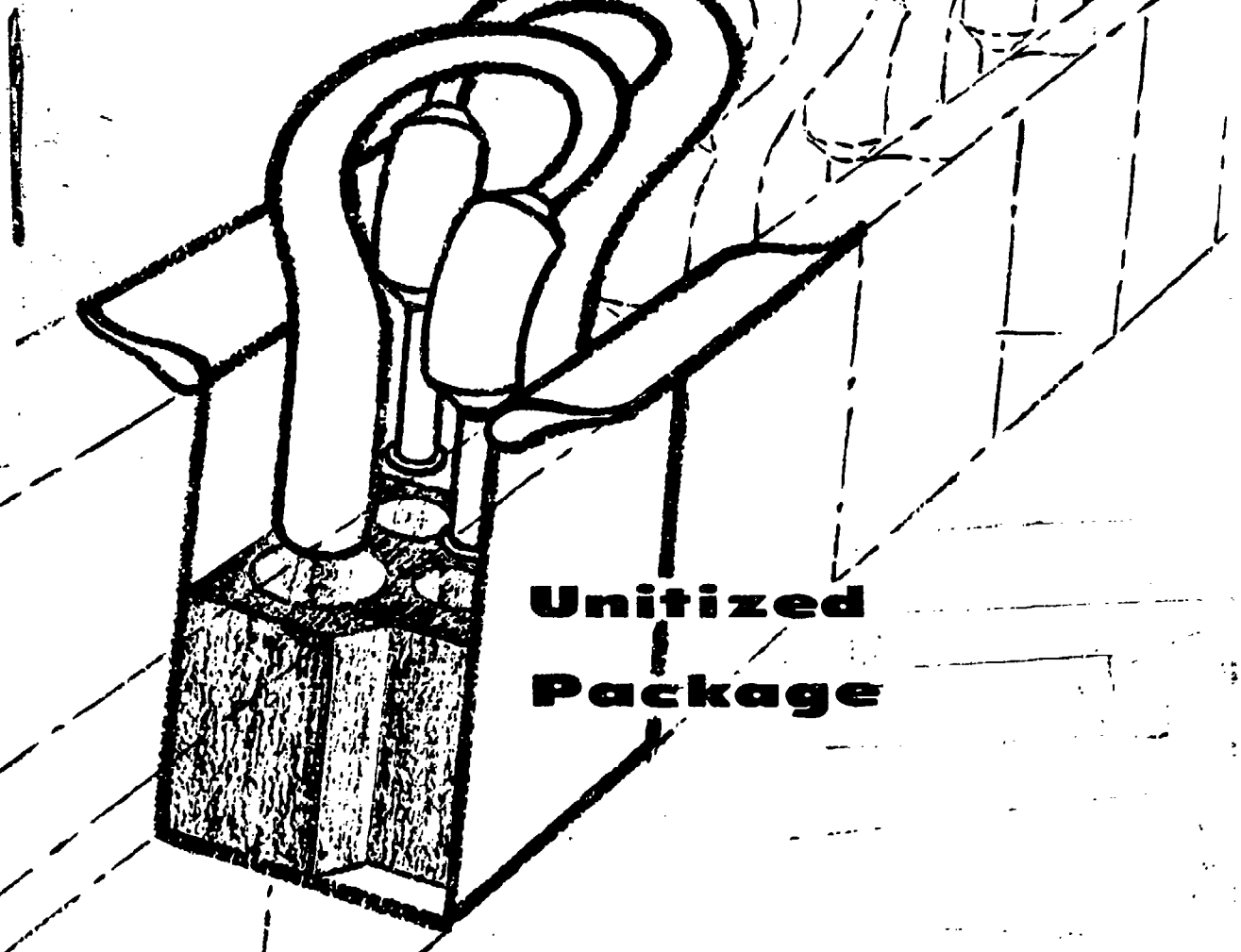
Hiller Pulse Reactor Lift Engine

AD-601 715

Final Report

ADVANCED RESEARCH
REPORT NO. ARD 308
MARCH 1963



Unitized Package

ILLER AIRCRAFT COMPANY DIVISION OF THE ELECTRIC AUTOLITE COMPANY

REPRODUCED BY
NATIONAL TECHNICAL
INFORMATION SERVICE
U.S. DEPARTMENT OF COMMERCE
SPRINGFIELD, VA. 22151

229

Report No. ARD-308

March 1963

PULSE REACTOR LIFT-PROPULSION SYSTEM DEVELOPMENT PROGRAM .

Final Report
Bureau of Naval Weapons
Contract NOw 61-0226-c

Approved: E. R. Sargent
Mgr. Propulsion Dept.

R. M. Lockwood
Project Engineer

J. B. Nicholls
Mgr. Advanced Planning
and Research

Key Members of Development Team:

J. E. Beckett, Development Engineer
W. G. Patterson, Research Engineer
H. W. Sander, Research Engineer
D. A. Graber, Chief Research Mechanic
R. J. Cullen, Research Mechanic
J. H. Awl, Research Engineer

ADVANCED PLANNING AND RESEARCH
DIVISION OF HILLER AIRCRAFT COMPANY

SUMMARY

The Pulse Reactor Engine Program is aimed at developing efficient, high performance lift-propulsion systems that have no moving parts. The Pulse Reactor engine is unique in that it rejects foreign particles that are denser than air; therefore, it can operate in the interface between ground and air that is denied to other aircraft lift-propulsion systems. In particular, development has been concerned with the performance effects of (1) engine size, (2) new shapes, (3) forward flight and vertical flight performance, (4) engine controls and accessories, (5) pulse reactor materials, construction techniques and engine durability.

Pulse Reactors of various sizes have been constructed and tested to determine the thrust/volume ratio versus engine size relationship. Combustor thrust/volume ratio varied from 60 lb/ft^3 for the HS-1B 9.1" diameter combustor to 150 lb/ft^3 for the HC-1 miniature combustor of 2.5" diameter. Improvements in the fuel injection system and combustor shell geometry applied to a 5.25" diameter combustor, designated HH(5.25")-5, resulted in a thrust/volume of 120 lb/ft^3, a 50% increase above that of previous 5.25" diameter combustors. When combined with the high performance intermittent jet thrust augmenters, this configuration produced 147 lb thrust with a thrust-specific fuel consumption (Tsfc) of less than 0.9 pph/lb thrust. A thrust-to-weight ratio of 10 is judged to be feasible at the current state of the art, based on component weight. Typical downwash jet velocities and temperatures are 200 ft/sec and 200°F.

The Pulse Reactor may be bent into a variety of shapes and configurations with little effect on performance if the internal surfaces remain fairly smooth and continuous and if the bends are not too sharp. A program for preliminary investigation of new Pulse Reactor shapes has been conducted under subcontract by SNECMA, the French jet engine company, to indicate the potential of essentially horizontal combustor tubes with short-coupled turns to provide vertical jet combinations of multiple

inlets and tailpipes, or modified Helmholtz resonators near the tailpipe exits.

The combustor shell durability problem is concerned with temperatures ranging as high as 1850°F and cyclic pressures nominally in the range of -5 psig to +30 psig at operating frequencies of about 120 cps. Shell construction using thin (0.010" to 0.018") Haynes 25 alloy (L-605) with circular circumferential stiffeners attached by furnace brazing has been investigated. No cooling by shrouding and ejector pumping is required in this approach. Over 51 hours of operation have been performed with a pair of lightweight combustors which were constructed of 0.017" thick Haynes 25 alloy, with circular circumferential stiffening rings. The best thrust-to-weight ratio of this combustor type (including fuel nozzles, manifold, igniter, attachments) was 76 lb thrust/11.0 lb st = 6.9. Recommended re-design as a result of the 50-hour durability tests would reduce the number, size and weight of the stiffening rings and also replace much of the tailpipe with thinner (0.010") material. Thrust/weight ratios as high as 12 to 1 for the separate augmenter component, along with excellent durability, have been achieved with augmenters of sandwich construction using fiberglas skins, and cores of honeycomb (fiberglas or aluminum), "Multiwave" (aluminum) and polyurethane foam.

A Pulse Reactor control system has been designed which includes features such as an automatic starting sequence, false-start sensor, "Blow-torching" limiter, and automatic re-start sequence.

Forward speed performance tests with both unshrouded and shrouded engines have been conducted with a trailer test rig which has been towed on the airstrip at Moffett Field at airspeeds up to 63 knots. Engine internal performance indications, based on measurement of average combustion chamber pressure, as well as preliminary measurements of lift and drag, showed continued improvement up to these maximum speeds tested. The initial HH-5.25-7 combustor configuration used in trailer speed tests had a tendency toward unexpected flameouts, but this was essentially corrected with the later HH-5.25-7 combustor configuration.

TABLE OF CONTENTS

		Page No.
SUMMARY		i
TABLE OF CONTENTS		iii
LIST OF FIGURES		v
1. INTRODUCTION		1
1.1	Pulse Reactor Concept	1
1.1.1	Pulse Reactor Definitions	
1.1.2	The Pulse Reactor Cycle of Operation	3
1.2	Pulse Reactor Development Program	5
1.3	Supplementary Programs	5
1.3.1	Energy Transfer from Intermittent Jet to Secondary Fluid in Jet Ejectors	5
1.3.2	Miniature Valveless Pulsejet Characteristics	6
1.3.3	Interrelation of Pulse Reactor Programs and Areas Needing Additional Work	7
2. COMBUSTOR DEVELOPMENT		9
2.1	Scale Effects	9
2.2	Improved Combustor Geometry	10
2.2.1	Effect of Combustor Tailpipe Length	10
2.2.2	Combustion Chamber Bulkhead Design	11
2.2.3	Breakthrough in Combustor Design	12
2.2.4	Inlet Lip Shape Effect	13
2.3	Fuel System Development	13
2.4	Combined Effects of Fuel System and Combustor Geometry	17
2.4.1	Lengthening the Combustion Chamber	18
2.4.2	Inlet Pipe Taper	19
2.4.3	Combined Effects of Inlet Pipe Taper and Chamber Length	19
2.5	Combustion Chamber Average Pressure Observations	21
2.6	Combustor Shape Investigation	23
2.6.1	Minor Changes in Pulse Reactor Configurations	23
2.6.2	Major Changes in Pulse Reactor Configurations (See Appendix)	26
3. THRUST AUGMENTER DEVELOPMENT		28
3.1	Augmenter Inlet Flare	28
3.2	Spacing Between Augmenter and Combustor Outlet	29
3.3	Augmenter Cluster Design	30
3.4	Augmenter-to-Combustor Tuning	31

TABLE OF CONTENTS (CON'T)

		Page No.
4.	MULTIPLE ENGINE OPERATION	33
4.1	Dual HH(5.25")-5-2 Pulse Reactor Tests	33
4.2	Multiple Miniature Engines	33
5.	PULSE REACTOR SUBSYSTEMS	34
6.	FORWARD FLIGHT PERFORMANCE OF PULSE REACTOR LIFT ENGINES	36
6.1	Connected-Pipe Tests	36
6.2	Trailer Test Rig Program	37
6.3	Demonstration of Operation over Dry Hay Field	41
7.	PULSE REACTOR DURABILITY AND MATERIALS	42
7.1	Augmenter Materials and Construction	42
7.2	Combustor Durability	43
7.2.1	Cyclic Pressure and Thermal Stress Loads	44
7.2.2	Combustor Materials	45
7.2.2.1	Attachment with Rubber Mounts	45
7.2.2.2	Improved Combustor Suspension Systems	46
7.2.3	Detail Design	47
7.2.4	Combustor Shell Material	49
7.2.4.1	Stainless Steel Combustors	49
7.2.4.2	Lightweight Combustor Materials and Weights	49
7.3	50-Hour Exploratory Durability Tests	50
8.	RECAPITULATION AND CONCLUSIONS	53
9.	REFERENCES	55
10.	FIGURES	57
11.	APPENDIX	167

LIST OF FIGURES

1. Pulse Reactor Cycle Diagram
2. Chart for Pulse Reactor Development Program
3. HS-1 Valveless Pulsejet Engine with Inlet Jet "Dilution Duct" Thrust Augmenter Mounted on Simple Thrust Stand
4. Components for Two Straight Pulse Reactors of 4.75" i.d. and 7.5" i.d. Combustion Chamber Diameter (HS-1 Type Geometry)
5. Trend of Thrust/Vol and Tsfc Vs. Volume for Pulse Reactor Combustors
6. Geometry of HS-1B Pulse Reactor
7. Effect of Reduced Combustor L/D on HS-1B (9.1" dia.) Performance
8. HS-1B 9.1" Diameter Pulse Reactor Effect on Engine Length on Thrust per Unit Volume
9. Effect of Combustor L/D on Tsfc for HS-1B 9.1"
10. Effect of Combustor L/D on Thrust for HS-1B 9.1" Combustor
11. Effect of Combustor L/D on Thrust/Vol. for HS-1B 9.1" Combustor
12. Effect of Combustor L/D on Tsfc for HS-1B 9.1" Combustor
13. Longitudinal Section Showing "Half Doughnut" Combustion Chamber Bulkhead for HS-1B (0.33) Combustor
14. Effect on Performance of a 30° and 45° Combustion Chamber Bulkhead
15. Effect of Reduction of Tailpipe Length on 5.0" Diameter Combustor
16. HH(5.25")-5 Combustor with 45° Bulkheads at Both Ends of Combustion Chamber and Excessively Long Tailpipe
17. Effect of Reduction in Combustion Chamber and Tailpipe Length on Combustor with 45° Bulkhead and 45° Transition
18. Major Changes to 5.25" i.d. Combustor Geometry
19. Effect of Modifications to 5.25" i.d. Combustor
20. Effect of Inlet Lip Configurations on HH(5.25")-5 Combustor
21. 5.25" Diameter Pulse Reactor Combustor, Model HS-1B(0.33), with 12-Line Fuel System
22. Fuel Nozzle Locations for 5.25" i.d. Pulse Reactor Combustor
23. Fuel Nozzles used successfully in 5.25" i.d. Pulse Reactor Combustor

LIST OF FIGURES (CON'T)

24. Lorgnette Type Fuel Nozzle for 5 $\frac{1}{4}$" i.d. Combustor

25. Lorgnette Fuel Nozzle Locations for 5$\frac{1}{4}$" i.d. Combustor

26. Effect of Fuel Nozzle Gap Width on Flat U-Shaped HH(5.25")-5 Combustor with 4 Each "Question-Mark" Nozzles

27. Effect of Fuel Nozzle Location on Thrust and Specific Fuel Consumption

28. Inlet and Combustion Chamber "Average Static" Pressure Probe Test HH(5.25")-5 Flat U-Shaped Combustor at 105 pph Fuel Flow Rate and 54 lb Thrust

29. Improved Performance from Changes in 5$\frac{1}{4}$" i.d. Combustion Geometry and Fuel System

30. Various Combustion Chamber and Inlet Pipe Configuration Modifications to Basic HH 5.25" i.d. Model

31. Comparison of Performance of Various Combustion Chamber Lengths and Inlet Taper Configurations

32. Comparison of Performance of Various Combustion Chamber Lengths and Inlet Taper Configurations

33. Comparison of Performance of Various Combustion Chamber Lengths and Inlet Taper Configurations and Tailpipe Bend

34. Various Combustion Chamber and Inlet Pipe Configuration Modifications to Basic HH 5.25" i.d. Model

35. Comparison of Performance of Various Combustion Chamber Lengths and Inlet Taper Configurations

36. Comparison Data of HH 5.25-6 Models in 90° (Right-Angled) Configurations

37. 180° -5.25-7 Combustor Layout Sketch

38. Typical Pulse Reactor Configurations

39. HS-1B 90° Pulse Reactor on Orthogonal Thrust Stand

40. Pulse Reactor Engine Package, Model HH(5.25") "Horsecollar"

41. HH(5.25") "Horsecollar" Combustor with Fuel Nozzles and Starting Air Tube Ready for Static Testing

42. HH(5.25")-5 "Horsecollar" Combustor with Bend Relocated to Aft Part of Combustion Chamber

43. HH(5.25") "Horsecollar" Combustor Preliminary Checkout

LIST OF FIGURES (CON'T)

44. Unitized Pulse Reactor Lift Engine Display Package Consisting of Twin Combustors, Augmenters, and Shroud Open for Operation

45. HH(5.25")-5-3 "Horsecollar" Combustor

46. Two Views of HH(5.25")-5-1

47. HH(5.25")-5-2 "Horsecollar" Combustor with Bend Located in Aft Part of Combustion Chamber

48. HH(5.25")-6 Combustor with 9.25" Radius Mitered Turn Section Modified from -5 "Horsecollar" Model by Removing Bend in Combustion Chamber

49. HH(5.25")-6 Combustor with 9.25" Radius Mitered Turn Section Modified from -5 Combustor by Changing to Cylindrical Combustion Chamber and Straight Tailpipe

50. HH(5.25")-5 "Horsecollar" Modified with Cylindrical Combustion Chamber and Straight Tailpipe

51. Flat U-Shaped HH(5.25")-6 Combustor with 7" Radius Turn Section on Test Stand. This Type Combustor was Used in the Initial Trailer Forward Speed Tests

52. Augmenter Flare Configurations

53. Effect of Lip Flare Configuration on Augmenter Thrust at "X" Spacing From Augmenter to Jet Outlet. Constant Fuel Flow to C-1 Combustor (4.0" H_2O Average Combustion Chamber Pressure)

54. Effect of Augmenter Lip Radius and Spacing on Combustion Chamber Average Pressure (Nominal Average Chamber Pressure 4.0" H_2O)

55. Exhaust Augmenter Tuning for the HH(5.25")-5, 90° Combustor

56. Exhaust Augmenter Tuning for the HH(5.25")-5,90° Combustor

57. HH(5.25")-5, 90° Pulse Reactor

58. Various Sandwich Construction Materials Considered in the Design and Construction of Augmenters and Engine Shrouds

59. Inlet Thrust Augmenters for HS-1B 9.1" Diameter Pulse Reactor Constructed of Fiberglas Skin and Honeycomb Core

60. Augmenter Cluster for a Pair of HH(5.25")-5 Combustors, Constructed of "Sta-Foam" Core and Fiberglas Skin - Weight 12½ lbs

61. Examples of Augmenters of Sandwich Construction Using Polyurethane Foam Core. The Augmenters with Rectangular Outlets Require Reinforcing of the Flat Surfaces

LIST OF FIGURES (CON'T)

62. Dual Mounted HH(5.25")-5-2 Engine (Combustor) Configuration (No Scale)

63. Effect of Engine Proximity

64. Dual HH(5.25")-5 U-Shaped Pulse Reactors

65. Diagram of Fuel and Starting Air System

66. Automatic Engine Control Circuit

67. Boxes in Foreground Contain Automatic and Semi-Automatic Control Systems for Pulse Reactor Start, Fuel Control and Re-start Sequences

68. A Pair of HS-1B(0.19) Pulsejet (4" dia.) Combustors Mounted for Static Testing

69. Connected-Pipe Test Set-Up for HS-1B(0.19) Pulse Reactors

70. Dual HS-1B(0.19") Pulse Reactors Shrouded for Connected-Pipe Testing with Axial Flow

71. Sketch of Hiller Truck-Trailer Low-Speed Test Rig

72. Hiller Aircraft Water Tunnel Used for Flow Visualization Testing of Trailer Test Rig

73. Trailer Test Rig with Accessory Equipment

74. Pulse Reactor Lift, Drag, and Pitching Moment Balance Mechanism for Trailer Test Rig

75. Balance Measurement System

76. Pulse Reactor Control Console for Trailer Test Rig

77. Block Diagram of Digital Data Conversion and Recording System

78. Two Unshrouded Pulse Reactor Engines Mounted on Trailer Test Rig

79. Air Supply Storage Tank and Air Compressor

80. Trailer Test Rig in Operation on Moffett Field Runway, 25 January 1962

81. Effect of Forward Speed on Pulse Reactor Thrust (Lift)

82. Comparison of Air Flow Paths for Hovering and Forward Speeds with Unshrouded Engines

83. Pulse Reactor Trailer Test Rig and Shroud Assembly with Two (2) HH(5.25")-6-7 Pulse Reactor Combustors Installed

LIST OF FIGURES (CON'T)

84. Forward Speed Tests on Runway at Moffett Field N.A.S. with Dual Shrouded Pulse Reactor Engines in Shroud Package Large Enough for Later Testing with Six Combustors

85. Comparison of Shrouded and Unshrouded Dual HH(5.25")-6-7 Pulse Reactor Engine Performance on Trailer Test Rig

86. Pulse Reactor Trailer Test Rig with Shrouded Engines Positioned 15° Up

87. View Looking Down on Test Site at N.A.S. Moffett Field, Showing Top View of Shrouded Pulse Reactor Engine Package

88. Shrouded Engines, Nose Down 30° Operating Over Dry Hay Field

89. View Showing Pulse Reactor Jet Downwash Effect as it Passes Over Dry Hay Field at Two Miles per Hour

90. Tailpipe Sections Stiffened by Rolled-In Corrugations

91. Testing of Corrugation Stiffened Tailpipe Section on HH(5.25") Combustor

92. HH(5.25") "Horsecollar" Lightweight Combustor with Ring Stiffeners and Shock Mounts

93. Shell Temperature Distribution HH(5.25")-5 (130 pph Fuel Flow)

94. Pulse Reactor Combustor Tubular Turn Section

95. Photo of Engine Crack in HH(5.25")-6-7 Stainless Steel (0.050" Type 321) No. 1 Combustor after 16 Hours of Operation. Field Repair was Made and Engine Performance Restored

96. Sketch of Various Configurations Available from Tyce Turn

97. Assembly Jig for 180° (5.25")-7 Combustor

98. (5.25"-7 Combustor Mounted in Assembly Jig

99. 180° (5.25")-7 Combustor Mounted on Test Stand. This Combustor was Fabricated Using Haynes 25 Alloy

100. Lightweight 220° Ring-Stiffened Combustor Turn Section Manufactured by Tyce Engr. Co., 0.017" Thick Material Haynes 25 (L-605); Weight 2.55 lb

101. Completed Lightweight HH(5.25")-7 Combustor of 0.017" Thick Haynes 25 Material

102. Uncoated Lightweight HH(5.25")-7 Combustor on Static Test Stand, Using Rubber Lord-Type Shock Mounts

LIST OF FIGURES (CON'T)

103. Solaramic Coated Lightweight (5.25")-7 Combustor Operating on Static Test Stand, Using Robinson-Type Shock Mounts with Attachments that Permit Differential Thermal Expansion of Combustor

104. Oblique Views of Improved Combustor Support Mechanism

105. Axial View of Improved Combustor Support Mechanism. Jointed Attached Arm on Combustor Permits Differential Motion Between Tailpipe and Inlet

106. Lightweight HH(5.25")-7 Pulse-Reactors Installed in Shroud on Trailer Test Rig for 50-hr Exploratory Durability Test Program

107. Close-up of Installation of Lightweight HH(5.25")-7 Engines

108. Faulty Brazed Joint in Uncoated Lightweight HH(5.25")-7 Combustor

109. Typical Fatigue Crack Developing Beneath Brazed-on Stiffening Ring on Lightweight HH(5.25")-7 Combustor

110. Small Fatigue Crack Developing Around Spark Plug Boss of Uncoated Combustor

111. Circumferential Fatigue Crack at Juncture of Inlet Tube and Combustion Chamber of Ceramic Coated Lightweight HH(5.25")-7 Combustor

112. Pulse-Reactor 50-Hour Durability Test, Power Settings, Cycles and Time

113. Lightweight HH-5.25-7 Pulse-Reactor Shell (Ceramic Coated) Showing Location, Time and Description of Key Repairs

114. Lightweight HH-5.25-7 Pulse-Reactor Shell (Uncoated) Showing Location, Time and Description of Major Repairs

115. Lightweight HH-5.25-7 Pulse Reactor (Ceramic Coated) Showing the Complete History of Location and Time in Hours of Engine Shell Repairs Including Incipient Cracks

116. Lightweight HH-5.25-7 Pulse-Reactor (Uncoated) Showing the Complete History of Location and Time in Hours of Engine Shell Repairs Including Incipient Cracks

117. Various Types of Fuel Used During Pulse-Reactor 50-Hour Exploratory Durability Test

LIST OF FIGURES (CON'T)

118. Average Temperature Reading at Augmenter Outlets

119. Mean Average Pressure Readings Taken at Augmenter Outlets

120. Maximum Pressure Reading Taken at Augmenter Outlets

121. Individual Operated HH(5.25")-7 Pulse-Reactor Engines without Augmenters, Prior to 50-Hour Durability Test Run

122. HH(5.25")-7 Pulse-Reactor Engine Performance at End of 50-Hour Durability Test Run

123. Dual HH(5.25")-7 Pulse-Reactor Engines After 50-Hour Durability Test, without Augmenters

124. Individual HH(5.25")-7 Pulse-Reactor Engines with Augmenters, After 50-Hour Durability Test Run

125. HH(5.25") Dual Pulse-Reactors in Shroud Assembly After 50-Hour Durability Test

126. Dual HH(5.25")-7 Pulse-Reactor Engines with Augmenters After 50-Hour Durability Test

127. HH(5.25")-7 Pulse-Reactor Engine with (3) Fuel Nozzles

128. Summary Tabulation of Best Pulse-Reactor Performance Data

129a. Best Pulse-Reactor Performance with Sketches Showing Various Configurations and Combinations

129b. Best Pulse-Reactor Performance with Sketches Showing Various Configurations and Combinations

129c. Best Pulse-Reactor Performance with Sketches Showing Various Configurations and Combinations

1. INTRODUCTION

From November 1961 to date, the Advanced Research Division of Hiller Aircraft Company has been developing a lift-propulsion engine, called the Pulse Reactor, under Bureau of Naval Weapons Contract NOw 61-0226-c.* This work is a continuation of the work done previously under Contract NOa(s)59-6055-c (Ref. 1, Hiller Report No. ARD-256).

1.1 The Pulse Reactor Concept

Development of VTOL aircraft over the past 20 years, from helicopters to tilt-wings, to pure jet VTOL, has resulted in a trend of higher disk loading and greater installed power. Following this upward trend are increased complexity and cost of the lift-propulsion system, and increased susceptibility to field environmental hazards. The Pulse Reactor lift-propulsion system sharply reverses these rising trends yet provides hovering performance which is competitive with that of turbojets. At this early stage of development, the Pulse Reactor lift engine has demonstrated a thrust-specific fuel consumption of better than 1.0 pph/lb and a thrust-to-weight ratio of 10 is feasible at the current state of the art, based on component weight, and with downwash temperatures of only 200°F and velocities in the order of 200 ft/sec, in contrast with a temperature of 750°F and a velocity of 1,000 ft/sec for a typical turbojet. Furthermore, the Pulse Reactor simply refuses to ingest heavier-than-air particles, a vitally important consideration when operating over unprepared surfaces. To further complement these characteristics is the basic simplicity of the Pulse Reactor. Since it has no moving parts, consisting mainly of three simple tubes, (a combustor and two thrust augmenters) it permits low cost development, production, maintenance and high reliability.

1.1.1 Pulse Reactor Definitions

In order to describe the Pulse Reactor and the development progress made to date, it is necessary that the following terms be defined:

---

*U. S. Army support (TRECOM) added under C.N. 7763-61

(1) combustor -- a valveless open-ended tube with intermittent efflux from both ends. The tube may be bent into a variety of configurations, the most common being a U-shape;

(2) combustion chamber -- that portion of the combustor in which ignition and combustion occ

(3) tailpipe or exhaust -- the longest portion of the combustor exclusive of combustion chamber. The largest portion of the combustion gases are exhausted through the tailpipe, producing approximately 60% of the combustor thrust. There is also considerable cyclic reverse flow of fresh air back into the tailpipe;

(4) inlet -- a short length of tube connected to the combustion chamber, through which the air for the combustion process enters the combustion chamber. It should be noted that both inflow and exhaust jet efflux occur from the so-called inlet, producing approximately 40% of the combustor thrust;

(5) augmenter -- an ejector-type device used to increase the thrust of the inlet and tailpipe of a combustor;

(6) pulse reactor -- combustor plus thrust augmenters.

The terms that are measures of Pulse Reactor performance are:

(1) combustion chamber average pressure, psig;

(2) thrust (F), in pounds;

(3) thrust-specific fuel consumption (Tsfc), in pounds of fuel per hour per pound of thrust;

(4) thrust augmentation ratio, which is the total thrust of augmenters and combustor divided by the thrust of the combustor when operating without thrust augmenters;

(5) thrust per unit volume, which is the total thrust in pounds divided by the volume in cubic feet of the thrust device;

(6) fuel flow rate (w), in pounds per hour (pph);

(7) corrected thrust and fuel flow rate (F_c and w_c), which are thrust and fuel flow rate corrected to standard atmospheric conditions. $F_c = F/\delta$ where δ = ambient pressure/standard pressure and $w_c = w/\delta\sqrt{\theta}$ where θ = ambient temperature/standard temperature. Due to the small variations in the corrected values (within 2 or 3%), F_c and w_c are determined only when a close comparison of the test data recorded over several days is made.

The independent variables that affect combustor performance are:

(1) combustor L/D ratio, which is the total combustor length along the centerline divided by the largest internal diameter of the combustion chamber;

(2) the total engine volume (including combustor and thrust augmenter), in cubic feet;

(3) augmenter L/D ratio, which is the centerline length divided by the minimum internal diameter of the augmenter;

(4) details of combustor geometry such as type of transition from inlet to cylindrical combustion chamber, transition from combustion chamber to tailpipe, divergence of tailpipe;

(5) interaction or matching of components;

(6) type and location of fuel injection system.

1.1.2 The Pulse Reactor Cycle of Operation

The Pulse Reactor cycle of operation may be described briefly with reference to Figure 1. Starting is accomplished by simultaneously turning on the ignition, fuel, and starting air. The resulting combustion causes a pressure build-up, and the air and combustion products expand out both ends of the combustor, introducing the exhaust phase. In this phase, the

ignition and starting air are turned off, and as the pressure in the combustion chamber is higher than the fuel pressure, the fuel flow ceases momentarily. The momentum of the exhaust gases causes an over-expansion in the combustion chamber and flow reverses in the inlet and tailpipe. During this inflow phase, as the combustion chamber pressure is substantially below the fuel manifold pressure, the fuel again flows into the chamber. The air flows which enter from both ends of the combustor collide in the combustion chamber and there is a vigorous mixing of the incoming air-charge and fuel. The hot products of combustion which didn't escape from the tailpipe during the previous phases are thoroughly mixed with the fresh charge and furnish multiple points of ignition for the next combustion phase. The cycle is then repeated at a frequency determined by the size of the combustor. The vigorous mixing and multiple-point ignition explains why the resonant combustor may be operated on a wide variety of fuels. The performance (at sea level) does not depend on the use of fuels with high flame speeds, but only on the heating value and the mixing efficiency. Of additional importance is the very rapid thrust response to changes in fuel flow rate. It is estimated that the Pulse Reactor's throttle response is complete within three to four combustion cycles, a small fraction of a second.

The intermittent jets from the ends of the combustor can be compared to one-way pistons as they travel through the augmenters forcing air out ahead and drawing ambient air in behind over the curved augmenter entrance. With optimum geometrical relationships between the augmenters and combustor, the thrust of the combustor can be more than doubled by the action of the augmenters.

During this last year of development, several changes have

been made to the qualitative Pulse Reactor cycle description. With the aid of high-speed schlieren motion pictures of a two-dimensional augmenter model, it was observed that the gas flow doesn't reverse direction in the augmenter as was previously postulated (Reference 1, Fig. 8). However, there is flow reversal over the rounded lip (from the jet spill-over) as the intermittent jet piston enters the augmenter. These schlieren flow visualization studies are presented in Reference 2 in the form of 35 mm color transparencies.

1.2 Pulse Reactor Development Program

The Pulse Reactor Development Program under Contract NOw 61-0226-c can best be summarized by referring to the chart of Figure 2. The first phases of the program were involved in testing Pulse Reactors of various sizes scaled from the 9.1" diameter combustor (Fig. 3) originally furnished by the French jet engine company, SNECMA. Investigation of fuel systems and combustor shell geometry preceded selection of a Pulse Reactor package for the trailer forward speed tests. The durability and subsystem development programs support the trailer test program so as to lead to Pulse Reactor lift-propulsion packages suitable for VTOL applications. The details of each phase are presented in sections 2 through 7 of this report.

1.3 Supplementary Programs

1.3.1 Energy Transfer from Intermittent Jet to Secondary Fluid in Jet Ejectors

A study of the energy transfer process from intermittent jets to the secondary fluid in ejector type thrust augmenters is currently being done under Office of Naval Research Contract Nonr 3082(00) (References 2 and 3). This work has produced important results which have greatly benefited the Pulse Reactor Development Program. For example, results from small scale tests under Nonr 3082(00) were

used to develop augmenter configurations which have produced augmentation ratios as high as 2.4. Excellent visualization of the jet interface and measurement of its velocity through the augmenter have been achieved using high-speed frame and streak color schlieren motion picture photography. "Instantaneous" pressure measurements in the augmenter have been made, and several methods for instantaneous temperature measurements are being evaluated. The results of this program are leading to an analysis and mathematical model which will contribute to the full development of intermittent jet thrust augmentation.

1.3.2 Miniature Valveless Pulsejet Characteristics

A program for the investigation of miniaturized valveless pulsejets in the thrust range of 5 to 15 lbs has been sponsored by the U. S. Army Transportation Research Command under Contract DA 44-177-TC-688 (Ref. 4). This program is aimed at determining miniature pulsejet operating characteristics in terms of thrust, Tsfc, thrust-to-weight ratio, and thrust-to-volume ratio, as well as investigating the problem areas of fuels, fuel injection, starting, thrust augmentation and noise. Particular emphasis is placed on operation in clusters and the effects of inter-connecting the combustors. These miniature pulsejets have shown a unique potential as extremely simple devices for applications such as direct lift and propulsion, and for the creation of an air cushion beneath vehicles where a variety of configurations and space limitations are of prime importance. The Pulse Reactors (valveless pulsejet combustor plus augmenters) also offer interesting possibilities for use as jet pumps, and heater-blower combinations. As heaters, they offer particular advantages since it is known that the unsteady or back-and-forth flow of gases contributes to an unusually high rate of

heat transfer as compared to the steady flow of gases. This high rate of heat transfer is attributed to the scrubbing off of the boundary layer by the unsteady or reciprocating flow (Reference 11). In certain cases the increase of heat transfer has been reported to be as high as sixfold over the steady laminar flow situation. The most recent development under this contract has been the successful miniaturization of a fuel injection system which will allow combustor operation with gasoline. Previously, these small combustors were tested with gaseous propane.

1.3.3 Interrelation of Pulse Reactor Programs and Areas Needing Additional Work

It is fortunate that these areas of investigation and development, described in the preceding sections, are being worked on concurrently with the Pulse Reactor Program (Contract NOw 61-0226-c) in that they dovetail together in a way to accomplish the overall research and development in a most efficient manner. Significant progress has been made by applying the results and knowledge derived from the supplementary programs. The Pulse Reactor Development Program itself has produced the most important recent breakthrough in the development of a new combustor geometry of 5-1/4" diameter which provides an unaugmented Tsfc of 1.8 pph/lb and an increase in maximum thrust-to-volume ratio of 50% over that which could be obtained from the previous state-of-the-art. This was accomplished without the benefit of quantitative combustor cycle analysis data. In spite of these accomplishments, the development of the intermittent combustor has been handicapped by the lack of adequate theory and analysis. This contractor strongly feels that additional substantial improvements can be achieved by research into the gas dynamics of the Pulse Reactor engine cycle. In particular, a program which would

provide experimental instantaneous pressure and temperature data for a cycle analysis, such as outlined in Reference 5, would greatly supplement the existing programs and speed the performance development of the Pulse Reactor, as well as provide basic data on the useful and efficient resonant combustion phenomenon. The interactions between the resonant combustor and the thrust augmenters must not be neglected. Optimum performance certainly requires a proper matching or "tuning" of all components.

2. COMBUSTOR DEVELOPMENT

2.1 Scale Effects

One of the most important aspects of the Pulse Reactor development program has been the determination of the effective scaling of the engine up and down in size. From preliminary tests it was known that the thrust-to-volume ratio increased as the size of the Pulse Reactor was reduced. To provide more information about this trend several combustors were constructed with dimensions scaled from the 9.1" diameter HS-1B combustor originally furnished by SNECMA, the French jet engine company. These scaled engines are designated with the HS-1B notation followed by the square of the ratio of the combustion chamber diameter over 9.1" (Fig. 4).

The thrust-to-volume ratio and Tsfc performance for the HS-1B, HS-1B(0.33), the HS-1B(0.19), and the C-1, a miniature combustor of approximately 2 inches diameter, are shown in Figure 5. The thrust-to-weight trend closely follows the thrust-to-volume trend down to the point where the construction difficulties of miniaturized components and accessories places a limit. The thrust-to-weight and thrust-to-volume trends for the augmenters have also shown an increase as the augmenter size is reduced.

A variety of problems developed when the combustors were reduced in size. A reduction of combustor size causes an increase of the resonant combustion frequency. The physical space and time for the mixing of the fuel and incoming air is also reduced. A point is finally reached where the performance is affected. Thus, in order to get the smaller combustors to run satisfactorily, it became necessary to develop new types of miniaturized fuel nozzles and to determine the proper location of these nozzles within the combustion chamber. Difficulty with the fuel injection system was quite apparent when testing the 4" diameter HS-1B(0.19). The Tsfc versus volume trend is dependent upon the fuel injection system

and combustor volume which determine the effectiveness of fuel-air mixing. This problem area will be discussed further in Section 2.3. Regarding the effects of scaling, as a matter of necessity, the greatest effort has been expended on combustor development.

Another trend which appeared that further complicated the test evaluation was the need for an increased length-to-diameter ratio as combustor size is reduced. This trend appeared when the lengths of the tailpipe and inlet of the HS-1B family were varied in order to improve the strength of resonant combustion and the operating range.

The scale-effect performance tests were carried out with engines scaled down, rather than up, from the HS-1B 9.1" diameter combustor in order to investigate and take advantage of the rising thrust-to- volume and thrust-to-weight trends. From the results of these tests, the 5-1/4" combustor was selected to be the basic development engine as it has the highest thrust-to-volume ratio and is the smallest of the scaled down combustors which did not initially show performance loss due to the fuel system miniaturization problems. Pulse Reactors larger than the 9.1" diameter can readily be built using the same principles and relations which have been derived in investigation of the smaller engines. Since the larger size engines are less sensitive to small dimensional changes, the construction and operation of engines greater than 9.1" diameter should present few problems.

2.2 Improved Combustor Geometry

2.2.1 Effect of Combustor Tailpipe Length

A few attempts to reduce the length of the HS-1B 9.1" diameter combustor and still maintain satisfactory performance were unsuccessful under the program described in ARD-256 (Ref. 1). However, since that time it was discovered that

with small combustors, the engine tailpipe length could be drastically reduced if a slightly convergent cone (2^{o} included angle) tapered towards the inlet opening, was subsituted for the cylindrical inlet tube. It was decided to test this effect on the 9.1" diameter HS-1B combustor (Fig. 6) in the hope that the thrust-to-volume ratio of the combustor might be improved. Just as in the case of the small combustor, it was possible to operate the large combustor with greatly reduced tailpipe lengths (Fig. 7). However, the thrust-to-volume ratio generally decreased (Fig. 8) and the Tsfc increased (Fig. 9). This suggested an investigation of the effect of extending the tailpipe length in order to find the optimum length for the maximum thrust-to-volume ratio. The results of this program are shown in Figures 10, 11 and 12, which indicate that the best thrust-to-volume ratio (Figures 8 and 11) is achieved with a tailpipe length that is close to the standard length (L/D of 18.5) as exemplified by the HS-1B geometry; however, the best Tsfc occurs with L/D ratios between 21 and 22-1/2. The best Tsfc is 1.8 pph/lbs. thrust at an L/D of 22.4 (Fig. 10).

The differences in performance at matching points between the earlier set of data shown in Figures 7, 8 and 9 and the later set of data shown in Figures 10, 11 and 12, are due to using an improved combustor for the latter tests. The combustor improvement stemmed mainly from a rebuilt combustion chamber and tailpipe. Figure 9 shows the large difference in the performance (Tsfc) of the two unaugmented combustors. As the earlier tests progressed, distortion of the shell occurred in the transition region between the combustion chamber and tailpipe, thereby causing the older combustor to perform poorly.

2.2.2 Combustion Chamber Bulkhead Design

The flat bulkhead or abrupt transition from the combustion

chamber to inlet proved to be an area of structural weakness. A semi-toroidal bulkhead (Fig. 13) temporarily eliminated this problem on the 5-1/4" diameter combustor. However, when lighter gage materials were used for combustor construction, this area again became a structural problem. Conical bulkheads were then tried. Figure 14 is a performance comparison between combustors with a 45° bulkhead and a 30° bulkhead. The 45° bulkhead has been used on subsequent combustor tests and has shown no signs of structural weakness.

2.2.3 Breakthrough in Combustor Design

Further improvement of combustor thrust and Tsfc was accomplished with the 5-1/4" diameter combustor that was designated in its original dimensions as Model HS-1B(0.33). Significant gains in thrust were first made by elongating the entire combustor. Changes in various section diameters were tried and showed little improvement. The combustors still required a long tailpipe for optimum thrust-to-volume ratio. Reduction in tailpipe length resulted in trends of reduced thrust and thrust-to-volume ratio and an increase in Tsfc (Fig. 15), trends which were similar to those of the 9.1" diameter combustor.

The major breakthrough occurred when the long transition from combustion chamber to tailpipe was replaced with a 45° bulkhead similar to the transition between combustion chamber and inlet (Fig. 16). With this configuration, combustor length could be reduced drastically. The previous gains in maximum thrust were retained and the Tsfc improved to less than 2.0 pph/lb (Fig.17). The most important result attributable to this new geometry was an increase of 50% in the maximum thrust-to-volume ratio. Figure 18 compares the breakthrough geometry, designated as Model HH(5.25")-5 with the elongated version and the original version of the 5-1/4" diameter combustor. Figure 19 shows the

thrust-to-volume ratio and Tsfc as functions of fuel flow rate for the three combustors, while the maximum thrust-to-volume ratio and best Tsfc are shown for comparison in Figure 5.

The straight section of the tailpipe following the 180° turn in the HS-1B configuration in both 5 inch and 5.25 inch combustion chamber diameters was tested with a conically divergent section of 3.3° instead of the more usual included angle of 2.3°. The smaller angle seems to give slightly better performance and has more significance in that the tailpipe exit diameter is reduced and thus the required augmenter diameter is reduced, resulting in a smaller Pulse Reactor package.

2.2.4 Inlet Lip Shape Effect

Inlet lip configuration affects the combustor performance by changing the aerodynamics of the inlet. A small lip is associated with greater thrust than a larger lip (Fig. 20). Apparently, there are conflicting requirements for the inlet lip shape. From the standpoint of maximum air inflow to the combustor a large bellmouth or lemniscate shape would be ideal. However, the pressure drop on the lip associated with inflow acts on the combustor as a negative thrust. The best total combustor performance is achieved by a compromise which results in a relatively small inlet lip of a shape that approximates a lemniscate.

2.3 Fuel System Development

In a fairly broad investigation of commercially available fuel nozzles, we did not find nozzles small enough and of adequate flow characteristics to operate successfully in the smaller Pulse Reactor combustors. The larger nozzles seemed to be bothered by a vapor lock condition which developed soon after starting the engine, resulting in very uneven operation, and drastically reduced performance

or actual stoppage of operation. Therefore, we were forced to design our nozzles with the first factor in mind being that of reducing the over-all size of the nozzles, so as to reduce the amount of heat absorbed from the combustion gases. In order to get the smaller combustors to operate, it was at first necessary to use small (0.125" o.d.) tubes with two 0.0180" holes drilled opposite each other. It was also necessary to insert these fuel tubes into the air inlet (Fig. 21) instead of directly into the combustion chamber. Total thrust was fairly satisfactory with this combination, but thrust-specific fuel consumption suffered; apparently because fuel was wasted by blowing out the inlet during the blowback portion of the cycle.

Further research resulted in two successful types of nozzles that could be operated within the combustion chamber in the location shown in Figure 22, position B-B. These nozzles, designated the LB-I jet impingement type, and the "Question Mark" type, are illustrated in Figure 23. Emphasis has been placed on the latter type because of its simplicity of construction and because it does not clog so readily as the LB-I type. The "Question Mark" type has evolved into the so-called "Lorgnette" type (Fig. 24) which is a further simplification from the standpoint of fabrication. In order to obtain smooth operation over a wide range of fuel flow rates, it was necessary to place a restrictor in the fuel line near the nozzle. The effect of the restriction in the fuel line is to prevent the blowback of fuel so far back into the fuel line that it does not re-enter the nozzle in time for the next cycle. A further modification of the Lorgnette type consists of making the restricting orifice by merely drilling a small hole (No. 69 drill) through the wall of the ring-shaped nozzle at the junction of the stem and ring. The currently favored fuel injection system consists of four Lorgnette type nozzles positioned as shown in Figure 25. Note that two of these nozzles have the spray gap located at the end of the nozzle and the other two have the spray

gap located at 45° to the axis of the stem. The effect of the fuel nozzle gap width on performance of the HH(5.25")-5 combustor is shown in Figure 26. All of the foregoing fuel systems have used a low pressure in the fuel lines of 6 to 10 psig near the nozzles. High speed motion pictures have been taken at 1000 frames per second of the luminous flames during combustion and of the fuel spray pattern in the HS-1B engine. This was accomplished by pointing the Fairchild HS-101 camera, equipped with four-inch lens, directly into the combustor inlet. With the camera at a distance of about seven feet from the inlet, the fuel nozzles were clearly visible during the engine cycle. Four General Electric RSP2 photospots were arranged around the camera to provide front-lighting of the fuel nozzles. Eastman 16mm Ektachrome ER Type 7258 type B color film was used at f2.7. The motion pictures indicated that there is complete cutoff of the fuel during the combustion (and accompanying pressure rise) phase of the cycle as was expected with the low pressure fuel system.

The fuel nozzle position inside the combustion chamber has a large effect on combustor performance. Figure 27 illustrates these effects on the HS-1B 9.1" diameter combustor. In addition to the thrust and Tsfc changes, there is also an influence on the starting and combustion characteristics, and the throttling range.

Figure 28 shows the results of a test in which a small diameter "static pressure" probe was inserted into the combustor inlet along the longitudinal axis of the cylindrical inlet. In interpreting the plotted data, it must be born in mind that the flow past this so-called static pressure pick-up is decidedly back-and-forth as contrasted to steady flow situations. It may be assumed that the flow becomes established parallel to the main axis of the cylindrical inlet tube throughout much of the operating cycle. However, when the flow enters the combustor, it is expected that the sudden expansion of the flow from the cylindrical inlet into the cylindrical com-

bustion chamber will cause the intermittent creation of an incipient ring vortex motion or possibly a well-established ring vortex motion. The probe orifice is surely exposed to ram pressure during a portion of the cycle due to the swirling motion of the gases. Notwithstanding all these unresolved restrictions on the meaning of the data, the data is submitted as casting some additional light on the basic phenomenon.

One of the reasons for conducting the test was to look for some simple correlation between the position of the fuel nozzles for optimum performance as determined on an experimental basis, and the possible presence of standing waves within the combustor. As background here, it is noted that several inventors of valveless pulsejet combustors have claimed that their combustors operated on a so-called acoustic cycle, and blow-back through the inlet was completely nullified, or at least drastically reduced, by the presence of a standing wave located in the vicinity of the juncture of the inlet and the combustion chamber. This is obviously not the kind of cycle on which the subject Pulse Reactor engines operate. This is at once apparent because our tests have, from the first, shown that we get nearly as much thrust from the so-called inlet as we do from the tailpipe of the combustor. Furthermore, we have shown that we get good performance in terms of total engine thrust, even when the fuel nozzles are located in the inlet of the combustor. However, specific fuel consumption suffers in the latter situation as fuel is blown back out the combustor inlet during the combustion pressure rise portion of the cycle. Based on these "average static" pressure readings shown in Figure 28, one might suspect that the best position for the fuel injection would be in the region where the average pressure is highest. That is at the station designated 15" from the combustor inlet. However, the best nozzle location is shown to be at a station about 13" from the inlet. This indicates that the best location results not just from the highest average pressure location. The effect of the large swirling and

mixing action due to the inflow from the inlet, sudden dumping and expansion into the combustion chamber and resultant flame-holder action, and mixing of fresh fuel and air with hot gases from the previous cycle is fully as important in the overall performance, if not more so, than the pressure effect.

2.4 Combined Effects of Improved Fuel System and Combustor Geometry

The combined effects of the changes in both combustor geometry and the fuel systems are summarized in Figure 29. Curve (1) shows the performance of the HS-1B(0.33) combustor just as it was scaled down from the 9.1" diameter combustor, but with straight jet fuel nozzles in the inlet. Curve (2) shows an improvement of the fuel system, but with the nozzles still in the inlet. Curve (3) represents a large jump in performance due to the improved geometry shown as the HH(5.25") model in Figure 18. Some of the increased thrust is attributed to the increased volume of the lengthened combustor. Curve (4) shows the effect of the improved fuel system whereby the LB-I and the "Question Mark" types of fuel nozzles permitted engine operation with the fuel nozzles inside the combustion chamber. Notice that the maximum thrust of (4) is the same as (3), but (4) occurs at a much [illegible] fuel flow rate, thus (4) has a much better Tsfc than (3). [illegible] improvement in Tsfc is achieved by the combination of t[illegible]d fuel system and the breakth[illegible]ough in combustor geometry. [illegible]ortant breakthrough in combustor performance has provided a 50% increase in the thrust-to-volume ratio of the HH(5.25")-5 model as compared with the HS-1B(0.33) combustor (5). The HS-1B(0.33) has a thrust/unit volume of 80 lb/ft^3 for a volume of 0.69 ft^3; whereas, the HH(5.25")-5 gives 120 lb/ft^3 with a volume of only 0.6 ft^3.

When the HH(5.25")-5 configuration was changed from a 90° shape to a U-shape, the designation was changed to -6 for the latter. These high performance combustors designated as HH(5.25")-6 were initially used on the trailer test rig but they had relatively poor starting character-

istics as compared to many of the Pulse Reactors, and experienced unexpected blow-outs at high fuel flow rates. These combustors were constructed with the rather crude 180° turns pictured in Figures 16 and 21. The improved turn of larger radius and more nearly circular cross-section was not yet available at this time.

Past experience (sec. 2.2.1 preceding) indicated that easier starting and more stable operation with less sensitivity to tailpipe tuning occurs with tapered inlets than with the cylindrical inlets. Another possibility for improving the starting characteristics was to make a small increase in the length of the combustion chamber. It was anticipated that one or a combination of both of these modifications would alleviate the starting problem. Accordingly, the HH-5.25-6 combustor configuration was initially modified by (a) increasing the combustion chamber from 11" to 12", and (b) by replacing the cylindrical inlet with tapered inlets of 1° and 2-1/4° included angle. The various configurations of inlet taper and combustion chamber length are shown in Figure 30.

2.4.1 Lengthening the Combustion Chamber

The 11" long combustion chamber of the standard HH(5.25")-6 model combustor was lengthened to 12", thereby increasing the combustion chamber volume 21.65 cubic inches and the total engine volume 0.0125 cubic feet. Figure 31 is a plot of corrected thrust vs. corrected fuel flow rate for combustor L/D = 16.7 with combustion chamber lengths and inlet taper as parameters. Performance for an L/D = 17.3 is shown in Figure 32.

All tests for the plotted data were made in the absence of augmenters. Holding inlet taper angle 2θ constant and considering only the effect of combustion chamber length on performance, it is seen that a loss in thrust occurred when the chamber was lengthened from 11" to 12". However, the combustor started more quickly and easily. Furthermore, as shown in Figure 33, when the tailpipe was lengthened in combination with a combustion chamber length of 12" to give an over-all L/D of 18.8, and an inlet taper of 2θ = 1° was used, the total thrust increased from 72.5 lbs to 77 lbs at a fuel flow rate of 150 pph.

2.4.2 Inlet Pipe Taper

The inlet tube was modified from a right circular cylinder (no taper) to a truncated conical shape, tapered as shown in Figure 30. For purposes of definition, the included angle of the cone is called 2θ. Tests were made initially on two inlet tapers of $2\theta = 1^{\circ}$ and $2\theta = 2\text{-}1/4^{\circ}$.

Figures 31 and 32 show that with combustion chamber length held constant an increase in thrust occurs for a given fuel flow for tapered inlets. For the 12" chamber, the better of the two tapers is $2\theta = 1^{\circ}$. Again the engines started quickly, ran stably, and had no blow-outs. It should also be noted that the larger 9.25" radius turn made with smooth surfaces by a drop-hammer forming and seam welding process was first used with the test results shown in Figure 33. The results are shown for a 12-inch combustion chamber and length-to-diameter ratios, L/D, of 16.8 and 18.8 as compared to an earlier configuration of 11 inch combustion chamber and L/D of 16.6 with a 180° turn of 7-inch radius.

2.4.3 Combined Effects of Inlet Pipe Taper and Chamber Length

From the foregoing results it was suspected that the optimum taper (2θ) of the inlet was somewhere between 1° and $2\text{-}1/4^{\circ}$ so it was decided to try an angle of $2\theta = 1.5^{\circ}$ in conjunction with combustion chamber lengths of 11", 11-1/2" and 12" (Fig. 34). The results for 90° combustor configurations are shown in Figure 35 which is a plot of corrected thrust versus corrected fuel flow rate. The length of the tailpipe has been varied in each case to give maximum thrust. Figure 35 shows that the -6 and -7 configurations with the 1.5° inlet taper are superior. The 12" combustion chamber is also shown to be superior to the 11-1/2" combustion chamber length in conjunction with the inlet taper of 1.5°. The maximum thrust of 86 lb for the HH 5.25-6-7 combustor represents the highest thrust yet achieved for the 5.25" combustor diameter. The minimum Tsfc of 1.6 for both the -6 and -7 modifications at a fuel flow rate of 110 pph is also the best performance yet achieved. Note that this performance is for combustors only(not in the presence of

augmenters). This performance should be compared with the Tsfc of 2.3 for the original HS-9.1" combustor in the 90° configuration. The improvement represents a reduction of over 30% in thrust specific fuel consumption. Comparisons of the most important HH 5.25-6 models is shown in Figure 36 in terms of length, volume, maximum thrust and thrust-to-volume ratio.

Comparing HH 5.25-6 to HH 5.25-6-7 the latter model has a 10% increase in thrust for a 15% increase in total engine volume, which corresponds to a 4.6% decrease in thrust-to-volume ratio. On the other hand, advantages of this model are much more stable operating characteristics, quicker starting, higher maximum thrust and better Tsfc. An engine package composed of two or more combustors, similar to the HH 5.25-6-7 model combustors, has been designed so that when the engine is not operating, each combustor can be retracted into its own set of augmenters, thereby reducing the total engine package volume. Thus, because of the different geometrical relationships that exist between combustors and augmenters, even though the HH 5.25-6-7 combustor is somewhat larger than the HH 5.25-6, the total retracted engine package volume for the HH 5.25-6-7 may be less than that of the HH 5.25-6 type. More recent investigations of U-shaped combustors have shown that the tapered inlet of angle $2\theta = 1.5^{\circ}$ permits again reducing the total length to an L/D of 16.4 by removing two inches from the inlet tube to reduce it to 10-5/8" and an 8" reduction of the length of the unbent section of the tailpipe to 18-3/4 inches. This modification (called HH 5.25-7, see Fig. 37), reduces the volume to 0.615 ft^3 as indicated on Figure 36.

2.4.4 3-Nozzle Heavy-Wall HH -5.25-7 Combustor

As a result of operational problems and experience during the combustor durability program (section 7.3) at the very end of the contract, a modification of fuel system of the HH 5.25-7 configuration was conceived and tested. It consisted of substitution of 3 (45°, Fig. 24) fuel nozzles of the same type and flow characteristics, but re-positioned symmetrically with 120° between nozzles on a diametral plane, and set at 45° as indicated by the upper and lower nozzles in Fig. 25. Starting characteristics and overall performance were the best yet tested for the U-shaped configurations, as indicated in Figure 127.

2.5 Combustion Chamber Average Pressure Observations

The trend of combustion chamber average pressure follows the trend of thrust at various fuel flow rates as has been evident with other (valved) pulsejet engines. Reference 7 indicates that time-averaged combustion chamber pressure is an excellent indicator of pulsejet internal performance, and since it is our only direct measurement of internal engine performance, it is of obviously great importance even for static operation. This report shows that combustion chamber pressure can also be used to determine drag in forward flight by noting the difference between the equivalent thrust pressure and the specific net thrust. Since the term equivalent thrust pressure is a rather unusual term, it will be defined as follows: equivalent thrust pressure is determined by first dividing peak thrust by a corresponding combustion chamber average pressure which occurs at peak thrust, to determine an "equivalent area". Specific thrust is defined as the pressure, psig, obtained when the engine thrust is divided by the maximum cross-sectional area of the engine. The combustion chamber average pressure is then multiplied by the ratio of "equivalent area" to pulsejet maximum cross-sectional area to give "equivalent thrust pressure" over the range of fuel flows. In this way, the curves of specific thrust and the "equivalent thrust pressure" are made to coincide at peak thrust fuel flow and then the curves can be readily compared over the rest of the range.

The tests reported in Reference 7 indicate that the effect of forward velocity is to cause a spread between the curves of equivalent thrust pressure and specific net thrust. This is reasonable if equivalent thrust pressure is an accurate indicator of internal performance. The difference between these parameters is named the "specific drag" which is the drag divided by the maximum cross-sectional area of the pulsejet. From this information "hot drag" coefficients may then be plotted from the specific drag values. These resultant drag coefficients were shown to be reasonable values and represent the

best check available on the use of equivalent thrust pressure as an indicator of internal performance. It is interesting to note in Reference 7 that the drag coefficients decreased generally with increasing fuel flow rate until peak thrust is reached. This seems logical, since increased mass flow through the engine, as indicated by increased fuel flow, should reduce the intermittent spillage around the inlet cowl; and increased mass flow through the exhaust exit may also tend to reduce the engine base drag. This parameter of average combustion chamber pressure is included in all of our engine tests, both in static and in forward velocity conditions. Since this is such a simple parameter to measure, it should also, in later stages, be of particular importance as a way of giving the pilot information concerning the internal performance of his power plants, which for a given configuration may be calibrated directly in terms of net thrust. This is especially important in the case of multiple engine packages.

2.6 Combustor Shape Investigation

One of the most important characteristics of the Pulse Reactor is that it may be built in a wide variety of configurations. Several aircraft types and applications which take advantage of the various shapes are illustrated and described in Reference 1. The configurations of most immediate interest, however, are shown in Figure 38. In all these configurations except number (6), the inlet and exhaust ends of the Pulse Reactor are pointed in the same direction so that the thrust from each end may be combined to greater advantage.

2.6.1 Minor Changes in Pulse Reactor Configuration

Minor changes in Pulse Reactor shape have been accomplished by bending and twisting the combustor tube into a variety of configurations. The combustor tube, however, retains its characteristic dimensions and component dimensional ratios which characterize its geometry. In Figure 38, number (6) is a special shape suited to the Hiller-designed orthogonal thrust stand (Fig. 39) which separately but simultaneously measures the thrusts of inlet, exhaust, inlet augmenter, and exhaust augmenter. Shape number (1) has been the subject of the majority of our combustor development tests (as in Fig. 16) while shape (3) is the original S.N.E.C.M.A. furnished HS-1 valveless pulsejet with the inlet "dilution duct" augmenter. Figure 3 shows this S.N.E.C.M.A. engine undergoing tests on a static thrust stand. Figure 4 illustrates two straight combustors which were constructed for the scaling trend tests and to provide a standard of maximum performance for comparison with the U-shaped combustors. This particular configuration requires a thrust plate type of test stand which turns the jet efflux 90°.

In the design and selection of a Pulse Reactor configuration for an aircraft application, the engine volume requirements must be minimized. The 5.25" i.d. size combustor was selected because it provides a high basic thrust-to-volume ratio (Fig. 5) with a minimum of fuel system and performance problems. This

medium-sized engine is interesting from the standpoint of packaging multiple Pulse Reactors in pods, giving possibilities of good aircraft control during hovering by selective throttling of engines from left to right and from front to rear for roll control and pitch control.

Figure 40 shows a Pulse Reactor configuration in which the HS-1B type combustors and the thrust augmenters are crowded as closely together as we estimate can be done without drastically interfering with engine performance, and about as compactly as the engine geometry will permit. The curvature of the combustors was established to minimize the over-all package size when two or more Pulse Reactors are placed in a row. These "horsecollar" Pulse Reactors are oriented with a 15° slant from the vertical, which gives a component of 26% of the total thrust for forward flight when the aircraft is level, and are bent forward 47° to minimize frontal area. In addition, the combustors may be retracted into the augmenters, thus reducing frontal area and volume for the case when Pulse Reactor power is not required in forward flight.

Several HH(5.25") type combustors were built in the "horsecollar" configuration (Figure 41). Eighteen mitered segments comprised the large 200° bend in the tailpipe while there were four mitered sections in the bend near the end of the tailpipe and five mitered sections in the bend near the inlet end of the combustor. The semi-toroidal bulkhead was one of the features originally included in this combustor (Fig. 41) but was later replaced by the 45° conical bulkhead for performance testing. Performance data is presented in Figure 43. Thrust and specific fuel consumption were considerably poorer than that of the HH(5.25") flat U-shaped combustor. Average combustion chamber pressure reached a maximum of only about 2.5 psig. Factors which caused poor performance of this configuration were thought to be the following:

(a) a bend in the combustor occurred in a critical region near the junction of inlet and combustion chamber;

(b) the use of mitered sections in the turns adversely affects internal flow characteristics;

(c) the bend near the end of the tailpipe was so sharp as to have caused significant performance loss;

(d) cross sectional deformation caused by thermal stresses and pressure loads in the mitered sections of the large turn contributed to performance loss.

A "horsecollar" type combustor was then constructed using the new HH(5.25")-5 geometry. One bend was relocated to the aft part of the combustion chamber and the radius of the tailpipe bend was increased. While having the same maximum thrust rating as the previous "horsecollar" combustor, the HH(5.25")-5 was much smaller and therefore, lighter. A comparison can be made between Figures 41 and 42. A full sized display package (Fig. 44) demonstrates how the HH(5.25")-5 "horsecollar" combustors may be retracted down into the augmenter and the flaps closed to provide an aerodynamically clean, minimum volume package for forward flight when lift from the Pulse Reactors is not required.

The static performance tests of the HH(5.25")-5 "horsecollar" combustor (Fig. 45) revealed that maximum thrust and Tsfc were again considerably poorer than that of the flat U-shaped combustor of the same geometry. As segmented turns were used in the construction, the performance losses were again attributed to those factors previously mentioned. To further pinpoint the performance problems of this particular combustor configuration, several modifications to the shape were made as indicated in Figures 46, 47 and 48. The first change consisted of replacing the curved combustion chamber with a straight cylindrical chamber and then cutting and rotating the tailpipe so that the inlet and tailpipe axes were again parallel. No improvement in performance over that in Figure 45 was achieved. The bent tailpipe was then re-

placed by a straight section (Fig. 49). The only improvements in performance (Fig. 50) noted were slight improvements in the throttling range and resonating characteristics.

Conclusions derived from these tests led to the procurement of tooling and manufacture of a close-tolerance smooth tubular turn to replace the mitered sections of the tailpipe turn. It was constructed of Haynes 25(L605) and will be used both as a component for combustors in further development testing and for the combustor durability test program. Close tolerances were required for the turn, primarily because the major source of combustor failure is due to the pressure stress reversals which occur at the engine operating frequency of approximately 120 cps. If the engine is not quite round in cross section to start with, there is an increasing tendency for the shell to ovalize cyclically with eventual fatigue failure appearing as longitudinal cracks.

Another configuration which is interesting from the viewpoint of compactness is the 1.5 turn Pulse Reactor illustrated in Figure 38, number (4). Construction of this combustor is somewhat difficult in that the mitered section construction has not proven entirely successful, and tooling to provide a full size smooth turn would be quite costly.

2.6.2 Major Changes in Pulse Reactor Configurations

Results of Hiller company-sponsored application studies of Pulse Reactor lift-propulsion systems as applied to various air vehicles indicate a need for Pulse Reactors that are essentially horizontal tubes, but which exhaust from short air inlet and jet outlet pipes arranged so that the jet efflux will exit pointing vertically downwards, somewhat as typified in Figure 38, number (2). The French jet engine company, SNECMA, has had actual test experience with several of the components illustrated in Figures (plances) 6-1, 6-2 and 6-3 of Appendix I.

This experience gave strong support to the belief that one or more combinations of these combustors and short-coupled outlet turns would be highly promising. The target was to (1) accomplish sharp turns in the outlets of the combustor, (2) obtain improved thrust specific fuel consumption and (3) obtain improved thrust-to-volume ratio. The results of the initial phase of the SNECMA program are reported in Appendix I entitled "Test Report on New Types of Pulse-Reactors Developed for Hiller Aircraft Corporation" by Pierre Servanty, Chief of the Experimental Propulsion Department of the SNECMA Company.

3. THRUST AUGMENTER DEVELOPMENT

The ejector-type thrust augmenters adapted to the intermittent jet have shown exceptional performance. As described in References 1 and 2, the intermittent jet thrust augmenter is superior in performance as well as being relatively much smaller in diameter and shorter in length than the typical single central nozzle steady flow ejector. For example, intermittent jet thrust augmentation ratios as high as 2.4 have been achieved using an 8° divergent augmenter with an augmenter throat cross-sectional-area to primary-jet-area ratio of only 4 and a length-to-throat diameter ratio (L/D) of only 1.5. Typical steady flow ejectors with single central nozzle, for example, have shown maximum thrust augmentation ratios of about 1.4 but with an area ratio of approximately 25 or higher and a length-to-diameter ratio of 5. This superior performance of the intermittent jet thrust augmenter is explained by considering the energy exchange process between the primary jet and the secondary fluid. From flow visualization studies (References 2 and 12) it is apparent that this process involves pressure exchange between the waves created by the jet interface as it moves through the augmenter, and the secondary fluid. The basic research on intermittent jet thrust augmentation is being accomplished under Contract Nonr 3082(00). In addition to its high augmentation performance, the intermittent jet thrust augmenter has the effect of reducing the jet wake velocity and temperature to approximately 200 ft/sec and $200^{\circ}F$ at seven combustor tailpipe exit diameters (8.5" dia) aft of the tailpipe exit, i.e., at five feet from the combustor jet outlets in the case of the HS-1B configuration whose tailpipe jet wake temperature distribution is shown in Fig. A-35 of Reference 1.

3.1 Augmenter Inlet Flare

The general rule for augmenter construction has been to use an augmenter inlet flare of generous radius. In order to determine how small the flare radius could be without a significant sacrifice in performance, a range of miniature pyrex glass augmenters was tested using the inlet

(approximately 0.85" i.d.) of the C-1 miniature valveless pulsejet combustor as the primary jet. Figure 52 shows the various flare configurations tested. Before each augmenter was tested, the fuel flow rate to the combustor was adjusted to give the same predetermined value of "average" combustion chamber pressure. Augmenter spacing from the jet outlet was varied from 0.5" to 2.5". Figure 55 shows the results of this test. The 8° divergent cylinder with no radius or lip flare beyond the tube thickness of 0.05" showed a drag rather than a thrust. This corresponds with the average negative gage pressures along the inside of the augmenter wall observed in other tests. The superior performance of the divergent augmenter with a moderate lip radius over the cylindrical augmenter with a similar lip must be explained then by an improved flow pattern and pressure distribution over the lip flare.

It is surprising to note that there is such little variation in thrust over the range of lip flares of 0.1" to 1.0" radius at each spacing. The fluctuation in each thrust curve can partly be attributed to various imperfections or ridges in the throats, caused during spinning of the glass augmenters.

3.2 Spacing Between Augmenter and Combustor Outlet

Augmenter thrust has, in general, increased with decreased spacing between the tailpipe outlet and the augmenter inlet until the plane of the inlet was nearly reached. The spacing was measured from the combustor jet tailpipe outlet to a plane tangent to the augmenter inlet flare as shown by the small sketch on the lower right hand corner of Figure 52. However, tests at spacings of less than 0.5" (L/D = 0.59) were not made since the adverse effect on combustor performance, as indicated by combustion chamber pressure (see section 2.5, page 21 for significance of this parameter) definitely would outweigh the increase in augmenter performance. Figure 54 shows the effect of lip configuration and spacing on the average combustion chamber pressure. Bearing in mind that the combustion chamber average pressure is a good indicator of combustor thrust static performance, we note that lip configura-

tions of small radius show less adverse effect on chamber pressure while the cylindrical augmenter with no flare causes a rise in chamber pressure at the spacing in the neighborhood of 1 inch (L/D = 1.18). Combining these results, we can tentatively conclude that augmenters with a lip flare radius of only 5% of the minimum diameter offer as good augmentation as those with larger radii (important from the aspect of space conservation), or even better augmentation due to the fact that they may be coupled to the combustor with less spacing and less of an adverse effect on combustion chamber pressure.

There are three things which may, however, modify these conclusions and which require further investigation. First, the tests were carried out with cylindrical augmenters rather than the better performing divergent augmenters. Second, it is known that the natural acoustic frequency of cylindrical tubes is affected by the lip flare, so even though all of the tubes tested were of the same total length and diameter, their "effective" lengths were probably quite different. Third, the tests were conducted with the inlet end of the combustor only and the effect of the presence of an augmenter at the tailpipe end was not considered.

3.3 Augmenter Cluster Design

In the design of a compact multi-augmenter package it is desirable, for space conservation, to flatten the walls of the divergent augmenters so that the outlets are rectangular. Problems and techniques of construction are discussed in some detail in section 7.1. In general, tests with these flat walled augmenters have shown that there is a much greater structural problem due to the pressure load fluctuations on the flat surfaces (Fig. 61). Flat surfaces require reinforcement; however, the augmenters of circular cross-section are quite satisfactory and can be used with only a small increase in package volume.

3.4 Augmenter to Combustor Tuning

The effect of changes in HS-1B 9.1" combustor L/D (changes

made by varying the tailpipe length as in Figure 6) on thrust augmentation are shown in Figures 7-12 inclusive. In Figure 8 it is important to note that at low fuel flow rates the augmentation ratio varies widely. During these tests the augmenter dimensions were not varied to tune the augmenter to the combustor, so these curves do not represent the best augmentation ratio for each combustor L/D. Another possibility suggested by these curves is that the combustor may be tuned to the augmenter by varying the combustor L/D. This approach is, however, somewhat limited by the effect on Tsfc and thrust-to-volume ratio if not by the resonant combustion geometry requirement itself. Additional work has been done which will give further insight into the relation between combustor geometry and augmentation capabilities.

The results of a program of augmenter tuning for an HH(5.25")-5 90° combustor are shown in Figures 55 and 56. Figure 55 is a plot that shows the effects of exhaust augmenter throat diameter and augmenter length-to-diameter ratio on total Pulse Reactor thrust. Inlet augmenter configuration was not changed during the test. The results show that the augmenter with a throat diameter of 9.625" gives the best performance of the four that were tested. Furthermore, it shows that there is little difference in the over-all engine performance when the L/D of the tailpipe augmenter is varied from 1.0 to 2.0. An augmenter of 9.25" diameter was also tested but not plotted, since in the region of augmenter lengths of interest, its performance was very similar to that of the 11.5" diameter augmenter. Figure 56 shows the effect of both tailpipe thrust augmenter throat diameter and augmenter L/D on over-all engine performance in terms of corrected thrust-specific fuel consumption, Tsfc, for a single fuel flow rate. Here again the tailpipe thrust augmenter of 9.625" throat diameter was the best of the four sizes tested. Low Tsfc is achieved at augmenter L/D's between about 0.7 and 2.0 with relatively small cyclic variations with varying L/D ratio. Figure 57 is a plot of thrust versus fuel flow rate for one of the best combinations with dimensions as indicated on the figure. These excellent results were obtained on the orthogonal test stand, wherein the inlet and tailpipe ends of the Pulse Reactor were widely separated so that there was no problem of wave effects or interference involved.

4.0 MULTIPLE ENGINE OPERATION

4.1 Dual HH(5.25")-5-2 Pulse Reactor Tests

A preliminary test was made to determine the effect of combustor proximity on the operating performance of HH(5.25")-5-2 unaugmented combustors. Two HH(5.25")-5-2 engines were mounted in an engine package similar to the mounting method to be used with the trailer rig tests. The test consisted of placing the two combustors (inlet to tailpipe of adjacent combustor) 14 inches apart on centerlines as shown in Figure 62. Each engine was run alone and data was recorded for fuel flow rate, combustion chamber average pressure and thrust. The engines were then run simultaneously as a unit and the total thrust and fuel flow rate were recorded. The chamber pressure of each engine was again recorded. From the test data, two curves of thrust vs. fuel consumption were plotted as shown in previously referenced Figure 63. The dashed line is the sum of the individual thrusts of each engine; whereas, the solid line is the measured combined thrusts of the two engines running simultaneously. Close agreement between these two thrust curves shows that there is no appreciable loss of thrust due to combustor proximity for this particular mounting configuration.

Since the U-shaped combustors run essentially as well in a dual combustor arrangement as they do separately, it may then be assumed that any reduction in performance as compared with the orthogonal arrangement is primarily due to the proximity of the inlet and tailpipe outlets of the same engine, as well as the lesser effect of the extent of turning (180° or more as compared to 90°), rather than interference between adjacent combustors.

4.2 Multiple Miniature Engines

The investigation of multiple miniature pulse reactors in a companion program is described in the preceding section 1.3.2. Information from that program about the operation of multiple miniature engines has been fed into the program for full-sized engines. In general there is sufficient evidence to indicate that multiple engines can be operated in close proximity without a performance penalty if the engines are arranged in a straight line or row.

5. PULSE REACTOR SUBSYSTEMS

Supporting developments which are necessary for the success of the Pulse Reactor program are the developments concerned with the engine accessory elements. Of particular importance is the Pulse Reactor Control system which comprises an automatic starting sequence, a flame-up limiter, a re-start sequence, and a shut-down sequence. Monitoring the combustion chamber average pressure provides an excellent means of checking combustor performance and also provides a good method of handling automatic engine start control. For example, in the automatic engine start sequence, the fuel, ignition and starting air are turned on simultaneously (Figs. 65 and 66). If resonant combustion with accompanying pressure rise does not occur, the lack of a positive signal from a fast-acting pressure switch causes the fuel and ignition to be shut off. The starting air is also shut off following a brief time lag which purges the combustor of unburned fuel. After a pre-set time delay the start sequence may be automatically repeated.

Another feature of the automatic control system that is under development is a system designed to prevent flame-ups following engine shut-down. These flame-ups are caused by stored heat from the engine shell which vaporizes fuel in the fuel nozzles and lines near the nozzles. This causes fuel vapor to enter the combustion chamber where it may be ignited by the still hot combustion chamber walls. The problem is alleviated in the shut-off procedure as follows: a three-way valve is used so that when the fuel flow is shut off, air is introduced into the last foot or so of the fuel line in order to purge the line of fuel. When this is done in the proper sequence, and with the correct air pressure, a smooth shut-down sequence is achieved. The major problem at the present time is in procuring reasonably compact, leak-proof, three-way valves of the proper size and speed of operation.

As previously noted in section 2.5, the combustion chamber average pressure is an excellent indicator as to engine internal operation and performance, and it differentiates between (a) proper resonant combus-

tion which occurs with an average positive combustion chamber pressure, and (b) a "blow-torching" type of combustion that sometimes occurs with ramjet and turbojet engines, in which case the combustion (as is typical of steady-flow combustion processes) is accompanied by a pressure drop in the combustion chamber. The use of average engine combustion chamber pressure to monitor pulse reactor engine internal performance is far superior to the use of engine temperatures because of the way in which it differentiates between these two kinds of combustion. The time delay feature is not used in the restart cycle portion of the sequence. As currently set up, if there is a blow-out during combustor operation, the engine automatically recycles by turning on starting air and spark. This recycle time may be extremely brief (as brief as a few milliseconds) and, in fact, it may not be audible to observers. The use of a flashing light to indicate a restart cycle has been used to observe restarts during operation. The control box that was used to demonstrate operation is shown in use in Figure 67 on the engine static thrust stand for operation of the heavy duty L-605 combustor that is shown in Figure 99. For the purpose of testing the automatic restart control, a blow-out condition was simulated by rapid "off-and-on" action of the fuel flow solenoid valve. Following this, a more realistic technique was used to simulate a sudden "engine-out" condition. The resonant engine operating cycle was interrupted by sudden brief blockage of the air inlet. In this case the fuel flow rate to the combustor remained essentially unchanged, causing a tendency to flood the engine, but the sudden brief blast of starting air gave consistent automatic re-starts.

6. FORWARD FLIGHT PERFORMANCE OF PULSE REACTOR LIFT ENGINES

The forward flight performance program for the Pulse Reactor engines consisted of three phases: (a) connected-pipe tests; (b) the trailer test rig program; and (c) preparation for a wind tunnel program. For these phases, Pulse Reactors in the medium size range, as typified by the 5-1/4" diameter type HH(5.25")-5 and -6, were used. Considerations of optimum thrust-to-volume ratio placed the upper restriction on Pulse Reactor size, while fuel injection system miniaturization and performance problems placed the lower limit. The 5-1/4" size engine was a compromise which provides an improved thrust-to-volume ratio from size reduction, but which was large enough to avoid the fuel system problems associated with miniature engines.

6.1 Connected-Pipe Tests

Initial tests of the Pulse Reactor forward flight characteristics were conducted using the fixed Hiller air supply system consisting of five Allison aircraft superchargers connected in parallel and driven by Ford industrial engines. A pair of 4" diameter HS-1B(0.19) Pulse Reactors (Fig. 68) was selected as being the largest the air supply equipment could handle. Shrouds and nozzles for this test rig were designed and constructed to provide axial flow (Figs. 69 and 70) and cross flow to the paired Pulse Reactors. Static check-out tests of the 4" diameter combustors revealed performance so marginal that a series of modifications was made in an effort to improve primarily the strength of resonant combustion and the throttling range, and secondarily, the maximum thrust and thrust-specific fuel consumption. These modifications were only partially successful and it appeared that the 4" diameter combustor was affected by the miniaturization problem of maintaining effective and efficient fuel injection. Distortion and deterioration of the mitered U-turn section also contributed to the performance problem.

Rather than retard the other aspects of the Pulse Reactor Program to undergo an extensive investigation of these problems at that

time, on this size engine, the connected-pipe tests were temporarily set aside, but some valuable information was gained from these tests when the air flow rate through a single engine operating within the shroud, was measured. The air supply was only adequate to provide a simulation of static operation of a single engine. The results agreed fairly well with similar data for very small engines and revealed that the Pulse Reactor provided about six pounds of thrust per pound of air-flow per second. However, it is expected that properly operating Pulse Reactor engines will provide as much as 12 pounds of thrust per pound of air-flow. This is based on the fact that the 4-inch diameter combustors were only operating at about one-half of normal combustion chamber pressure. Subsequent performance development of the 5-1/4" diameter combustor, which resulted in the HH(5.25)-5,-6 and -7 shell geometries and improved fuel nozzles, has now made it possible to build 4" and smaller diameter combustors so that it will be practicable in the future to use the connected-pipe test technique.

6.2 Trailer Test Rig Program

An important aim of the current Pulse Reactor test program was to determine the effect of the performance of the lift engine as it moves from the hovering condition through speeds sufficient to achieve transition to wing lift. An effective and relatively inexpensive method was conceived for investigating the hovering and low-speed performance range, which consisted of towing a trailer test bed on which the Pulse Reactors are mounted. Figure 71 illustrates the concept of the trailer test rig on which from two to six Pulse Reactors of the 5-1/4" diameter size can be tested. A very important function of the trailer test program was emphasized by NASA engineers who pointed out that the most important transition trends and problem areas for most VTOL lift-propulsion systems have become evident (even though not necessarily maximized) by the time a forward speed of 50 to 60 knots has been attained. The Pulse Reactor trailer test program also provided further opportunity to gain experience in operating the engine test package with its instrumentation. From this experience, the

incidence of delays due to equipment malfunction and personnel errors during the later wind tunnel program should be reduced.

The airflow pattern of the trailer test rig and towing vehicle was checked in a brief preliminary flow visualization test in the Hiller Aircraft water tunnel (Fig. 72). The water tunnel tests indicated that there should be relatively little disturbance on the Pulse Reactors in the pod when attached to the test fixture if a low silhouette towing vehicle is used. In order to expedite the initial tests, however, a pickup truck was used for a tow vehicle. There was some concern about the higher silhouette of this vehicle, but as it turned out, the airflow pattern was marginally satisfactory. For use in future programs, a 1957 Mercedes Benz 300 SL sports coupe was procured after discovery on U. S. Government Excess Property Lists and it was planned to modify this vehicle for higher speed tests. The MB 300 SL would provide a very well stream-lined tow vehicle.

Figure 73 shows details of the trailer rig and its associated equipment, while Figure 74 is a close-up of the force-balance mechanism which is shown schematically in Figure 75. This unit contains three Hagan pneumatic null-balance thrust cells which were used to measure thrust and drag and to calculate the pitching moment. The direct lift and pitching moment loads were taken on two single-acting No. 30 Thrustorq units and the thrust-drag loads taken on a double-acting, No. 12 Thrustorq unit. A Ratio Totalizer was used to automatically take the difference between the two vertical loads in order to give the resultant static lift force.

Parameters, in addition to the Pulse Reactor thrust and pitching moment, which were observed and recorded during each test run included the following:

a. Individual Pulse Reactor combustion chamber average pressure.
b. Static and total pressures of the free air stream at three points ahead of the shroud.
c. Fuel flow rates to each engine.

Figure 76 shows the panel for control, direct monitoring and photograph-

ically recording data.

Considerable study was given to the problem of data recording equipment. A digital type system was finally selected, with system engineering and design by the DYMEC division of the Hewlett-Packard Company in Palo Alto, California. A schematic of the system is shown in Figure 77. This system satisfies all the minimum requirements for the program as well as having the advantages of relatively low cost, fast response, conversion of signal inputs to an engineering unit readout in some cases, adequate accuracy and resolution, expandable to more channels at small cost per additional channel, completely automatic, and provides immediate indication of test results. The transducers consist of thermocouples for temperature measurement and a Scanivalve for pressure measurements. The Scanivalve is a mechanical valve which sequentially exposes the pressure taps or lines to a single pressure transducer at a rate of up to 48 channels per second, thus eliminating the need for a separate and costly transducer on each line. The sequencing of the Scanivalve is automatically synchronized to the scanners of the DYMEC recording system. Until the DYMEC system is completed, basic data indication and recording must be accomplished by recording of fuel flow rates on a Foxboro pen recorder and photographing the gages and instruments mounted in the control console on the pick-up truck as shown in Figure 76.

The trailer test program began with tests of a dual Pulse Reactor package as indicated in Figure 78. Two U-shaped HH(5.25")-5 combustors with augmenters were mounted on the trailer with a vertical thrust axis. The performance of this package as tested on the static thrust stand is shown in Figure 64. The trailer test program was planned to eventually culminate with tests of a Pulse Reactor package of six engines (Fig. 2). The pair of unshrouded engines were tested first in order to determine the effect of cross-flow on engine performance. The trailer test rig is shown in operation in Figure 80 on the Moffett Field runway. The effect of forward speed is revealed in Figure 81. The important improvement in performance at low speeds is

explained in terms of the reduction of recirculation of exhaust gases as the engines translate from the hovering situation (Figure 82).

Following the tests of the pair of engines in the unshrouded condition, the engines were placed in a shroud assembly as shown in Figures 83, 84, 86 and 87. In this situation the inflow air was forced to enter from the top of the package. The performance was further improved as shown in Figure 85. The engines whose performance is reported here were not the same as the engines whose performance is reported in Figure 81. The major differences in the engines were discussed in the preceding section 2.4. As indicated therein, the main reasons for development of the -6 and -7 configurations were to improve the starting, the stability of operation and ease of re-start on the trailer test rig. However, as previously discussed in section 2.4, the total thrust and the Tsfc were improved coincidental to improvement in the other features mentioned.

A feature built into the trailer test rig is that of tilting the engine test package. This feature is illustrated in Figures 86, 88 and 89. Either a nose-up or nose-down angle can be set, up to 15° nose up and 30° nose down, in order to simulate various VTOL approach and transition situations.

6.3 Demonstration of Operation over Dry Hay Field

The results of a very brief check-out test to demonstrate the operation of the Pulse Reactor trailer test rig (at a fuel flow rate of approximately 250 pph) when moving across a dry hay field, are shown in Figures 88 and 89. In order to get the engine within three feet of the ground, the rig was tilted downward at about 30°. Although the basic design of the rig would permit it, time did not permit lowering of the engine package to this level in the horizontal position. However, the lower augmenter centerlines were within about 2-1/2 to 3 feet above the ground and it was noted that there was no indication at all of any tendency to ignite the dry hay. In fact, by using the typical Pulse Reactor wake temperature distribution information in Figure A-35 of Reference 1

(for an HS-1B size engine) and applying it to the scale of the smaller HH5.25-7 engine, it is estimated that the maximum temperature may be as low as about 140°F at 2-1/2 to 3 feet above ground. Although three feet above the ground may be quite adequate, based on various VTOL aircraft design and operational requirements, this indicates that the lift system, i.e., thrust augmenter, outlets may be placed much closer to the ground without danger of igniting dry, dibrous material on exposure to the jet wake or downwash. This illustrates the suitability of the Pulse Reactor for military operation in the field over rough and difficult terrain that might be encountered under realistic operational conditions.

7. PULSE REACTOR DURABILITY AND MATERIALS

The selection of materials and construction techniques for the Pulse Reactor is a problem of compromise between durability requirements and weight penalties. The cyclical pressure loads and temperatures definitely are the factors which affect the fatigue life of the various components. The combustor is the most crucial area and several novel techniques and promising materials were investigated, at least in a preliminary manner. The augmenter problem has been successfully handled with the use of plastics and fiberglas sandwich construction. Reduction in size of the Pulse Reactor has also proven to be helpful in the attack on weight and durability problems.

7.1 Augmenter Materials and Construction

Augmenter wall temperatures typically run in the range of 300°F or less, which opens the possibility of using a wide range of materials. Plastics, fiberglas and honeycomb structures received considerable attention because they satisfy the structural requirements and permit inexpensive construction methods and techniques. High internal damping and reduction of noise and vibration transmission make them even more attractive. As described in reference 1, two inlet thrust augmenters of 8° included angle of divergence, with a throat diameter of 14 inches and length of 40 inches were constructed of fiberglas laminate and a 1/2 inch thickness of fiberglas honeycomb (Fig. 59). Many hours of testing in conjunction with the 9.1" diameter HS-1B have indicated an excellent ability to accept the loading and temperatures involved. A third augmenter of aluminum "Multi-wave" core material was constructed and has been operated for a total of 46 hours with no structural failures. The combination of fiberglas skin and "Multi-wave" core construction yielded an augmenter which weighed 8 lbs, and contributed 96 pounds of thrust, giving a nominal thrust-to-weight ratio of 12, for the augmenter alone.

Figure 60 shows a cluster of augmenters for the HH(5.25")-5 combustor which was constructed from high temperature "Sta-Foam" polyurethane plastic foam (approximate density of 1.5 lb/ft^3) and covered with

fiberglas cloth and epoxy resin 820. The approximate weight for the cluster without the covering was 4.5 lbs. The weight is approximately doubled with a single fiberglas covering when using a "B-stage" mold technique with oven cure, but the weight goes higher when using a "cold layup" technique on initial models. The final weight for the cluster shown is 12.6 lbs, a nominal thrust-to-weight ratio of 13. This unitized geometry possesses, in general, sufficient rigidity and strength such that several units may be placed adjacent to each other to form a larger integral Pulse Reactor lift package.

Testing of the polyurethane-fiberglas augmenters indicated that the natural bond between the inner fiberglas skin and the plastic foam was not strong enough to endure the fluctuating pressure loads in the case of a flat-walled augmenter (e.g., Fig. 61). Failure of the type shown in Figure 61, center photo, occurred in less than four minutes. A possible remedy to this problem is to increase the contact surface area between the high strength inner skin and the foam. By laying up the inner shell first and then bonding to it either chopped glass roving or a thin layer of honeycomb material, the polyurethane may then be foamed into place, greatly increasing the bond surface area. From all indications, however, the augmenters of circular cross section will prove successful in all aspects with the materials and techniques currently at hand.

7.2 Combustor Durability

The combustor durability problem has been approached from several different directions. Combustor shell geometry changes which gave improved performance in terms of thrust-to-volume ratio and thrust specific fuel consumption (Tsfc), have also contributed to a more durable construction. The use of cooling fins and shrouds was partially investigated under the previous development Contract NOa(s)59-6055c (Ref. 1, Appendix A-5). The potential of high temperature alloys has also been investigated. In order to define the durability problem, Figure 93 represents the temperature distribution of the hottest portion

of an uncooled 5-1/4" i.d. combustor constructed of .050" thick 17-7 PH stainless steel. A portion of the tailpipe near the juncture with the combustion chamber operates in the range of 1800°F. This, coupled with the cyclically reversing pressure loads, represents the crux of the durability problem. The major effort, thus far, has been the development of a light-weight shell of material and design which will withstand these temperatures without the added weight and complexity of cooling fins and shrouds.

7.2.1 Cyclic Pressure and Thermal Stress Loads

The first critical area which appeared in the HS-1 type combustor shell was the flat combustion chamber bulkhead to which the inlet tube was welded. The cyclically reversing pressure loads on this flat surface caused frequent failures until this section was replaced with the 45° conical bulkhead as described in section 2.2.2.

In testing combustors which had turn sections constructed of mitered segments, it became apparent that stress concentrations in each segment would cause excessive deformation and resultant loss of performance as well as eventual shell failure. As the combustor cross-section would become egg-shaped, stresses from the reversing pressure and vacuum loads would progressively increase, greatly accelerating shell failure. Sections have also shown a tendency to vibrate when the ovalizing frequency of the section is approximately that of the engine operating frequency. In constructing the light-weight combustor, then, it is imperative to provide a smooth tubular turn and to preserve its circular cross section by providing sufficient circular stiffness.

Several methods have been investigated to preserve the circular cross-section on a light-weight shell without causing undue additional stress concentrations or complicated construction problems. One method is to roll circular beads or corrugations into the combustor shell. Figure 90 shows several tailpipe sections stiffened by rolled-in corrugations. A performance test of the corrugation-stiffened tailpipe (Fig. 91) revealed little effect on combustor internal (thrust) performance. Another method to preserve circular stiffness is to braze

thin rings to the combustor shell at various intervals determined by shell thickness and diameter. This has the advantage of leaving a smooth internal surface. Several 5-1/4" i.d. combustors of the "horse-collar" configuration were built of 0.020" stainless steel, using the brazed ring stiffener technique for light-weight construction. Figure 92 illustrates this construction technique.

The use of flexible shock mounts has greatly reduced the failures which have occurred due to stress concentrations in the area where the mount attaches to the combustor. Thermal expansion, which tends to change the distance between tailpipe and inlet axes, must also be effectively handled with these mounts.

7.2.2 Combustor Attachment and Mounting

7.2.2.1 Attachment with Rubber Mounts

The engine shock mounts using rubber Lord mounts are shown in Figure 102. There has been only one occasion requiring replacement of the rubber Lord-type mount due to deterioration of the rubber. This was required after about 17 hours of engine operating time. Replacement was required because of breakdown of the silicone rubber due to excessive exposure to radiant heating from the hot combustors. The excessive exposure to radiant heating was caused by the fact that only 60% of the engine mount was shielded. A thin aluminum metal shield was then installed to shield the entire engine mount, and to further minimize heat conduction from the engine support to the Lord mount, standoff spacers were used at the four bolt attachment points. It is believed that this action will be adequate to take care of the durability problem concerning flexible rubber engine mounts. However, the use of stainless steel metal fiber engine mounts, currently available commercially, was studied.

A major improvement in the combustor suspension system was next achieved by attaching to the combustor at sections that are relatively cool, and thus stronger than the hotter sections.

Furthermore, the attachment points were then located at sections that are large in cross-section. Whereas formerly there was evidence that most failures in the turn sections were caused by thermal stresses, this source of failure seems to have been reduced by the improved method of suspension. The combustors were then supported by very soft, flexible Lord mounts which permitted relieving of thermal stresses by allowing small changes in combustor alignment. Over 16 hours of running time were logged on a pair of stainless steel combustors prior to structural failures. This has included a large number of starts and stops, which is considered to be the most severe operating condition.

7.2.2.2 Improved Combustor Suspension System

When the lightweight HH-(5.25")-7 combustors were received for initial checkout, the uncoated shell was received first. It failed within a few seconds at the critical section at the juncture of the tailpipe and the combustion chamber as shown in Figure 108. Unsuccessful attempts were made to repair this lapped brazed joint with three techniques. First, the new Aerojet braze gun was tried, but it was designed and pre-set for a lower temperature than required for this application. Second, the technique clled TIG brazing was attempted. This is quite similar to tungsten-inert-gas welding. Instead of using braze materials in a powder form, the braze material was applied in rod form. Finally, repair was attempted with inert gas purging, gas torch, brazing powder and flux. Apparently the initial joint was faulty. In any case attempts to repair the joint were unsuccessful so the section was replaced as indicated in Figure 114, region 2. A section of 0.050" thickness was butt-welded to the adjacent material of 0.017" thickness. As a result of the very rapid initial failure of this lapped brazed joint it was decided to redesign the engine support mechanism so as to permit a greater differential movement between the inlet and tailpipe ends of the combustor. The new suspension system is shown in Figures 103, 104, and 105. It utilizes Hiller-modified Robinson shock mounts that consist essentially of springs whose motions are damped with steel

wool. The new suspension system is credited with an important contribution towards engine durability during the exploratory 50-hour durability test program.

7.2.3 Detail Design

A number of advances in engine durability have been made during the current program. Early structural failures were primarily associated with the combustor and were located generally in two regions: (a) the front bulkhead of the combustion chamber and (b) the narrowest section, which is at the juncture of the combustion chamber and the tailpipe. Failures at the front bulkhead stemmed from the use of a flat section at the juncture of inlet and combustion chamber as shown in Figure 18. This flat bulkhead was supported by the gussets. Failures occurred as cracks along the welded joint formed by the intersection of the flat bulkhead and the cylindrical combustion chamber. A satisfactory solution has been achieved by substituting a 45° conical section for the flat bulkhead and reinforcing gussets. This change has not hurt engine performance in terms of thrust and thrust specific fuel consumption (Section 2.2.2). On the other hand, the substitution of a 45° conical transition section for the much more gradual transition previously used to connect combustion chamber and tailpipe has been the source of a large improvement in engine performance (see Section 2.2.3) as well as an improvement in combustor durability. The improvement in durability may be attributed to the increased stiffness of the 45° conical transition section. However, equal credit for improvement in durability of the entire U-turn section of the combustor should go to the improved methods of combustor suspension.

In order to construct a smooth turn with reasonably circular cross-sections it was decided to make the turns in two pieces "on the half-shell" using a drop-hammer or press technique. The mating halves of the turn shell would then be assembled by butt-welding along two longitudinal seams. This job was performed by the Tyce Engineering Co. of Chula Vista, California. The sections were initially formed as

indicated in Figure 94. The purpose of this nearly complete ring shape was to permit variation of the size of the minimum diameter of the combustor so as to determine the effect on engine performance of this critical section at the juncture of the combustor tailpipe and the combustion chamber.

Eight turn sections of the improved shape were completed of 0.050" thickness. These heavy duty sections were primarily planned for use in the trailer and wind-tunnel test programs. They were made extra heavy so as to reduce the possibility of breakdowns during wind tunnel operation. By using the shape of turn shown in Figure 94 several different combustor configurations can be made as shown in the sketch in Figure 96. The configuration picked for testing was designated HH(5.25")-7 (Figures 97 and 98) and it incorporates the new modifications of inlet taper of 1.5° included angle and a slightly longer combustion chamber (12 inch) than the immediately preceding models. A complete combustor using heavyweight construction of HH(5.25")-7 configuration was fabricated and tested as indicated in Figure 99. It was used to check out the performance (thrust, starting, Tsfc, etc.) of the combustor geometry to be later used on the lightweight combustors for the 50-hour exploratory durability tests.

For the lightweight combustor, turns of 0.017" thickness were fabricated. These turns were reinforced with stiffening rings that were attached to the shell by furnace-brazing as shown in Figure 100. The first completed lightweight combustor is shown in Figure 101. The tailpipe was built about six inches longer than necessary in order to be able to "tun" the combustor by varying the tailpipe length.

7.2.4 Combustor Shell Material

7.2.4.1 Stainless Steel Combustors

Durability and performance of the pulse reactor combustors has been encouraging, even with the 321 and 17-7 PH stainless steel materials. Figure 95 shows the first combustor shell failure which occurred during trailer test runs at Moffett Field, described

under section 6, after 16 hours of operation. Following the speed test runs the engine was restarted again statically and further enlargement of the crack was observed during the static run. The crack showed up initially as a small, longitudinal crack about three inches long. When the engine was restarted statically, it was allowed to run for approximately 3 to 4 minutes in order to observe its performance. During this time the small crack opened up as shown in the photograph. It is important to note that even in this condition the engine would still restart and operate. Thrust performance deteriorated to about three-fourths normal for a flow rate of about 80% maximum. The crack was re-welded and trailer test runs were continued in the same afternoon.

7.2.4.2 Lightweight Combustor Materials and Weights

Design for a 50-hour minimum life expectancy must consider cyclic stresses at elevated temperatures, a total of about 20 million cycles, in addition to oxidation resistance. This requires a material with excellent fatigue strength as well as creep-rupture strength. Data on strength properties of materials in the 1600 to 1900°F range is still rather scarce, but based on the information available, Haynes 25 alloy (L605) was selected for the initial durability tests. Advantage is being taken of the most extensive and successful past program of combustor durability concerned with resonant combustion, which resulted in over 120 hours of continual operation of a valved pulsejet engine on a whirlstand (References 8, 9 and 10). The results of this program indicate that Haynes 25 alloy will probably be the most satisfactory material for the uncooled Pulse-Reactor combustor. Heat treating after welding is not recommended beyond that which occurs naturally as a result of engine operation. The first lightweight combustor (Fig. 102) was fabricated using a brazing compound that met the specifications of AMS 4775 (like Coast No. 62) but G. E. No. 81 (like Coast No. 60) was used for the second combustor. The furnace brazing was processed in accordance with Specification No. AMS 2675 in both cases. The re-melt temperature of the second brazing compound is approximately 100°F higher than that used for the first

combustor. This may have been the margin between success and failure of the critical joint at the juncture of the tailpipe and the combustion chamber. This critical joint did not fail on the second combustor. However, there was another important difference between the first and second combustors. The second combustor (Fig. 103) was coated with a ceramic coating called Solaramic 6100A. The coating job was performed by the Solar Aircraft Company of San Diego, California.

Weights of the combustor components are listed in the following table:

LIST OF WEIGHTS OF HH(5.25")-7 PULSE REACTOR COMBUSTOR SHELL WITH SOLARAMIC COATING AND COMPONENTS

Combustor and Nozzles		9.50 pounds
Fuel Manifold and Nozzles	.187	
Starting Air Nozzle		.275
Older Engine Mounts (Lord) and Aluminum Attachments		.97
New Engine Mount - Robinson Mount Modified Permitting Differential Expansion (mild steel - no attempt at min. wt. here; estimated weight reduction to 1.0 lb)	2.5	
Hayden Pressure Switch		.25
	Total	11.00

7.3 50 Hour Exploratory Durability Tests

The lightweight HH(5.25")-7 engines are shown in Figure 106 as installed in the shroud on the trailer test rig for the 50-hour exploratory durability tests. Figure 107 is a closeup of the same installation. The test program, including power settings, etc., to which the combustors were submitted is listed in Figure 112. The first failure occurred in what was later determined to be a faulty joint in the uncoated combustor. This situation was previously discussed in the preceding section 7.2.4 and pictured in Figure 108. The type and

position of major repairs are listed in Figures 113 and 114, and all repairs that were required are listed in Figures 115 and 116. The most common and typical type of failure is pictured in Figure 109, which shows a fatigue crack developing beneath one of the ring stiffeners. Most of the fatigue failures were of this type. Because all braze bonding was done at one time in the furnace there was a difference in the amount of filling of braze material beneath the rings, which contributed to the fatigue failures. It is agreed that better braze fillets can be achieved, particularly if the combustor is assembled a section at a time, rather than having all joints furnace-brazed simultaneously. It is of particular interest to note that no failures occurred of the type that is considered most typical of past experience with pulsejet type combustors, to wit, ovalizing of the cross-sections of the shell. The use of stiffening rings completely prevented any failure of that type. However, it appears that the rings were much stiffer than necessary. In a re-design it is proposed to reduce the height of the rings to about one-half and to use only a very small flange (1/16") to stiffen the outer edge of the rings. Figure 110 shows a minor fatigue crack that developed around the spark plug boss on the uncoated combustor. A circumferential fatigue crack at the juncture of the inlet tube and the combustion chamber of the coated combustor is shown in Figure 111.

Although the durability of the ceramic coated combustor was decidedly superior to the uncoated combustor there was one noticeable superiority of the uncoated shell. There was a much greater plastic swelling deformation of the tube between the stiffening rings in the case of the coated combustor. This is thought to be due to the insulating effect of the outer coating of ceramic which apparently causes the metal to operate at a higher temperature than in the case of the uncoated shell. A design recommendation for the next phase is to experiment with a shell which is coated on the inner surface only. Other recommendations for re-design are, to use no stiffening rings on the first 90° of the turn section, and to go to a thickness of approx-

imately 0.030" for that section only. This increase in weight can be more than compensated for by going to sections of only 0.010" for the remainder of the tailpipe, as well as for the inlet section, and by reduction in the size of the stiffening rings. The deterioration of engine performance due to shell deformation was not excessive except for the previously mentioned failure of the uncoated shell. However, replacement of the failed section brought the engine performance back to essentially the same as original.

The performance of the individual combustors prior to the 50-hour exploratory durability tests is given in Figure 121 and performance after the 50-hour tests is given in Figure 122. The performance of the dual combustors (without augmenters) is shown in Figure 123 and the performance of individual engines operating with augmenters is shown in Figure 124. This figure shows the effect a crack in the coated combustor has on engine performance. Figures 125 and 126 permit a comparison of the performance of the dual engine shrouded package in operation on the trailer test rig with the same dual engines operating in the unshrouded condition on the static test stand. A comparison of Figures 125 and 126 reveals that there is not much difference in the performance of the dual engines in operation in the shrouded package on the trailer test rig and in the unducted condition on the static test stand. This is important because it shows that the problem of operation within the shroud is not as great as might have been anticipated. On the other hand Figure 126 reveals that there was a rather poor match between the augmenters and the combustors in that less than 100% of thrust augmentation was achieved. This mismatch was due to the fact that the augmenters were originally sized to the HH(5.25")-5 combustors and there were insufficient funds to develop a new set of augmenters to match the -7 combustors. Figure 125 gives the key dimensions of the shrouded package. The dashed lines on the inside of the package walls above the augmenters represent the presence of fiberglas bats that were inserted in order to determine the effects of such material on wave reflection.

Measurements od downwash characteristics were obtained during the durability runs in terms of total pressure readings and temperature reading (by thermocouple). Readings at the outlets of the augmenters for average temperatures are given in Figure 118 and average pressures in Figure 119. Maximum pressure readings at the same location are given in Figure 120.

8. RECAPITULATION AND CONCLUSIONS

1. The best Pulse Reactor configurations and combinations that were tested under the subject contract are listed in Figure 128 and presented in Figures 129a, 129b, and 129c. In order to help evaluate progress, specific advances accomplished on the current contract are listed as follows:

A. Combustor thrust/volume ratio increased by reducing size (to take advantage of scaling trend) 33%

B. Combustor thrust/volume ratio increased by "breakthrough" in geometry and fuel system 55%

C. Combustor combined thrust/volume ratio improvement 107%

D. Combustor plus augmenters thrust/volume ratio increased 80%

E. Combustor Tsfc (90° configuration) reduced 27%

F. Combustor Tsfc (180° - U-shaped) reduced 29%

G. Combustor plus augmenters Tsfc (90° configuration) reduced 13%

H. Pulse Reactor "unitized" twin combustor arrangement allowing retraction of combustors down into augmenters for in-flight storage.

I. Control system milestones -
   (1) Automatic restart cycle,
   (2) Automatic fuel line purge at shut-down,
   (3) Remote controls for engine throttling, air-start and shut down fuel purging.

J. Forward Speed program -
   (1) Trailer test rig operational,
   (2) Preliminary tests indicate that the shrouded engine package increases thrust about 10% from static to a forward speed of about 63 knots.
   (3) Instrumentation designed and partially procured for multi-engine package.

K. Durability -

A durable, lightweight (12:1 T/W ratio without attachments) sandwich type construction augmenter, has had approximately 44 hours operation with no sign of structural failure.

A pair of lightweight HH-5.25-7 combustors have been taken through an exploratory durability program for more than 51 hours. One combustor was coated with Solaramic 6100 both inside and out, whereas the other was uncoated. Definitely better durability was achieved with the coated combustor. However, it is believed that better performance would be obtained by coating the inside surface only.

Recommendations for the next stage of a durability program include reduction of the combustor skin thickness from 0.017" to 0.010", in all regions except for the first 90° of the turn section aft of the combustion chamber where it is recommended to remove the stiffening rings and increase the skin thickness to 0.024" or 0.030". Furthermore, it is recommended that each alternate stiffening ring be removed from the tailpipe section and that the remaining rings be reduced in stiffness to less than one-half the present value.

2. It is concluded that feasibility has been demonstrated in all critical areas, including starting, rapid control response, throttling range from 25% to full throttle, durability (for lift engine applications), maintenance of thrust level to at least 63 knots forward speed.

3. It has been demonstrated that the system can be readily scaled over a wide range of geometric sizes.

4. Demonstrations have been conducted that indicate that the system has the unique capability of being able to live under practically all rough terrain conditions without either setting the terrain on fire or being damaged by environments such as brush, trash, sand, mud, slush, etc.

5. The Pulse Reactor system continues to be the only one which, because it has no moving parts, gives promise of providing a low-cost lift-propulsion system with simple low-cost field maintenance.

8. REFERENCES

1. Lockwood, R. M., Sargent, E. R., and Beckett, J. E.: "Thrust Augmented Intermittent Jet Lift-Propulsion System - 'Pulse Reactor', Final Report", Contract NOa(s)59-6055c, Hiller Aircraft Corp., Report No. ARD-256, February 1960.

2. Lockwood, R. M.: "Interim Summary Report on Investigation of the Process of Energy Transfer from an Intermittent Jet to a Secondary Fluid in an Ejector-Type Thrust Augmenter", Contract Nonr 3082(00), Hiller Aircraft Corp. Report No. ARD-286, 31 March 1961.

3. Lockwood, R. M., and Patterson, W. G.: "Summary Report on Investigation of Miniature Valveless Pulsejets", Contract DA 44-177-TC-688, Hiller Aircraft Company Report No. ARD-307, July 1962.

4. Lockwood, R. M., Patterson, W. G.: "Interim Summary Report on Investigation of Miniature Interconnected Pulsejet Clusters", Contract DA 44-177-TC-688, Hiller Aircraft Corp. Report No. ARD-293, July 1961.

5. Lockwood, R. M.: "Proposal for Pulse Reactor Instantaneous Pressure and Temperature Measurements to Provide Data for Cycle Analysis", Hiller Aircraft Corp. Report No. ARD-283, July 1960. (Available on request to Hiller Aircraft Company).

6. Henry, John R.: "Design of Power Plant Installations Pressure Loss Characteristics of Duct Components", NACA Wartime Report ARR L4F26 (L-208), June 1944.

7. Lockwood, R. M., and McJones, R. W.: "Combustion Chamber Average Pressure as a Pulsejet Internal Performance Indicator", American Helicopter Division of Fairchild Engine and Airplane Corporation Report No. 1949-B-423, 10 December 1954.

8. Lambert, C. G.: "Review and Evaluation of Past Pulse-Jet Engine Structural Development Programs", American Helicopter Division of Fairchild Engine and Airplane Corporation Report No. 1949-S-401, 1 July, 1954.

9. Lambert, C. G.: "Analysis of Structural Results from Tests of 7.5 Inch Pulse-Jets", American Helicopter Division of Fairchild Engine and Airplane Corporation Report No. 1949-S-403, October 15, 1954.

10. Avant, William W.: "Results of 50-Hour Preliminary Flight Rating Tests of the Model AJ-7.5-1 Rotary Wing Tip-Mounted Pulse-Jet Engine". American Helicopter Co., Inc. Report No. 194-B-2, 3 March 1953.

REFERENCES (CON'T)

11. Layton, J. P.: "Heat Transfer in Oscillating Flow, Final Report on Work Performed 1 July 1953 to 30 September 1954", Princeton University, Department of Aeronautical Engineering, Report No. 266a, 15 May 1956.

12. Lockwood, R. M., and Patterson, W. G.: "Interim Summary Report Covering the Period from 1 April 1961 to 30 June 1962 on Investigation of the Process of Energy Transfer from an Intermittent Flow to Secondary Fluid in an Ejector-type Thrust Augmenter", Hiller Aircraft Corp. Report No. 305, June 30, 1962.

PULSE REACTOR CYCLE DIAGRAM

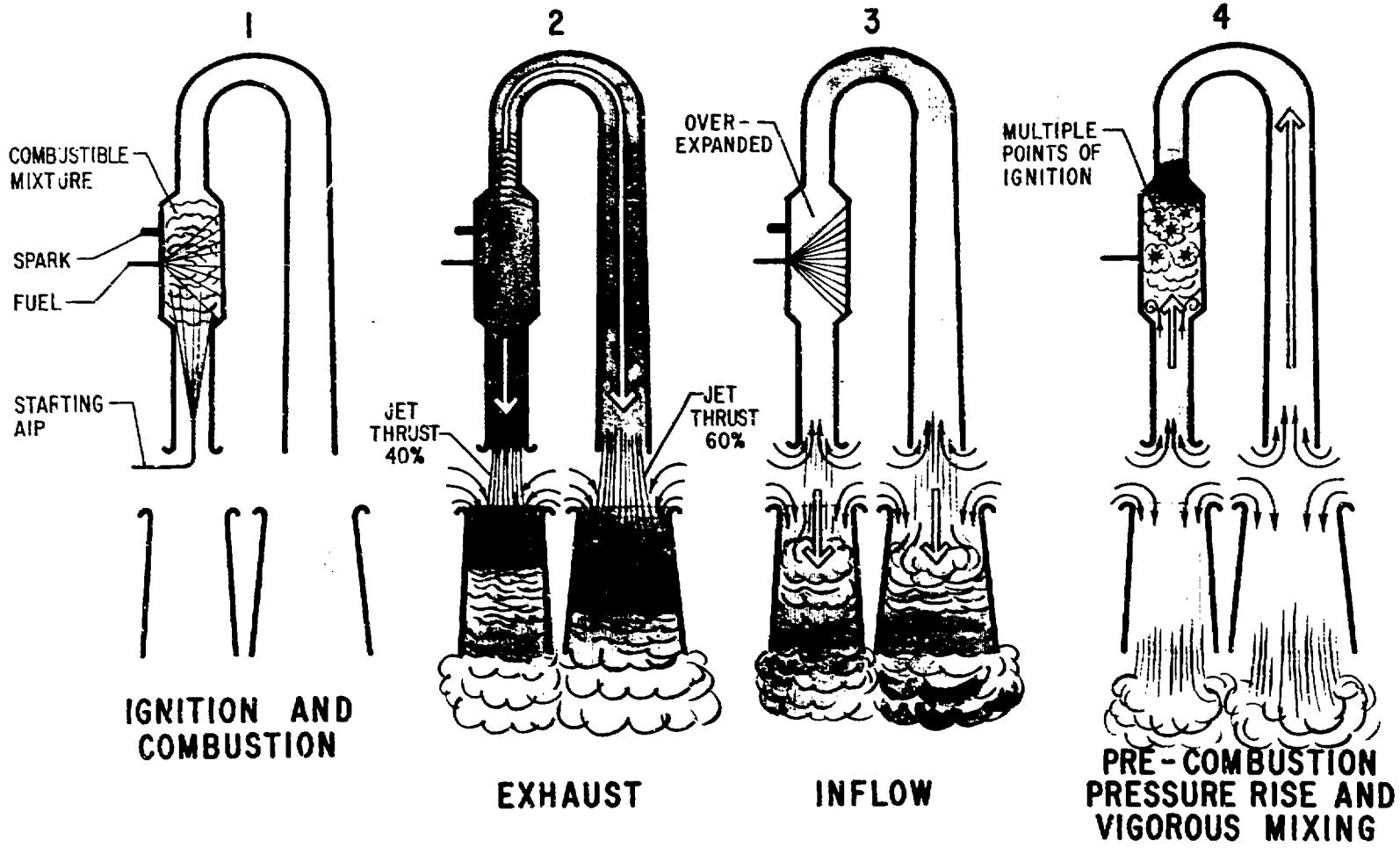


FIGURE 1

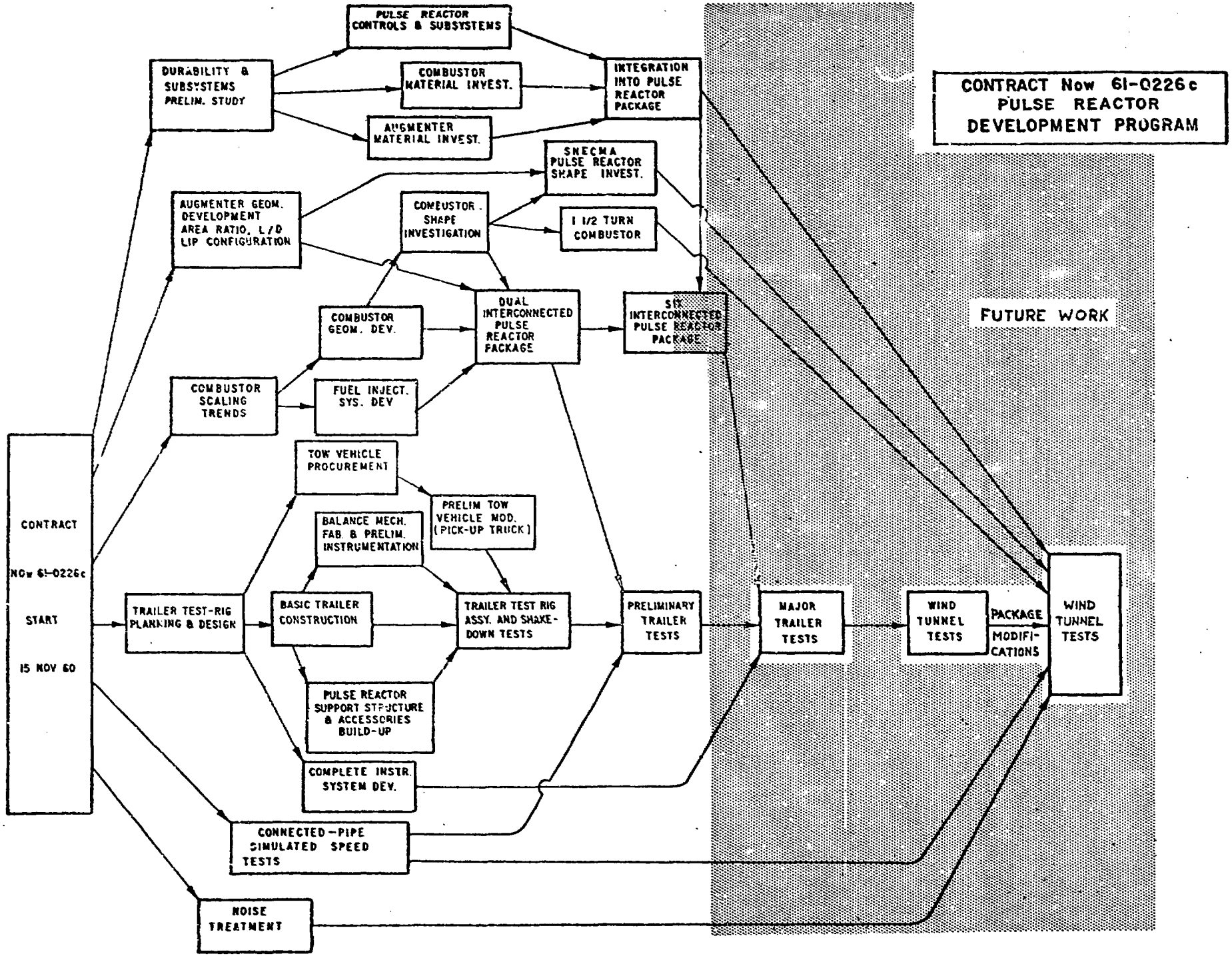

CONTRACT Now 61-0226c
PULSE REACTOR
DEVELOPMENT PROGRAM
FUTURE WORK
PULSE REACTOR CONTROLS & SUBSYSTEMS
DURABILITY & SUBSYSTEMS PRELIM. STUDY
COMBUSTOR MATERIAL INVEST.
AUGMENTER MATERIAL INVEST.
INTEGRATION INTO PULSE REACTOR PACKAGE
SNECMA PULSE REACTOR SHAPE INVEST.
AUGMENTER GEOM. DEVELOPMENT AREA RATIO, L/D LIP CONFIGURATION
COMBUSTOR SHAPE INVESTIGATION
1 1/2 TURN COMBUSTOR
COMBUSTOR GEOM. DEV.
DUAL INTERCONNECTED PULSE REACTOR PACKAGE
SIX INTERCONNECTED PULSE REACTOR PACKAGE
COMBUSTOR SCALING TRENDS
FUEL INJECT. SYS. DEV
TOW VEHICLE PROCUREMENT
PRELIM TOW VEHICLE MOD. (PICK-UP TRUCK)
BALANCE MECH. FAB. & PRELIM. INSTRUMENTATION
CONTRACT
NOw 61-0226c
START
15 NOV 60
TRAILER TEST-RIG PLANNING & DESIGN
BASIC TRAILER CONSTRUCTION
TRAILER TEST RIG ASSY. AND SHAKE-DOWN TESTS
PRELIMINARY TRAILER TESTS
MAJOR TRAILER TESTS
WIND TUNNEL TESTS
PACKAGE MODIFICATIONS
WIND TUNNEL TESTS
PULSE REACTOR SUPPORT STRUCTURE & ACCESSORIES BUILD-UP
COMPLETE INSTR. SYSTEM DEV.
CONNECTED-PIPE SIMULATED SPEED TESTS
NOISE TREATMENT

FIGURE 2

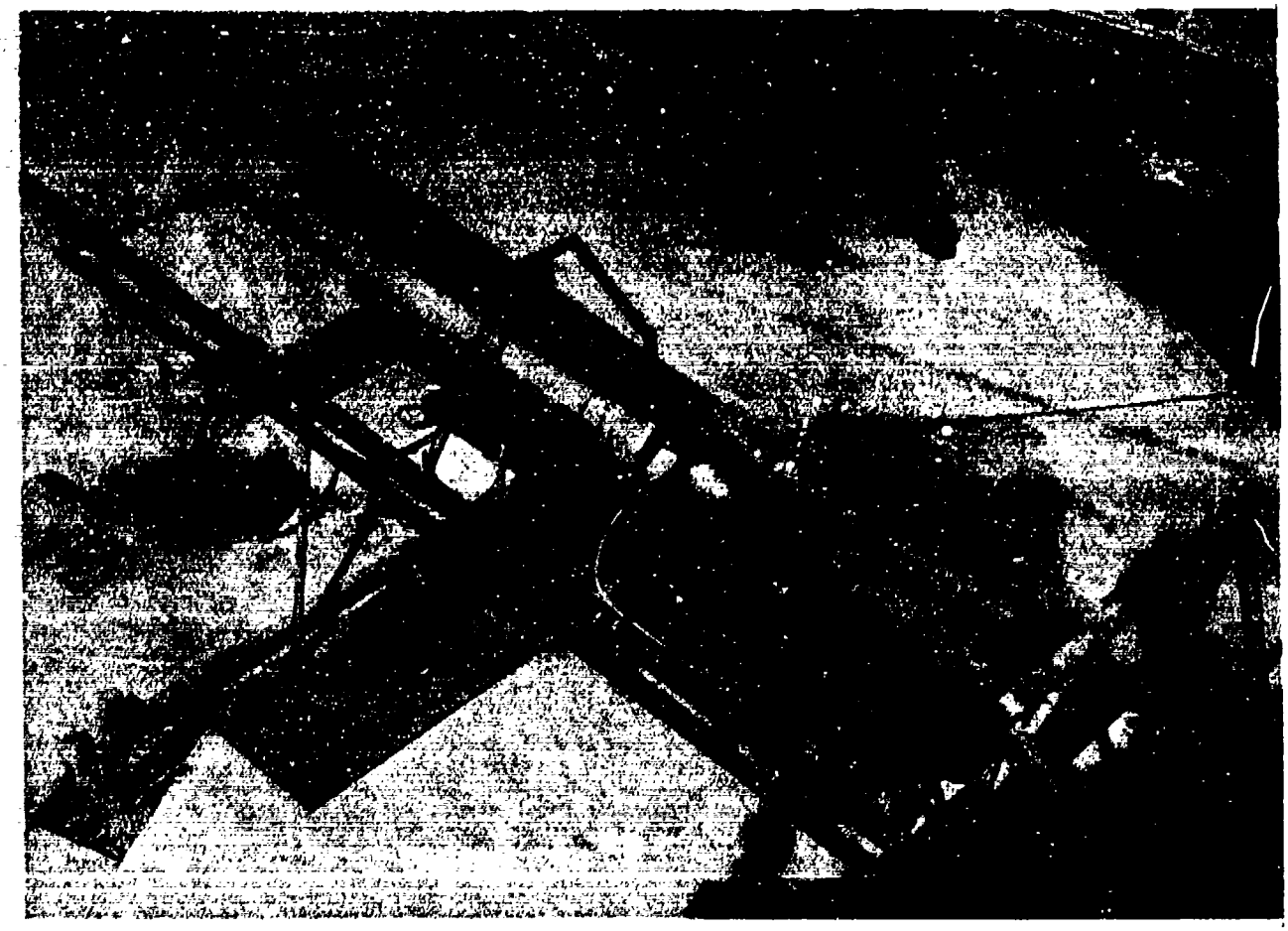


FIGURE 3 HS-1 VALVELESS PULSEJET ENGINE WITH INLET JET "DILUTION DUCT" THRUST AUGMENTER MOUNTED ON SIMPLE THRUST STAND

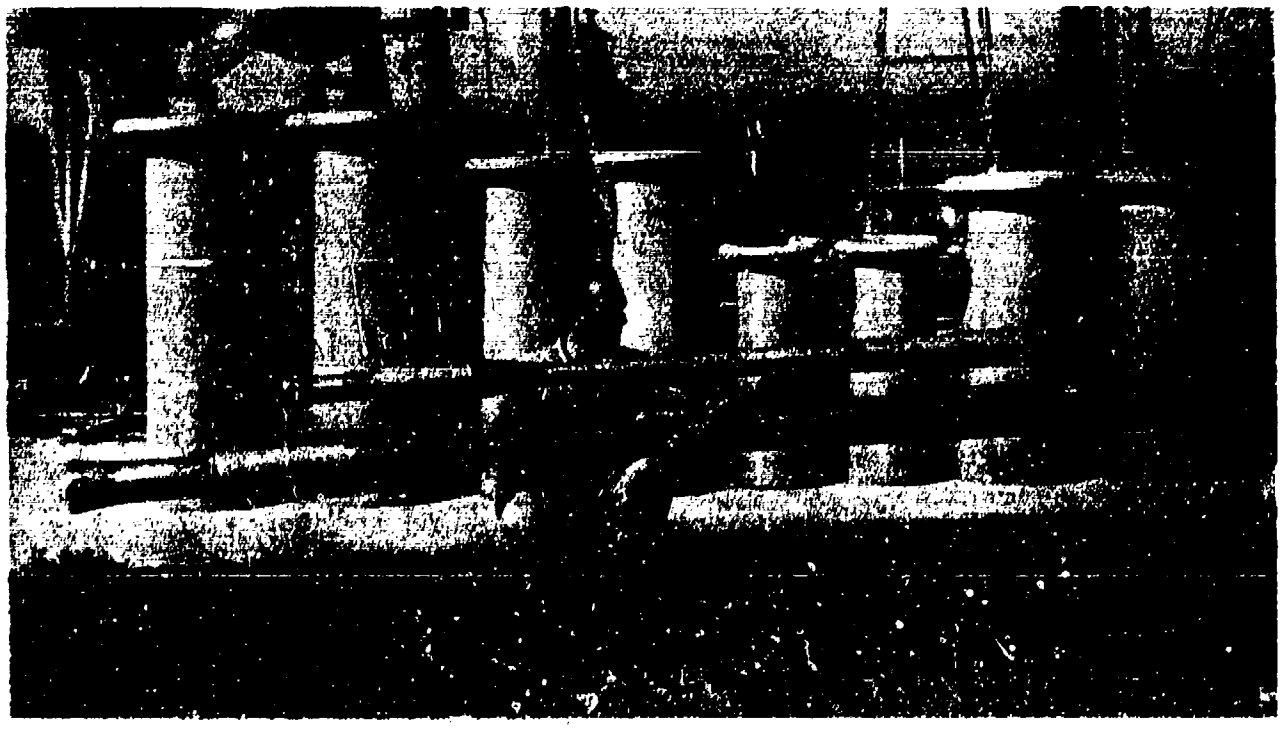


FIGURE 4 COMPONENTS FOR TWO STRAIGHT PULSE REACTORS OF 4.75" i.d. AND 7.5" i.d. COMBUSTION CHAMBER DIAMETER (HS-1 TYPE GEOMETRY)

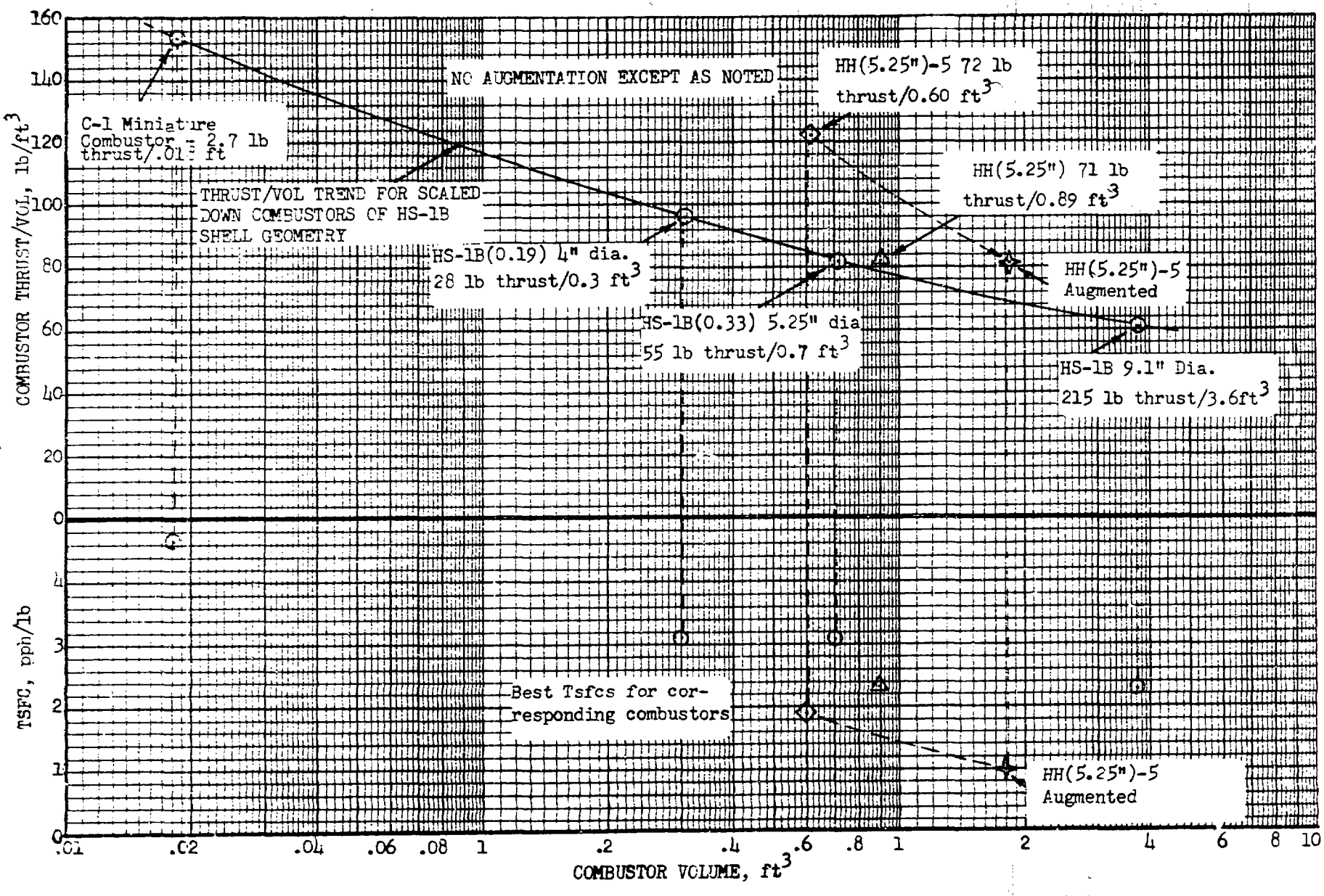


FIGURE 5: TREND OF THRUST/VOL AND TSFC VS VOLUME FOR PULSE REACTOR COMBUSTORS

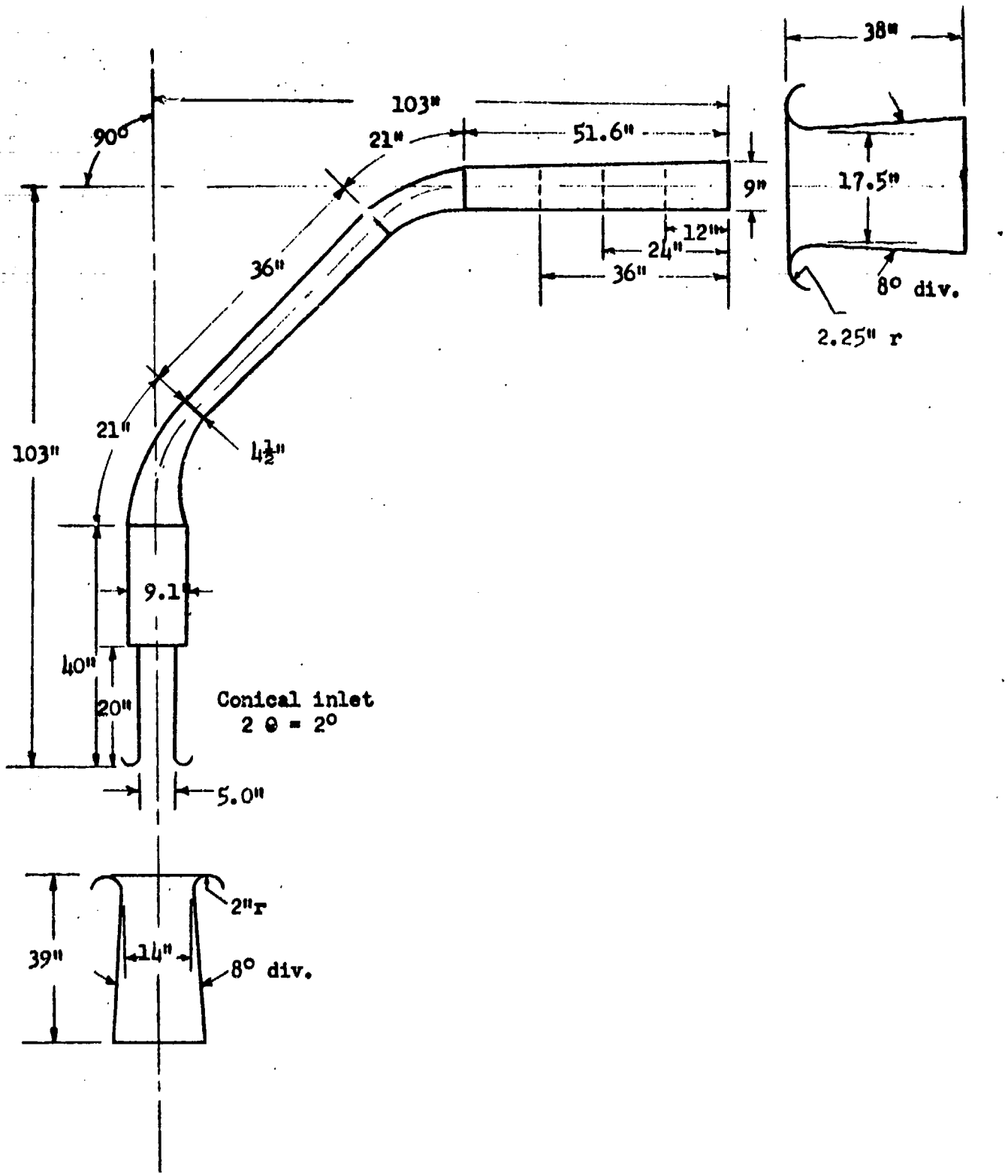


FIGURE 6: GEOMETRY OF HS-1B PULSE REACTOR

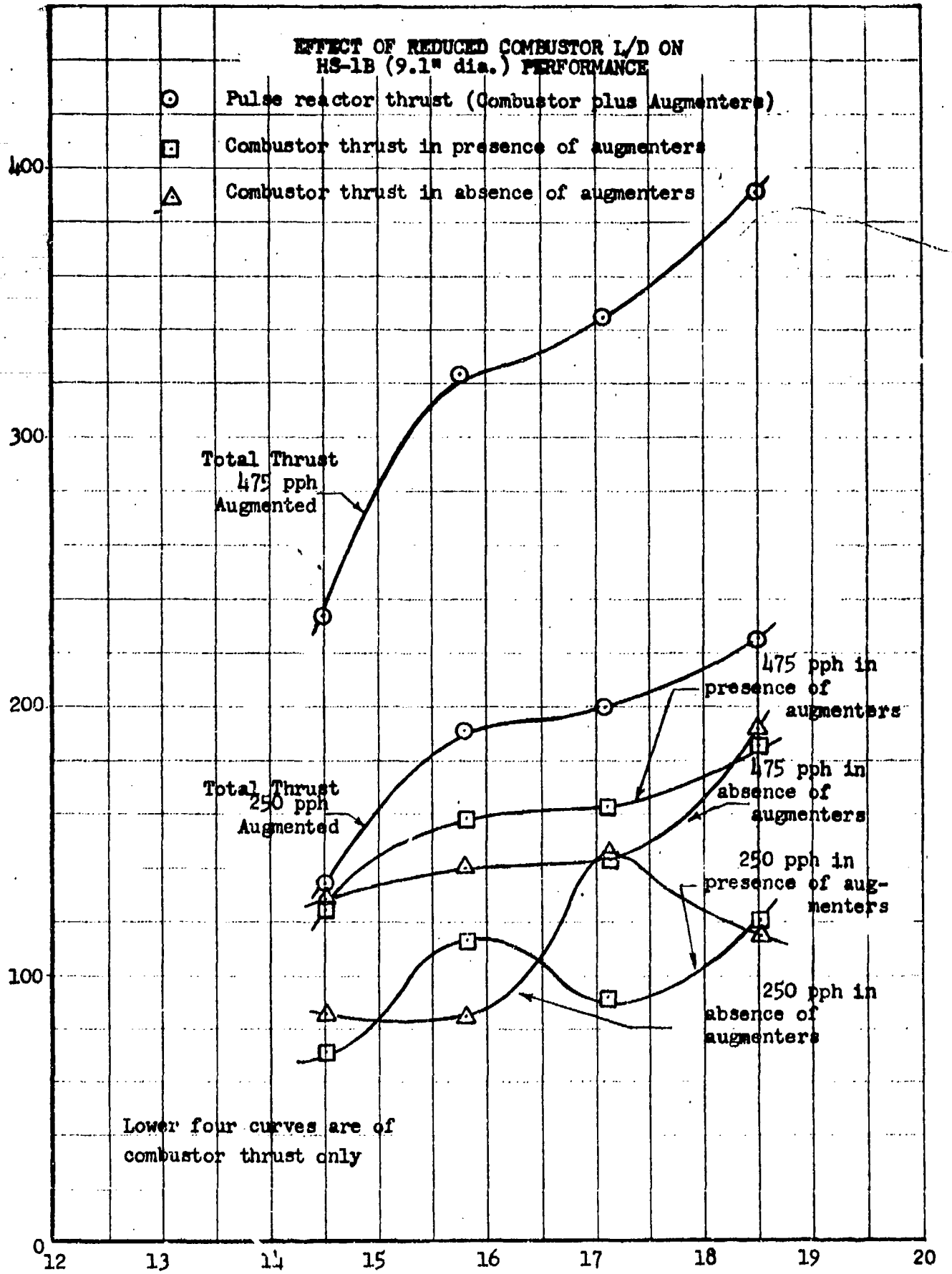

EFFECT OF REDUCED COMBUSTOR L/D ON
HS-1B (9.1" dia.) PERFORMANCE
Pulse reactor thrust (Combustor plus Augmenters)
Combustor thrust in presence of augmenters
Combustor thrust in absence of augmenters
THRUST, lbs.
400
300
200
100
0
Total Thrust
475 pph
Augmented
Total Thrust
250 pph
Augmented
475 pph in
presence of
augmenters
475 pph in
absence of
augmenters
250 pph in
presence of aug-
menters
250 pph in
absence of
augmenters
Lower four curves are of
combustor thrust only
12
13
14
15
16
17
18
19
20
COMBUSTOR LENGTH TO DIAMETER RATIO, L/D

FIGURE 7

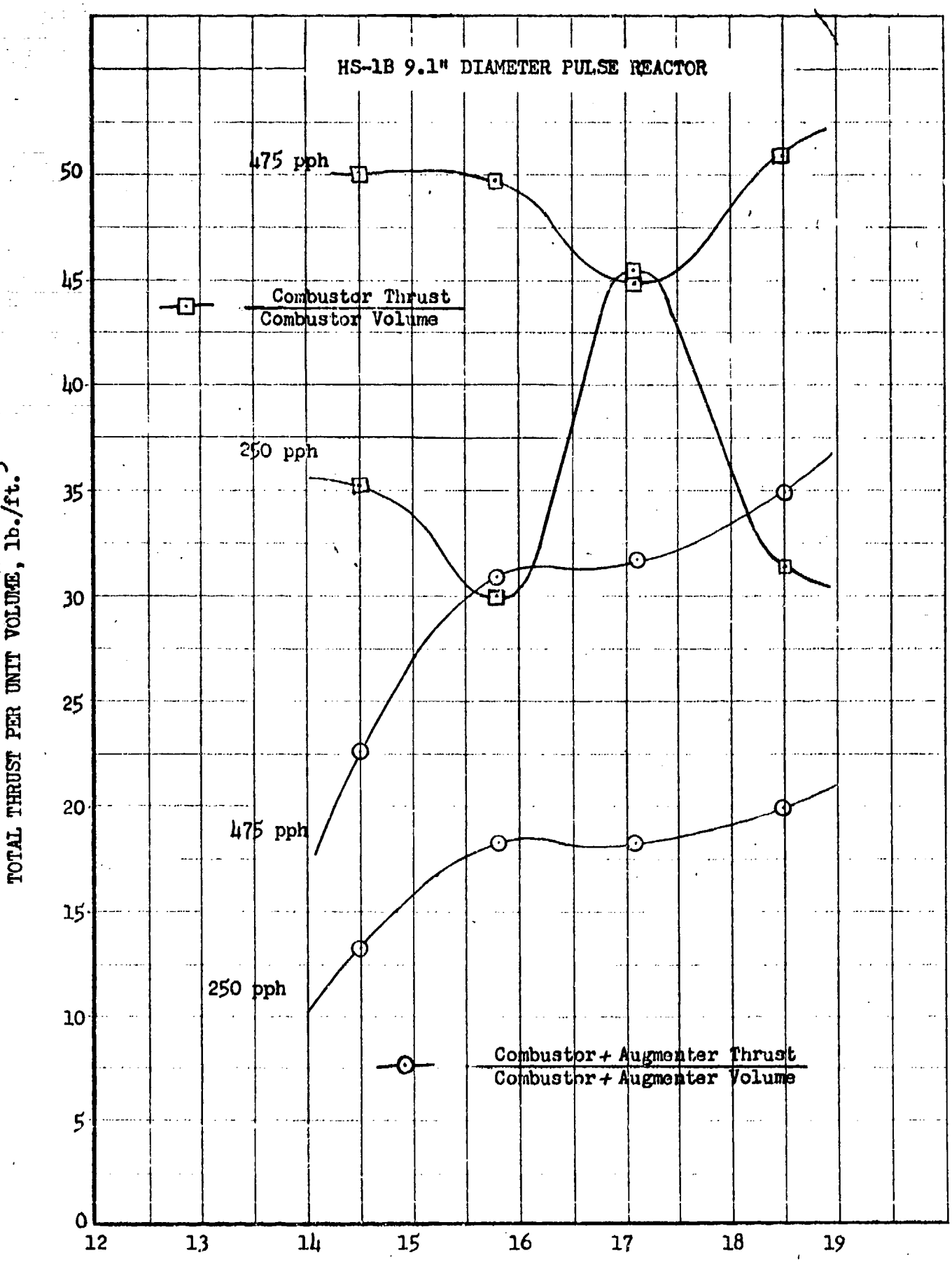

HS-1B 9.1" DIAMETER PULSE REACTOR
475 pph
250 pph
475 pph
250 pph
Combustor Thrust / Combustor Volume
Combustor + Augmenter Thrust / Combustor + Augmenter Volume
TOTAL THRUST PER UNIT VOLUME, lb./ft.3
0
5
10
15
20
25
30
35
40
45
50
12
13
14
15
16
17
18
19
ENGINE LENGTH TO DIAMETER RATIO, L/D

FIGURE 8

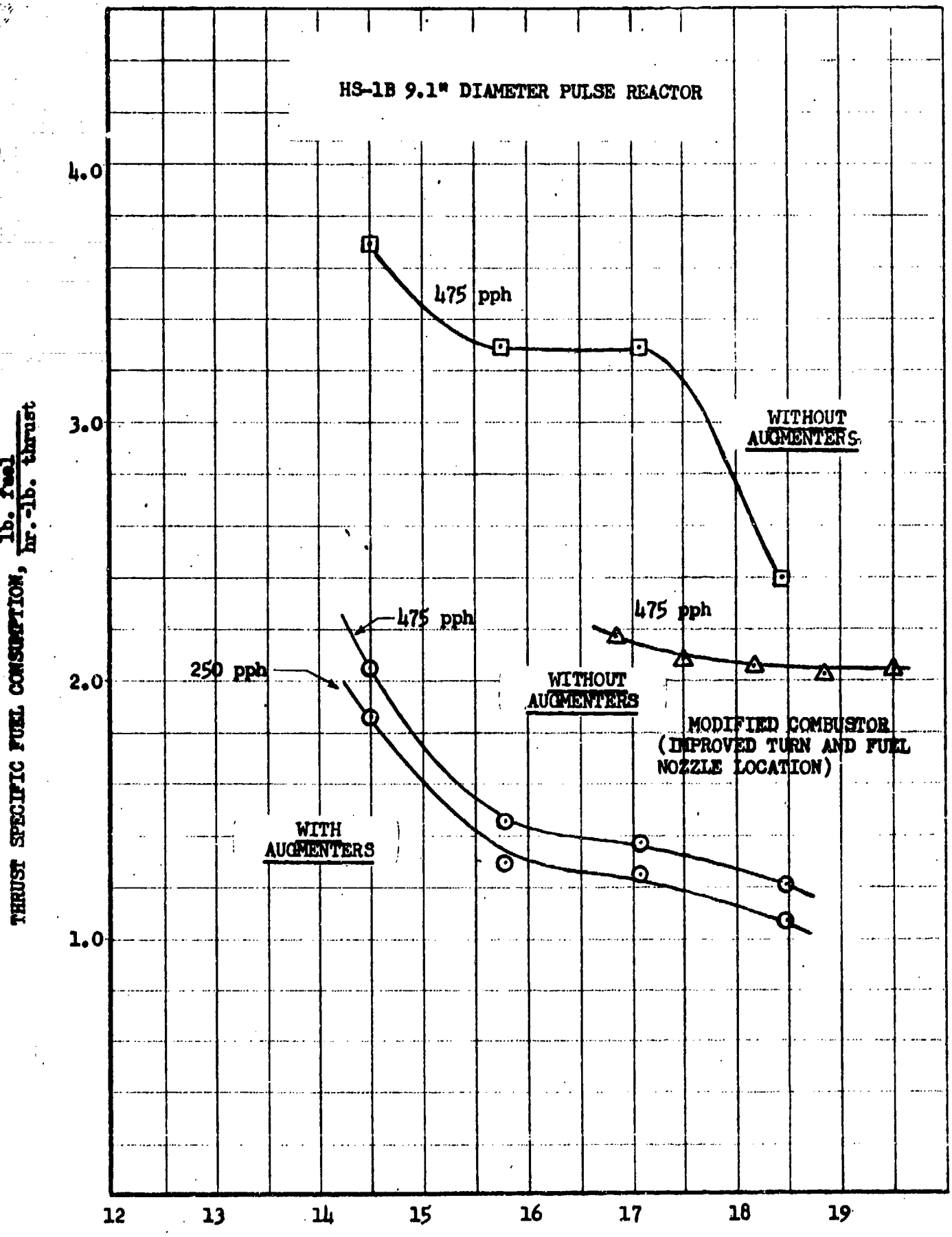

HS-1B 9.1" DIAMETER PULSE REACTOR
THRUST SPECIFIC FUEL CONSUMPTION, lb. fuel / hr.-lb. thrust
4.0
3.0
2.0
1.0
475 pph
WITHOUT AUGMENTERS
475 pph
250 pph
WITHOUT AUGMENTERS
475 pph
MODIFIED COMBUSTOR (IMPROVED TURN AND FUEL NOZZLE LOCATION)
WITH AUGMENTERS
12
13
14
15
16
17
18
19
ENGINE LENGTH TO DIAMETER RATIO. L/D

FIGURE 9

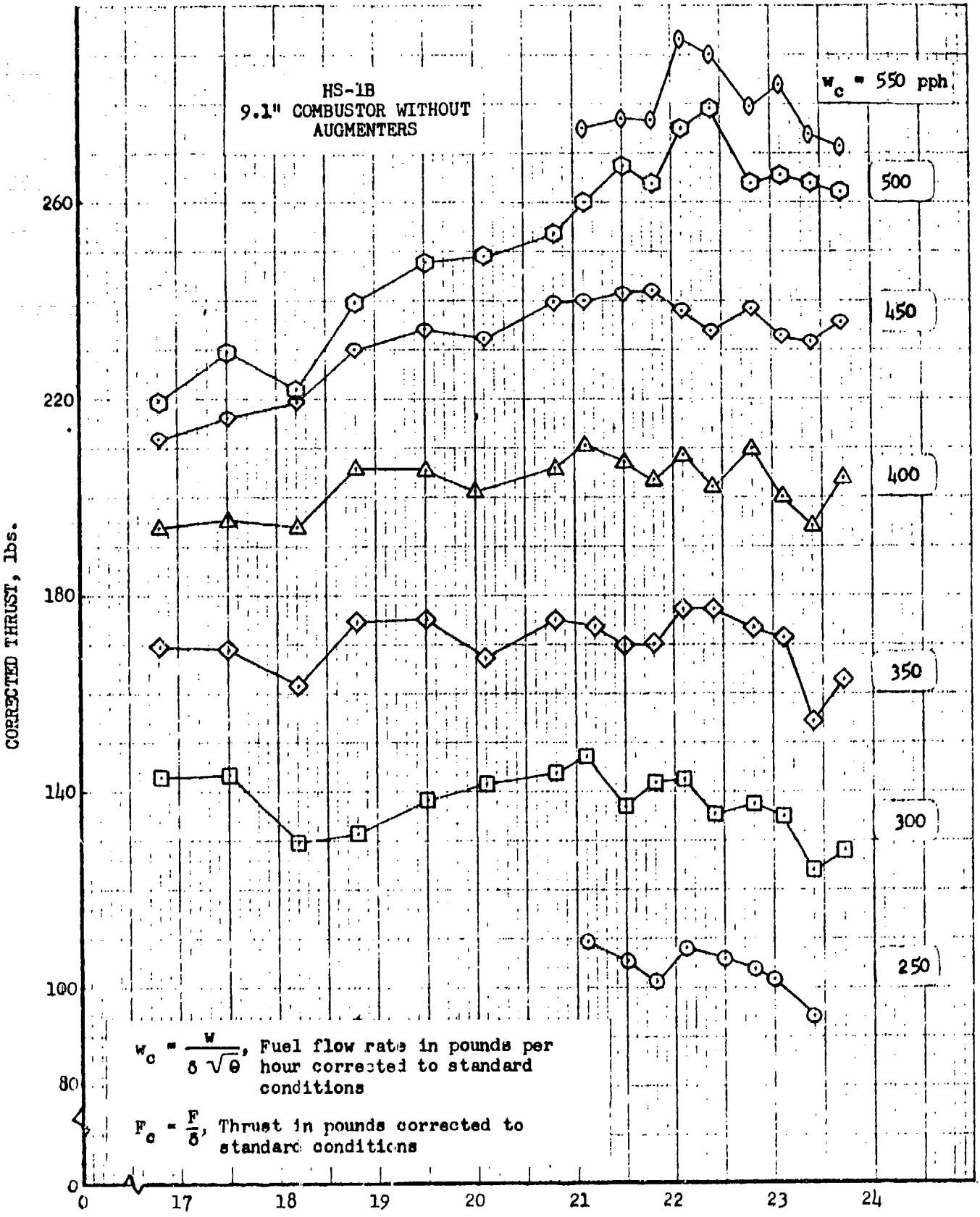

HS-1B
9.1" COMBUSTOR WITHOUT
AUGMENTERS
w_c = 550 pph
500
450
400
350
300
250
CORRECTED THRUST, lbs.
260
220
180
140
100
80
0
0
17
18
19
20
21
22
23
24
$w_c = \frac{w}{\delta\sqrt{\theta}}$, Fuel flow rate in pounds per hour corrected to standard conditions
$F_c = \frac{F}{\delta}$, Thrust in pounds corrected to standard conditions
L/D = TOTAL COMBUSTOR LENGTH / COMBUSTION CHAMBER DIAMETER

FIGURE 10

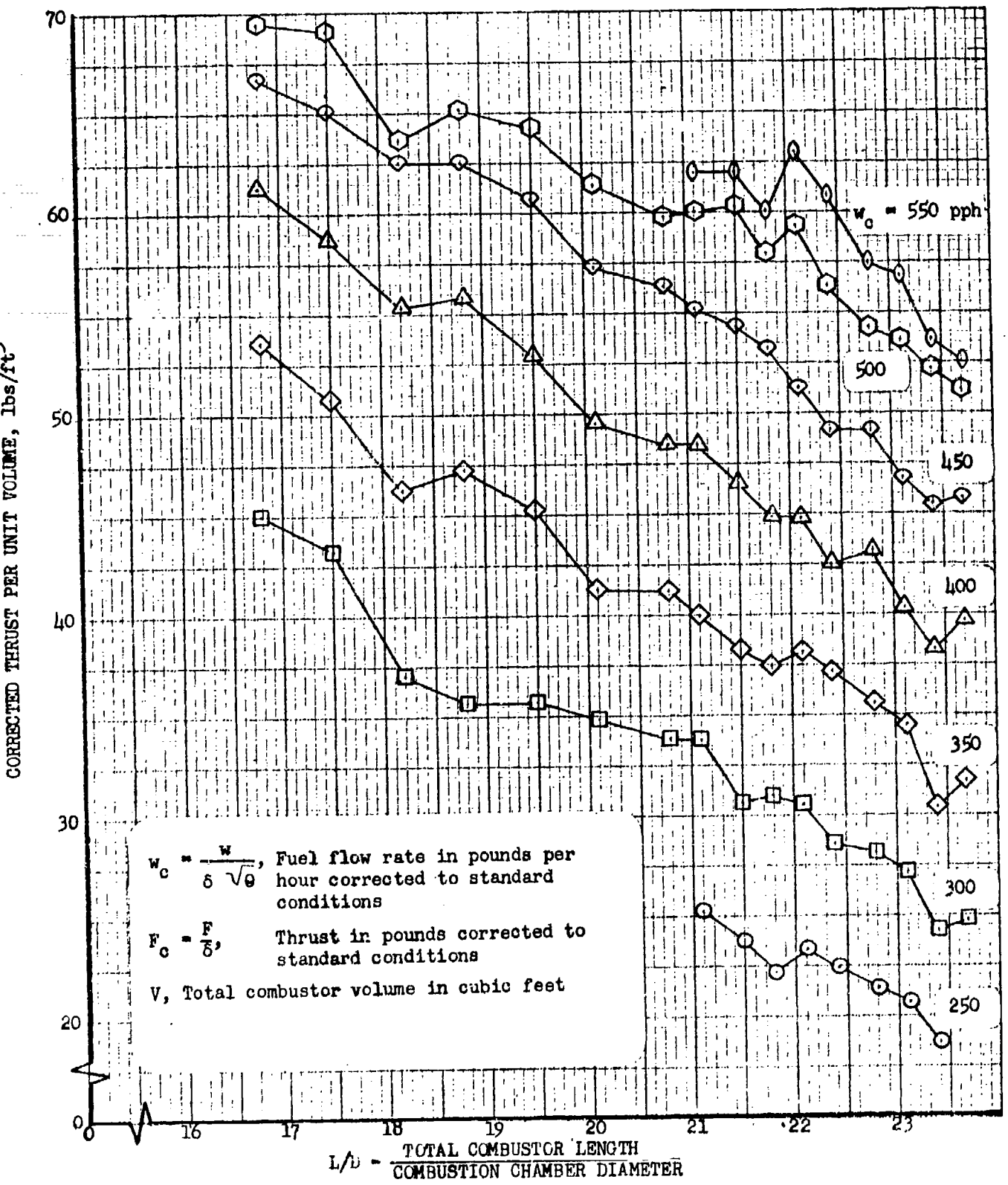


FIGURE 11: HS-1B(9.1") DIAMETER COMBUSTOR WITHOUT AUGMENTERS

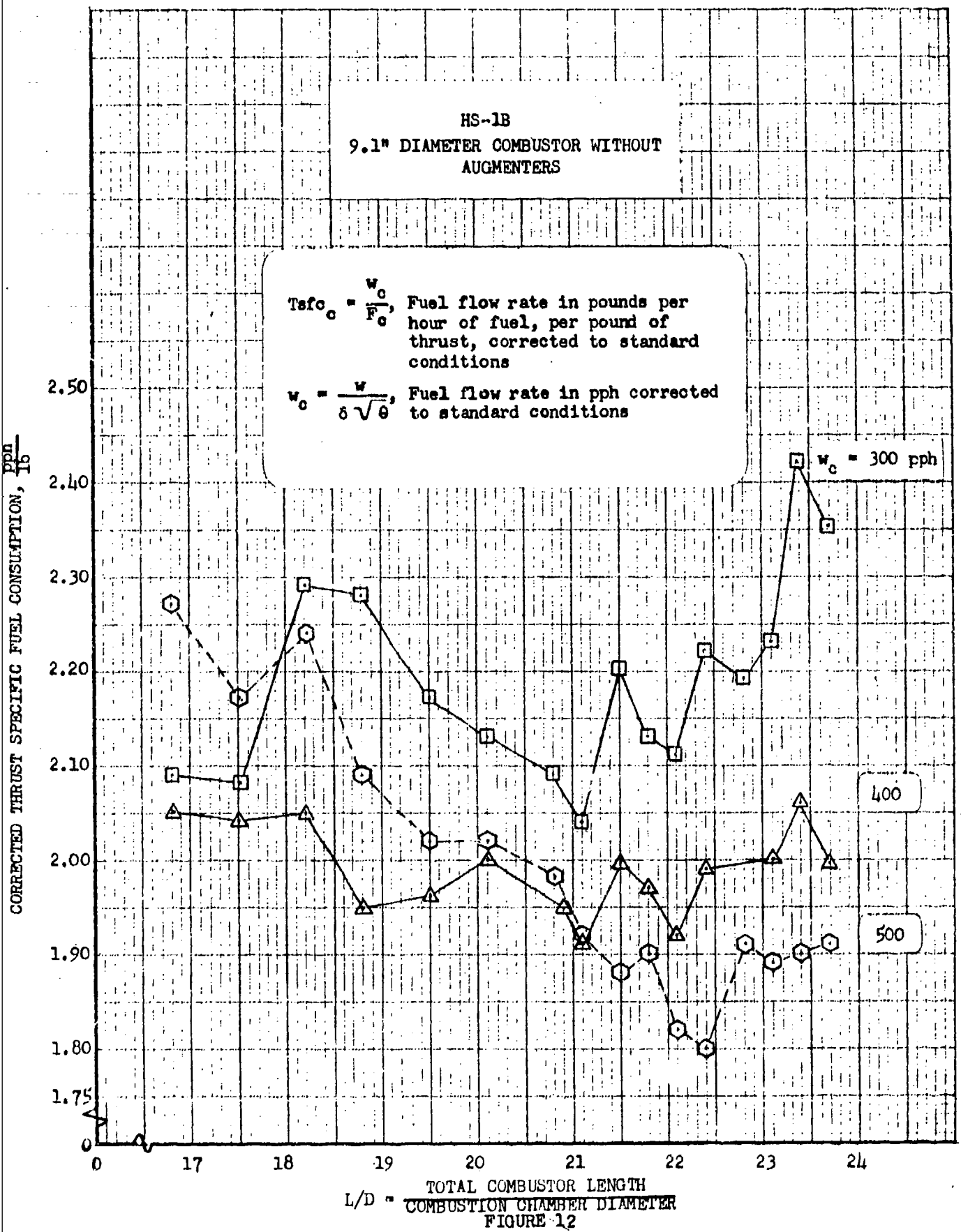

HS-1B
9.1" DIAMETER COMBUSTOR WITHOUT AUGMENTERS
$Tsfc_c = \frac{w_c}{F_c}$, Fuel flow rate in pounds per hour of fuel, per pound of thrust, corrected to standard conditions
$w_c = \frac{w}{\delta\sqrt{\theta}}$, Fuel flow rate in pph corrected to standard conditions
w_c = 300 pph
400
500
CORRECTED THRUST SPECIFIC FUEL CONSUMPTION, $\frac{ppm}{lb}$
2.50
2.40
2.30
2.20
2.10
2.00
1.90
1.80
1.75
0
0
17
18
19
20
21
22
23
24
L/D = TOTAL COMBUSTOR LENGTH / COMBUSTION CHAMBER DIAMETER

FIGURE 12

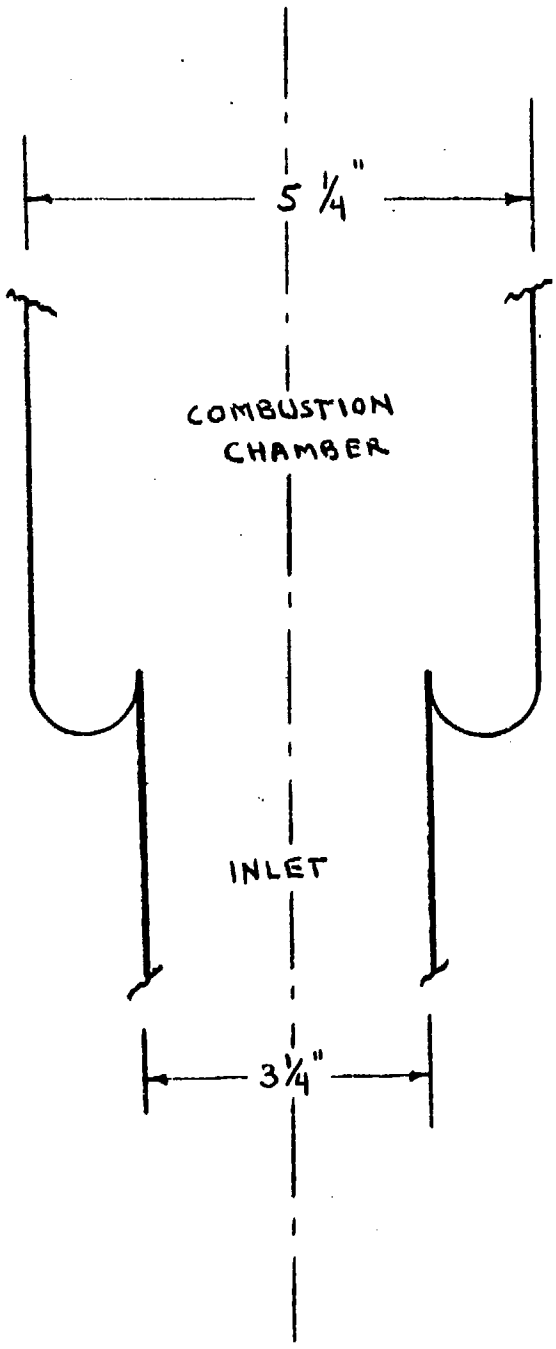


FIGURE 13: LONGITUDINAL SECTION SHOWING "HALF DOUGHNUT" COMBUSTION CHAMBER BULKHEAD FOR HS-1B (0.33) COMBUSTOR

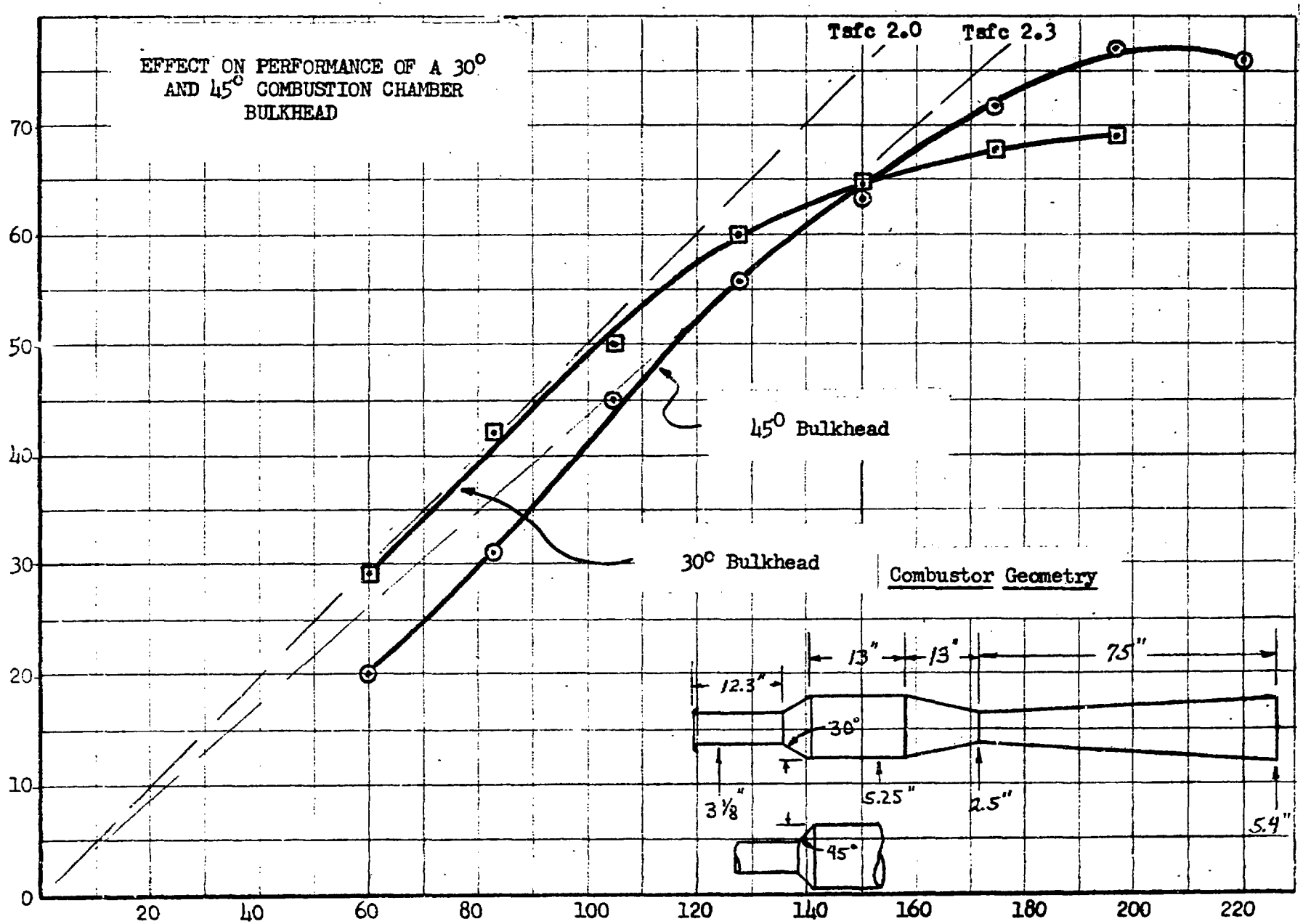

EFFECT ON PERFORMANCE OF A 30° AND 45° COMBUSTION CHAMBER BULKHEAD
Tsfc 2.0
Tsfc 2.3
45° Bulkhead
30° Bulkhead
Combustor Geometry
13"
13"
75"
12.3"
30°
3⅛"
5.25"
2.5"
5.4"
45°
THRUST, lb (NO AUGMENTATION)
FUEL FLOW RATE, pph
0
10
20
30
40
50
60
70
20
40
60
80
100
120
140
160
180
200
220

FIGURE 14

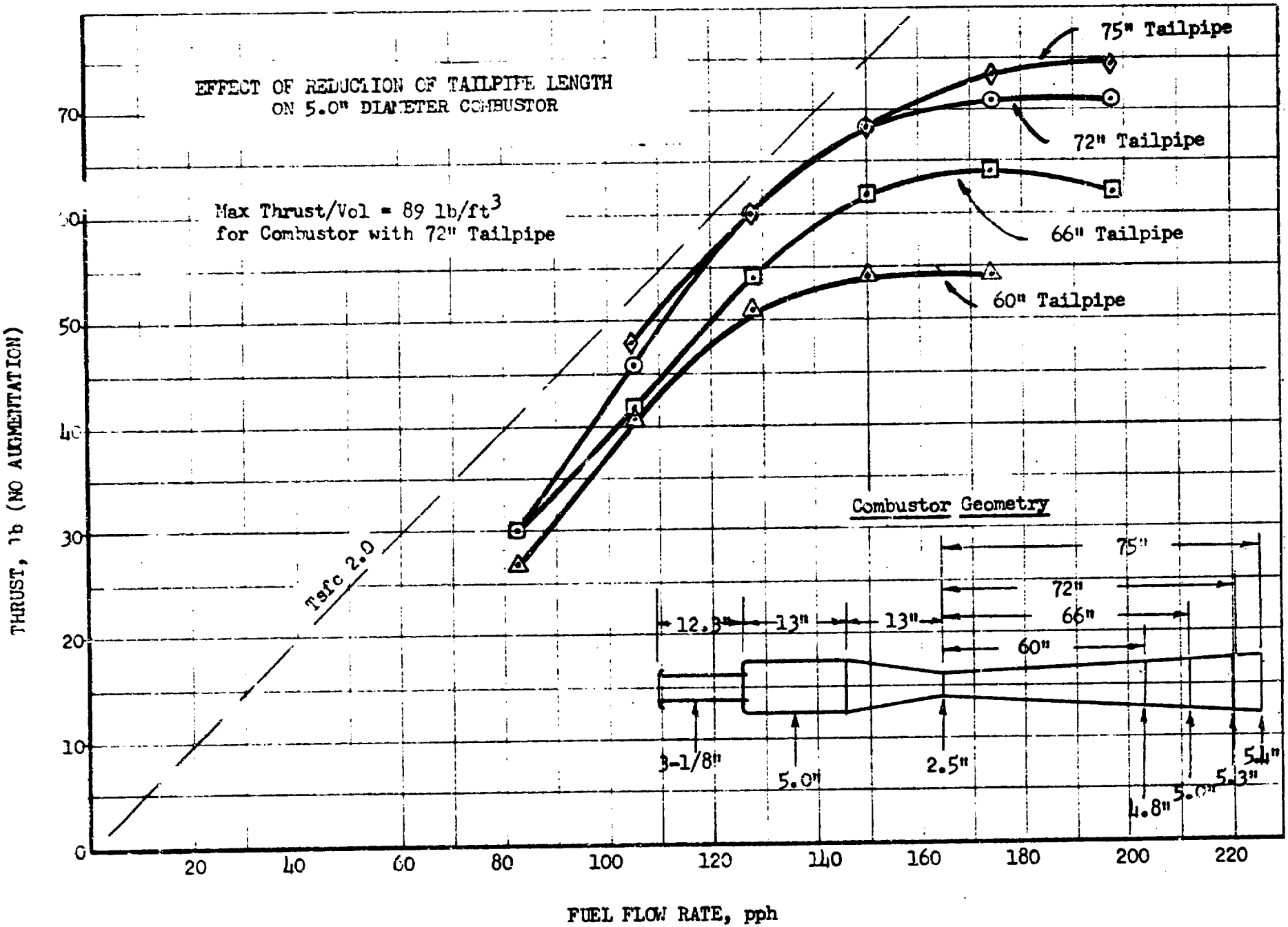

EFFECT OF REDUCTION OF TAILPIPE LENGTH
ON 5.0" DIAMETER COMBUSTOR
Max Thrust/Vol = 89 lb/ft3
for Combustor with 72" Tailpipe
75" Tailpipe
72" Tailpipe
66" Tailpipe
60" Tailpipe
Tsfc 2.0
Combustor Geometry
75"
72"
66"
60"
12.3"
13"
13"
3-1/8"
5.0"
2.5"
4.8"
5.0"
5.3"
5.4"
THRUST, lb (NO AUGMENTATION)
FUEL FLOW RATE, pph
0
10
20
30
40
50
70
20
40
60
80
100
120
140
160
180
200
220

FIGURE 15

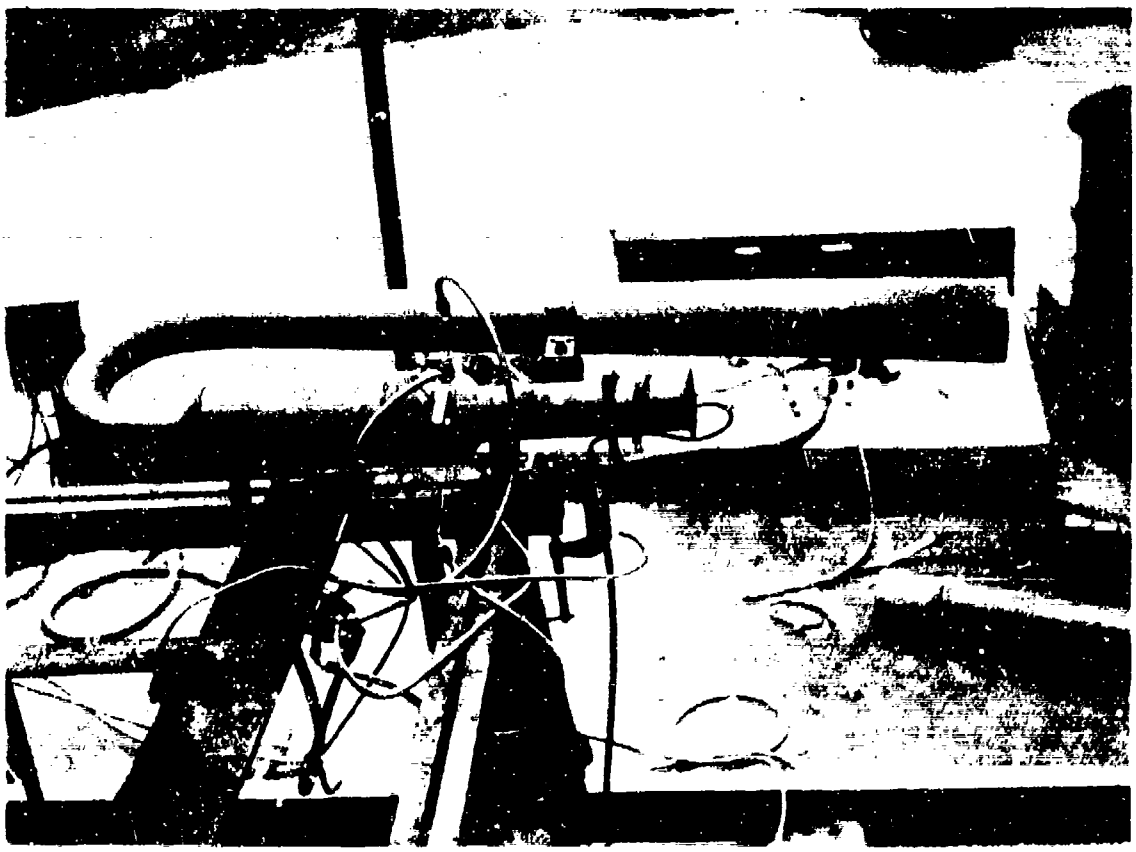
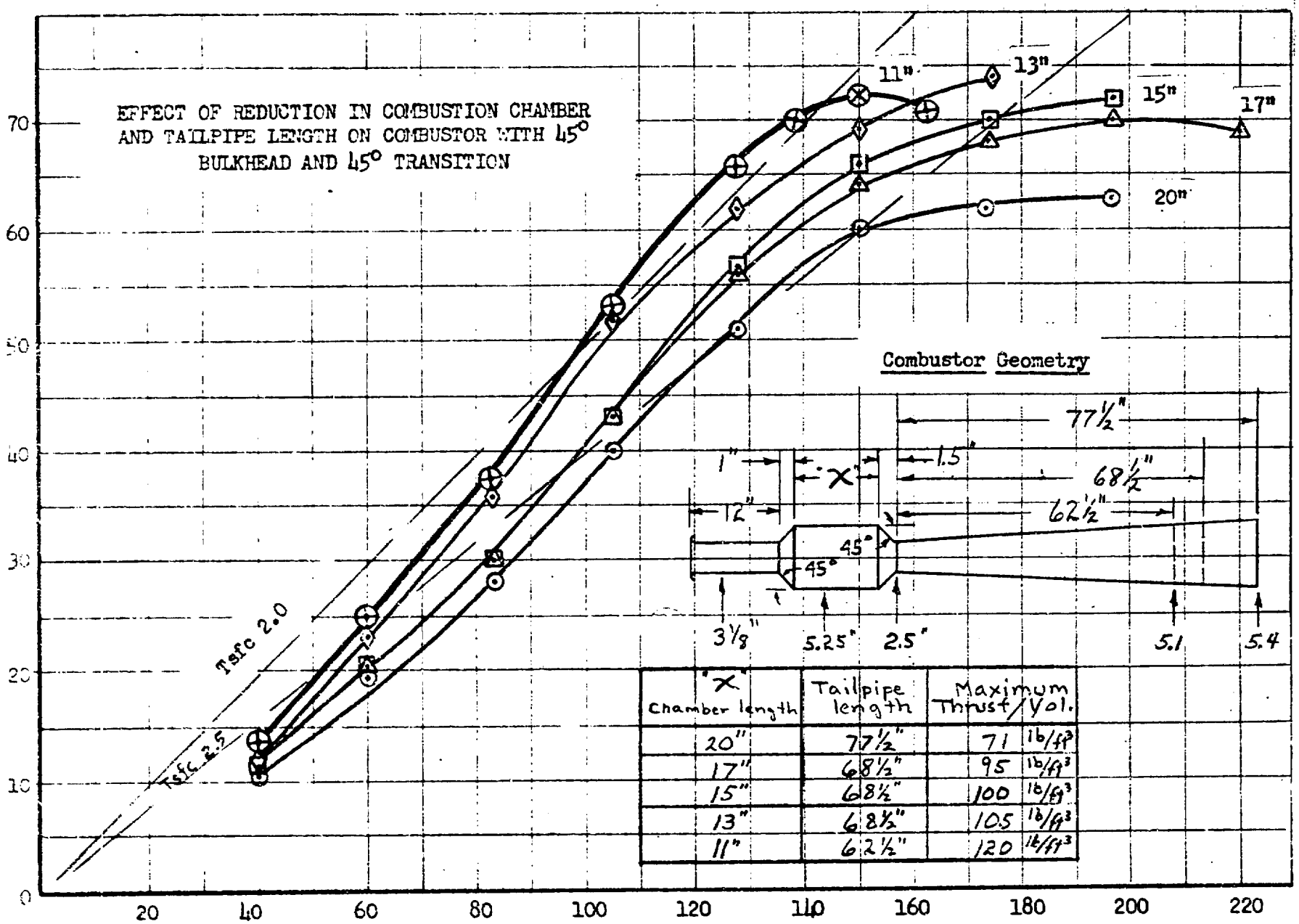


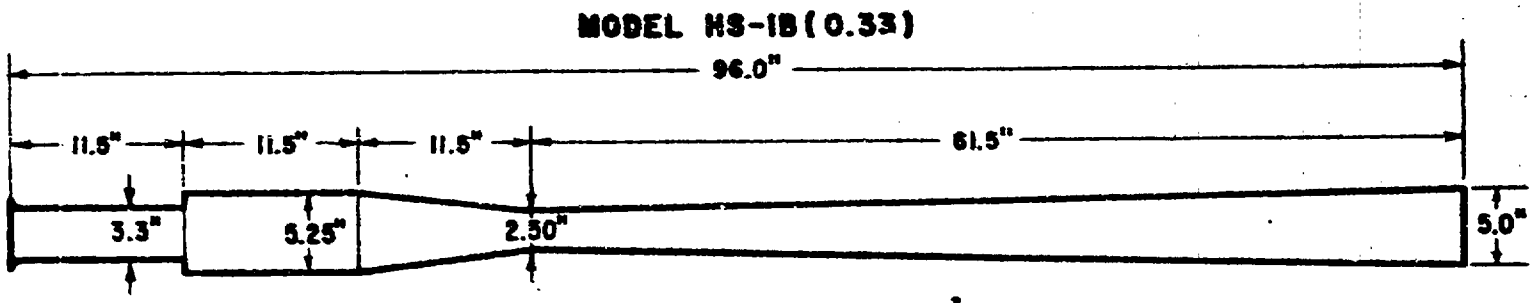
FIGURE 16: HH(5.25")-5 COMBUSTOR WITH 45° BULKHEADS AT BOTH ENDS OF COMBUSTION CHAMBER AND EXCESSIVELY LONG TAILPIPE.

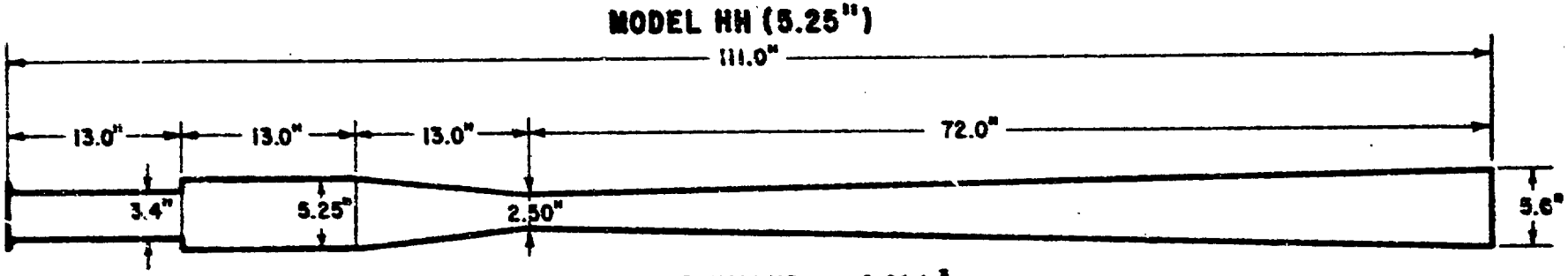


"X" Chamber length	Tailpipe length	Maximum Thrust/Vol.
20"	77½"	71 lb/ft³
17"	68½"	95 lb/ft³
15"	68½"	100 lb/ft³
13"	68½"	105 lb/ft³
11"	62½"	120 lb/ft³

FIGURE 17

MAJOR CHANGES TO 5.25" I.D. COMBUSTOR GEOMETRY





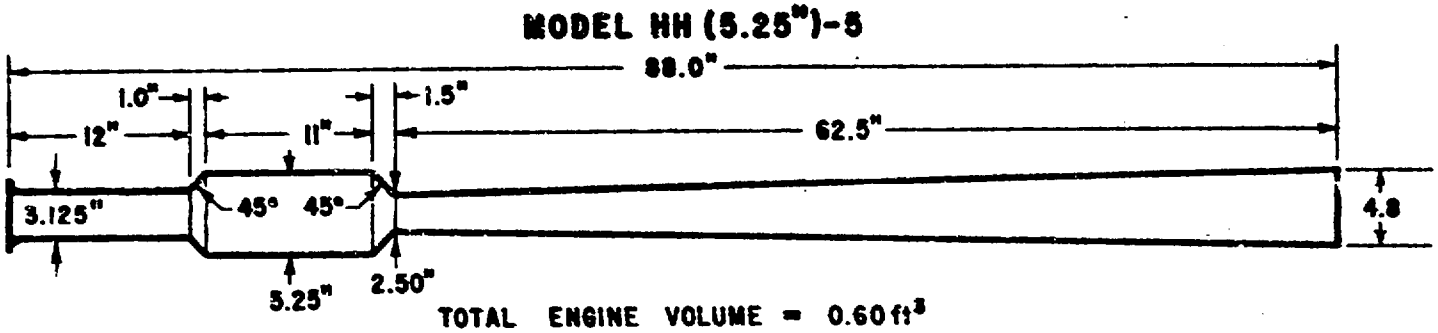


FIGURE 18

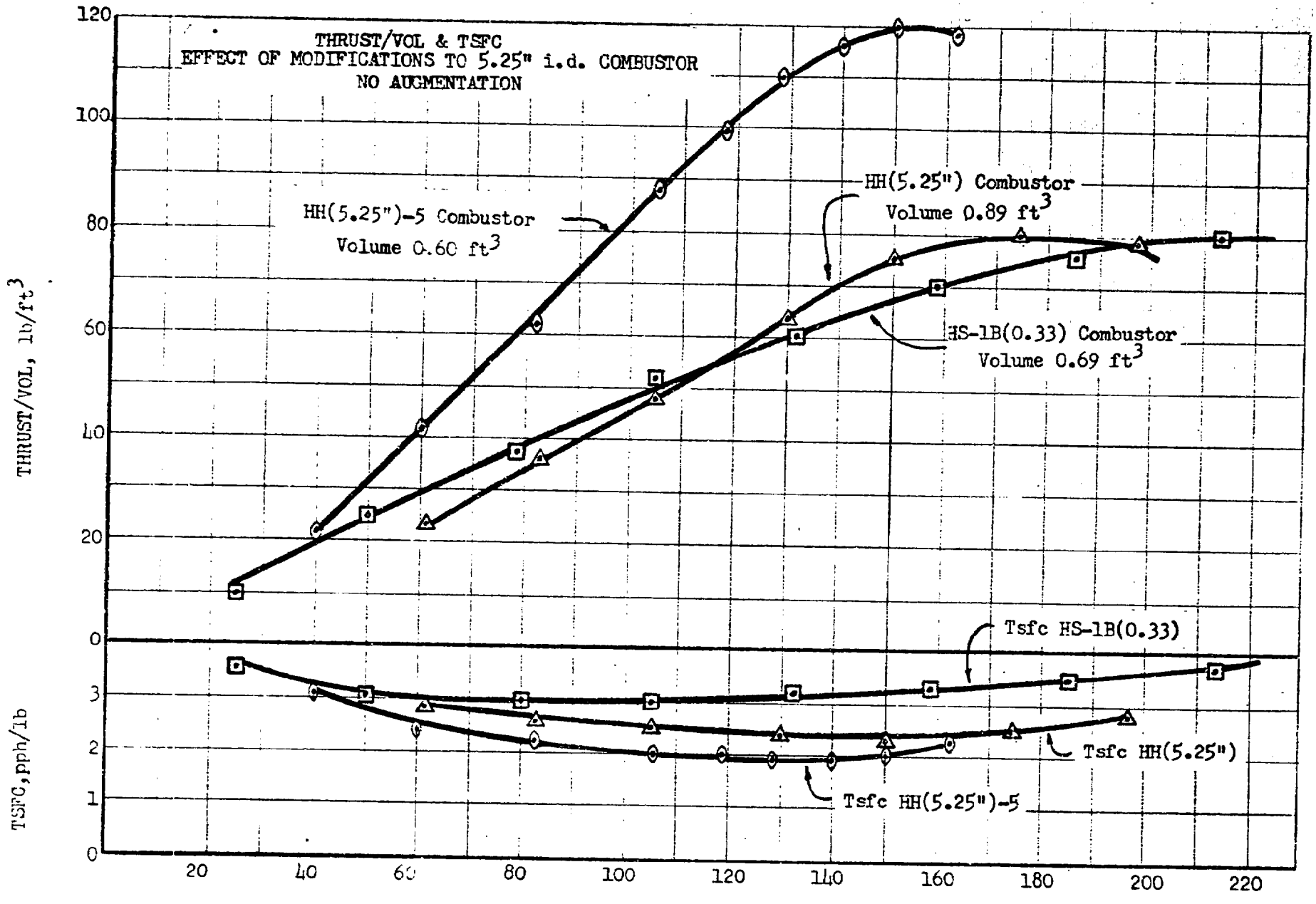

THRUST/VOL & TSFC
EFFECT OF MODIFICATIONS TO 5.25" i.d. COMBUSTOR
NO AUGMENTATION
HH(5.25")-5 Combustor
Volume 0.60 ft3
HH(5.25") Combustor
Volume 0.89 ft3
HS-1B(0.33) Combustor
Volume 0.69 ft3
Tsfc HS-1B(0.33)
Tsfc HH(5.25")
Tsfc HH(5.25")-5
THRUST/VOL, lb/ft3
TSFC, pph/lb
FUEL FLOW RATE, pph
120
100
80
60
40
20
0
3
2
1
0
20
40
60
80
100
120
140
160
180
200
220

FIGURE 19

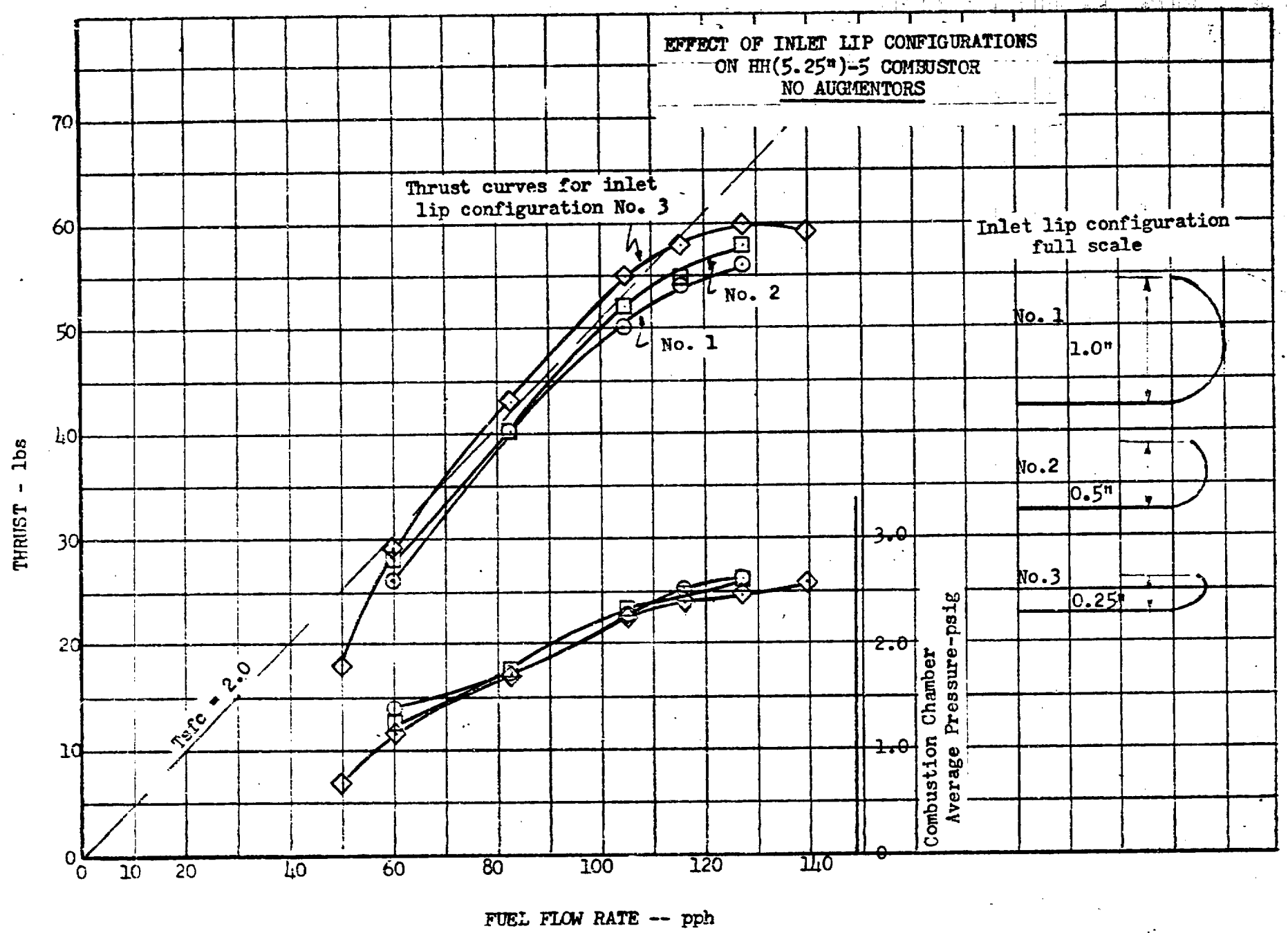

EFFECT OF INLET LIP CONFIGURATIONS
ON HH(5.25")-5 COMBUSTOR
NO AUGMENTORS
Thrust curves for inlet
lip configuration No. 3
No. 2
No. 1
Tsfc = 2.0
Inlet lip configuration
full scale
No. 1
1.0"
No.2
0.5"
No.3
0.25"
THRUST - lbs
Combustion Chamber
Average Pressure-psig
FUEL FLOW RATE -- pph
0
10
20
40
60
80
100
120
140
70
50
30
3.0
2.0
1.0

FIGURE 20

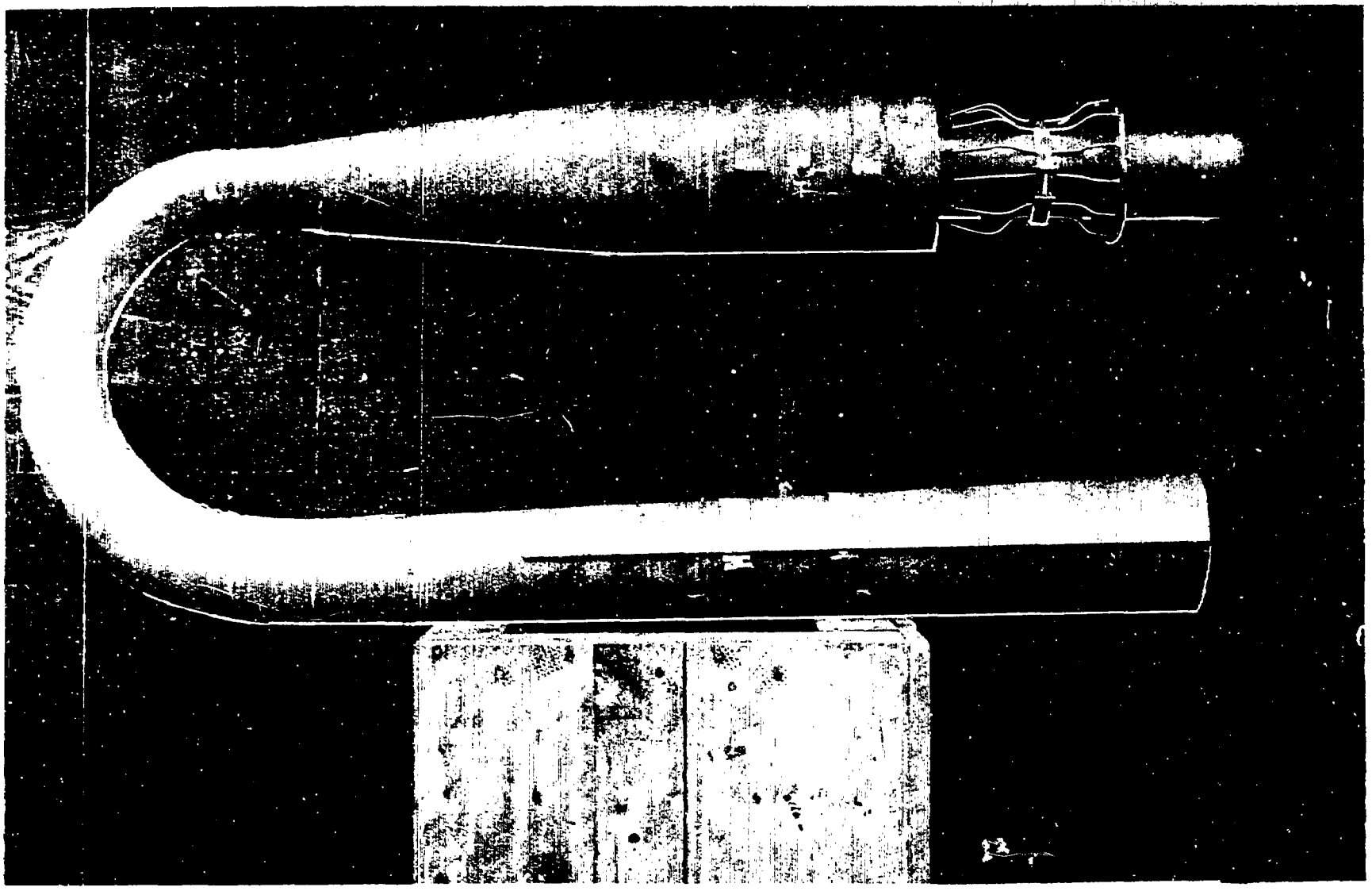


FIGURE 21: 5.25" DIA. PULSE REACTOR COMBUSTOR, MODEL HS-1B(0.33), WITH 12-LINE FUEL SYSTEM

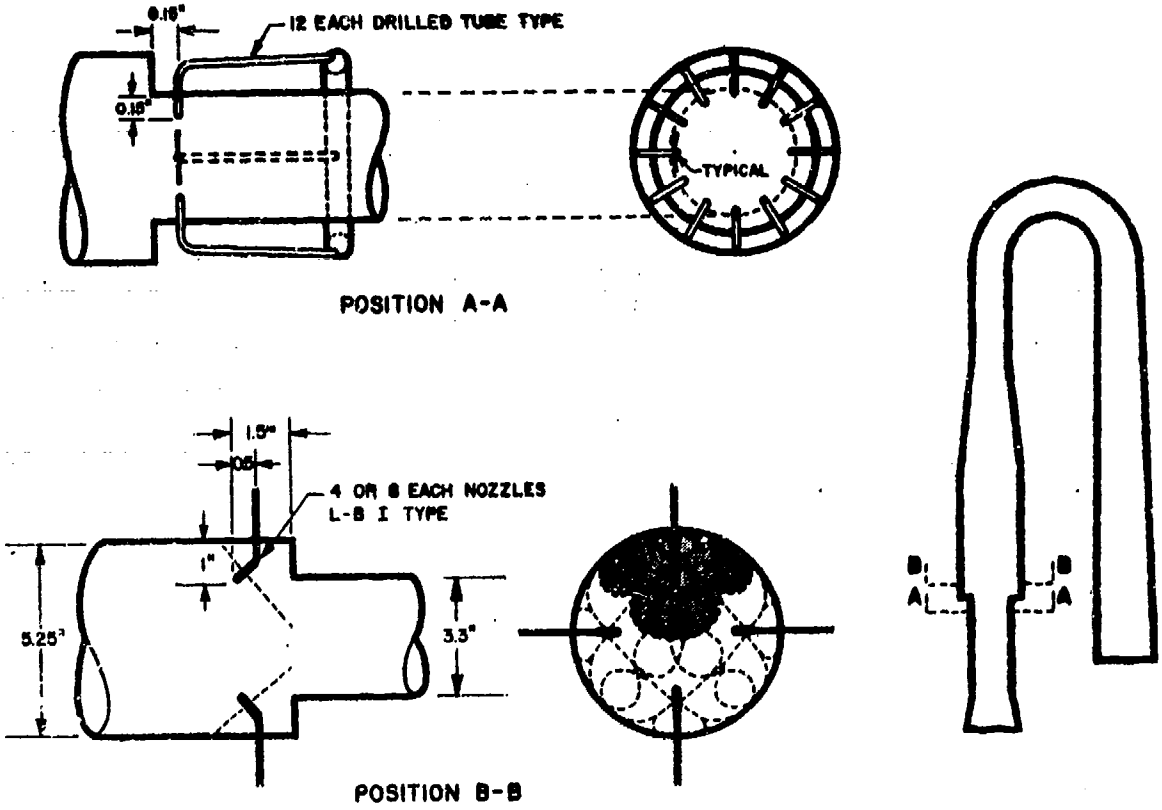


FIGURE 4.2: FUEL NOZZLE LOCATIONS FOR 5.25" I.d. PULSE REACTOR COMBUSTOR

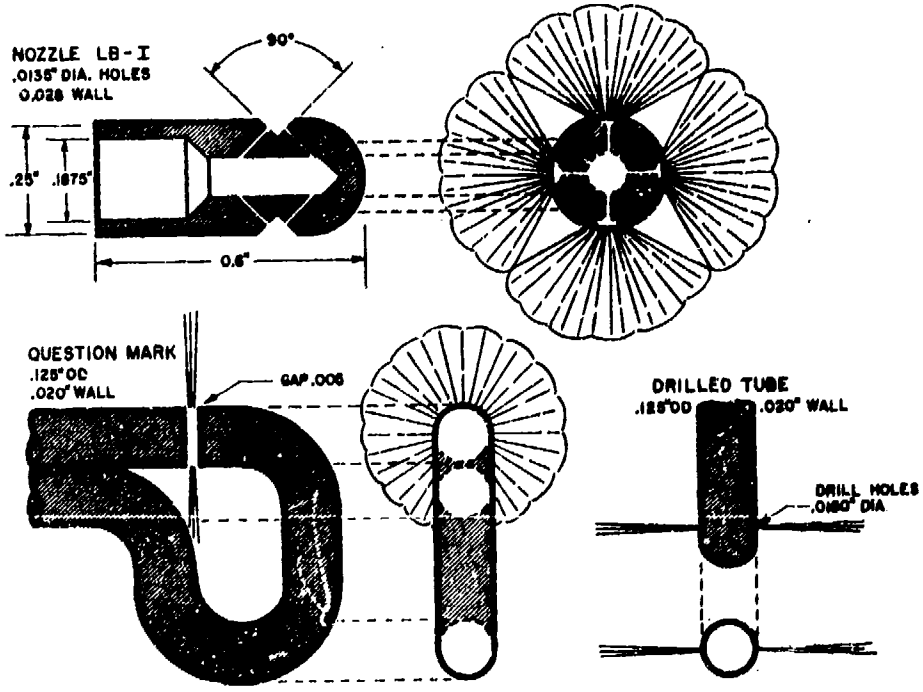


FIGURE 4.3: FUEL NOZZLES USED SUCCESSFULLY IN 5.25" I.d. PULSE REACTOR COMBUSTOR

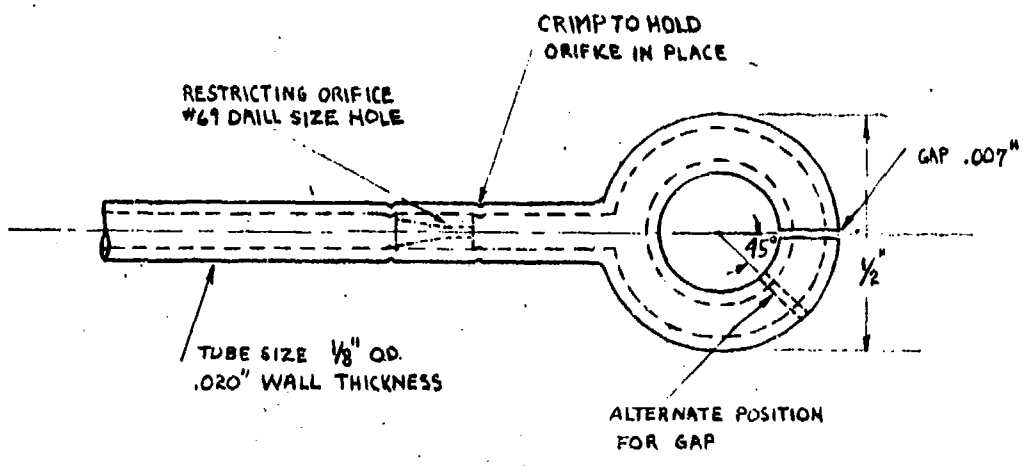
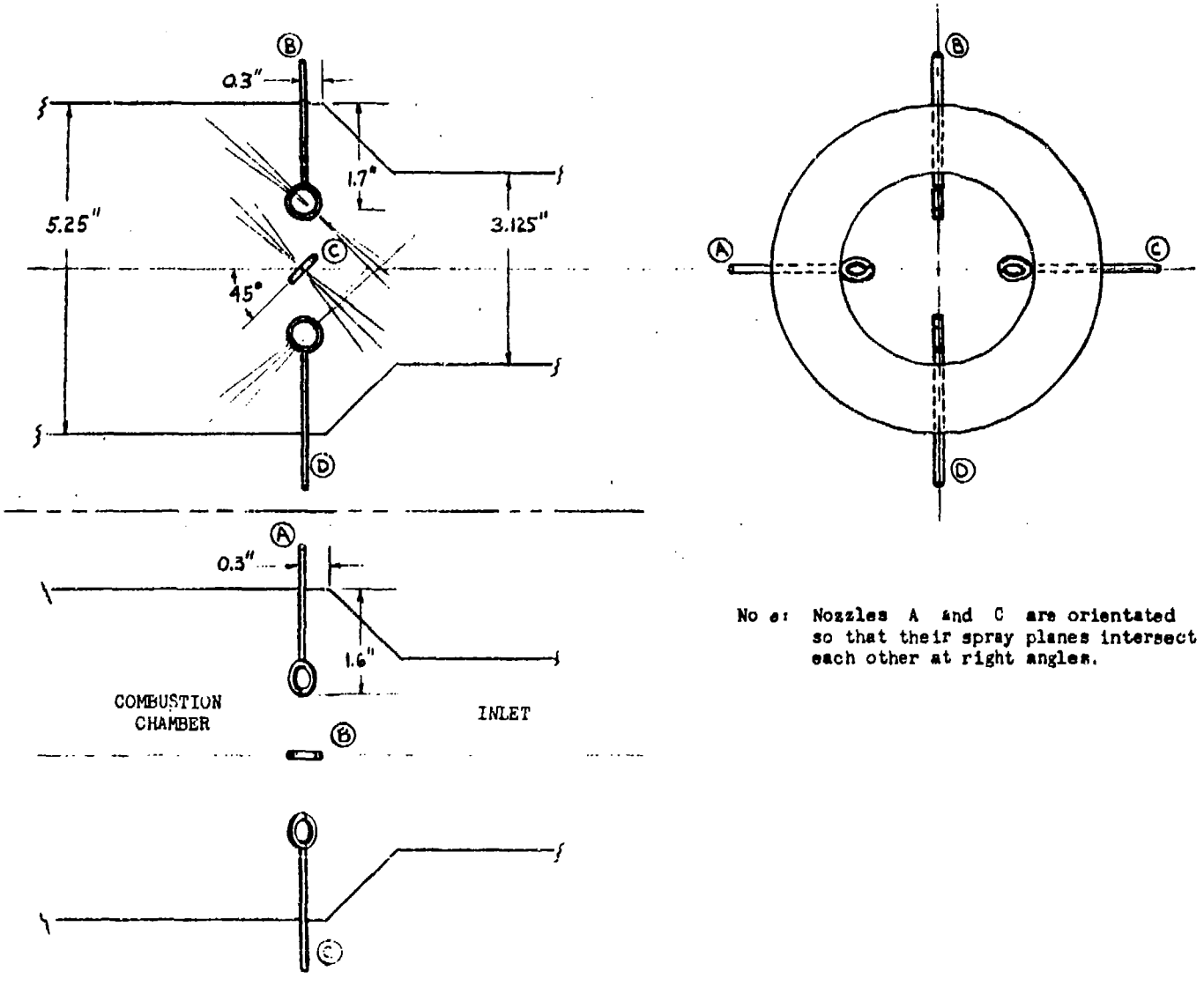


FIGURE 24: LORGNETTE TYPE FUEL NOZZLE FOR 5 ¼" i.d. COMBUSTOR



Note: Nozzles A and C are orientated so that their spray planes intersect each other at right angles.

FIGURE 25: LORGNETTE FUEL NOZZLE LOCATIONS FOR 5¼" i.d. COMBUSTOR

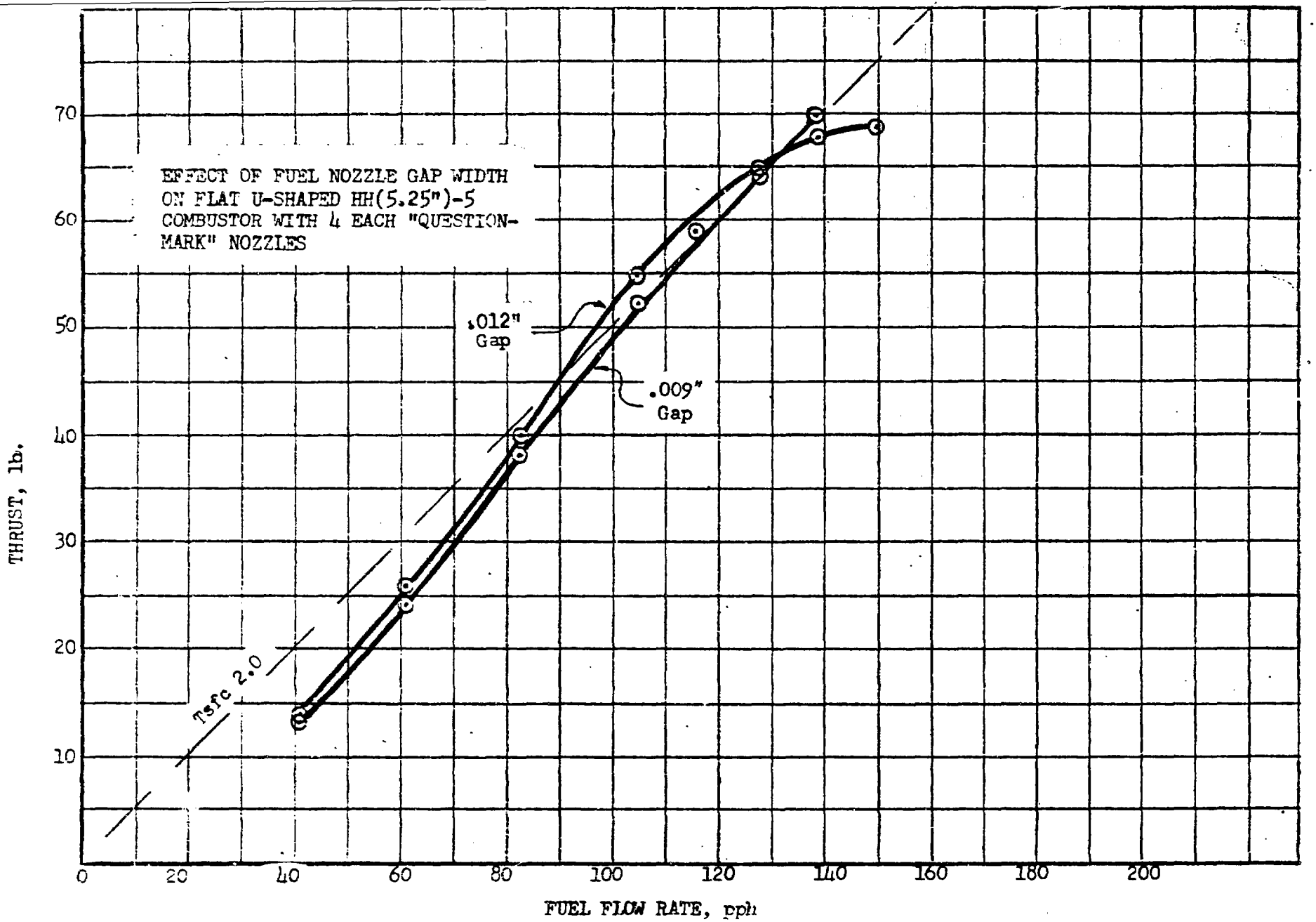
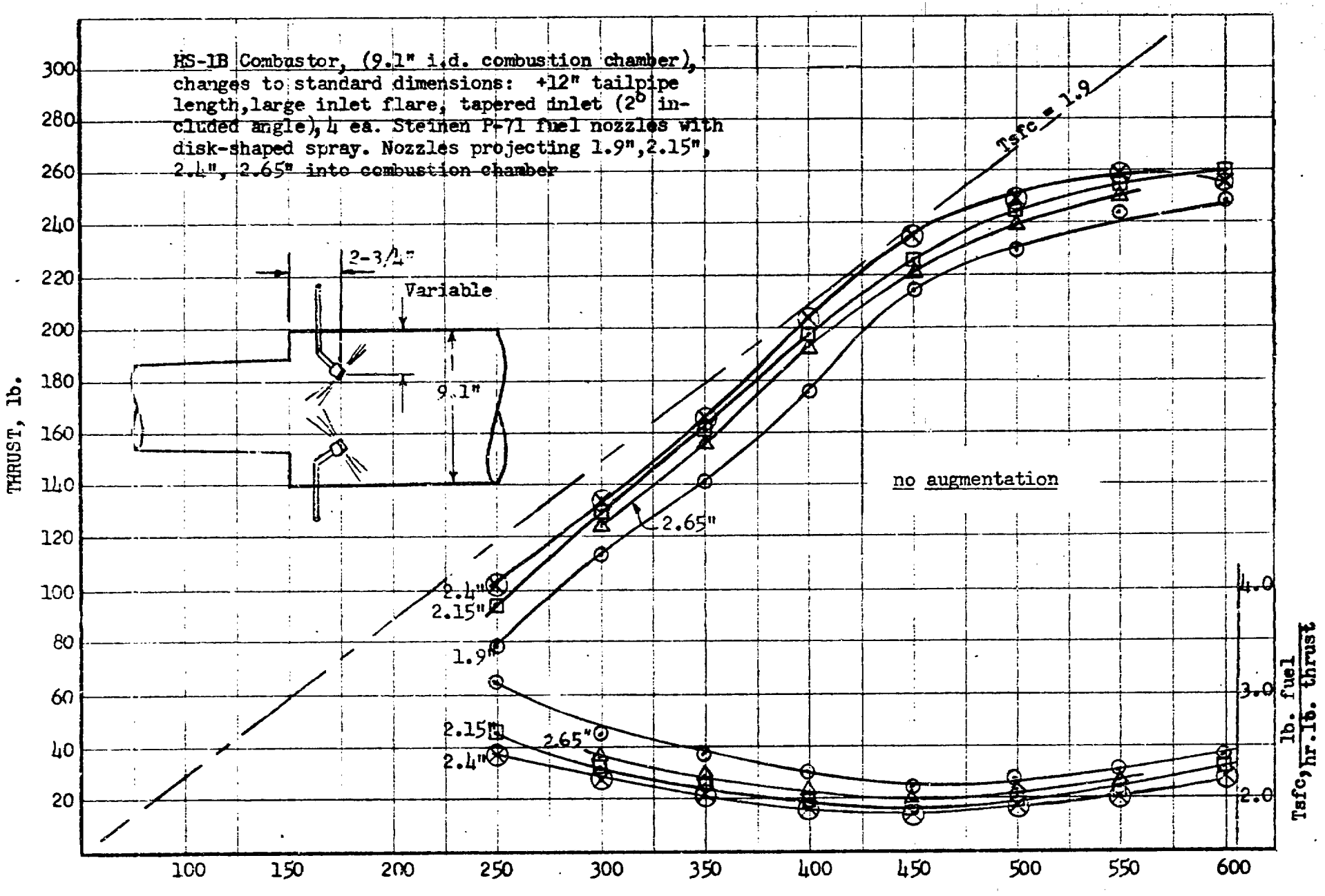

EFFECT OF FUEL NOZZLE GAP WIDTH
ON FLAT U-SHAPED HH(5.25")-5
COMBUSTOR WITH 4 EACH "QUESTION-
MARK" NOZZLES
.012"
Gap
.009"
Gap
Tsfc 2.0
THRUST, lb.
FUEL FLOW RATE, pph
0
20
40
60
80
100
120
140
160
180
200
10
20
30
40
50
60
70

FIGURE 2[illegible]



EFFECT OF FUEL NOZZLE LOCATION ON THRUST AND SPECIFIC FUEL CONSUMPTION

FIGURE 27

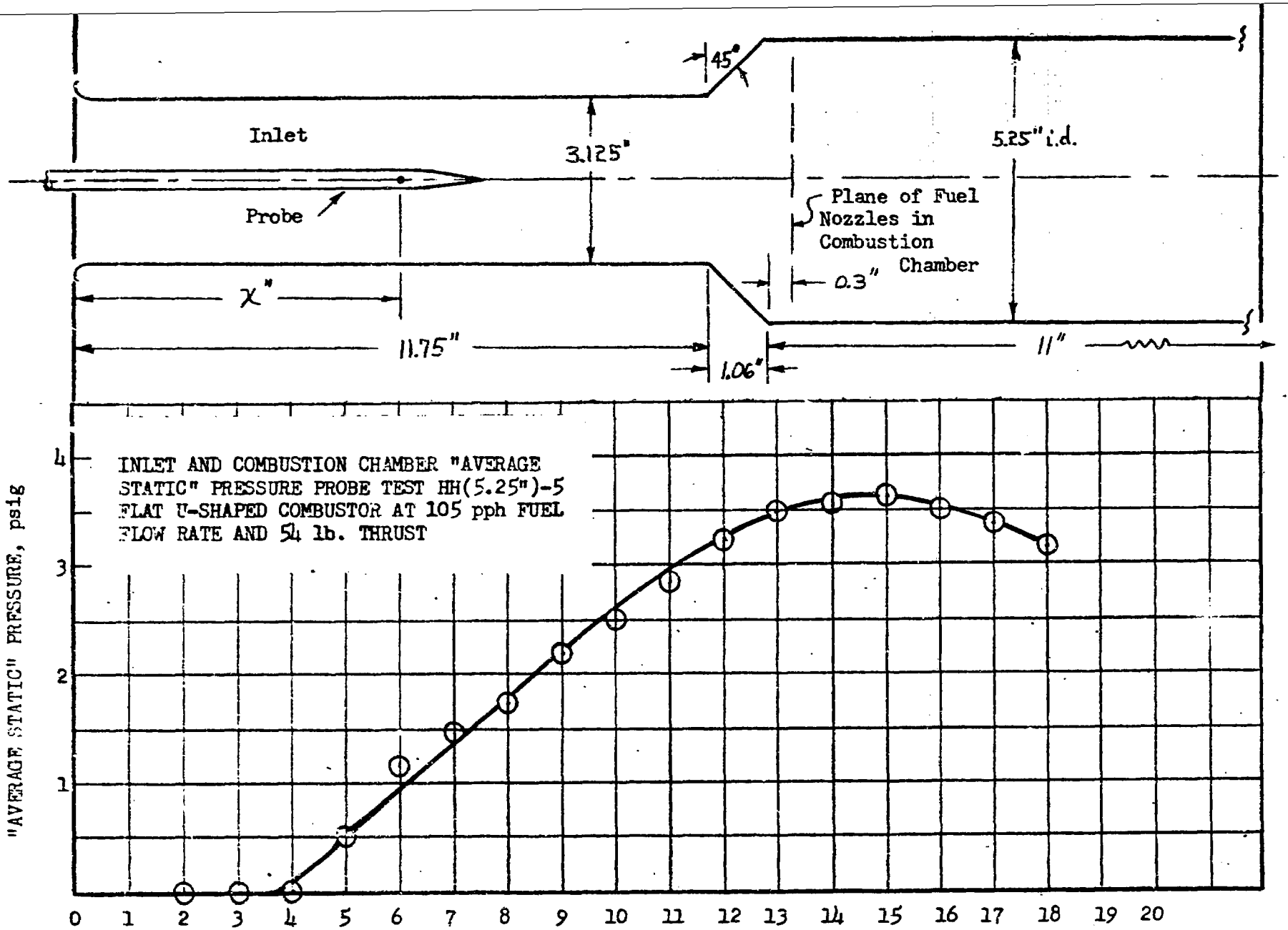

45°
Inlet
3.125"
5.25" i.d.
Probe
Plane of Fuel Nozzles in Combustion Chamber
0.3"
X"
11.75"
1.06"
11"
INLET AND COMBUSTION CHAMBER "AVERAGE STATIC" PRESSURE PROBE TEST HH(5.25")-5 FLAT U-SHAPED COMBUSTOR AT 105 pph FUEL FLOW RATE AND 54 lb. THRUST
"AVERAGE STATIC" PRESSURE, psig
1
2
3
4
0 1 2 3 4 5 6 7 8 9 10 11 12 13 14 15 16 17 18 19 20
DISTANCE INTO INLET, inches

FIGURE 28

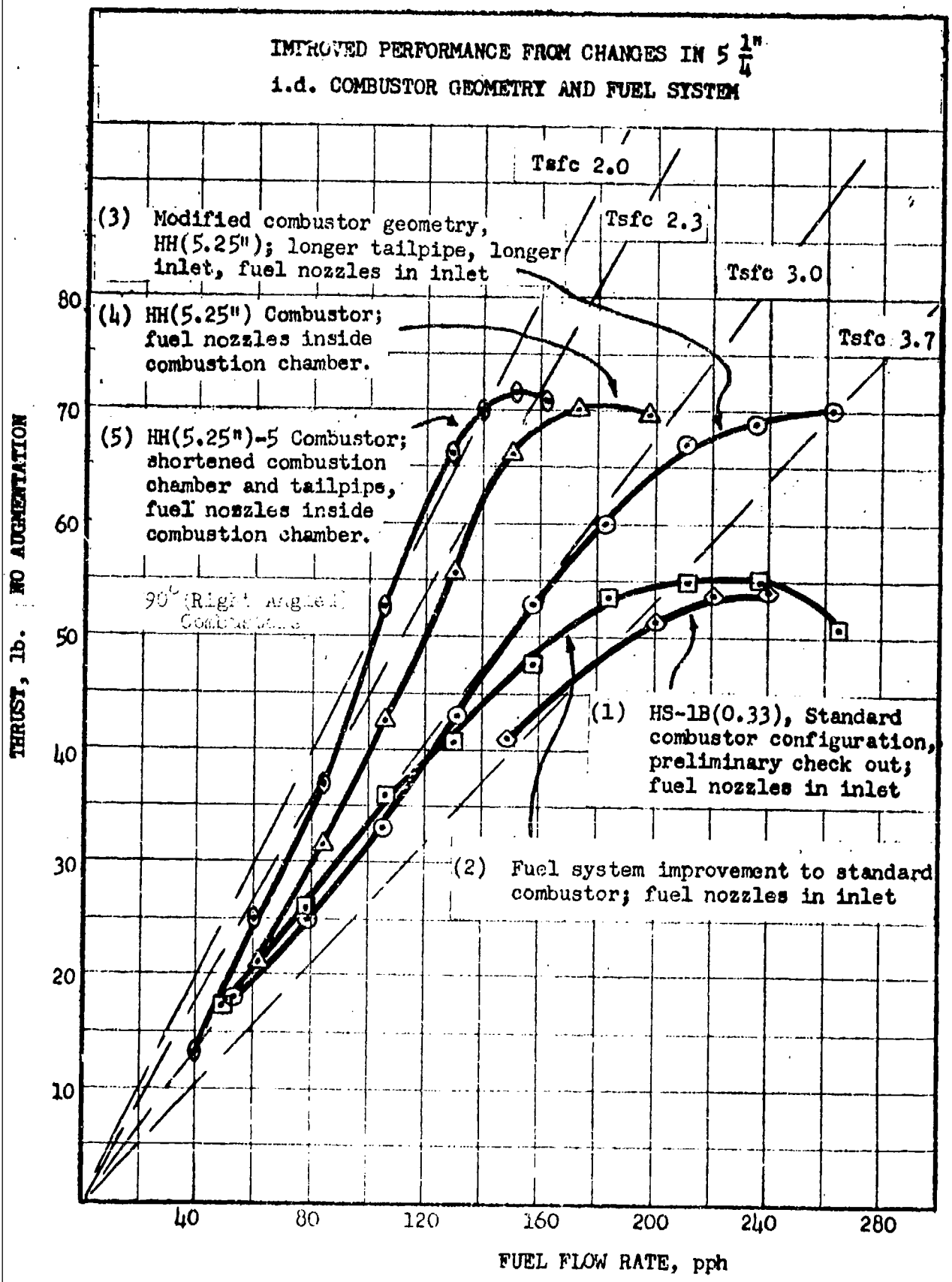

IMPROVED PERFORMANCE FROM CHANGES IN 5 1/4" i.d. COMBUSTOR GEOMETRY AND FUEL SYSTEM
Tsfc 2.0
Tsfc 2.3
Tsfc 3.0
Tsfc 3.7
(3) Modified combustor geometry, HH(5.25"); longer tailpipe, longer inlet, fuel nozzles in inlet
(4) HH(5.25") Combustor; fuel nozzles inside combustion chamber.
(5) HH(5.25")-5 Combustor; shortened combustion chamber and tailpipe, fuel nozzles inside combustion chamber.
90° (Right Angled) Combustors
(1) HS-1B(0.33), Standard combustor configuration, preliminary check out; fuel nozzles in inlet
(2) Fuel system improvement to standard combustor; fuel nozzles in inlet
THRUST, lb. NO AUGMENTATION
80
70
60
50
40
30
20
10
40
80
120
160
200
240
280
FUEL FLOW RATE, pph

FIGURE 2

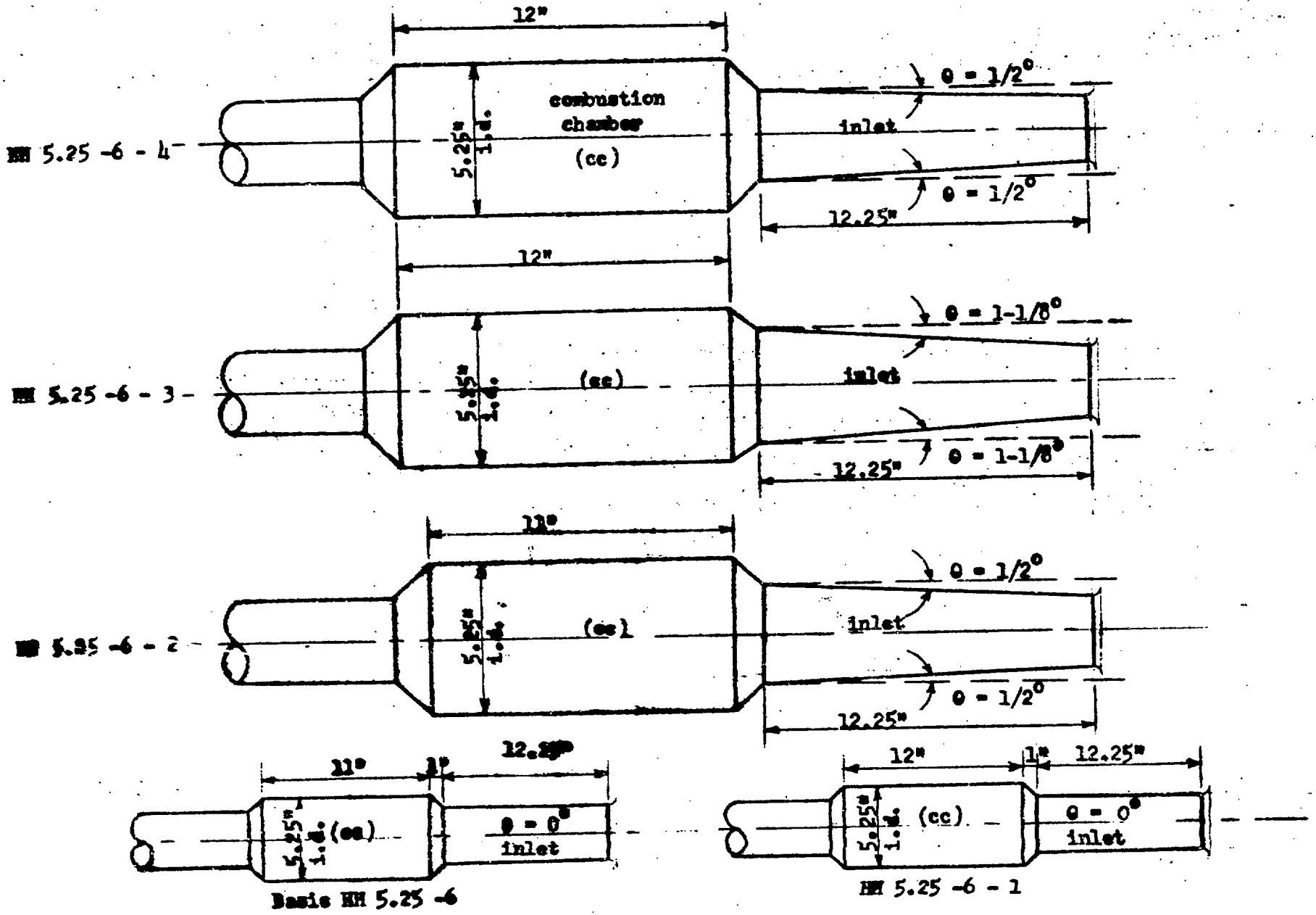


FIGURE 30: VARIOUS COMBUSTION CHAMBER AND INLET PIPE CONFIGURATION MODIFICATIONS TO BASIC HH 5.25" i.d. MODEL.

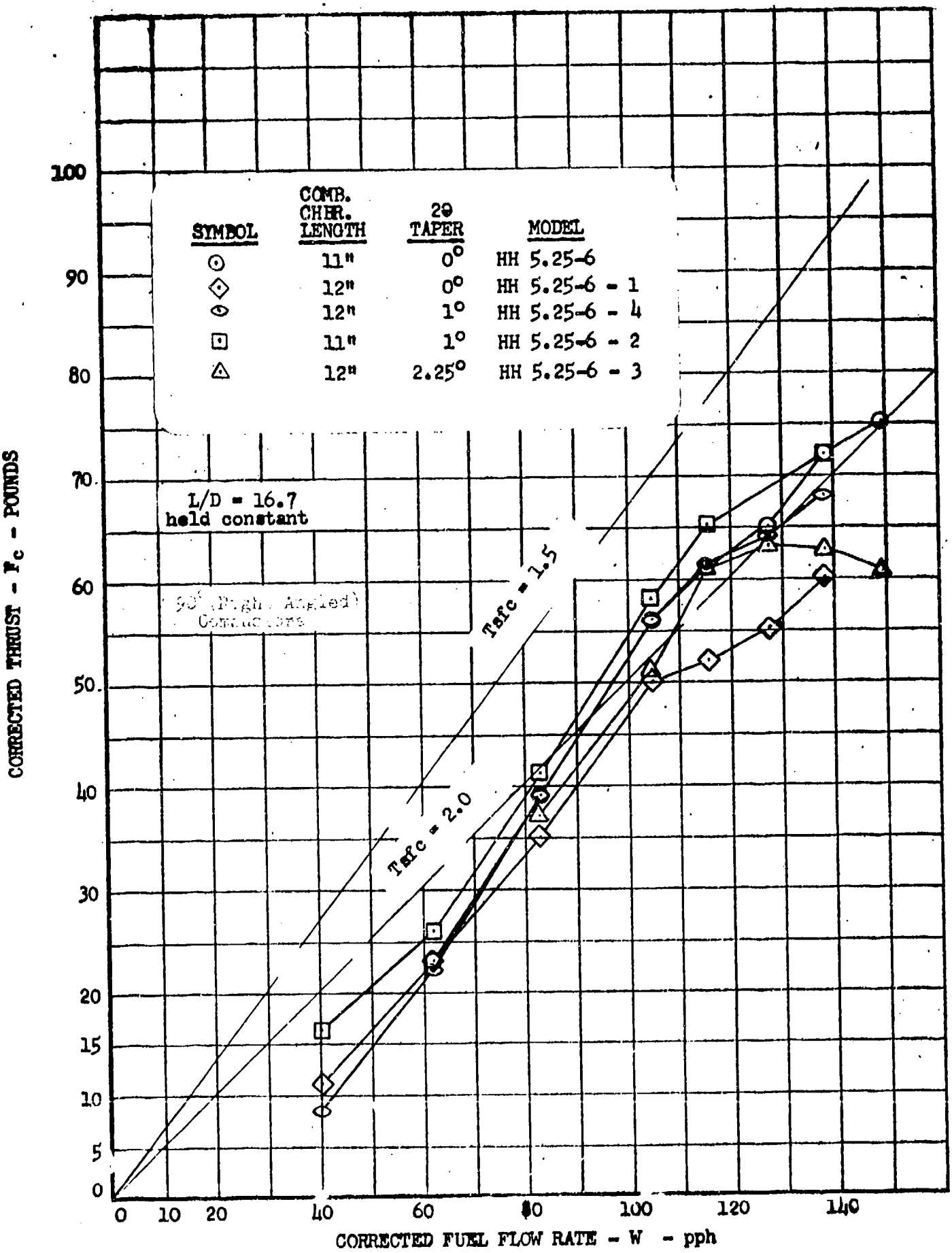


FIGURE 31 COMPARISON OF PERFORMANCE OF VARIOUS COMBUSTION CHAMBER LENGTHS AND INLET TAPER CONFIGURATIONS

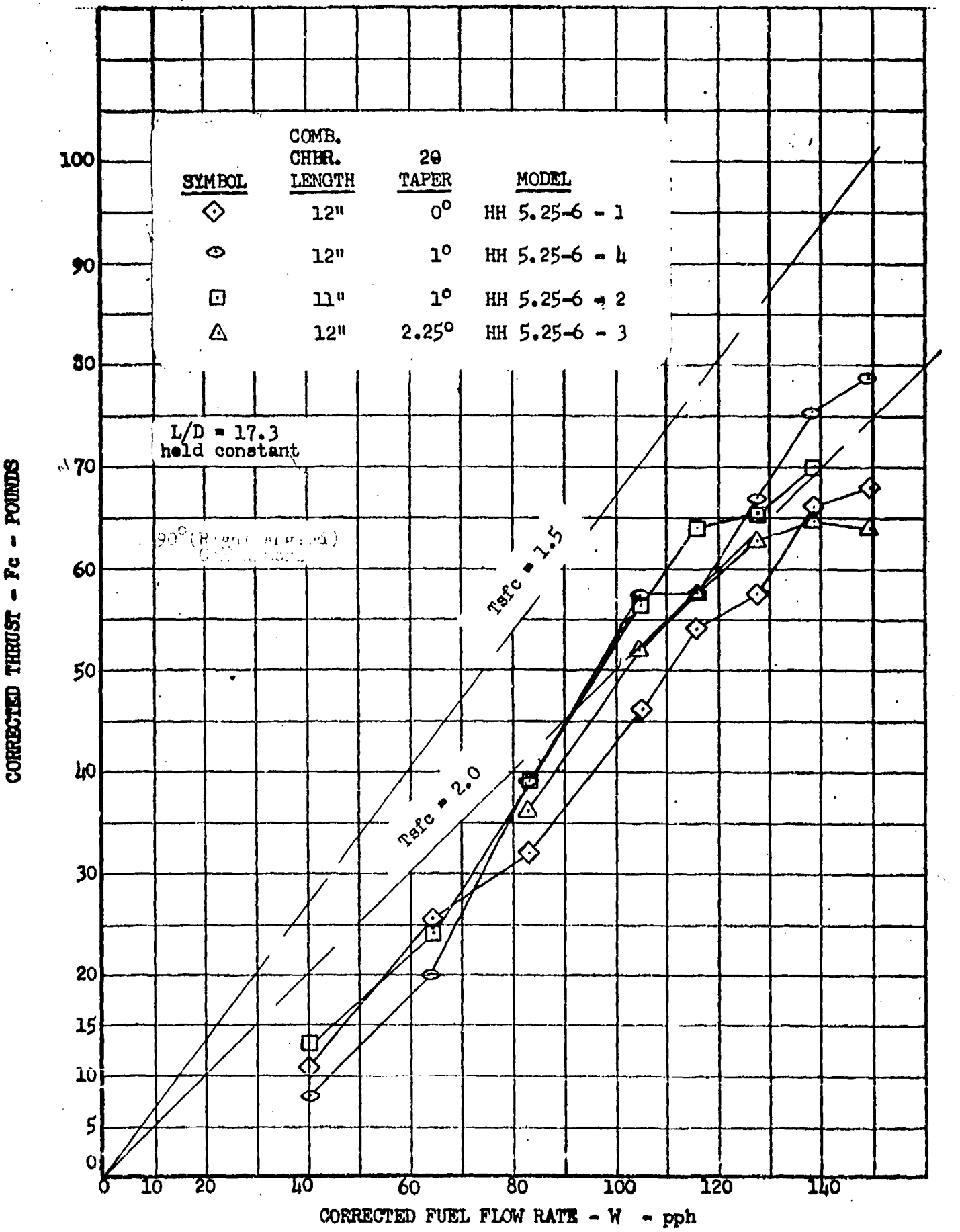


FIGURE 32: COMPARISON OF PERFORMANCE OF VARIOUS COMBUSTION CHAMBER LENGTHS AND INLET TAPER CONFIGURATIONS

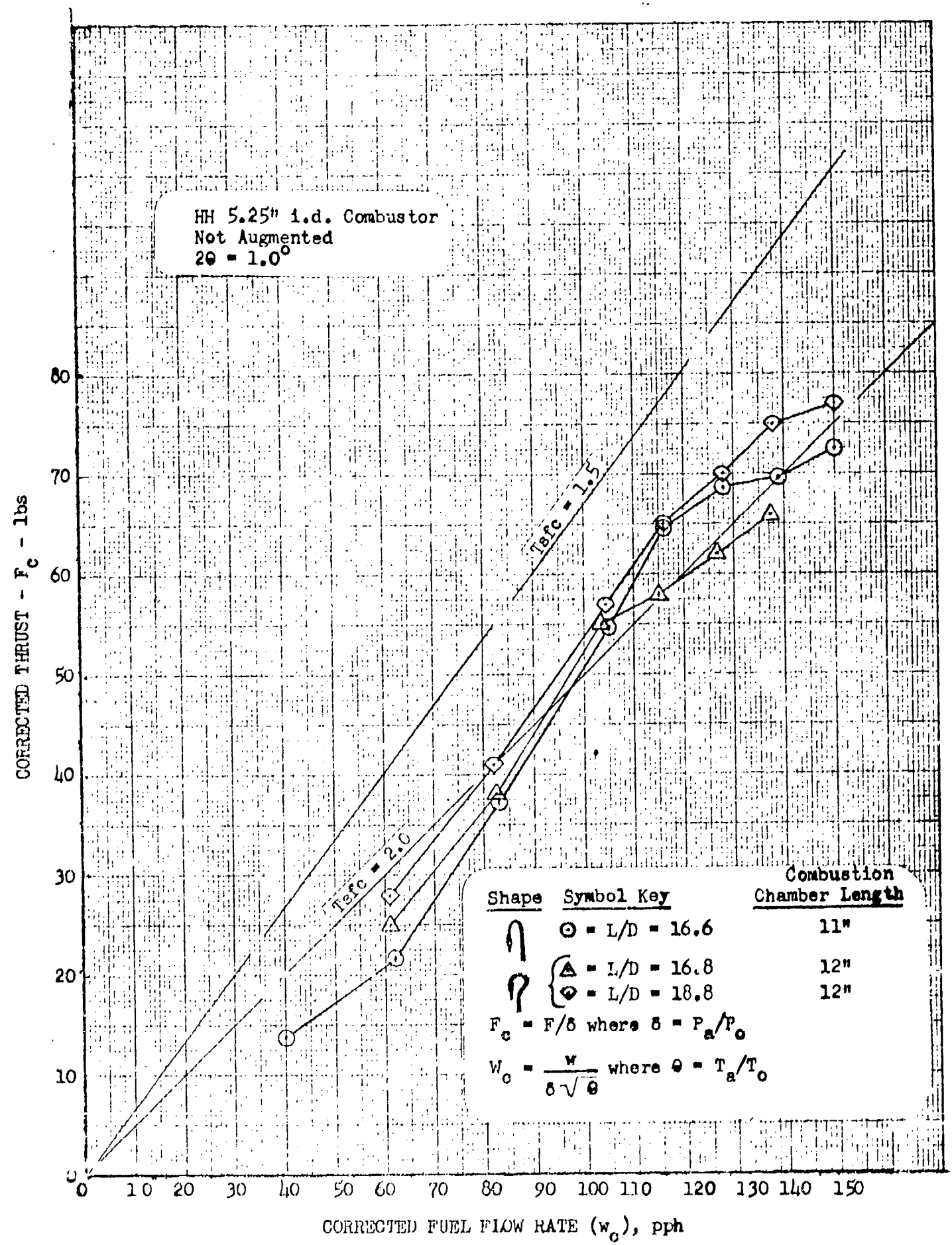


FIGURE COMPARISON OF PERFORMANCE OF VARIOUS COMBUSTION CHAMBER LENGTHS AND INLET TAPER CONFIGURATIONS AND TAILPIPE BEND

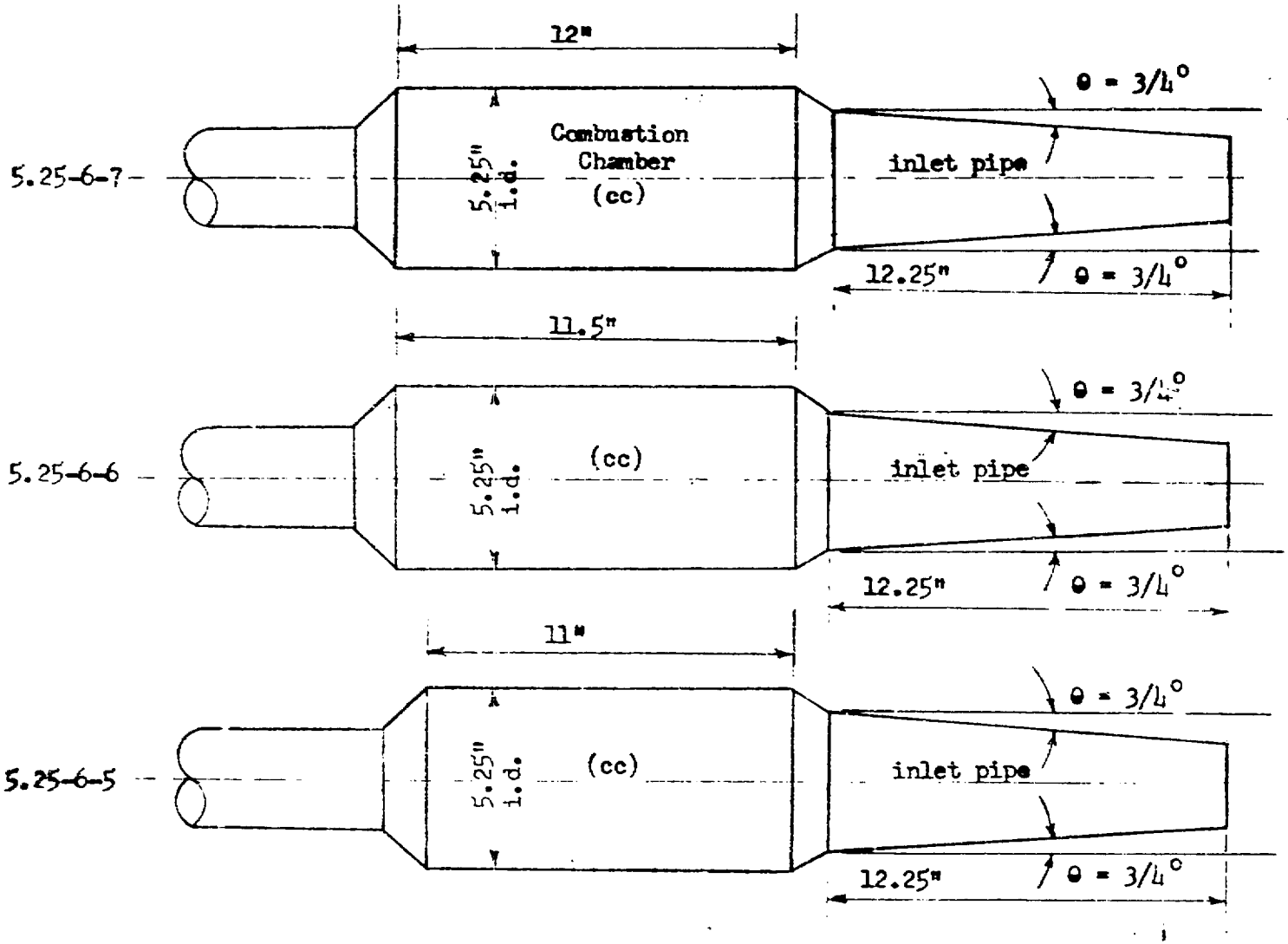


FIGURE 3. VARIOUS COMBUSTION CHAMBER AND INLET PIPE CONFIGURATIONS MODIFICATIONS TO BASIC HH 5.25" i.d. MODEL.

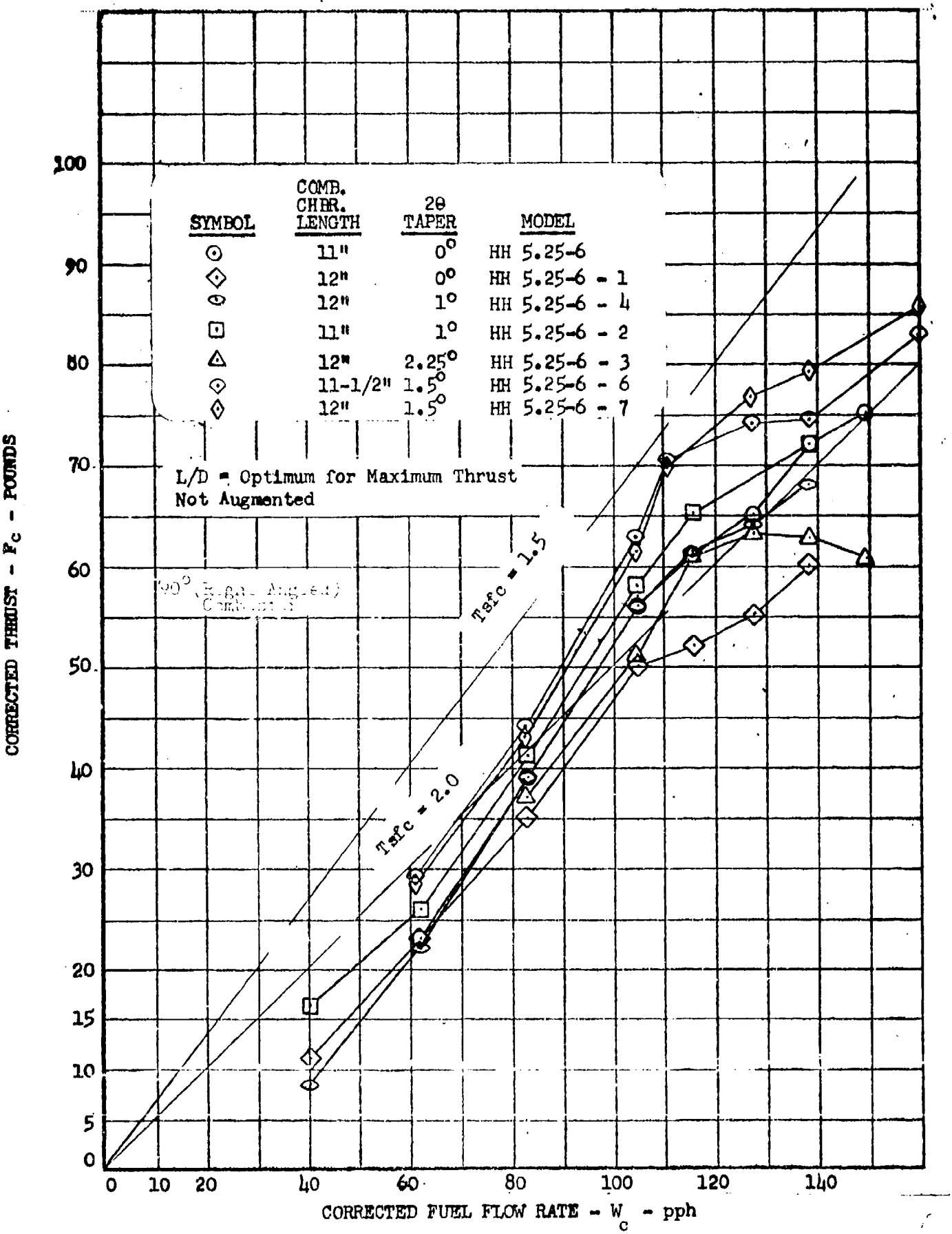


FIGURE 3.: COMPARISON OF PERFORMANCE OF VARIOUS COMBUSTION CHAMBER LENGTHS AND INLET TAPER CONFIGURATIONS

Model	Combustion Chamber Length	Inlet Taper	Optimum L/D	Volume V-ft^3	Maximum Thrust T-lbs.	T/V lbs/ft^3
HH 5.25-6	11"	0°	16.7	0.60	78	130
HH 5.25-6-6	11½"	1½°	18.35	0.69	83	121
HH 5.25-6-4	12"	1°	17.3	0.63	79	125
HH 5.25-6-7	12"	1½°	18.44	0.695	86	124
[illegible]	[illegible]	[illegible]	[illegible]	[illegible]	[illegible]	118

L = total engine length in inches

D = combustion chamber diameter in inches

V = total engine volume in cubic feet

T = combustor thrust in pounds

T/V = thrust per unit volume

FIGURE [illegible] COMPARISON DATA OF HH 5.25-6 MODELS IN 90° (RIGHT-ANGLED) CONFIGURATIONS

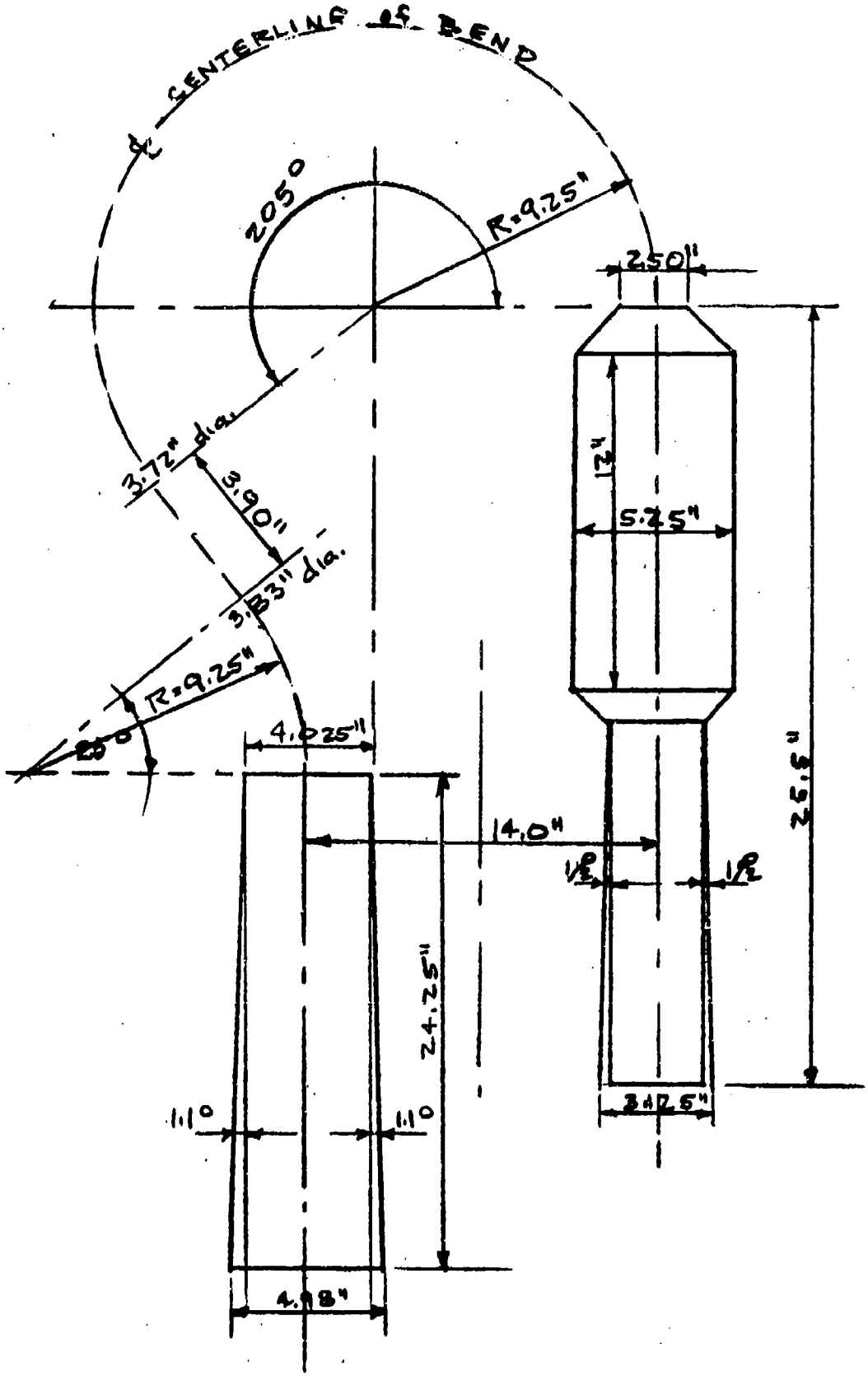


FIGURE 7. 180° - 5.25-7 COMBUSTOR LAYOUT SKETCH

TYPICAL PULSE REACTOR CONFIGURATIONS

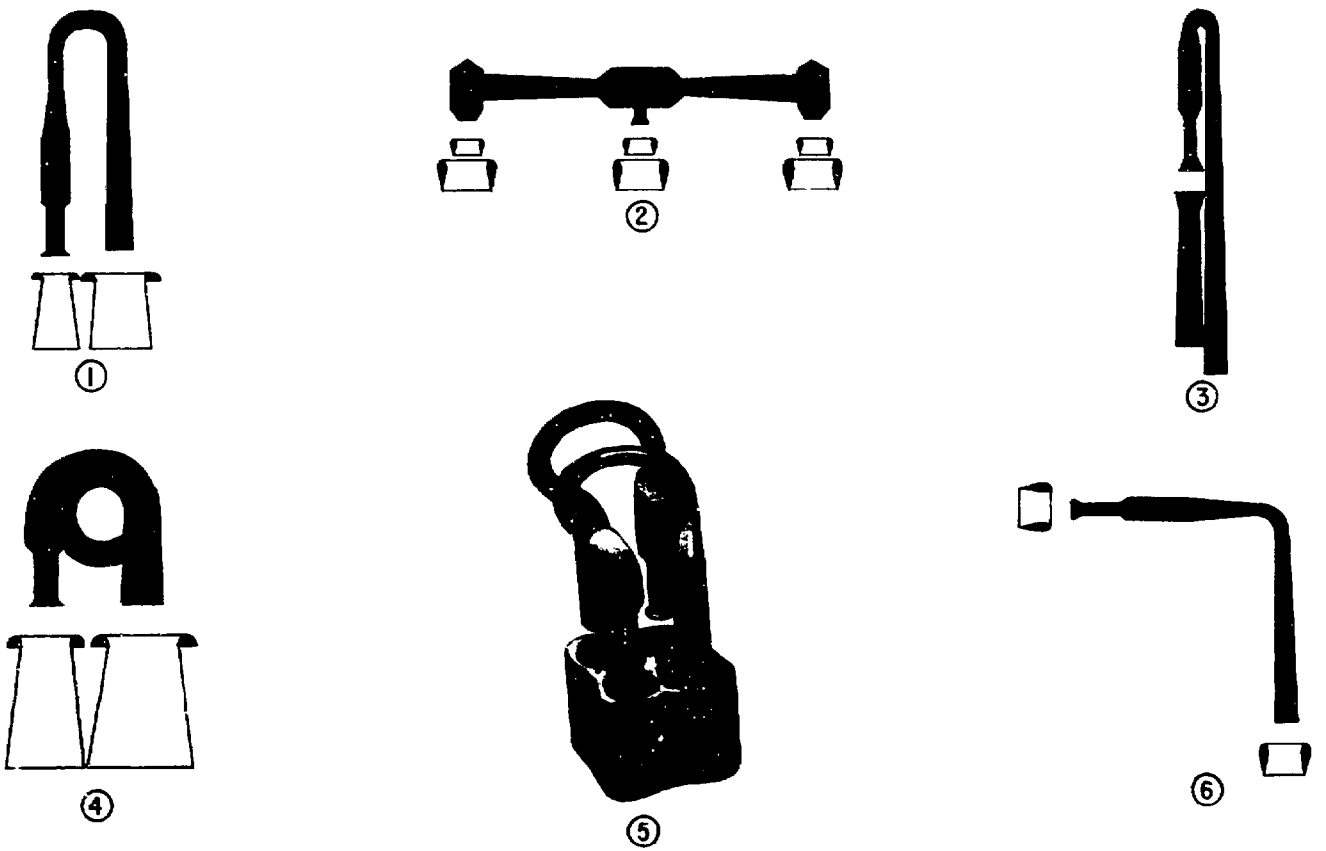


FIGURE 38

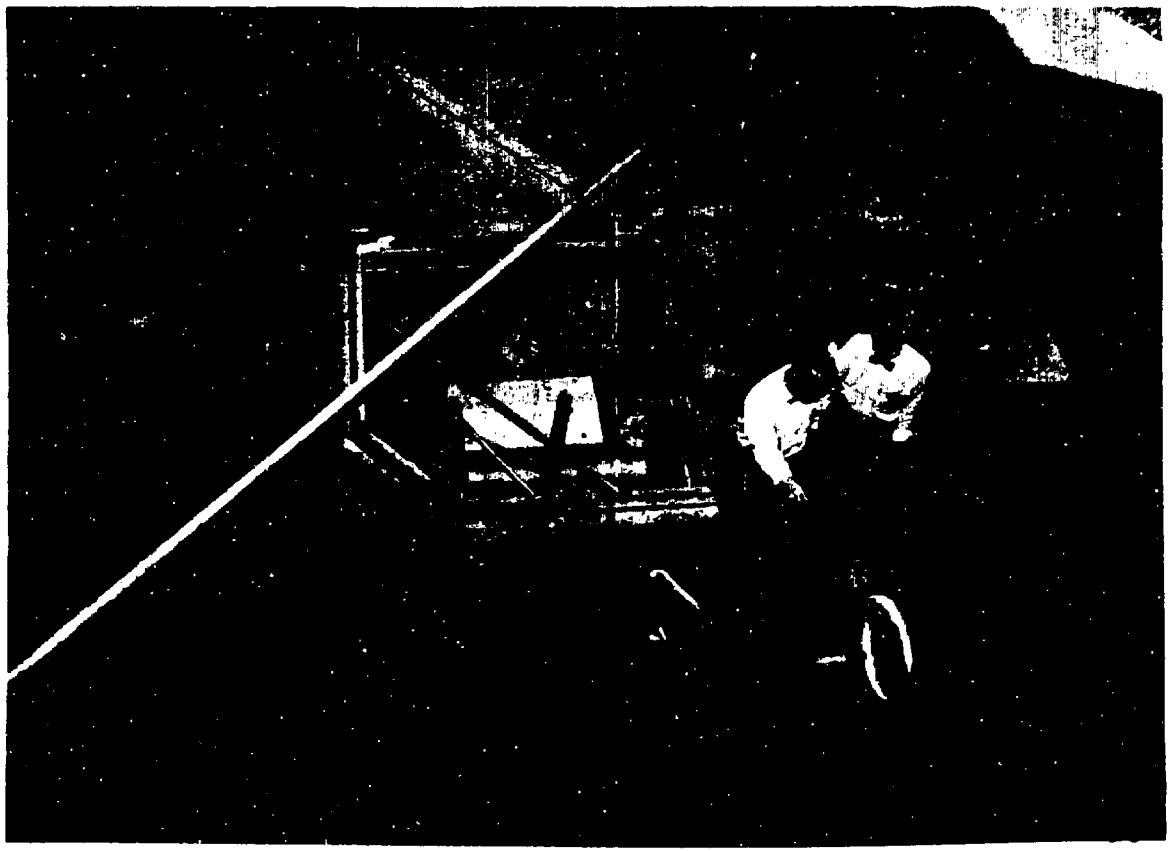


FIGURE 39: HS-1B 90° PULSE REACTOR ON ORTHOGONAL THRUST STAND

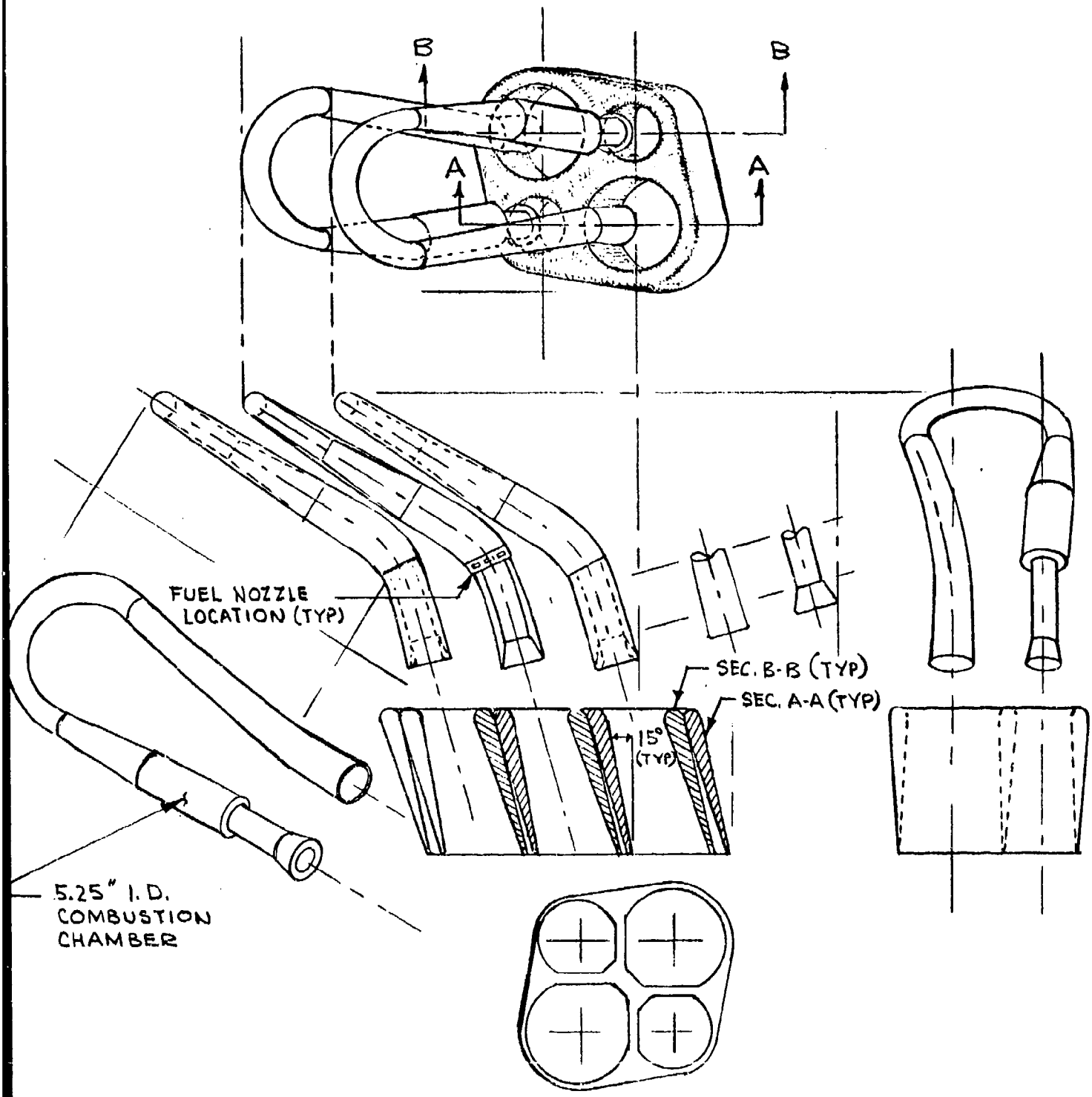


FIGURE 40: PULSE REACTOR ENGINE PACKAGE, MODEL HH(5.25") "HORSECOLLAR"

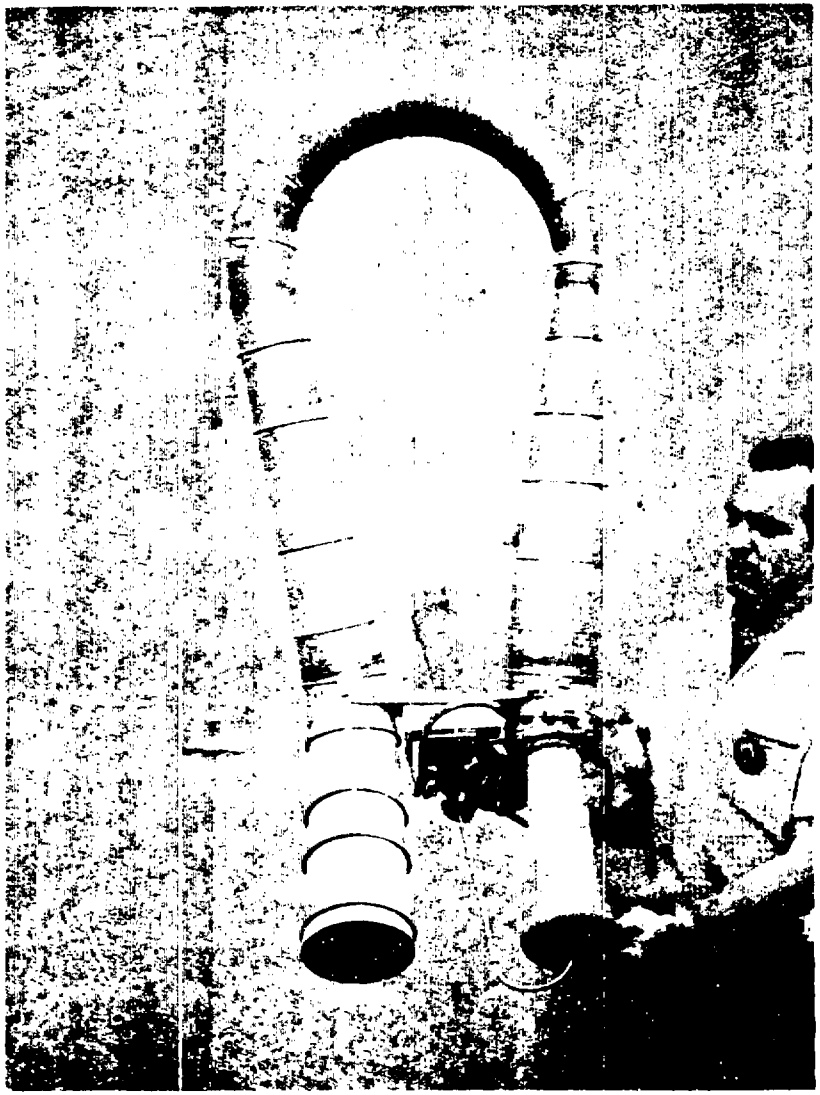


FIGURE 41: HH(5.25") "HORSECOLLAR" COMBUSTOR WITH FUEL NOZZLES AND STARTING AIR TUBE READY FOR STATIC TESTING



FIGURE 42: HH(5.25")-5 "HORSECOLLAR" COMBUSTOR WITH BEND RELOCATED TO AFT PART OF COMBUSTION CHAMBER

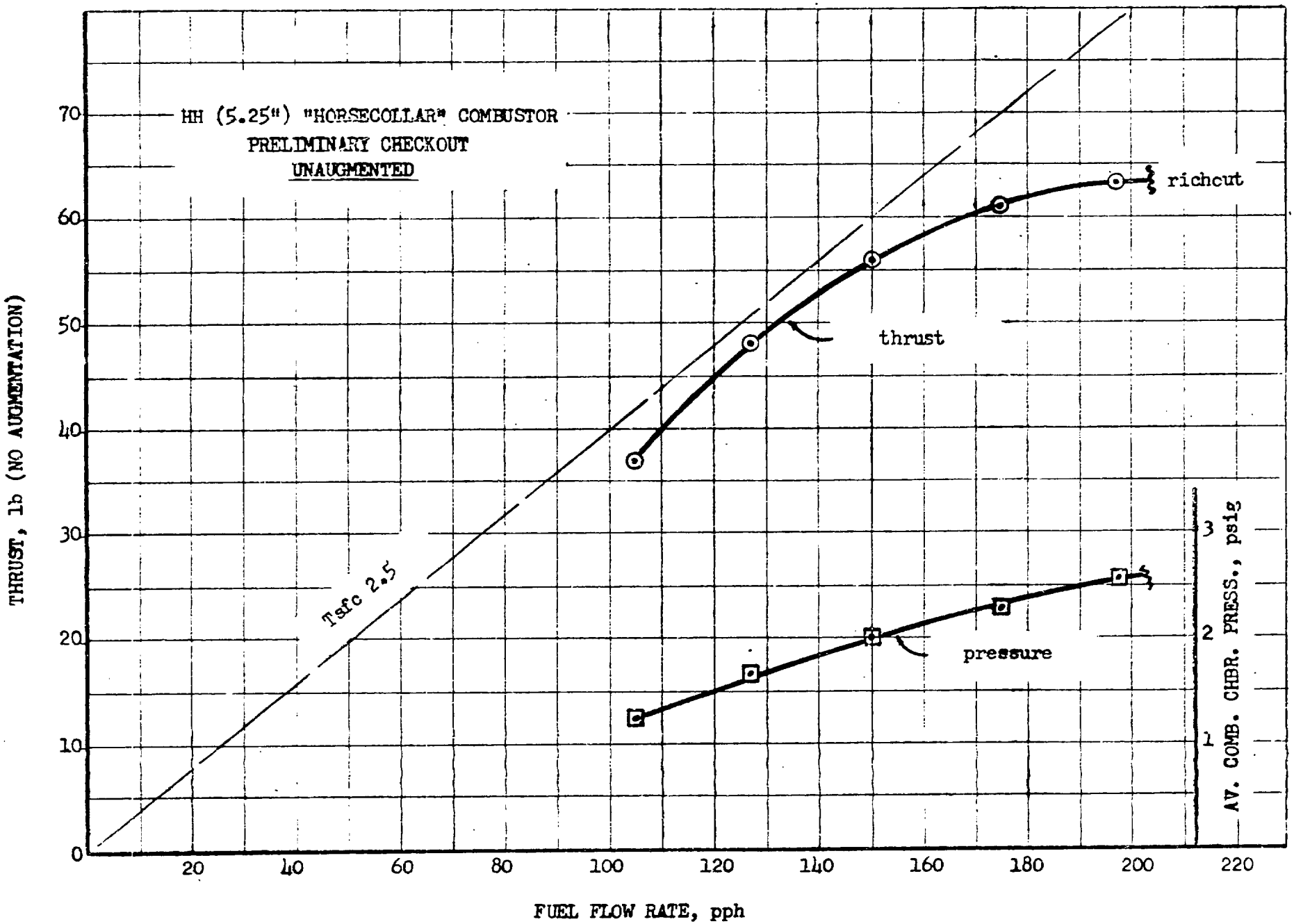

HH (5.25") "HORSECOLLAR" COMBUSTOR
PRELIMINARY CHECKOUT
UNAUGMENTED
richcut
thrust
pressure
Tsfc 2.5
THRUST, lb (NO AUGMENTATION)
AV. COMB. CHBR. PRESS., psig
FUEL FLOW RATE, pph
0
10
20
30
40
50
60
70
1
2
3
20
40
60
80
100
120
140
160
180
200
220

FIGURE 43

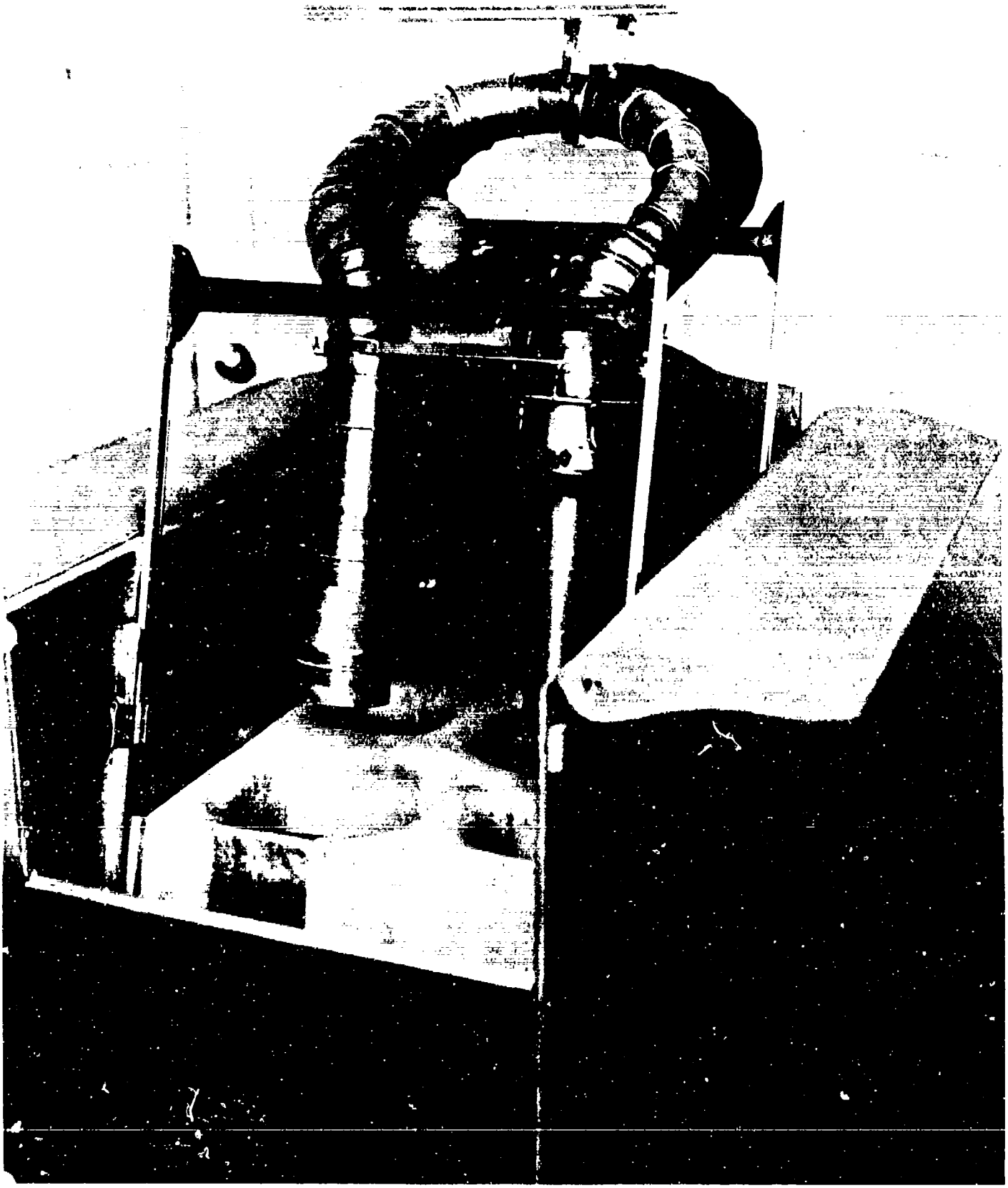
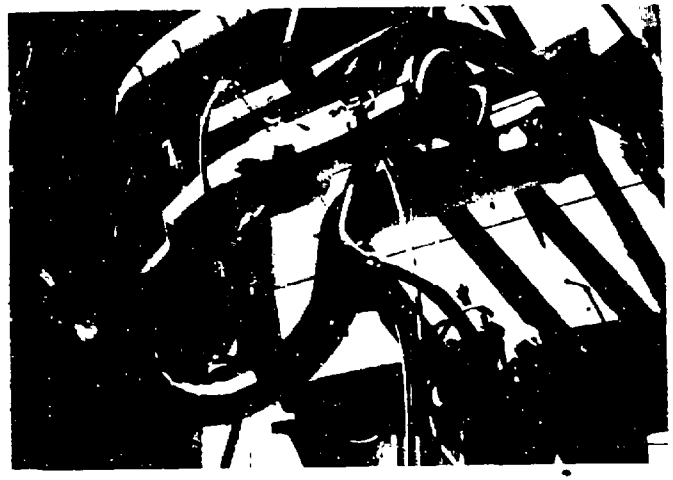


FIGURE 44: UNITIZED PULSE REACTOR LIFT ENGINE DISPLAY PACKAGE CONSISTING OF TWIN COMBUSTORS, AUGMENTERS, AND SHROUD OPEN FOR OPERATION



Rich out
HH(5.25")-5 "HORSECOLLAR"
UNAUGMENTED
Thrust
Pressure
Tsfc 2.0
Tsfc 2.5
THRUST, LB.
AV. COMB. CHBR. PRESS., psig
FUEL FLOW RATE, pph
0
10
20
30
40
50
60
70
20
40
60
80
100
120
140
1
2
3

FIGURE 45

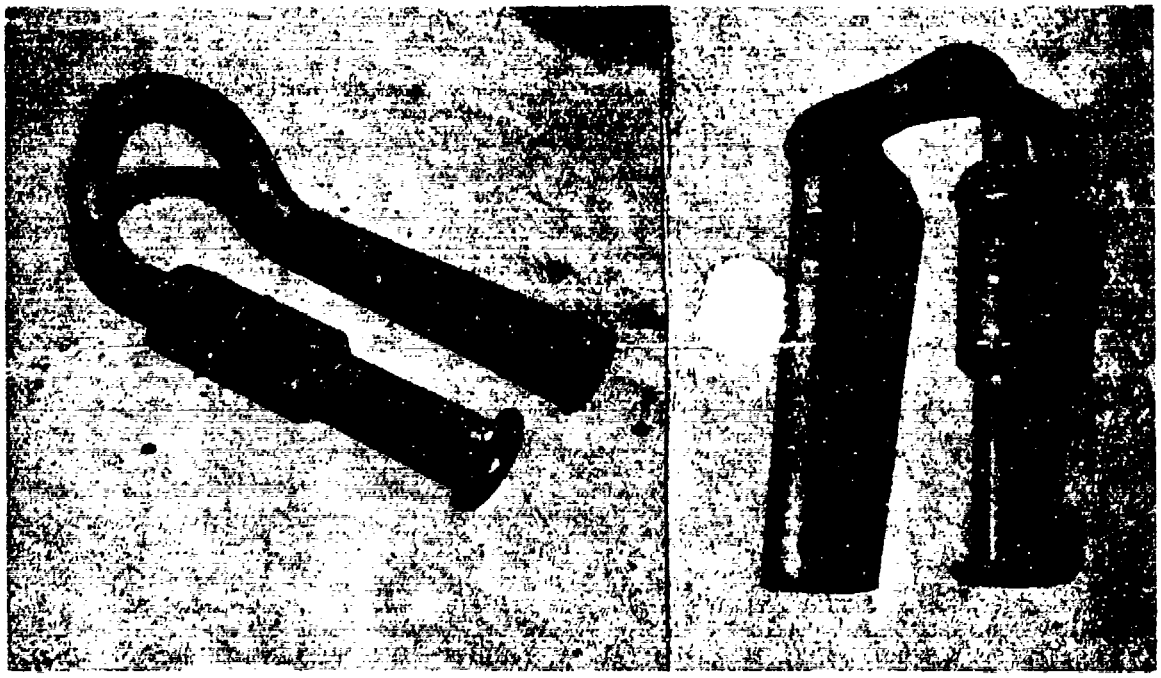


FIGURE 46: TWO VIEWS OF HH(5.25")-5 COMBUSTOR WITH BOTH ENDS ALIGNED AND WITH SHARP BEND IN TAILPIPE



FIGURE 47: HH(5.25")-5 COMBUSTOR WITH BEND LOCATED IN AFT PART OF COMBUSTION CHAMBER

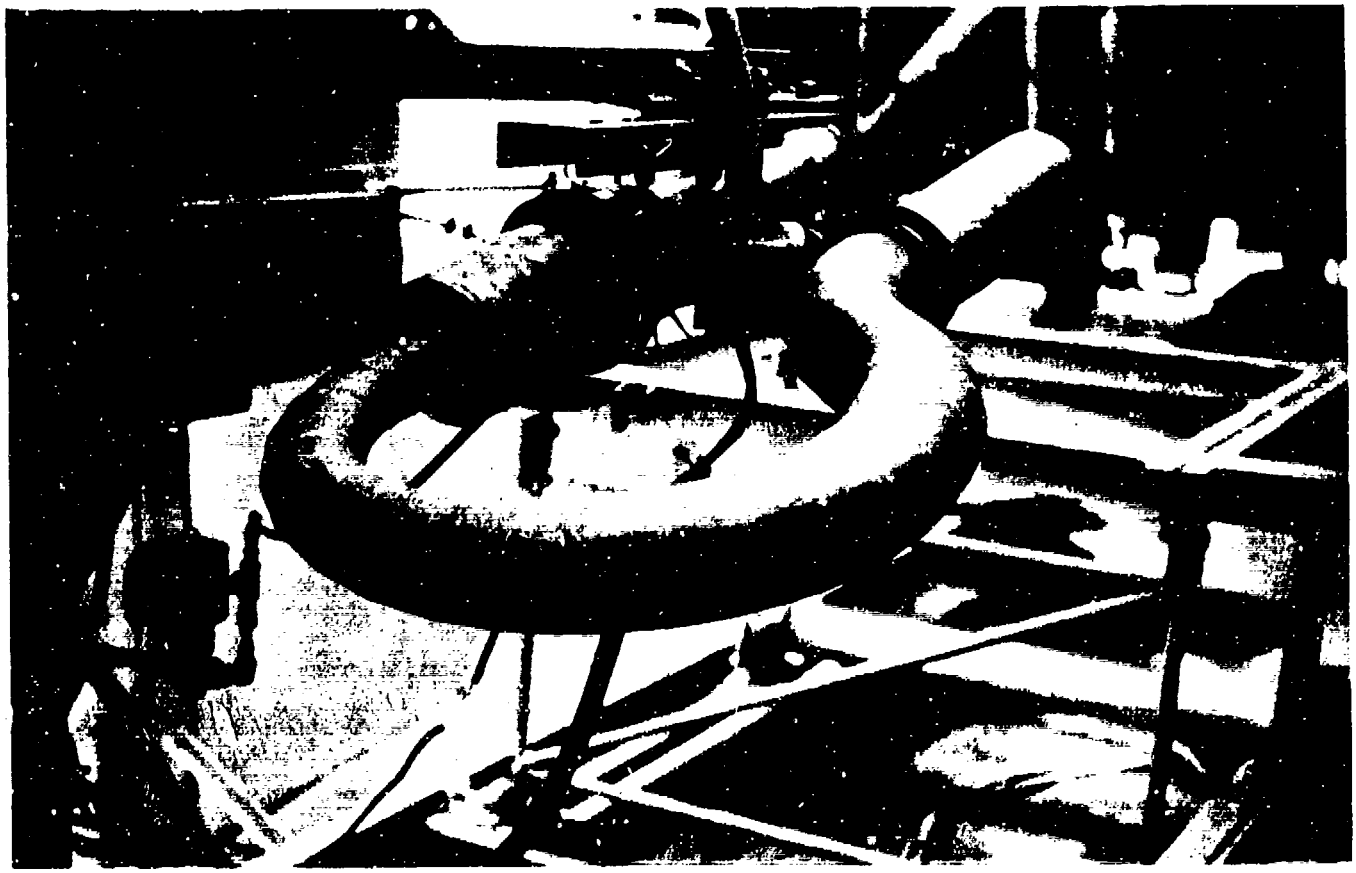


FIGURE 48: HH(5.25")-6 COMBUSTOR WITH 9.25" RADIUS MITERED TURN SECTION MODIFIED FROM -5 "HORSECOLLAR" MODEL BY REMOVING BEND IN COMBUSTION CHAMBER

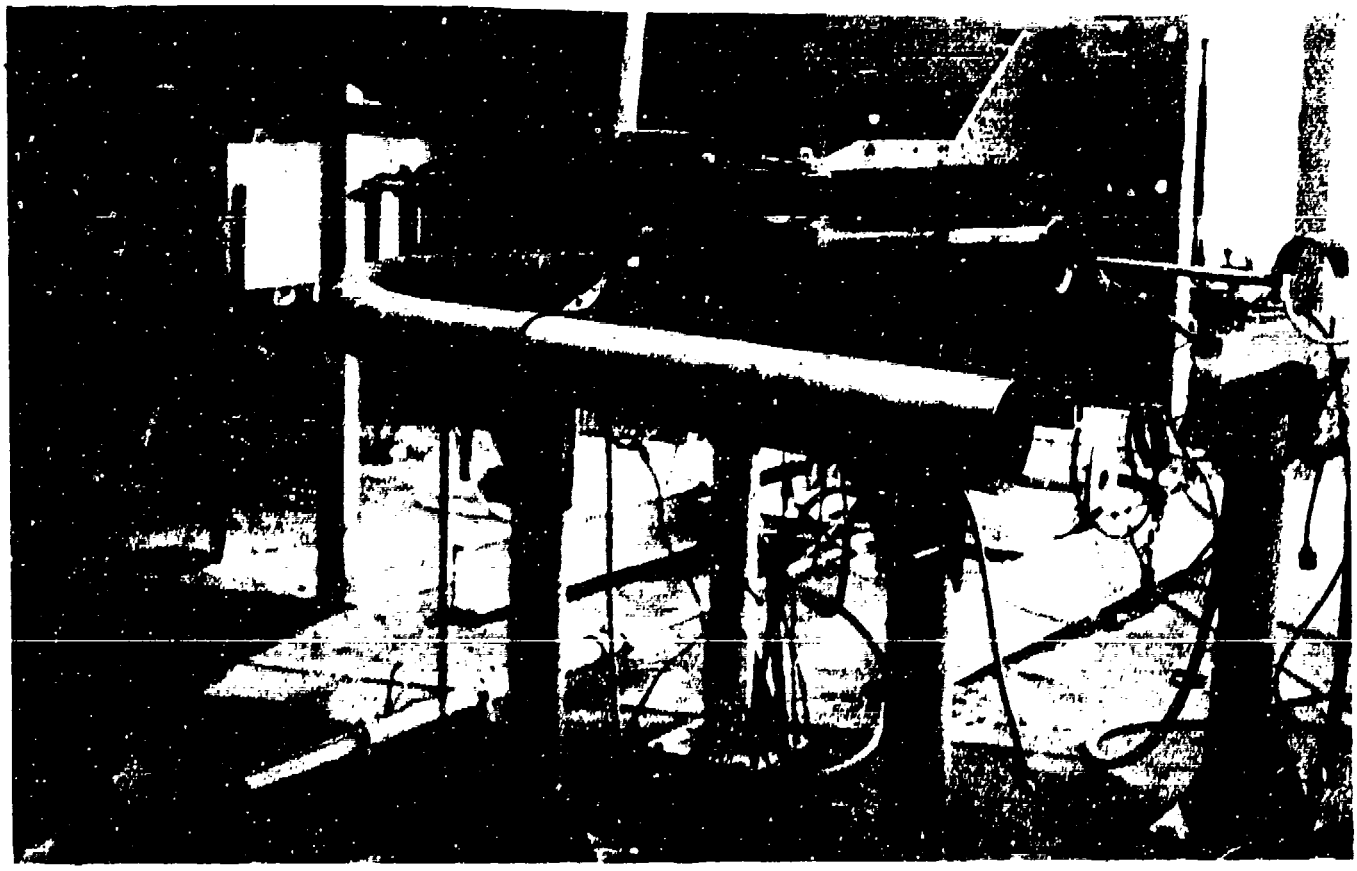


FIGURE 49: HH(5.25")-6 COMBUSTOR WITH 9.25" RADIUS MITERED TURN SECTION

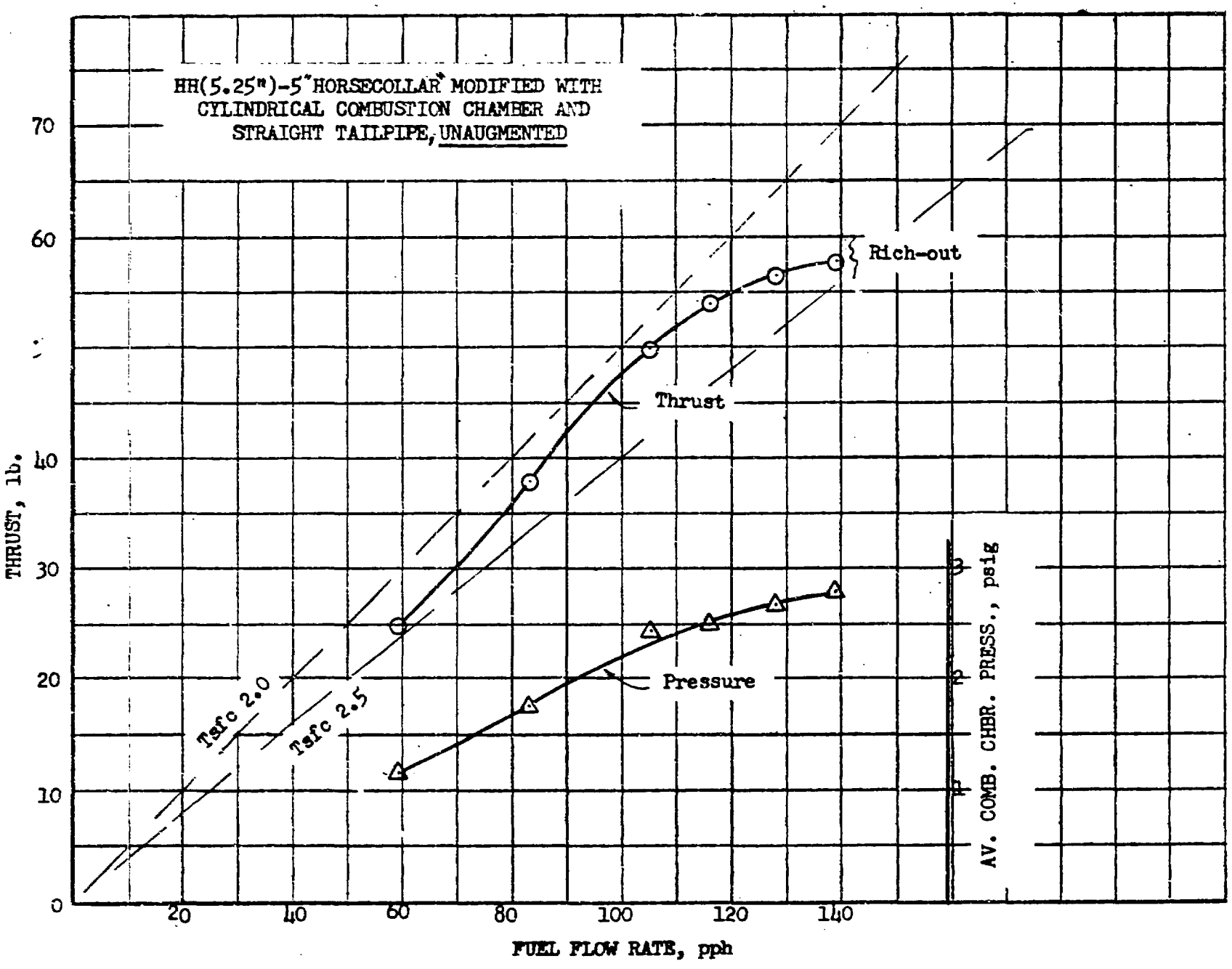

HH(5.25")-5" HORSECOLLAR MODIFIED WITH
CYLINDRICAL COMBUSTION CHAMBER AND
STRAIGHT TAILPIPE, UNAUGMENTED
Rich-out
Thrust
Pressure
Tsfc 2.0
Tsfc 2.5
THRUST, lb.
AV. COMB. CHBR. PRESS., psig
FUEL FLOW RATE, pph
0
10
20
30
40
60
70
20
40
60
80
100
120
140

FIGURE 50

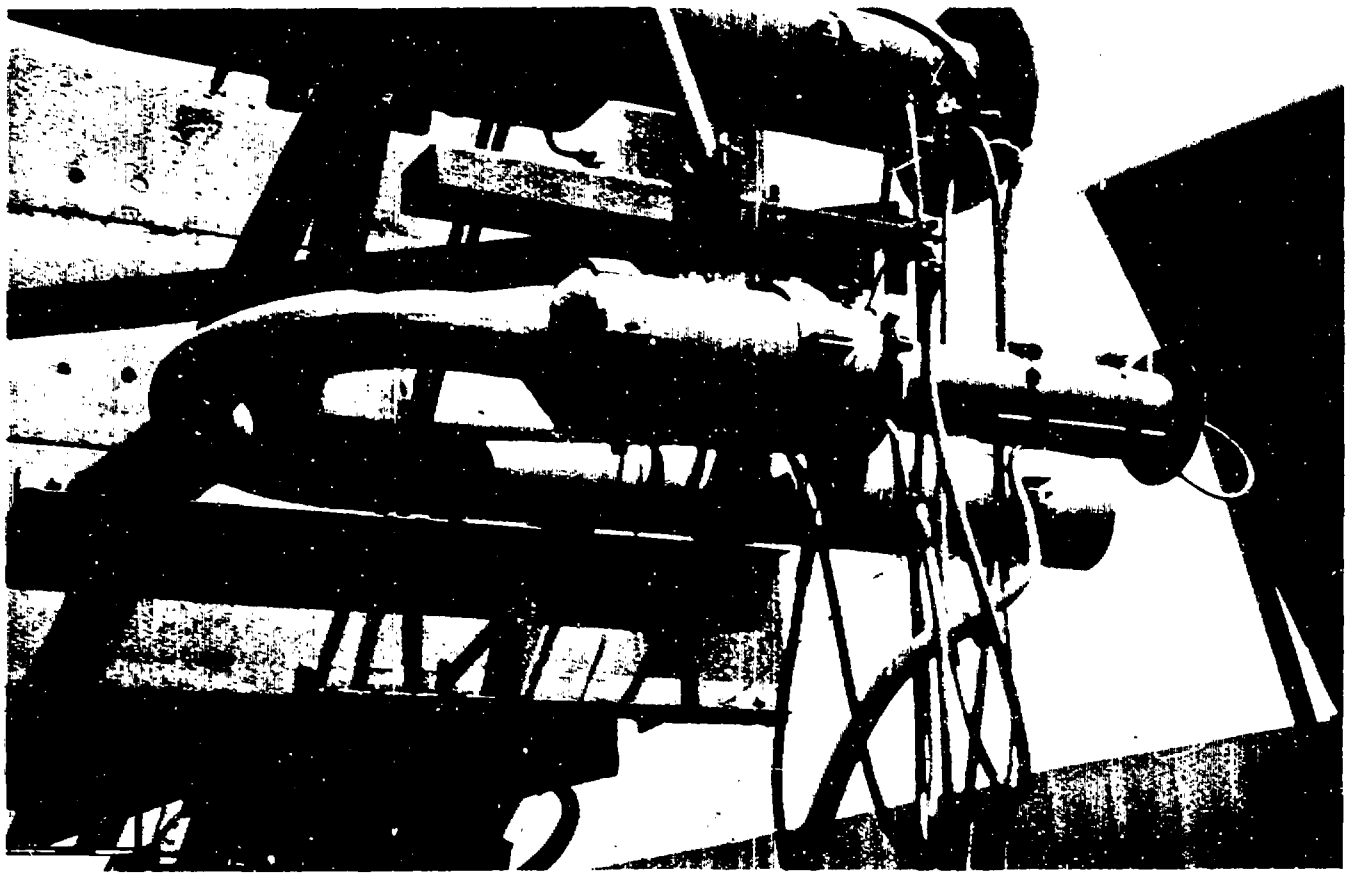
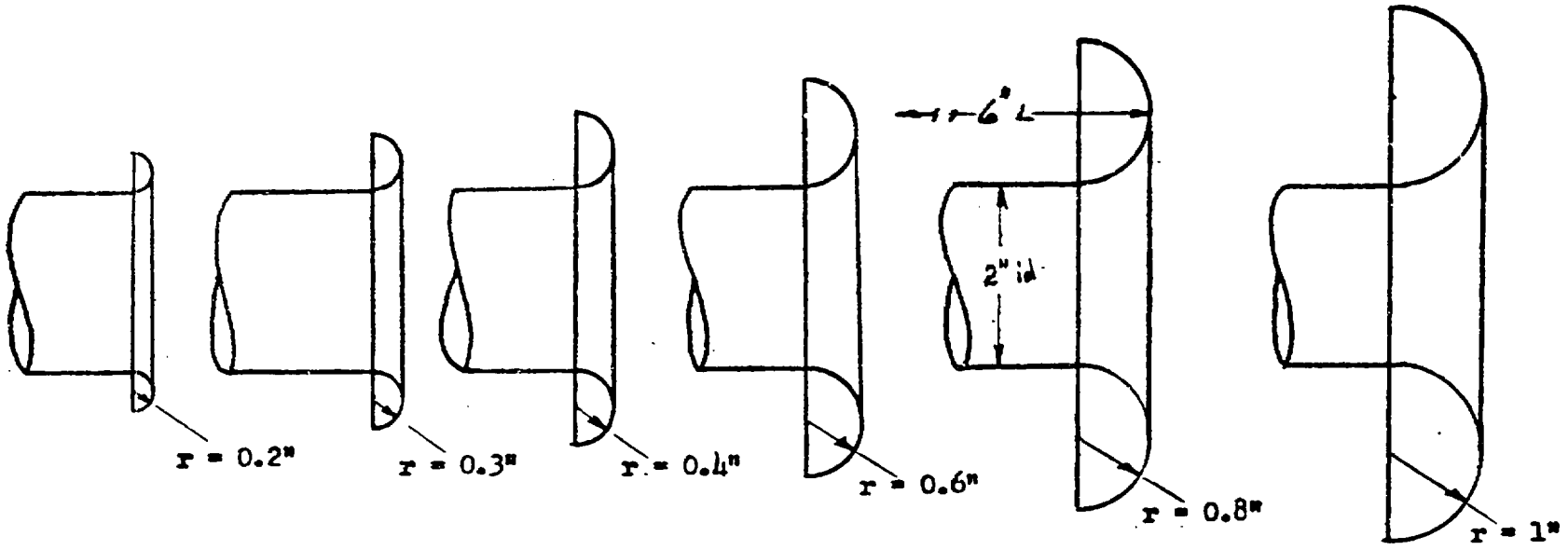


FIGURE 51: FLAT U-SHAPED HH(5.25")-5 COMBUSTOR ON TEST STAND



Cylindrical Augmenters
2" i.d. by 6" L

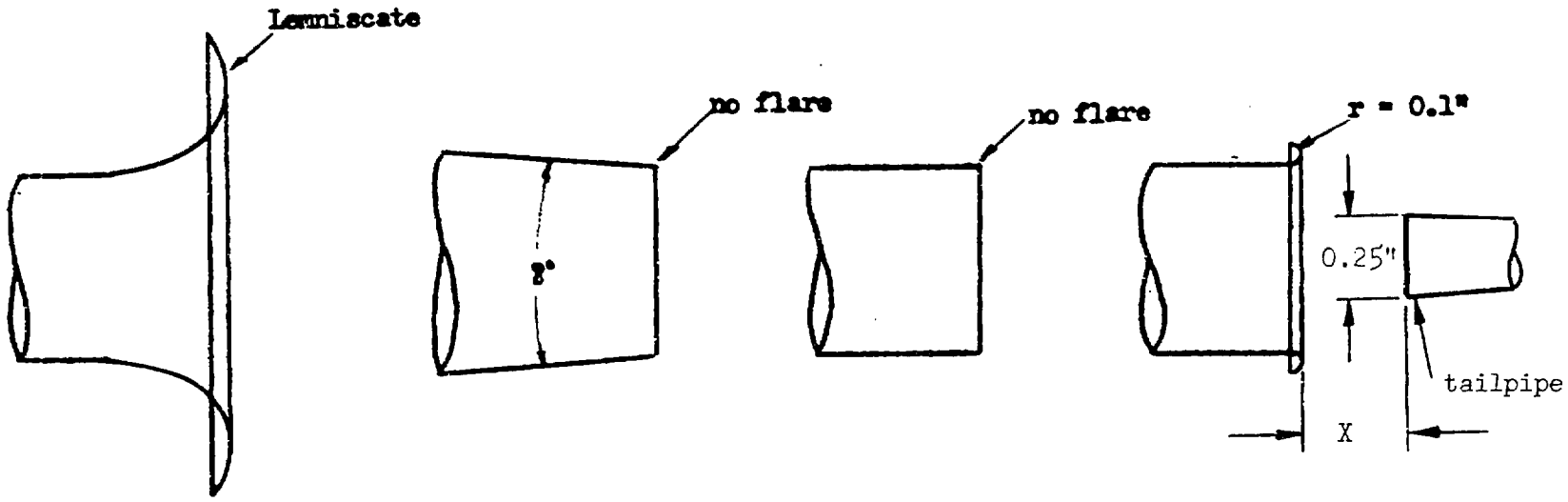


FIGURE 52: AUGMENTER FLARE CONFIGURATIONS

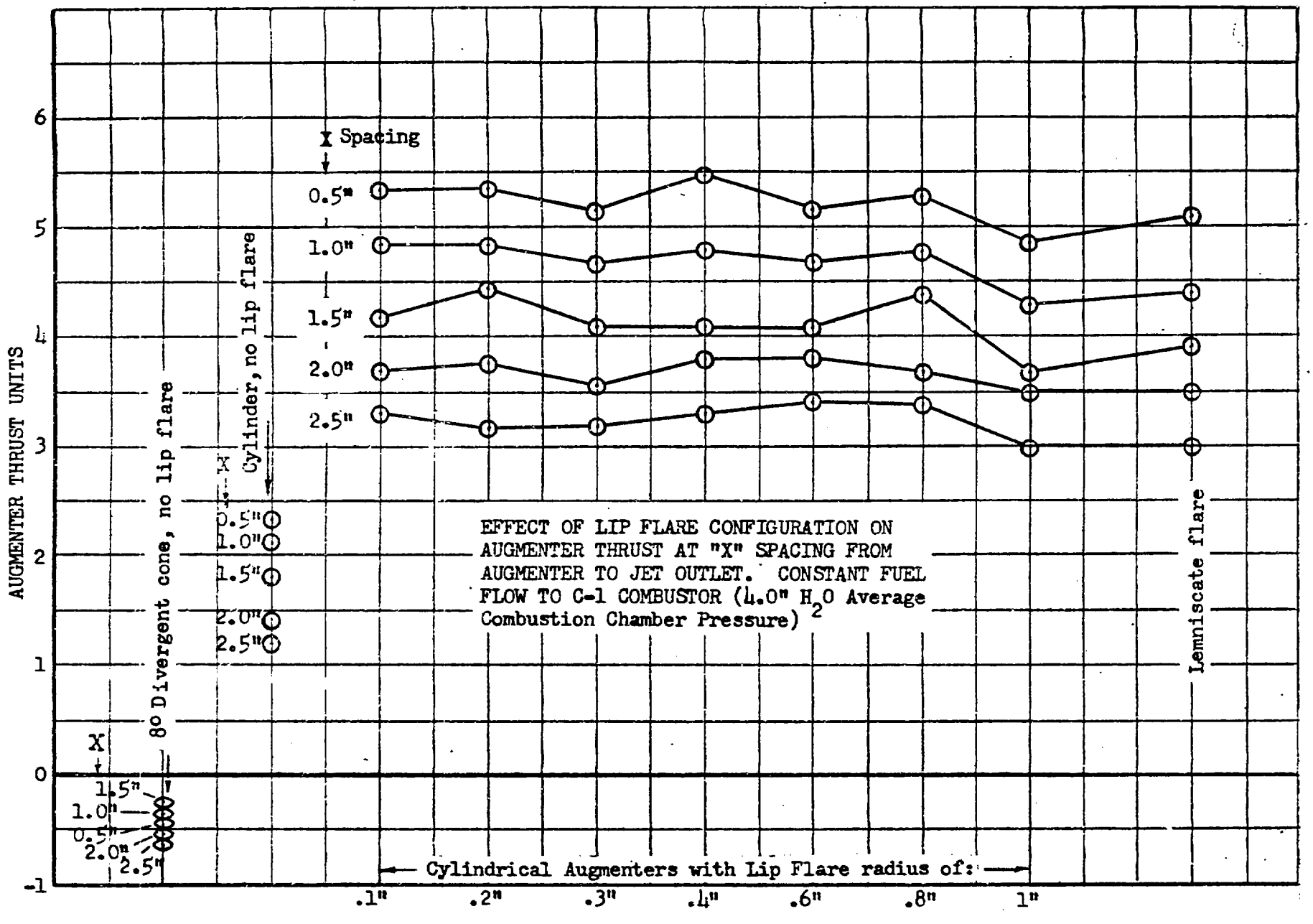

AUGMENTER THRUST UNITS
6
5
4
3
2
1
0
-1
X Spacing
0.5"
1.0"
1.5"
2.0"
2.5"
Cylinder, no lip flare
8° Divergent cone, no lip flare
Lemniscate flare
EFFECT OF LIP FLARE CONFIGURATION ON AUGMENTER THRUST AT "X" SPACING FROM AUGMENTER TO JET OUTLET. CONSTANT FUEL FLOW TO C-1 COMBUSTOR (4.0" H_2O Average Combustion Chamber Pressure)
Cylindrical Augmenters with Lip Flare radius of:
.1"
.2"
.3"
.4"
.6"
.8"
1"
LIP CONFIGURATION

FIGURE 53

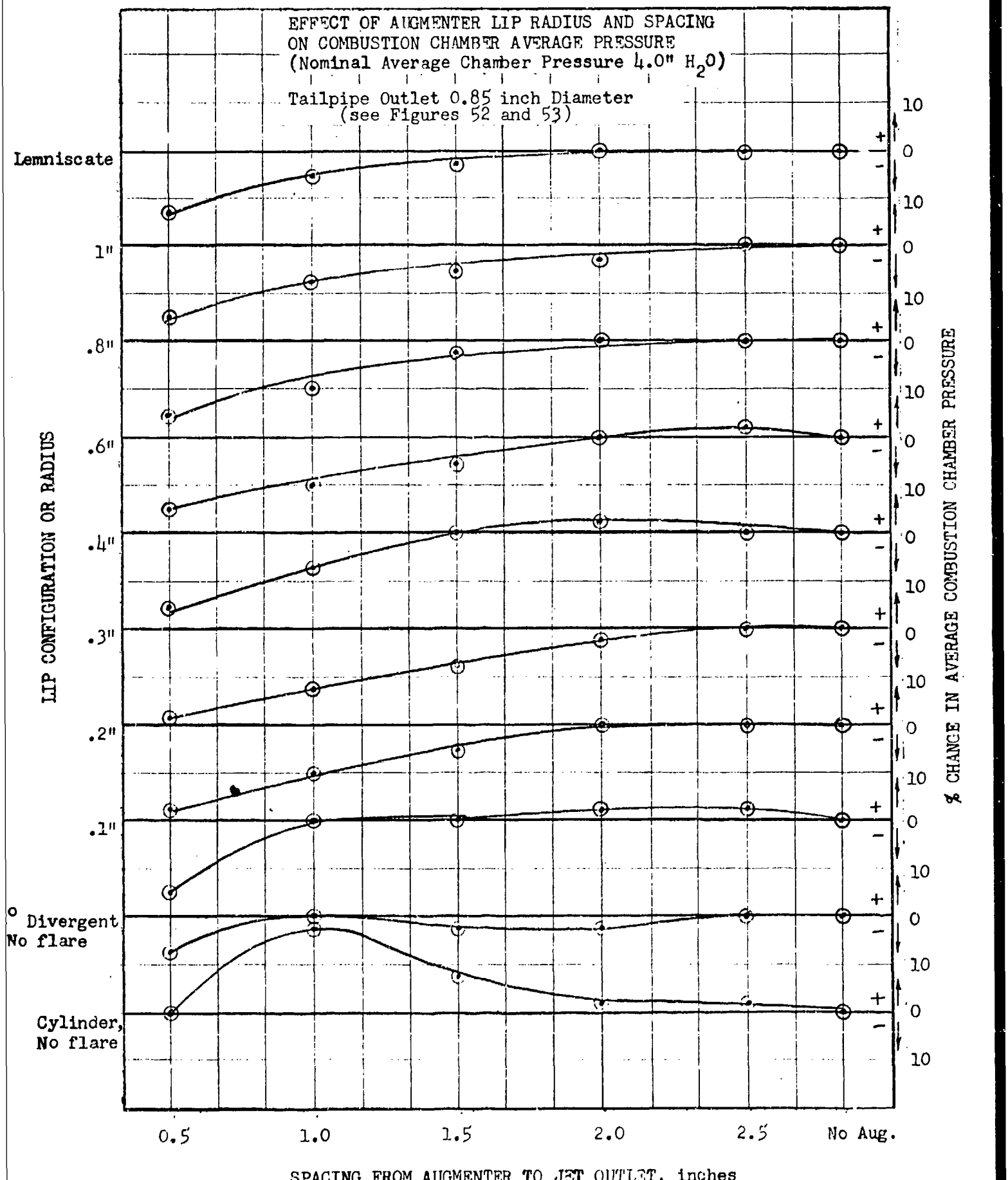

EFFECT OF AUGMENTER LIP RADIUS AND SPACING
ON COMBUSTION CHAMBER AVERAGE PRESSURE
(Nominal Average Chamber Pressure 4.0" H_2O)
Tailpipe Outlet 0.85 inch Diameter
(see Figures 52 and 53)
Lemniscate
1"
.8"
.6"
.4"
.3"
.2"
.1"
0° Divergent
No flare
Cylinder,
No flare
LIP CONFIGURATION OR RADIUS
0.5
1.0
1.5
2.0
2.5
No Aug.
SPACING FROM AUGMENTER TO JET OUTLET, inches
% CHANCE IN AVERAGE COMBUSTION CHAMBER PRESSURE
10
0
10
0
10
0
10
0
10
0
10
0
10
0
10
0
10
0
10
0
10
+
-

FIGURE 54

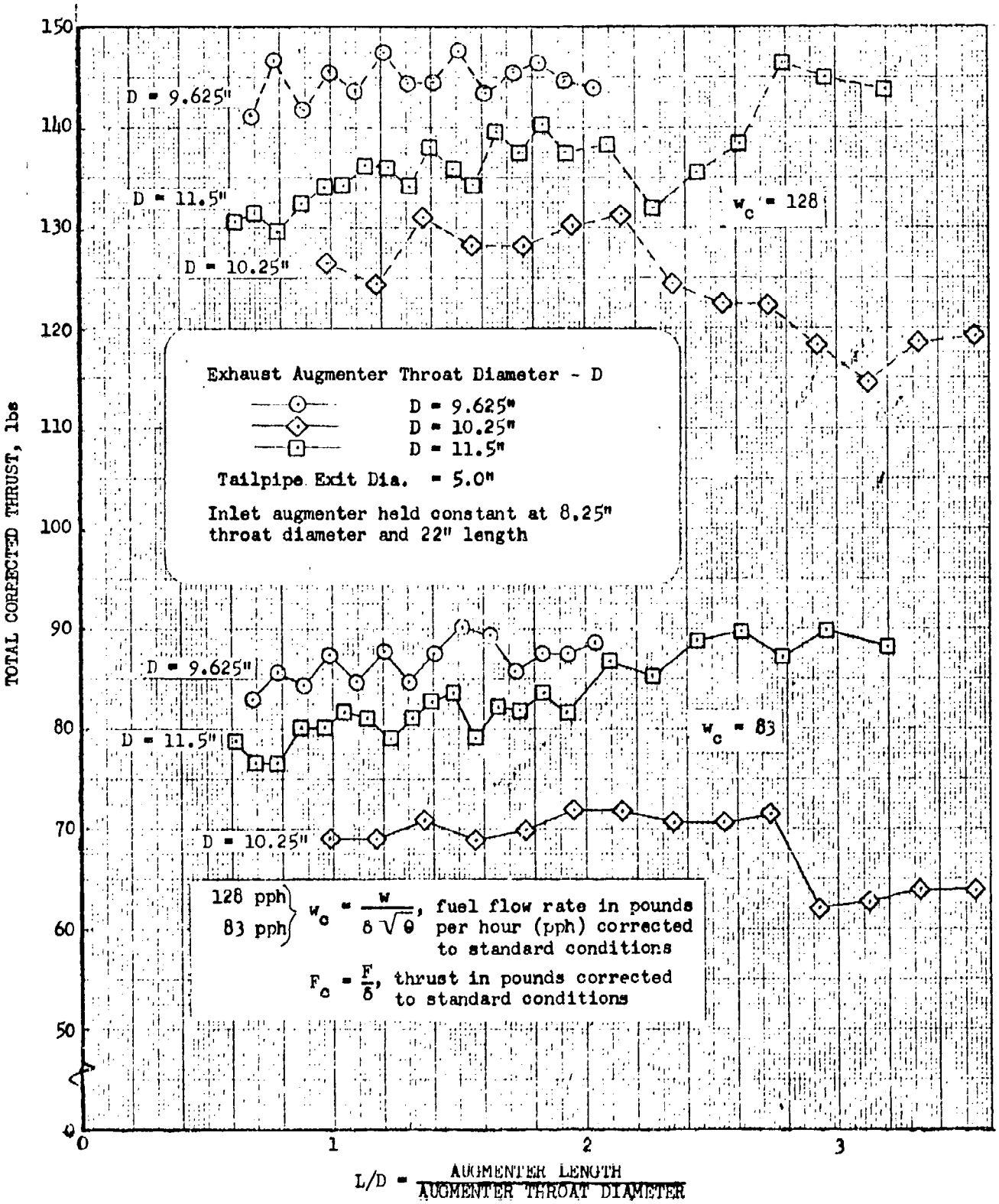


FIGURE 55: EXHAUST AUGMENTER TUNING FOR THE HH 5.25-5 90° COMBUSTOR

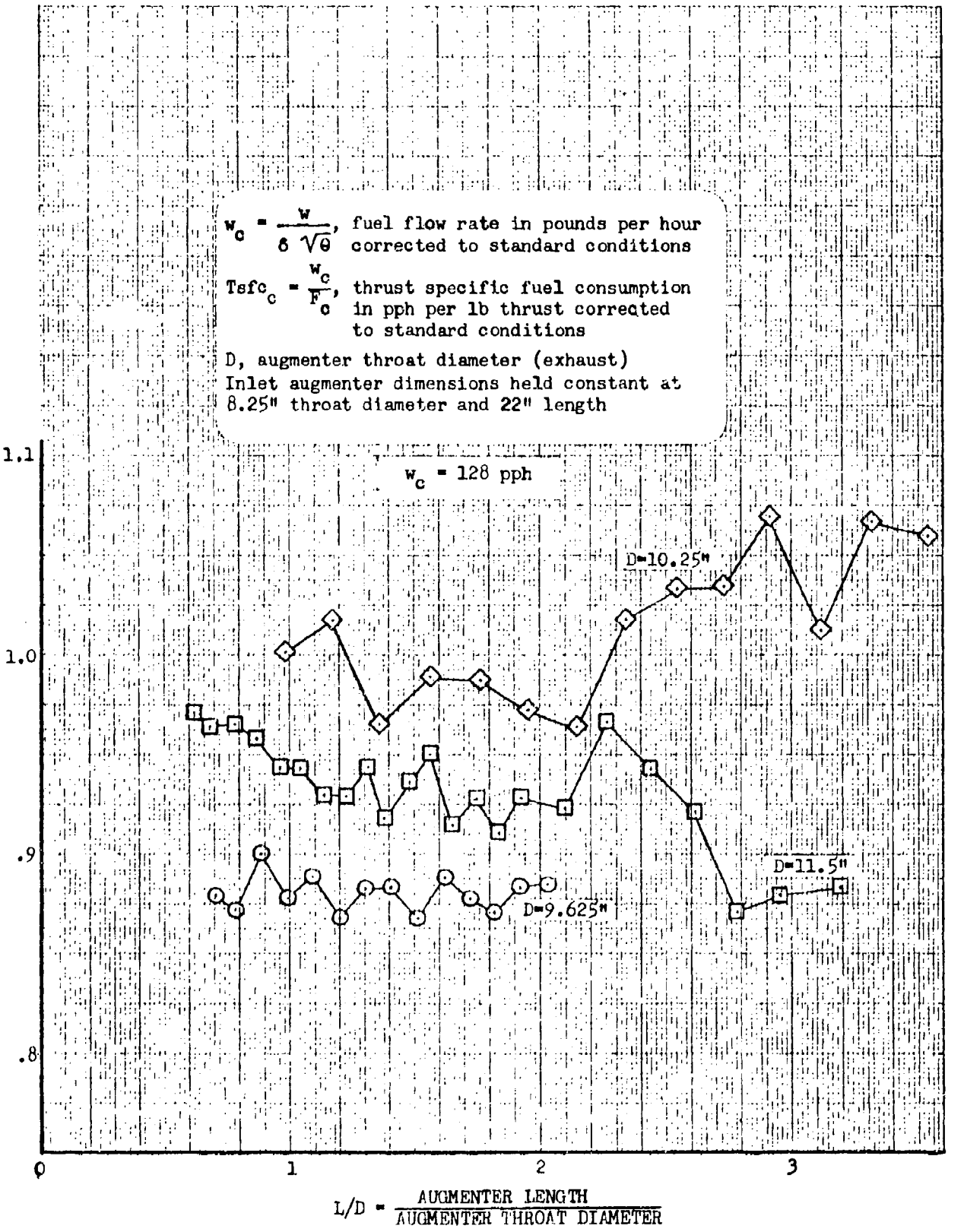


FIGURE 56: EXHAUST AUGMENTER TUNING FOR THE HI(5.25")-5 90° COMBUSTOR

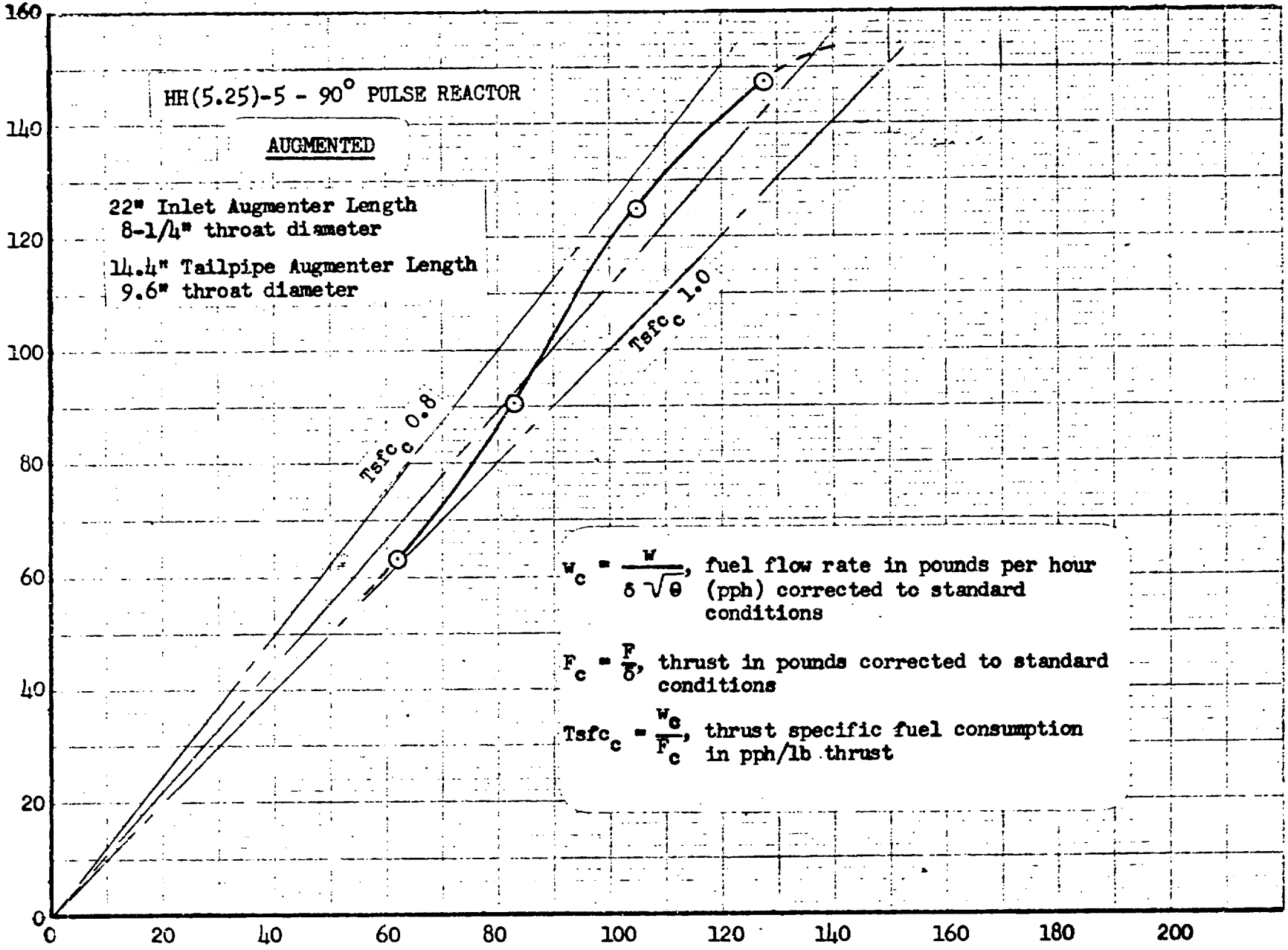
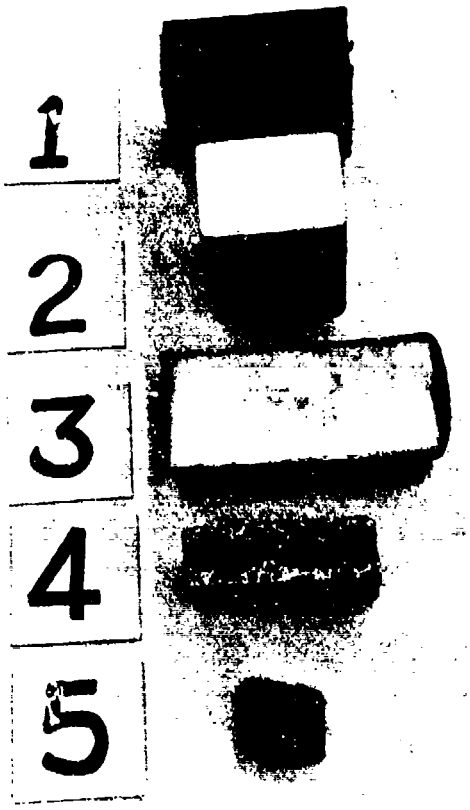

HH(5.25)-5 - 90° PULSE REACTOR
AUGMENTED
22" Inlet Augmenter Length
8-1/4" throat diameter
14.4" Tailpipe Augmenter Length
9.6" throat diameter
Tsfc c 0.8
Tsfc c 1.0
$W_c = \frac{W}{\delta\sqrt{\theta}}$, fuel flow rate in pounds per hour (pph) corrected to standard conditions
$F_c = \frac{F}{\delta}$, thrust in pounds corrected to standard conditions
$Tsfc_c = \frac{W_c}{F_c}$, thrust specific fuel consumption in pph/lb thrust
CORRECTED THRUST, lbs.
0
20
40
60
80
100
120
140
160
180
200
CORRECTED FUEL FLOW RATE, pph

FIGURE 57



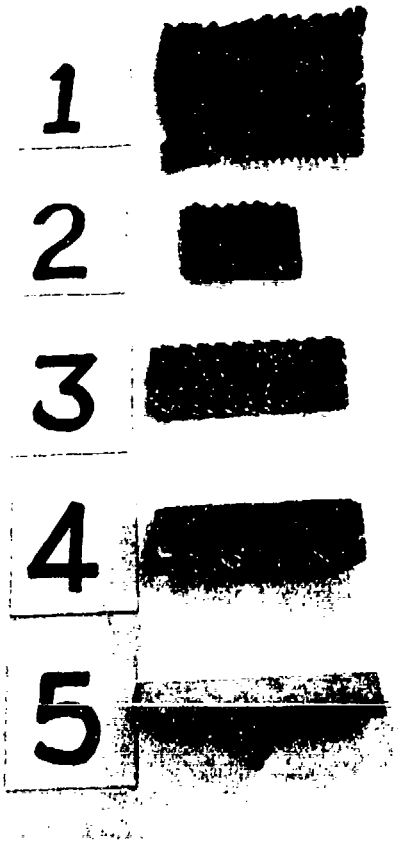


FIGURE 58: VARIOUS SANDWICH CONSTRUCTION MATERIALS CONSIDERED IN THE DESIGN AND CONSTRUCTION OF AUGMENTERS AND ENGINE SHROUDS

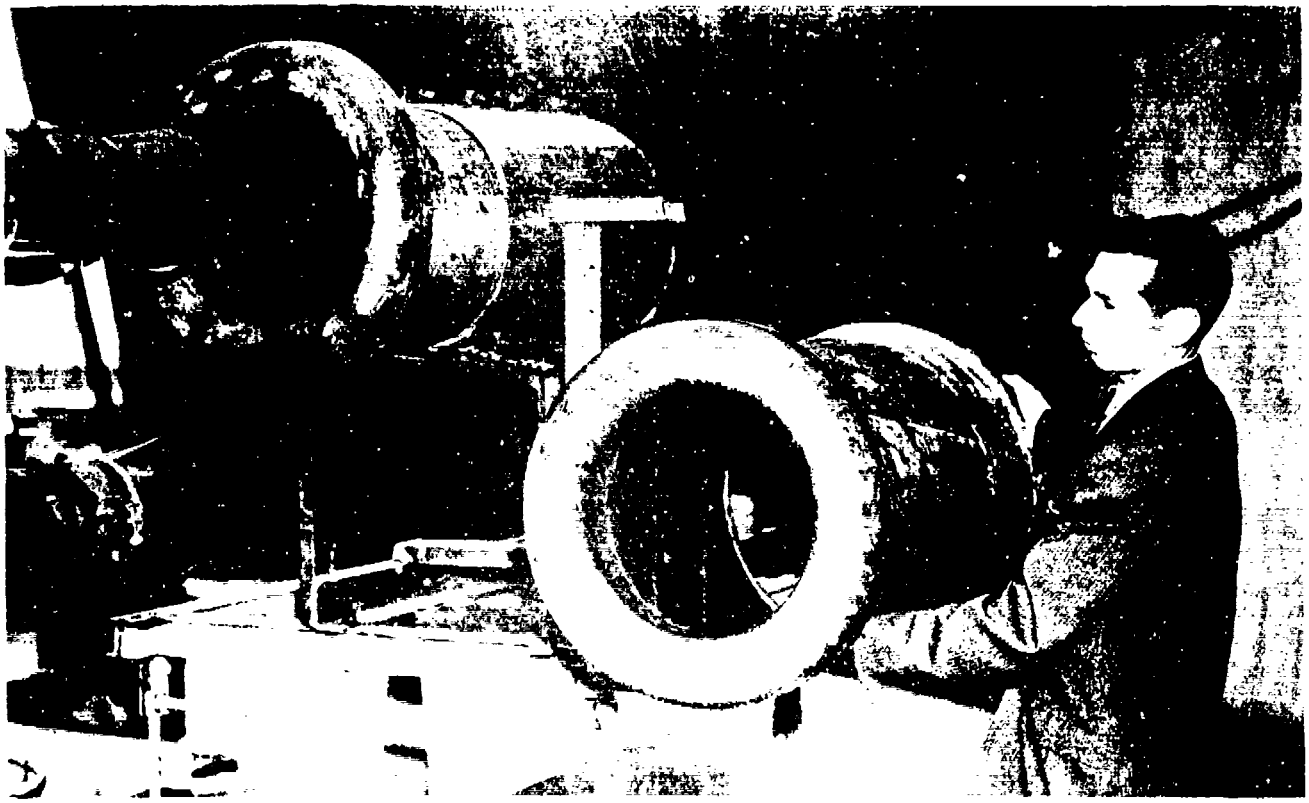


FIGURE 59: INLET THRUST AUGMENTERS FOR HS-1B 9.1" DIAMETER PULSE REACTOR CONSTRUCTED OF FIBERGLASS SKIN AND HONEYCOMB

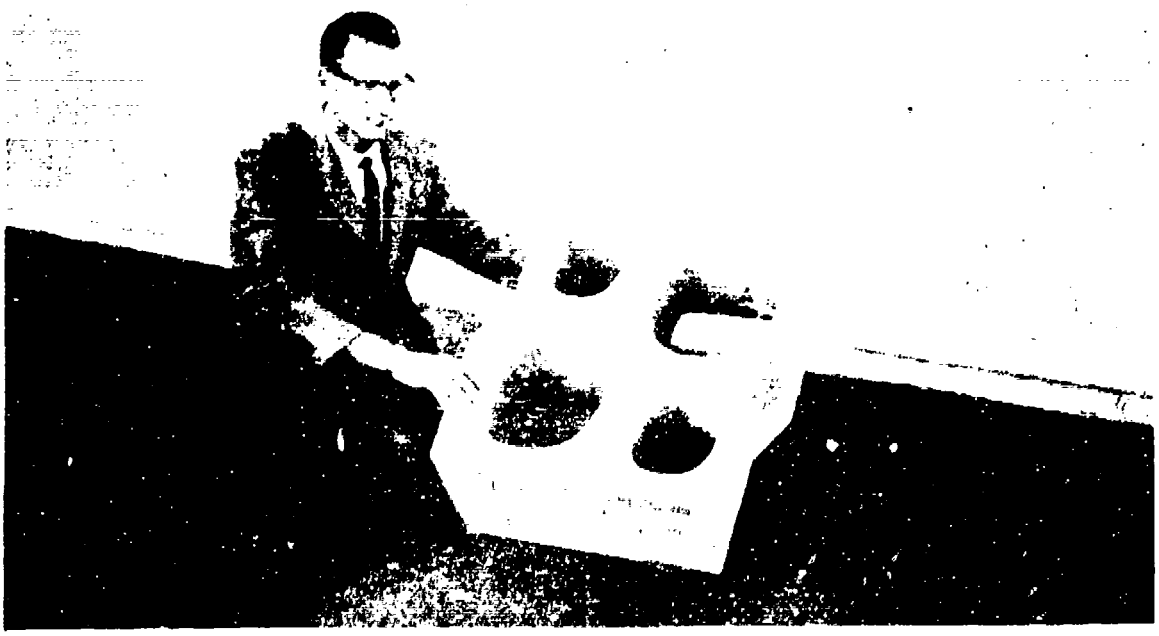
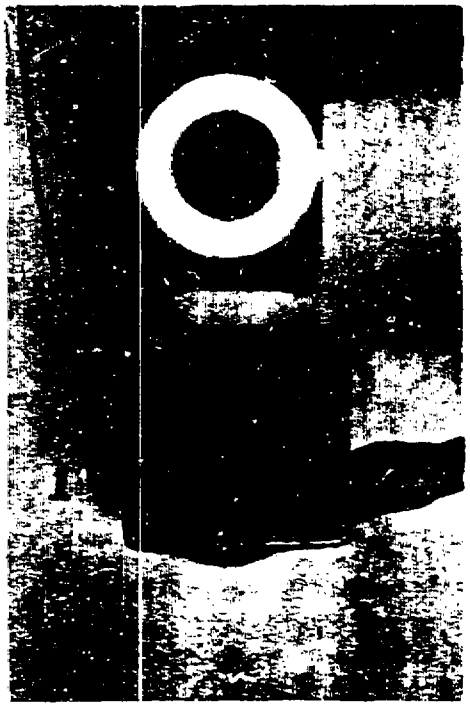
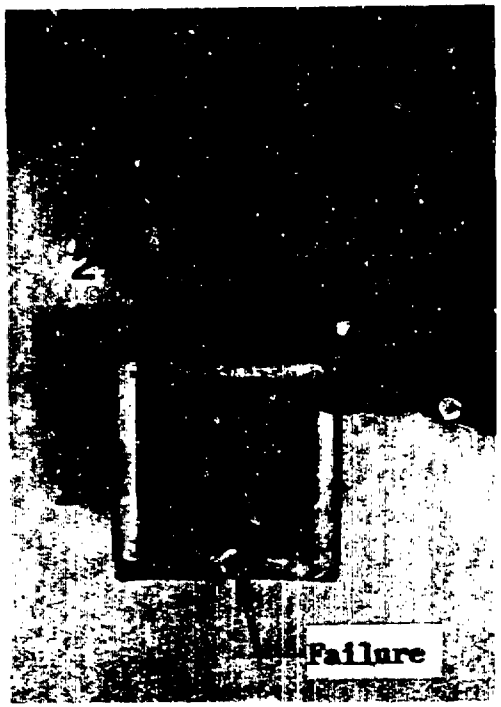


FIGURE 60: AUGMENTER CLUSTER FOR A PAIR OF HH(5.25")-5 COMBUSTORS, CONSTRUCTED OF "STA-FOAM" AND FIBERGLAS REINFORCED PLASTIC - WEIGHT 12½ lb.





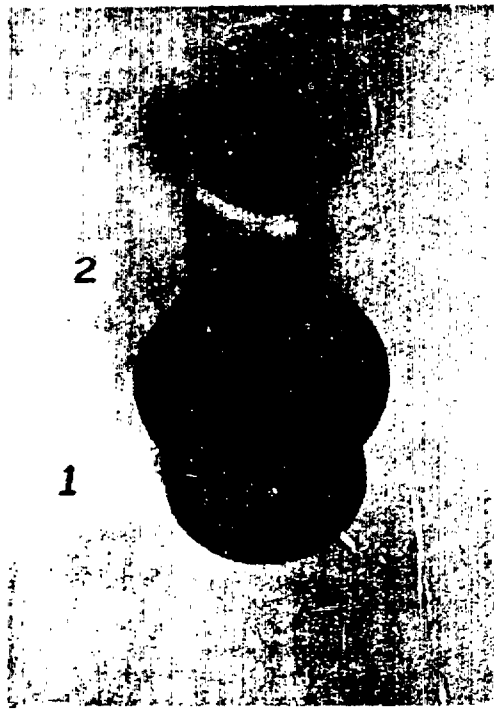


FIGURE 61: EXAMPLES OF AUGMENTERS OF SANDWICH CONSTRUCTION USING POLYURETHANE FOAM CORE. THE AUGMENTERS WITH RECTANGULAR OUTLETS REQUIRE REINFORCING OF THE FLAT SURFACES

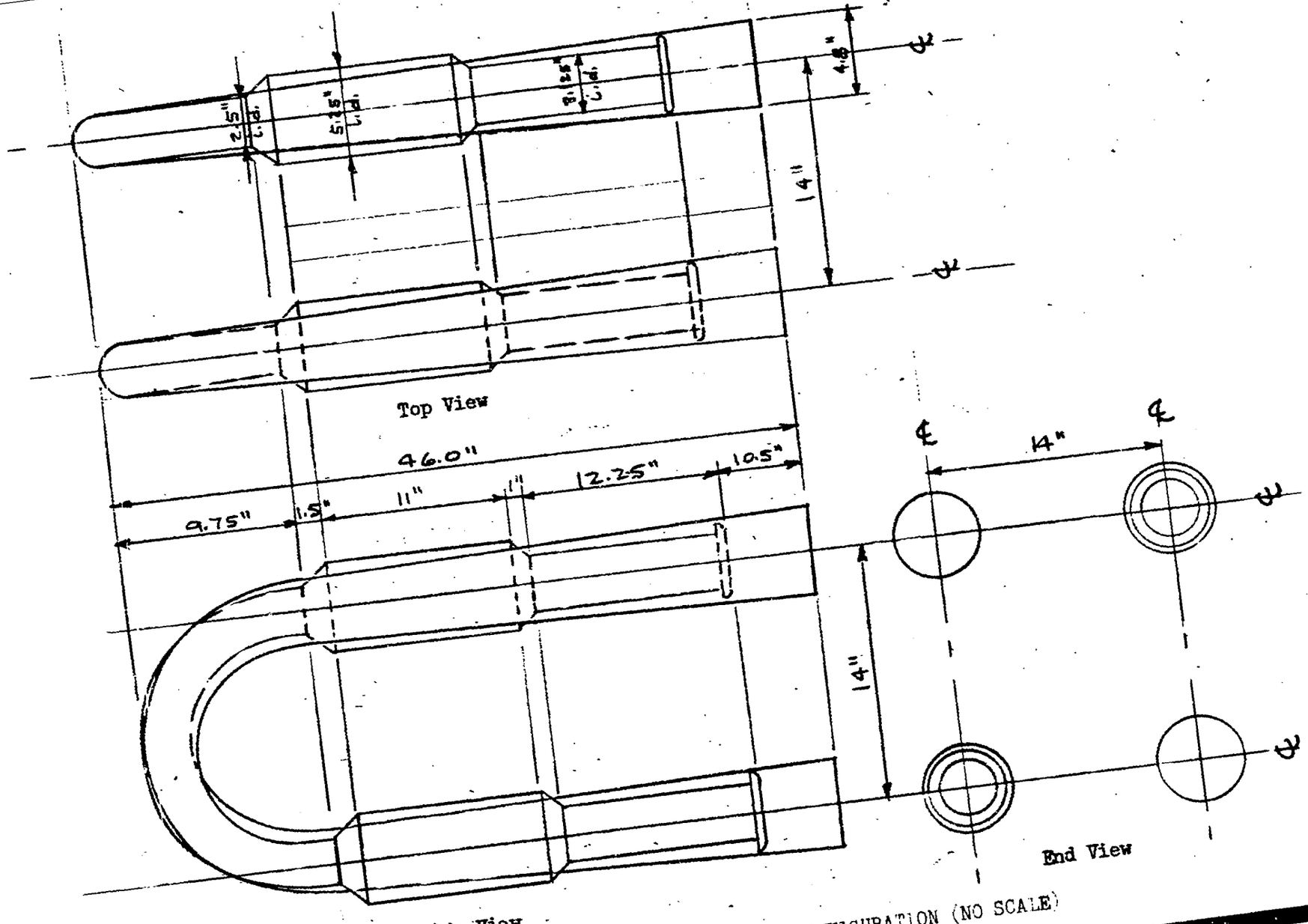


FIGURE 61: DUAL MOUNTED HH(5.3[illegible])-5-? ENGINE (COMBUSTOR) CONFIGURATION (NO SCALE)

11c

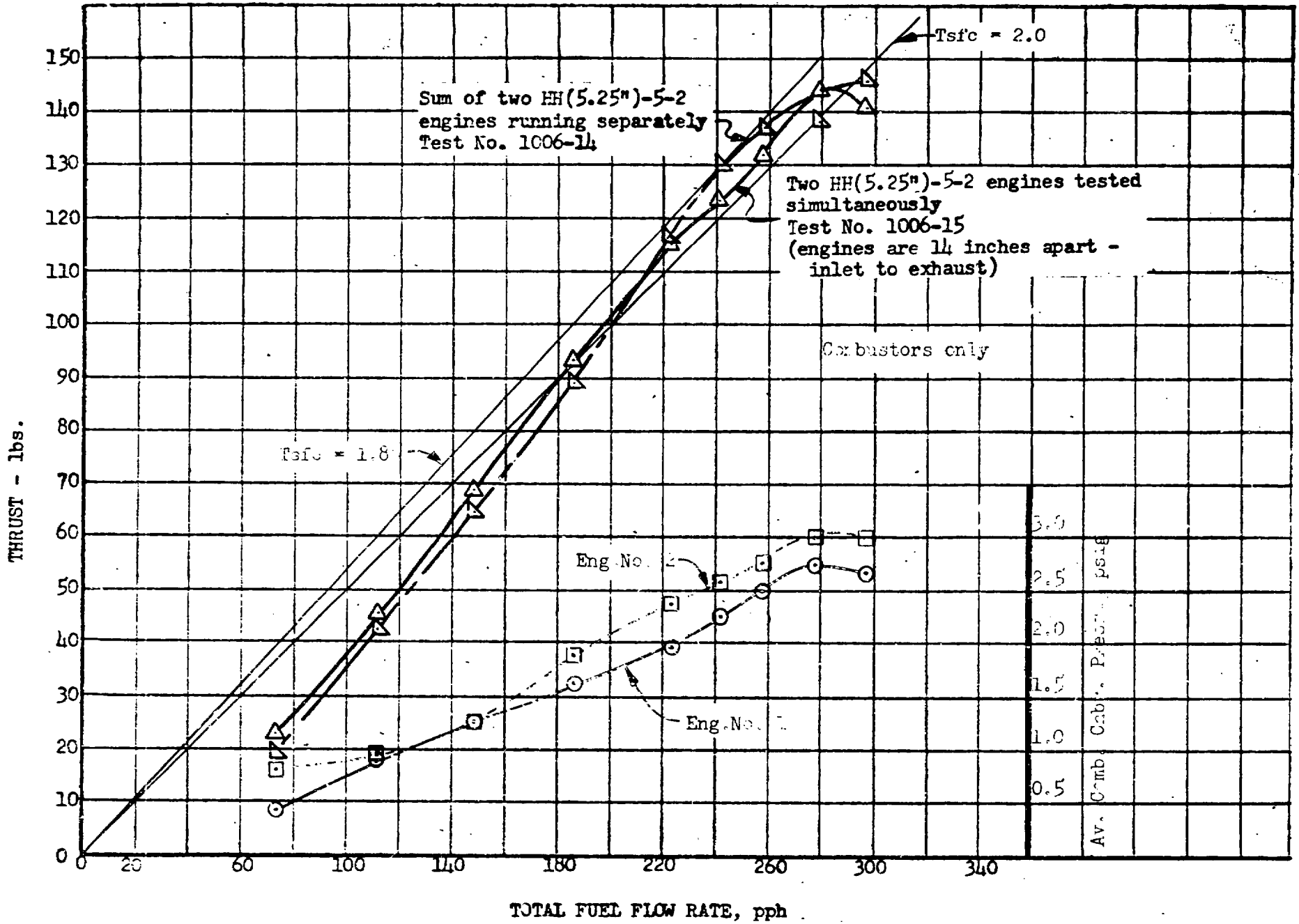


FIGURE 63: EFFECT OF ENGINE PROXIMITY

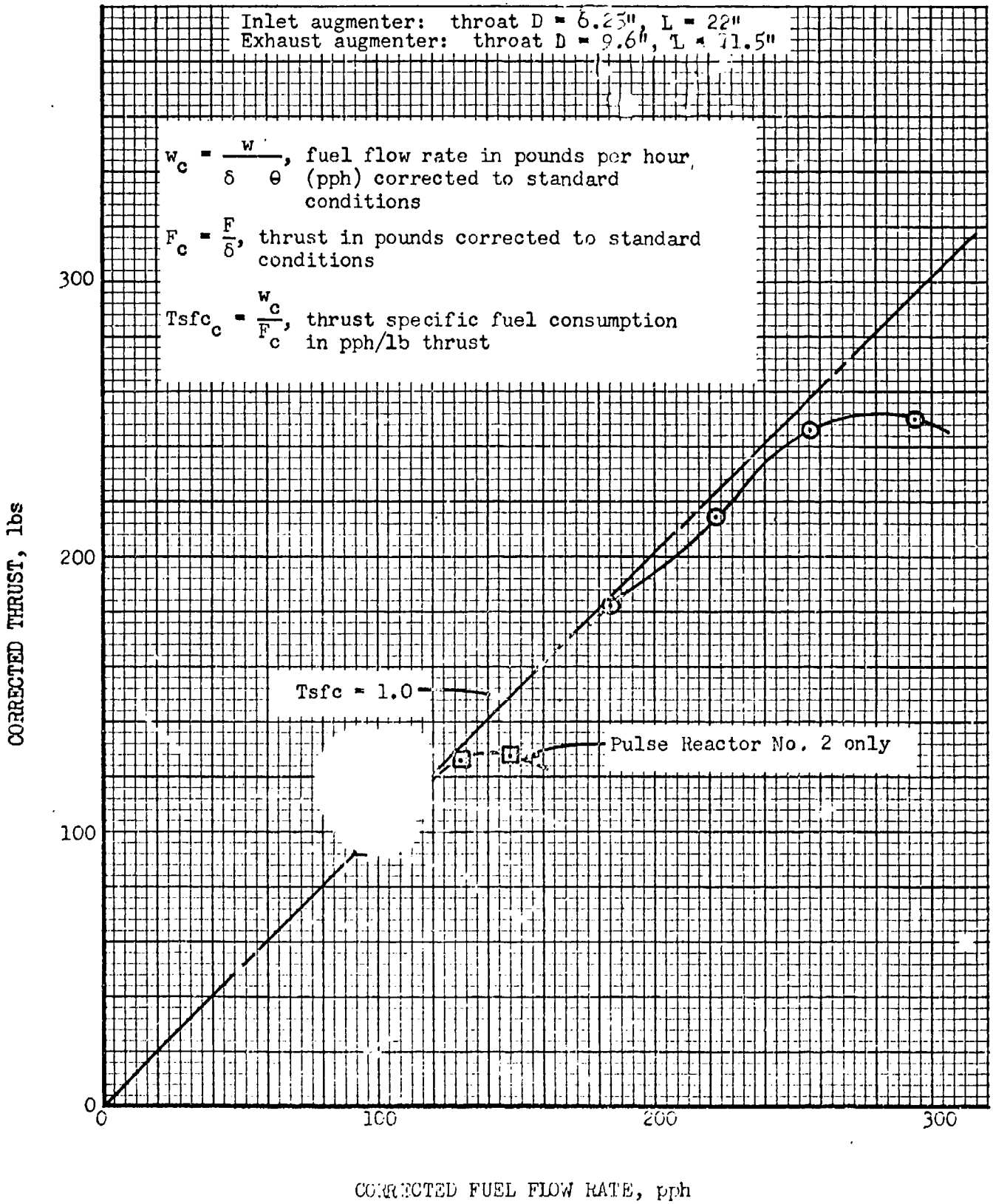


FIGURE 64: DUAL HH(5.25")-5-2 U-SHAPED PULSE REACTOR AUGMENTED

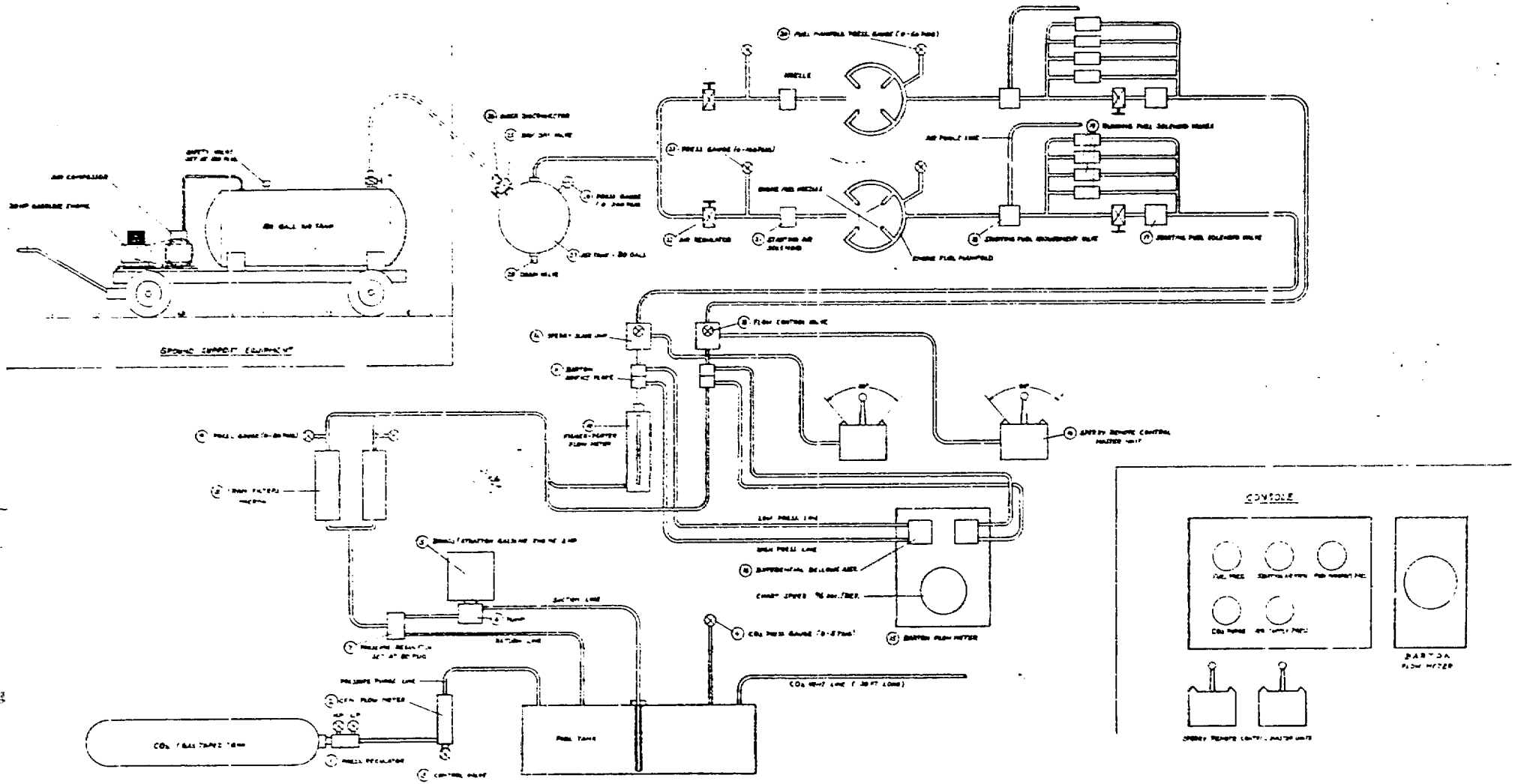
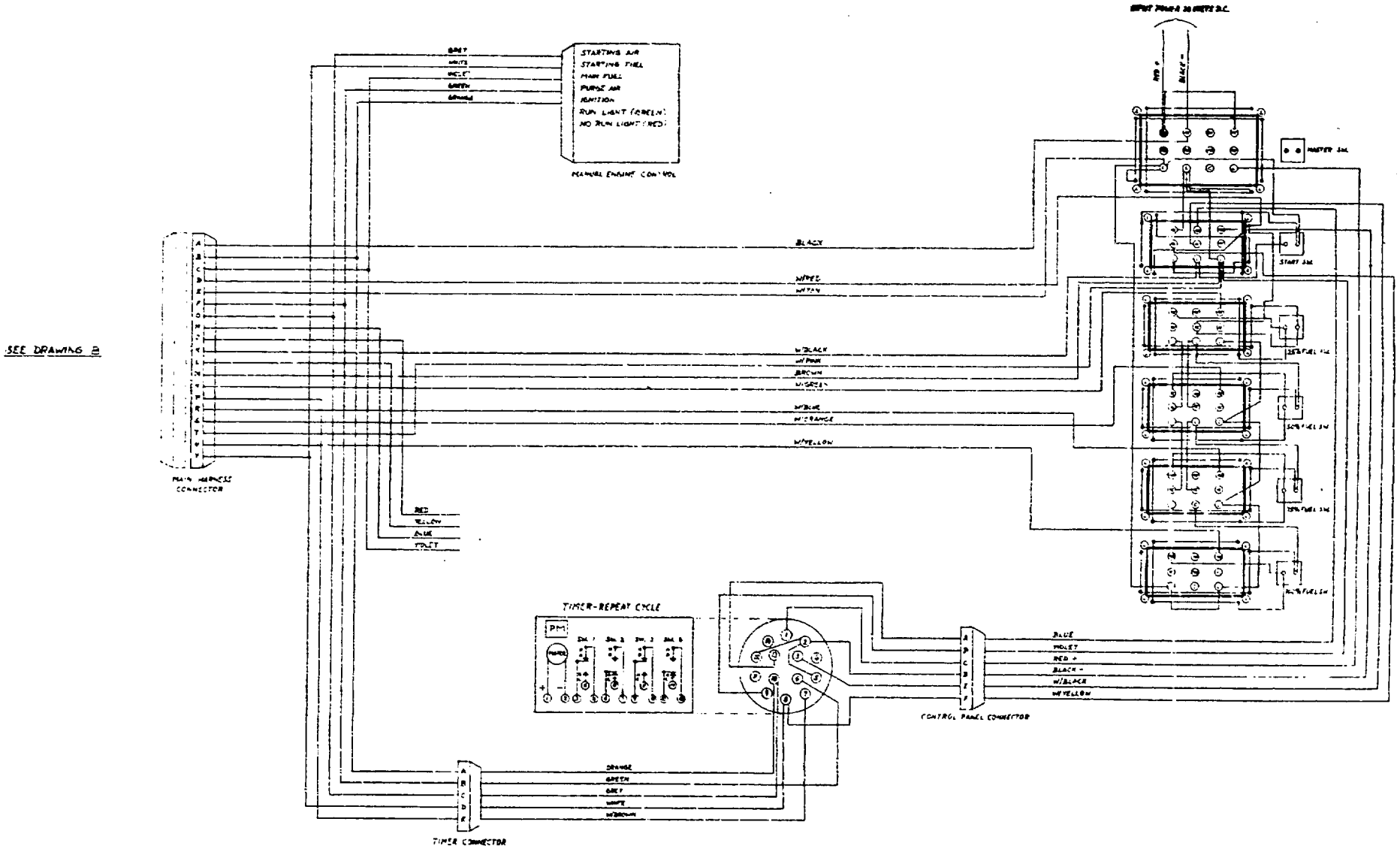


DIAGRAM OF FUEL AND STARTING AIR SYSTEM

FIGURE



AUTOMATIC ENGINE CONTROL CIRCUIT

FIGURE

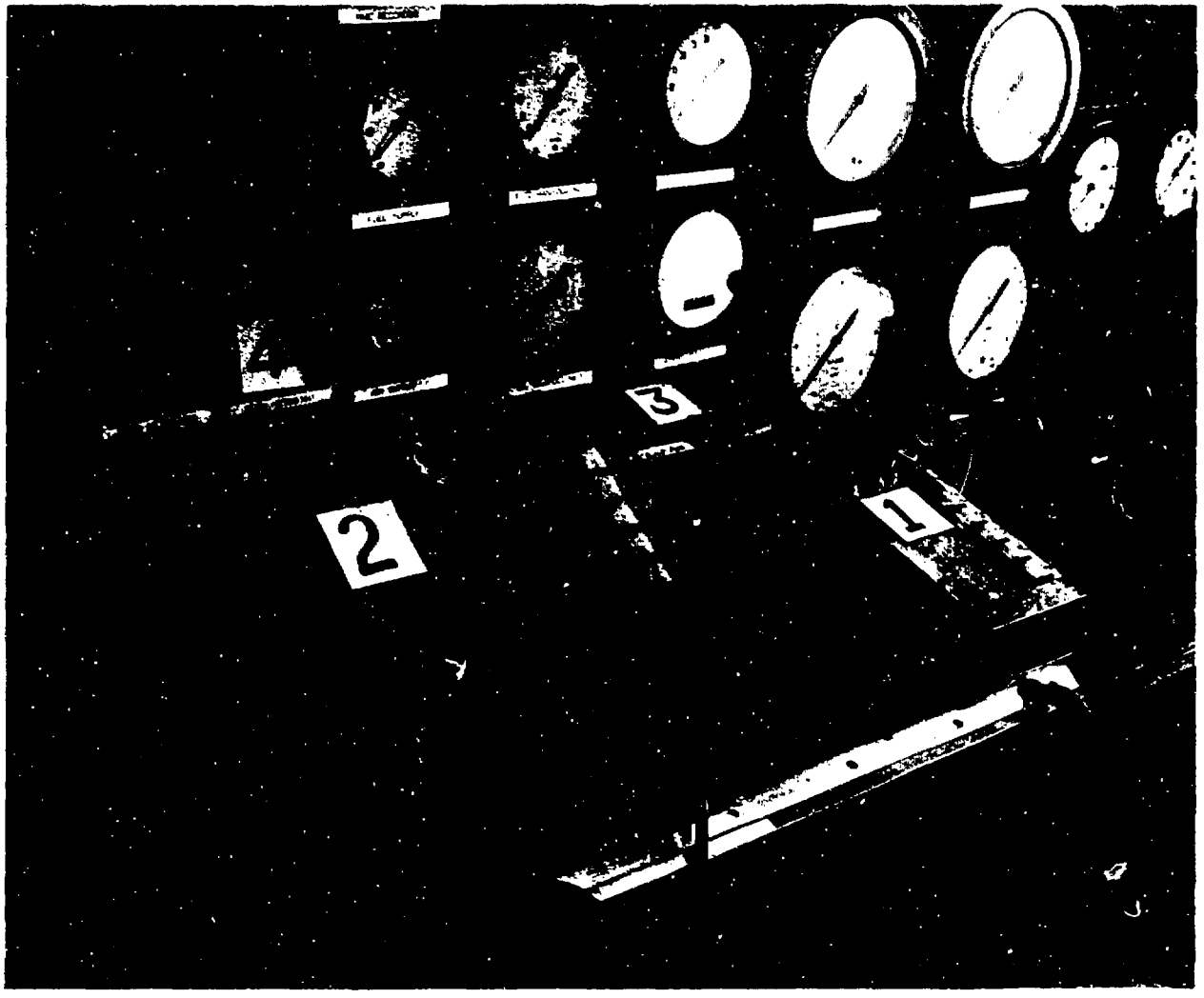


FIGURE 67: BOXES IN FOREGROUND CONTAIN AUTOMATIC AND SEMI-AUTOMATIC CONTROL SYSTEMS FOR PULSE REACTOR START, FUEL CONTROL AND RE-START SEQUENCES

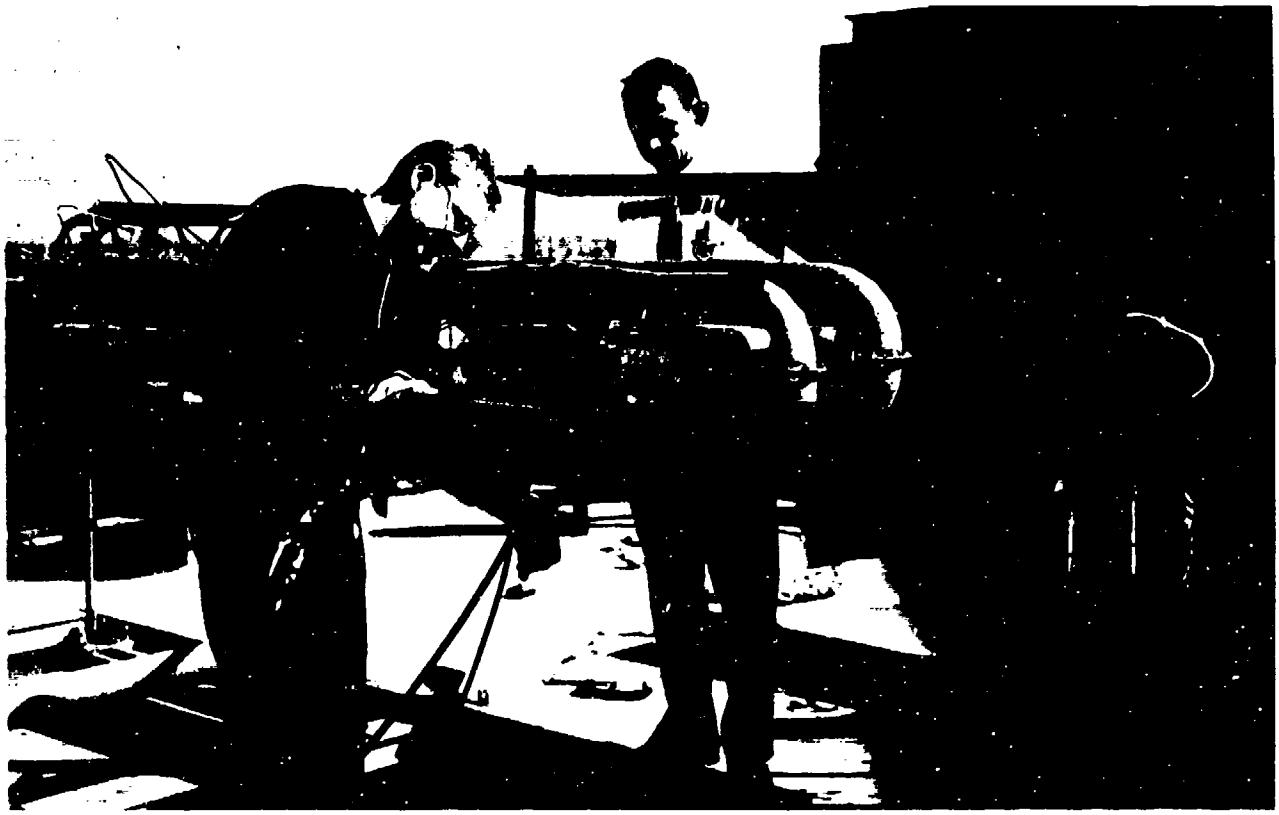


FIGURE 68 A PAIR OF HS-1B(0.19) PULSEJET COMBUSTORS MOUNTED FOR STATIC TESTING

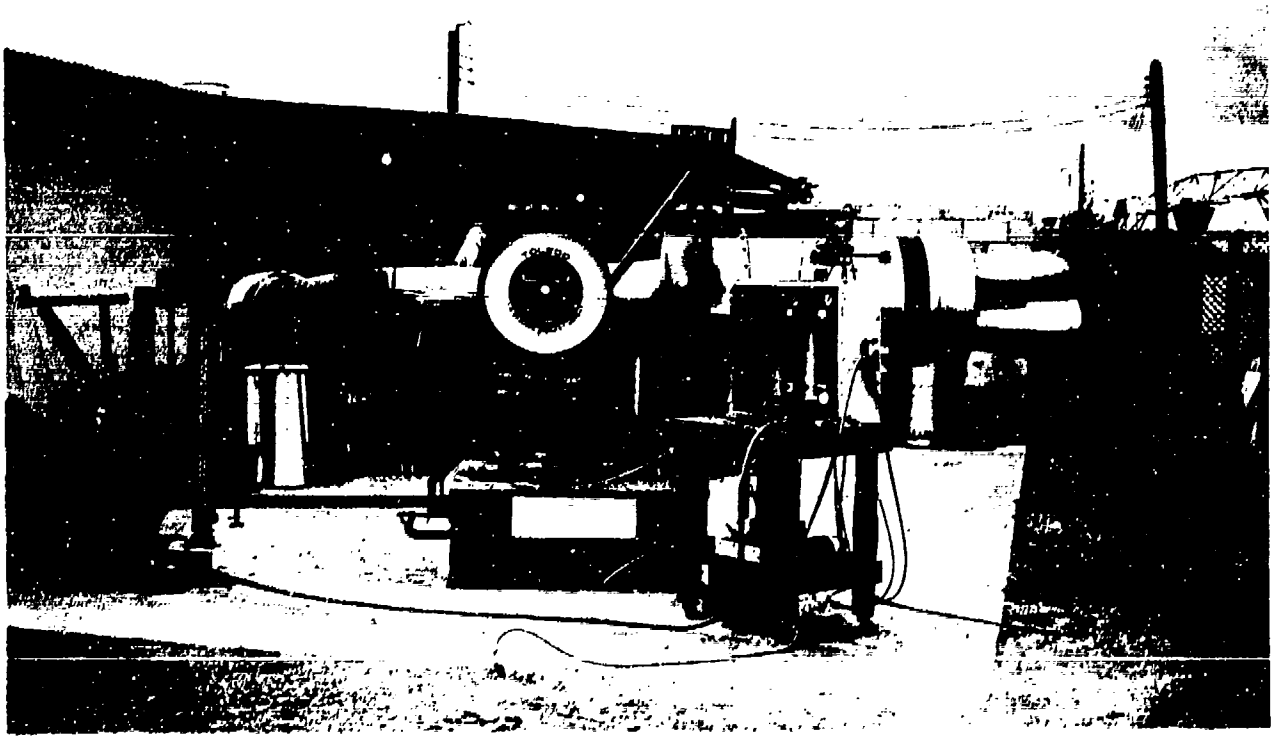


FIGURE 69: CONNECTED-PIPE TEST SET-UP FOR HS-1B(0.19) PULSE REACTORS

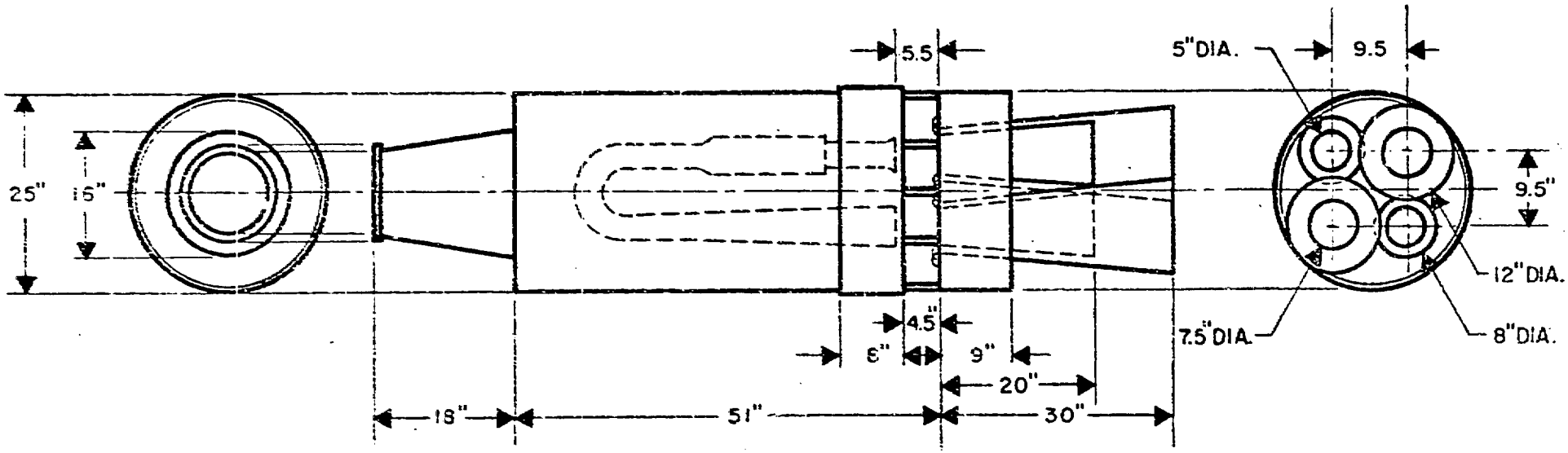


FIGURE 13 DRAWING OF FLOW PULSE REACTORS SHOWING FOR CORRUGATED-PIPE TESTING WITH AXIAL FLOW

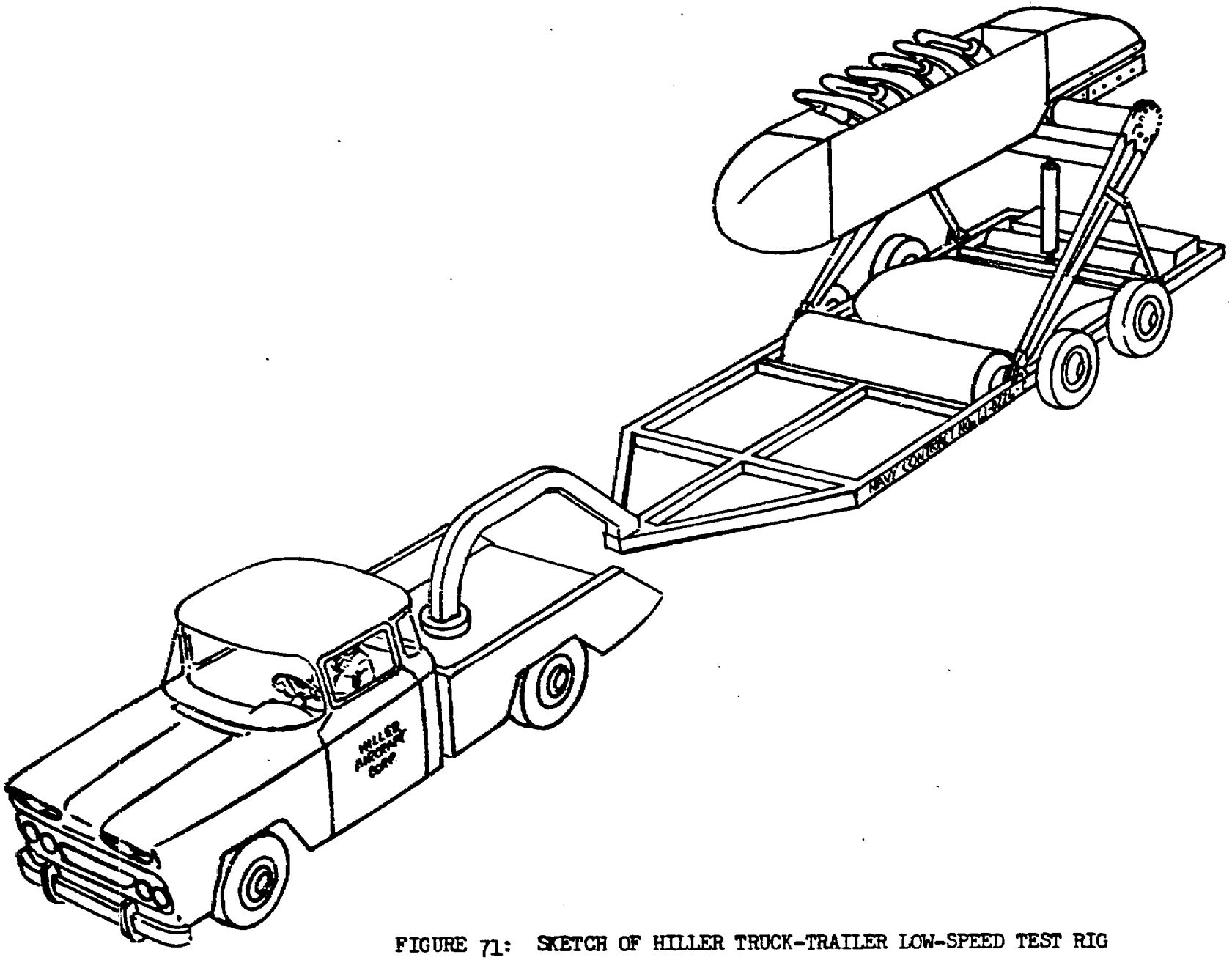


FIGURE 71: SKETCH OF HILLER TRUCK-TRAILER LOW-SPEED TEST RIG



FIGURE 72: HILLER AIRCRAFT WATER TUNNEL USED FOR FLOW VISUALIZATION TESTING OF TRAILER TEST RIG

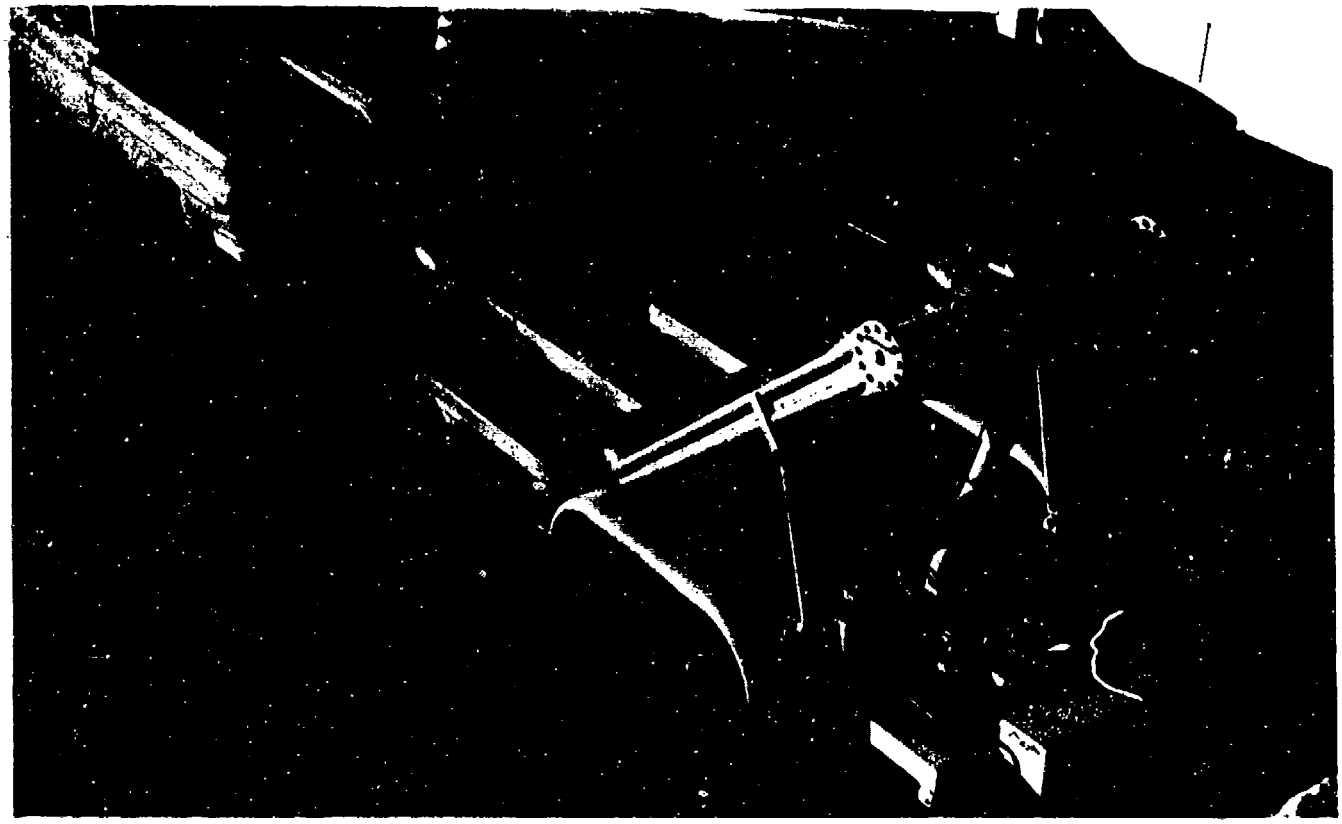


FIGURE 73: TRAILER TEST RIG WITH ACCESSORY EQUIPMENT

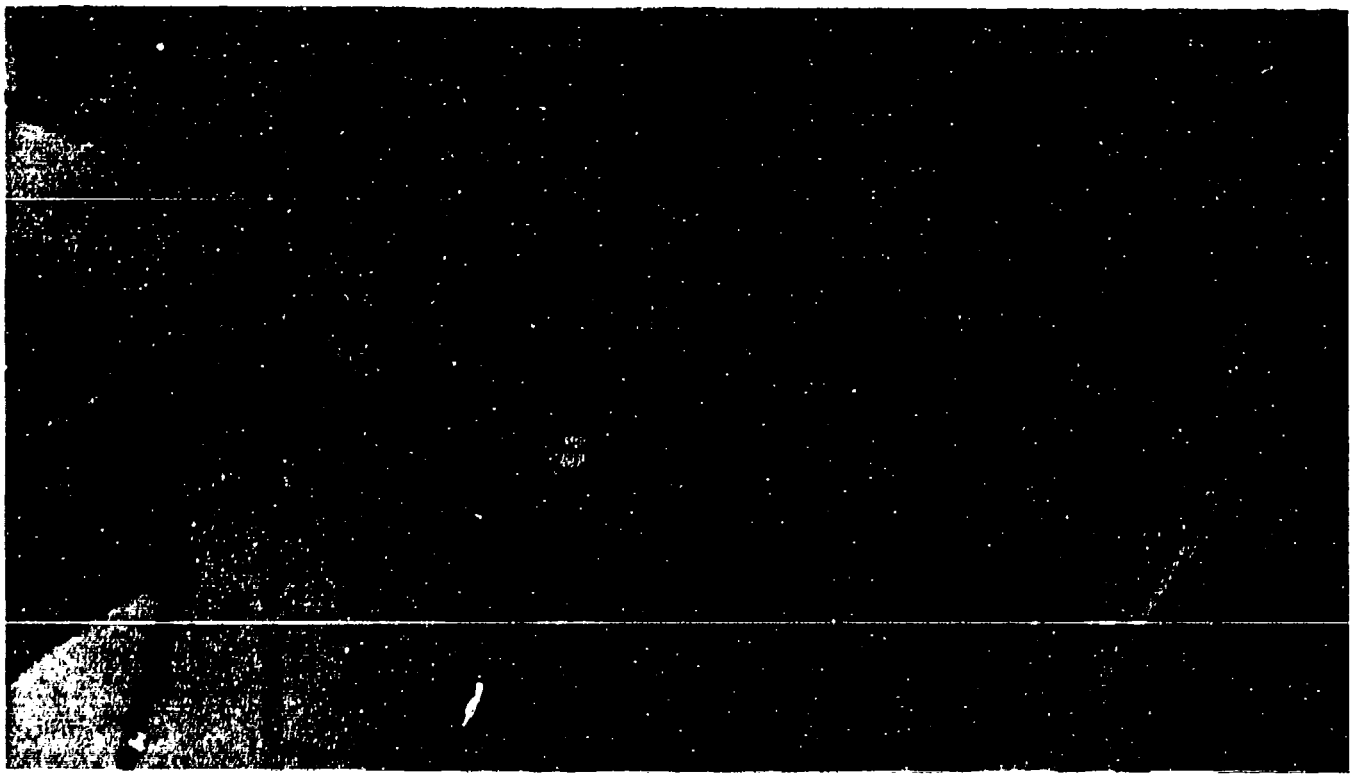
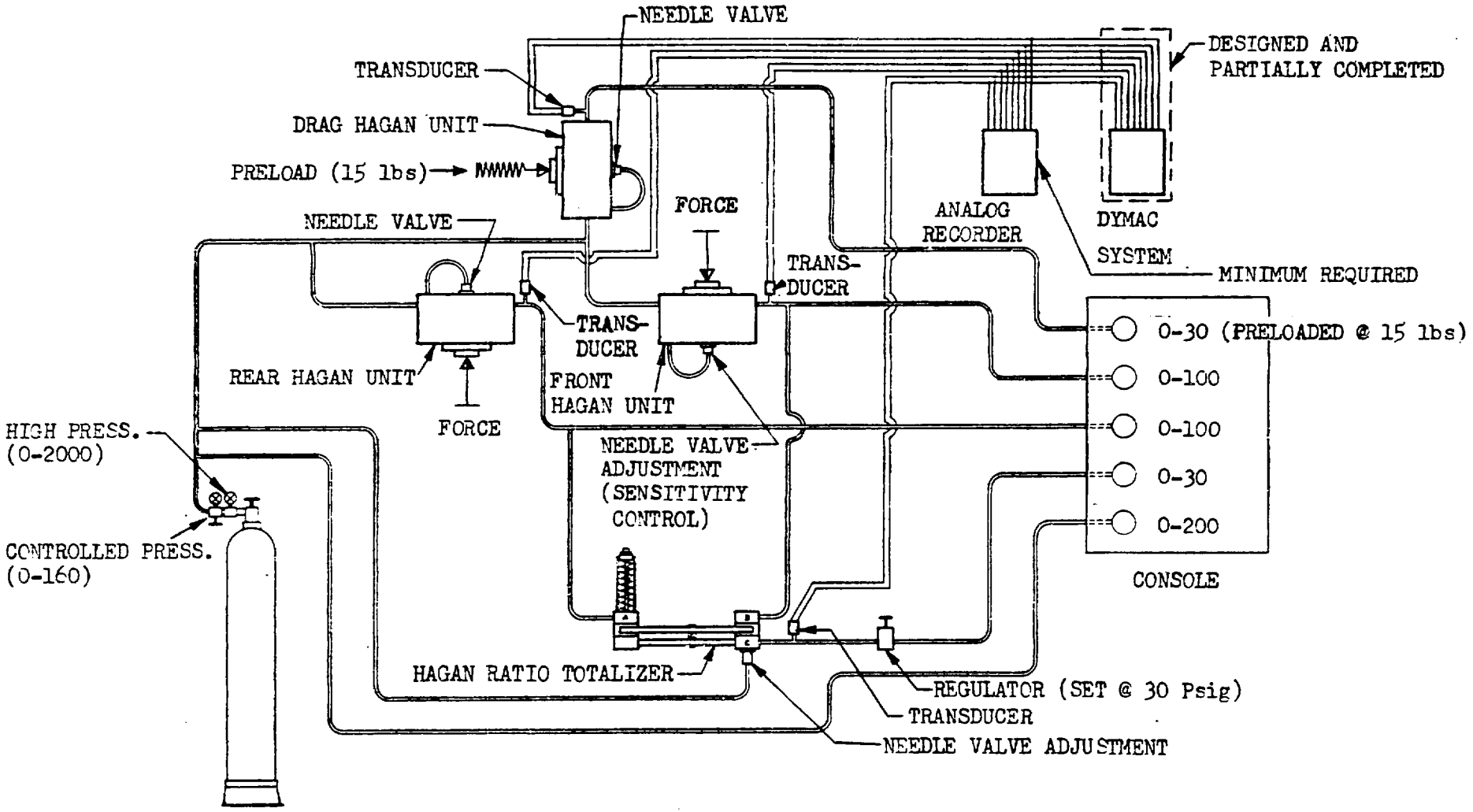


FIGURE 74: PULSE REACTOR LIFT, DRAG, AND PITCHING MOMENT BALANCE MECHANISM FOR TRAILER TEST RIG



BALANCE MEASUREMENT SYSTEM

FIGURE 75

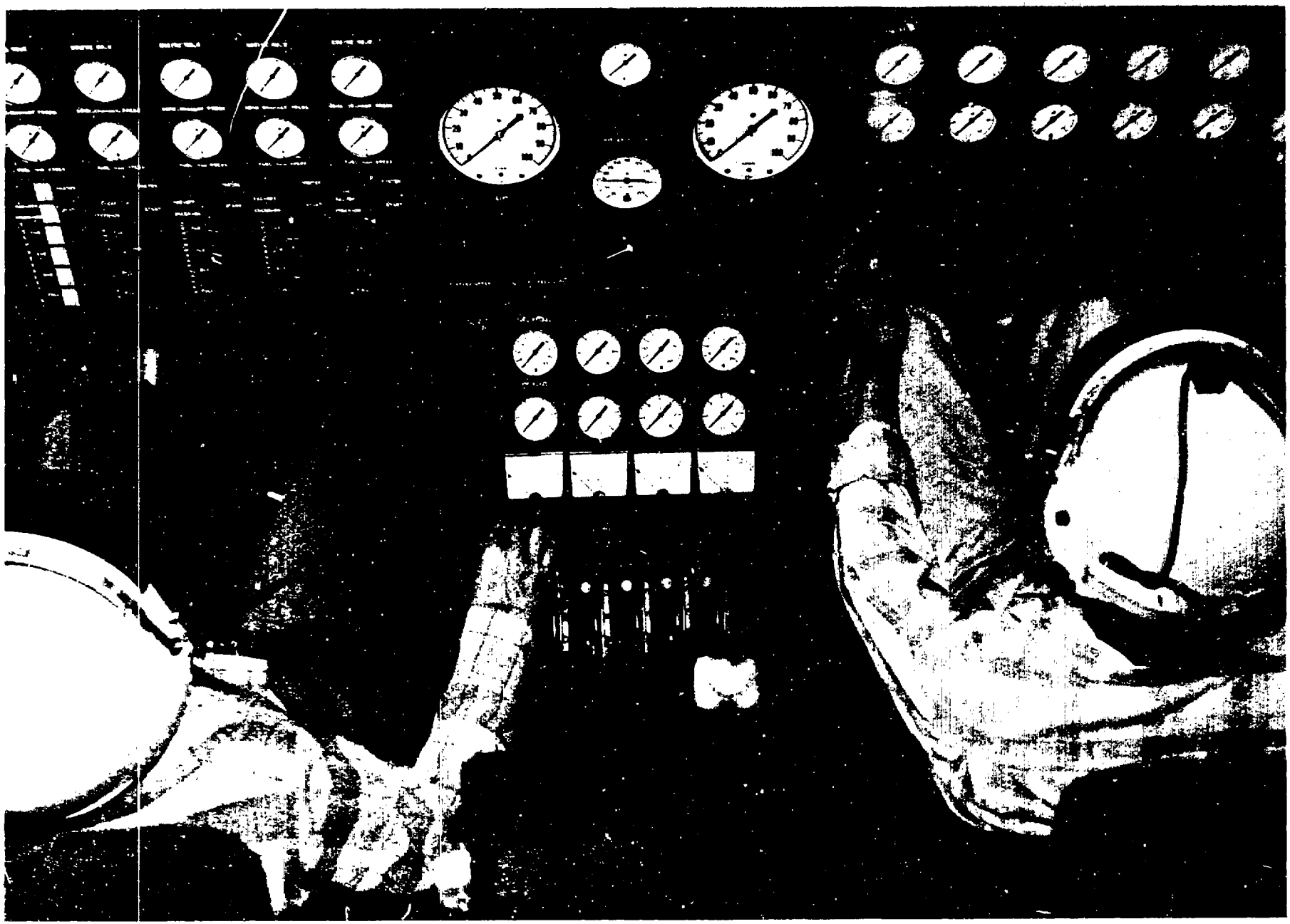


FIGURE 76: PULSE REACTOR CONTROL CONSOLE FOR TRAILER TEST RIG

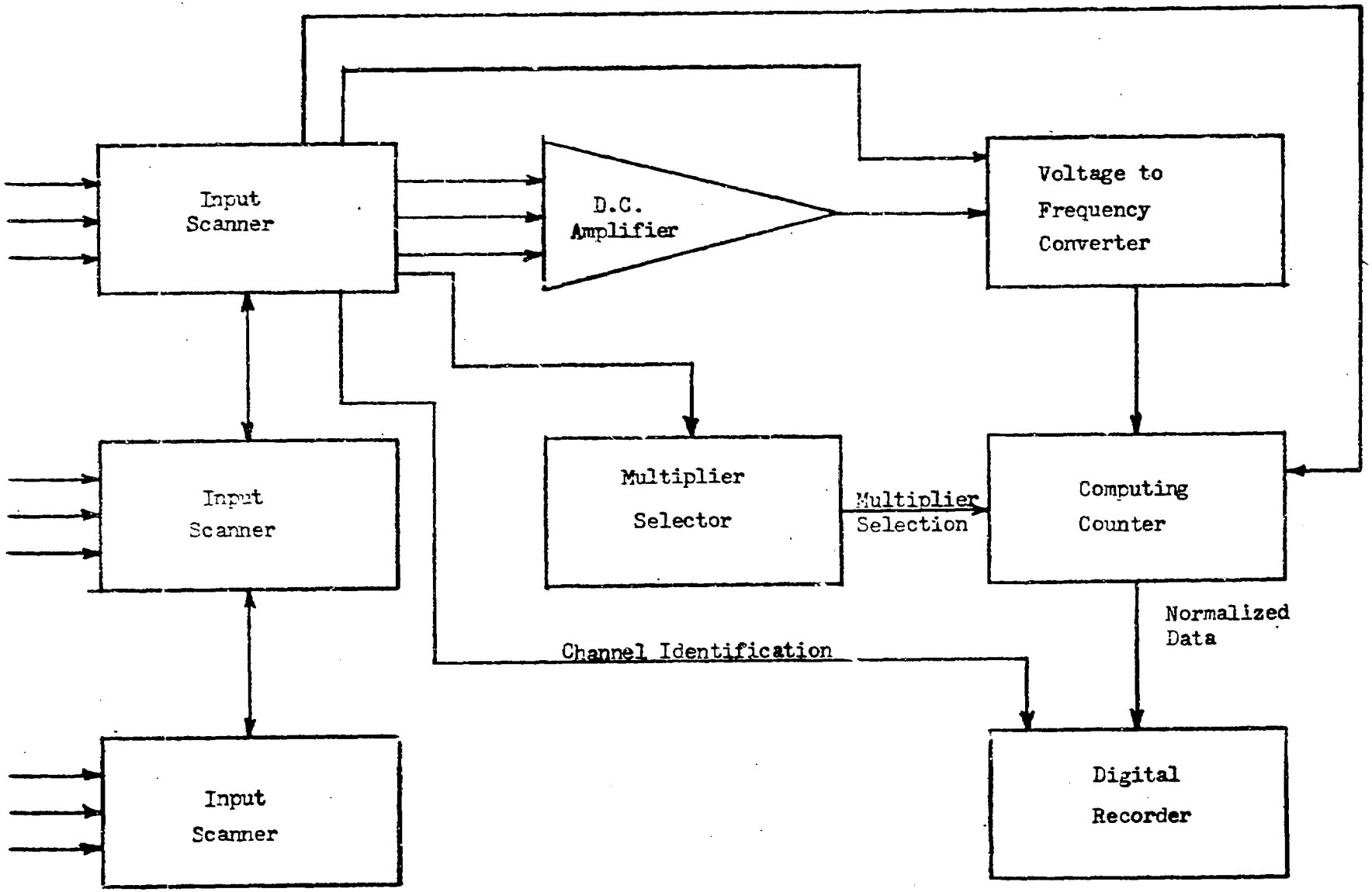


FIGURE 7: BLOCK DIAGRAM OF DIGITAL DATA CONVERSION AND RECORDING SYSTEM

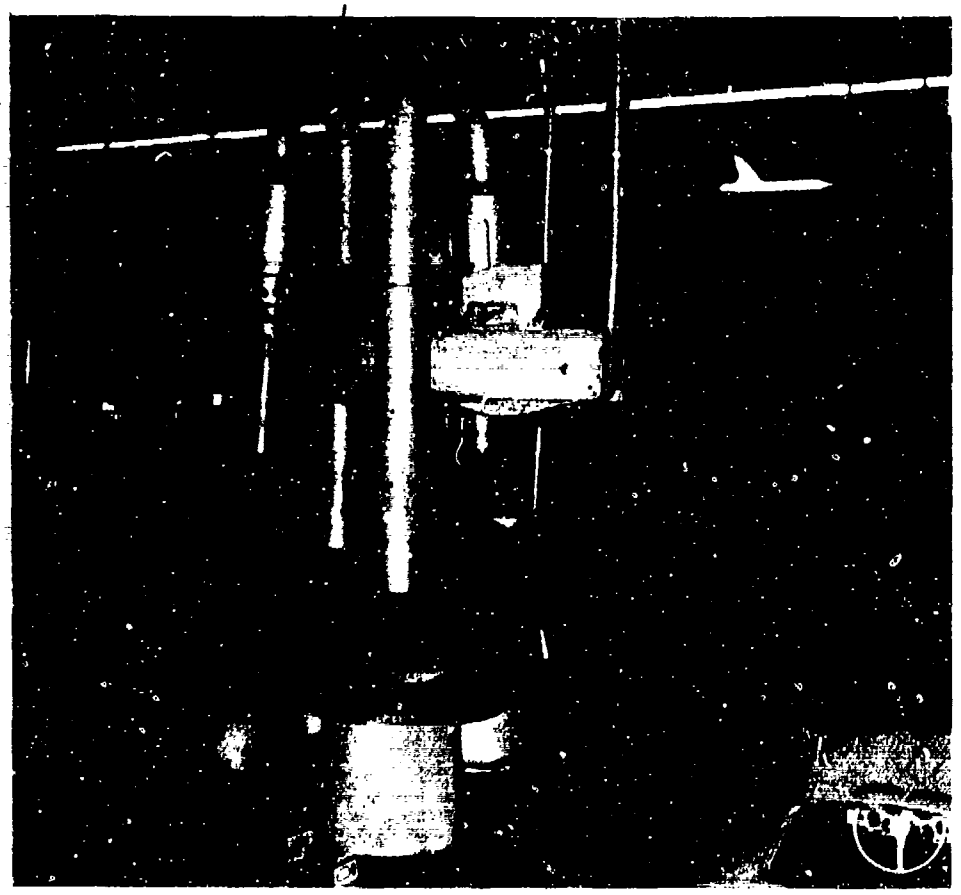


FIGURE 78: TWO UNSHROUDED PULSE REACTOR ENGINES MOUNTED ON TRAILER TEST RIG.

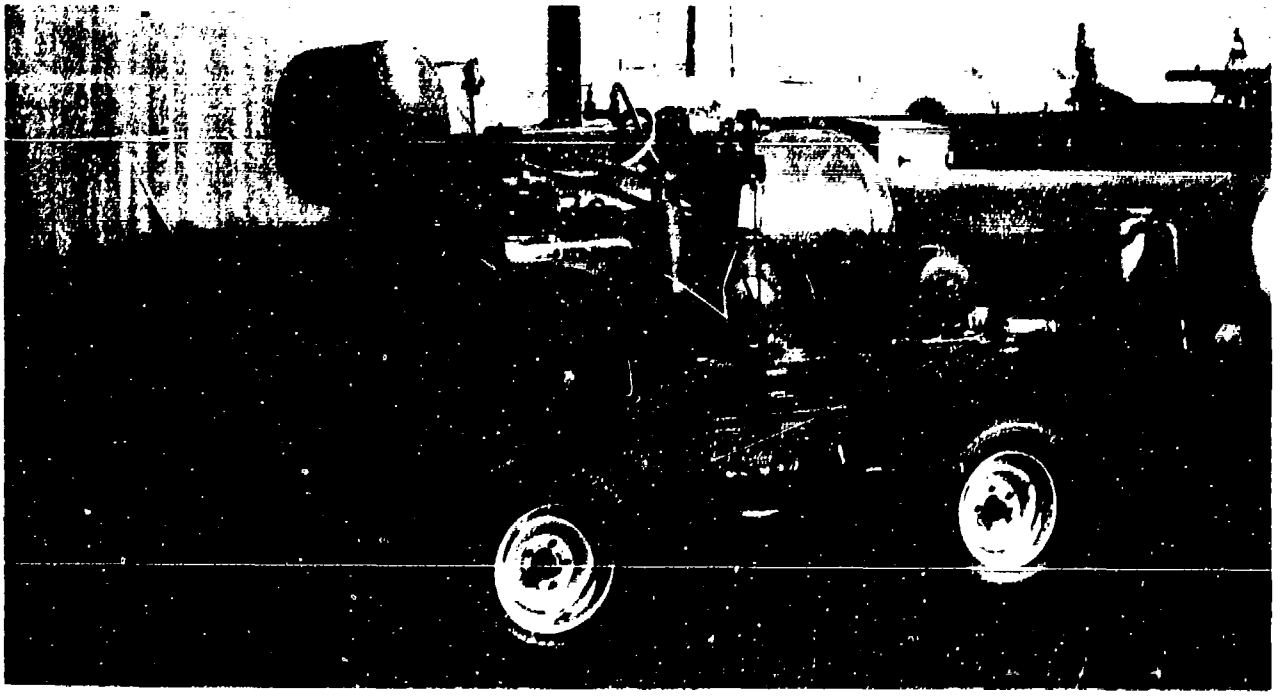


FIGURE 79: AIR SUPPLY STORAGE TANK AND AIR COMPRESSOR.

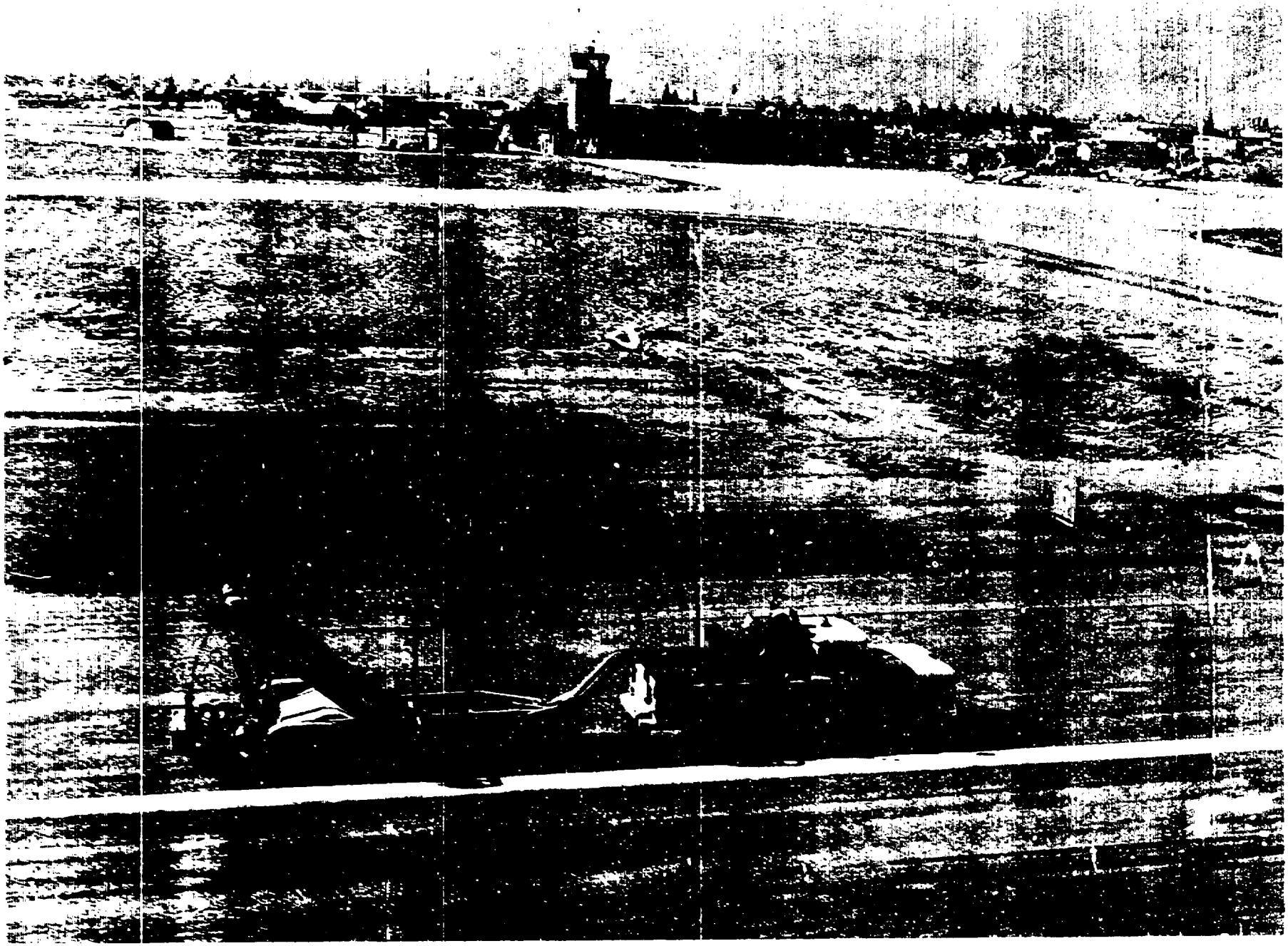


FIGURE 60: TRAILER TEST RIG IN OPERATION ON MOFFETT FIELD RUNWAY,
25 JANUARY 1962.

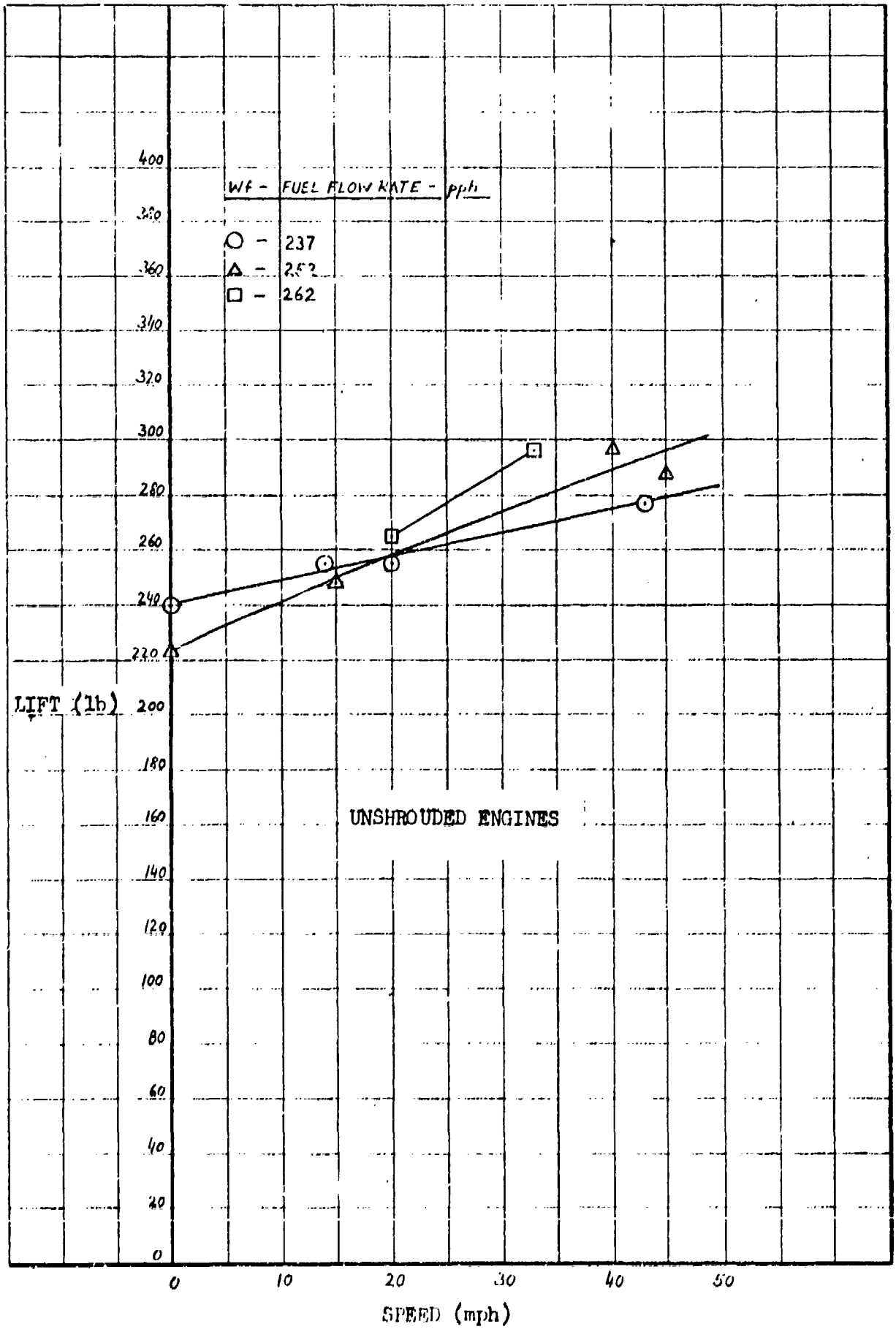
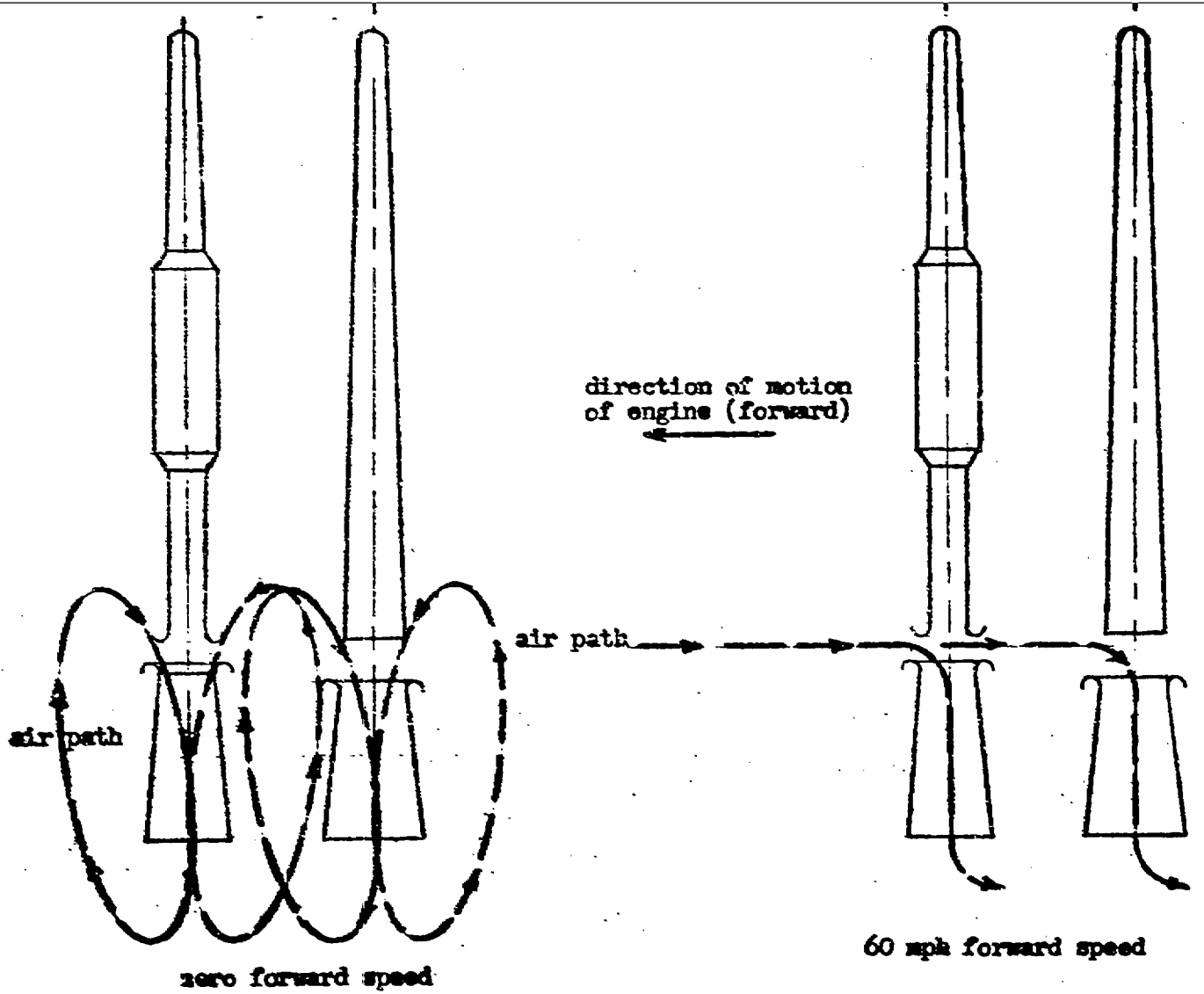


FIGURE 81: EFFECT OF FORWARD SPEED ON PULSE REACTOR THRUST (LIFT)



COMPARISON OF AIR FLOW PATHS FOR HOVERING AND FORWARD SPEEDS

FIGURE 8

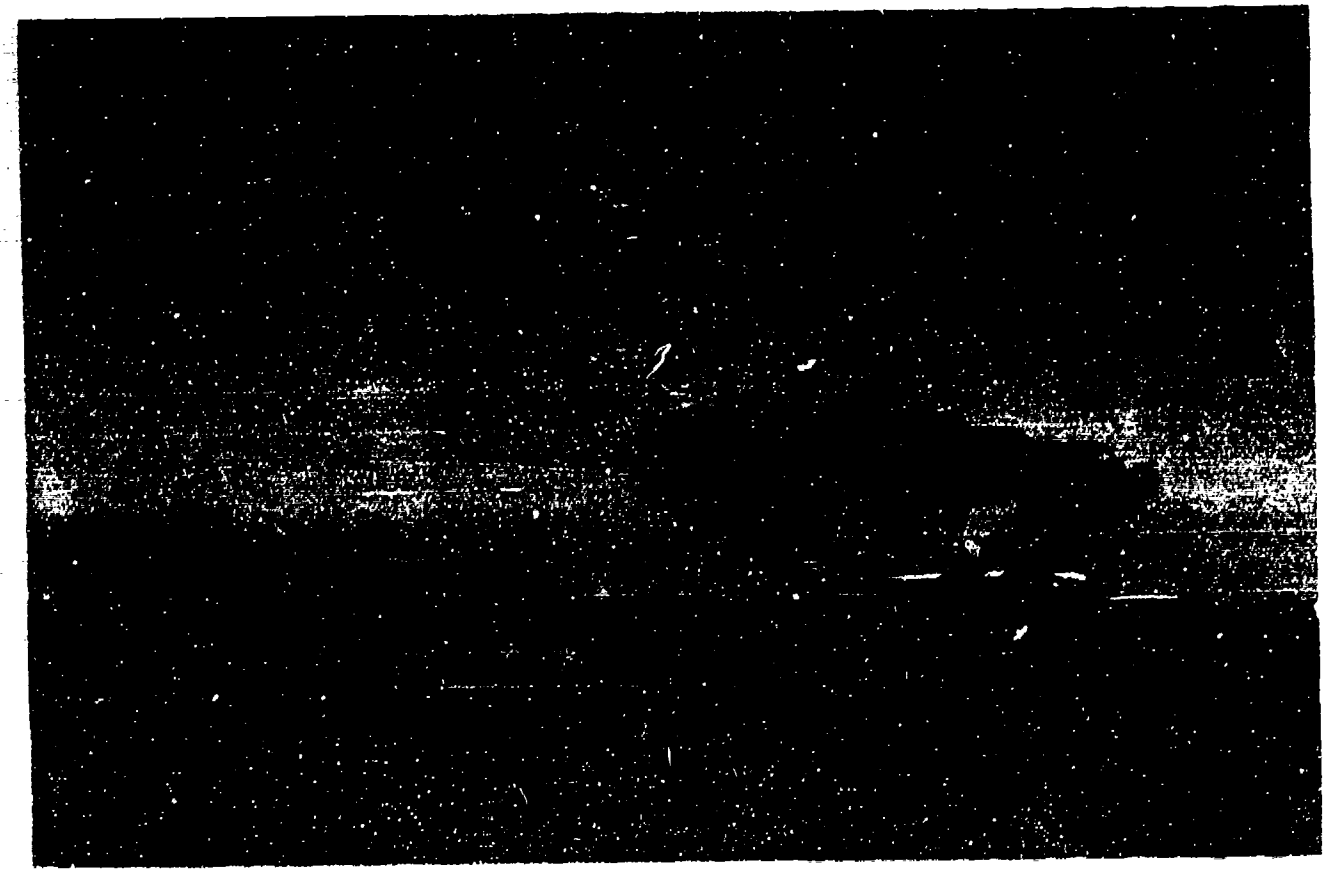


FIGURE 83: PULSE REACTOR TRAILER TEST RIG AND SHROUD ASSEMBLY WITH TWO (2) HH-5.25-6-7 PULSE REACTOR COMBUSTORS INSTALLED

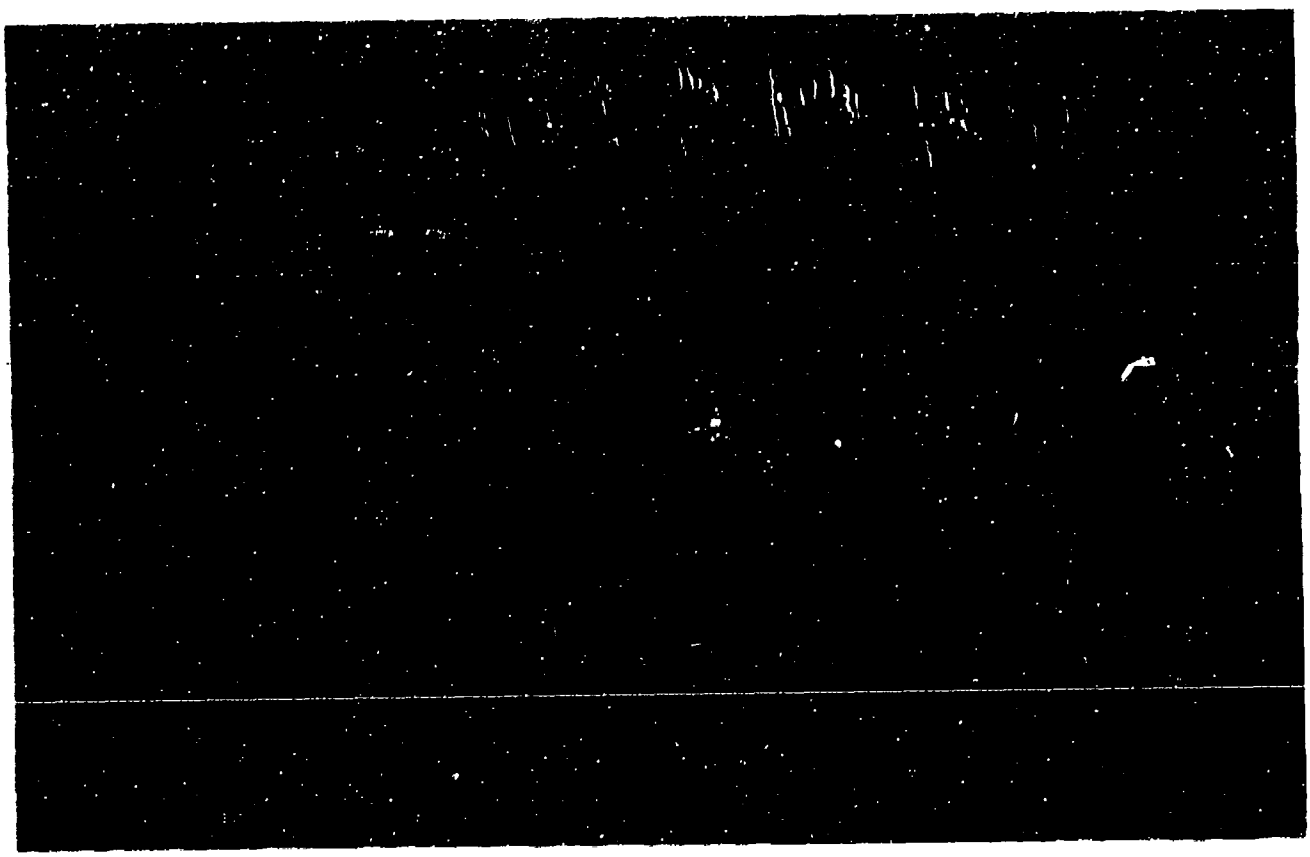


FIGURE 84: FORWARD SPEED TESTS ON RUNWAY AT MOFFETT FIELD N.A.S. WITH DUAL SHROUDED PULSE REACTOR ENGINES IN SHROUD PACKAGE LARGE ENOUGH FOR LATER TESTING WITH SIX COMBUSTORS

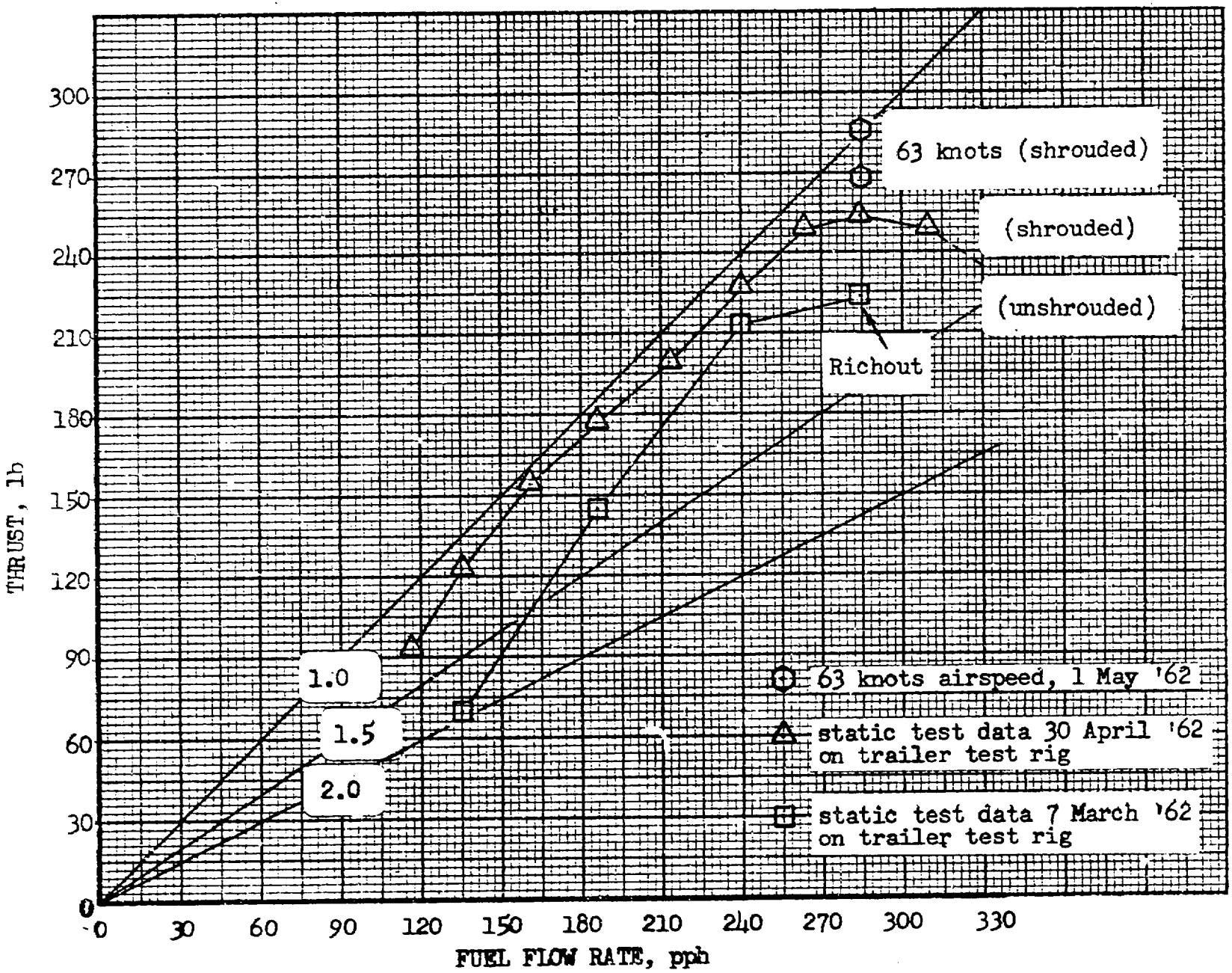


FIGURE 85: COMPARISON OF SHROUDED AND UNSHROUDED DUAL PULSE REACTOR ENGINE PERFORMANCE ON TRAILER TEST RIG

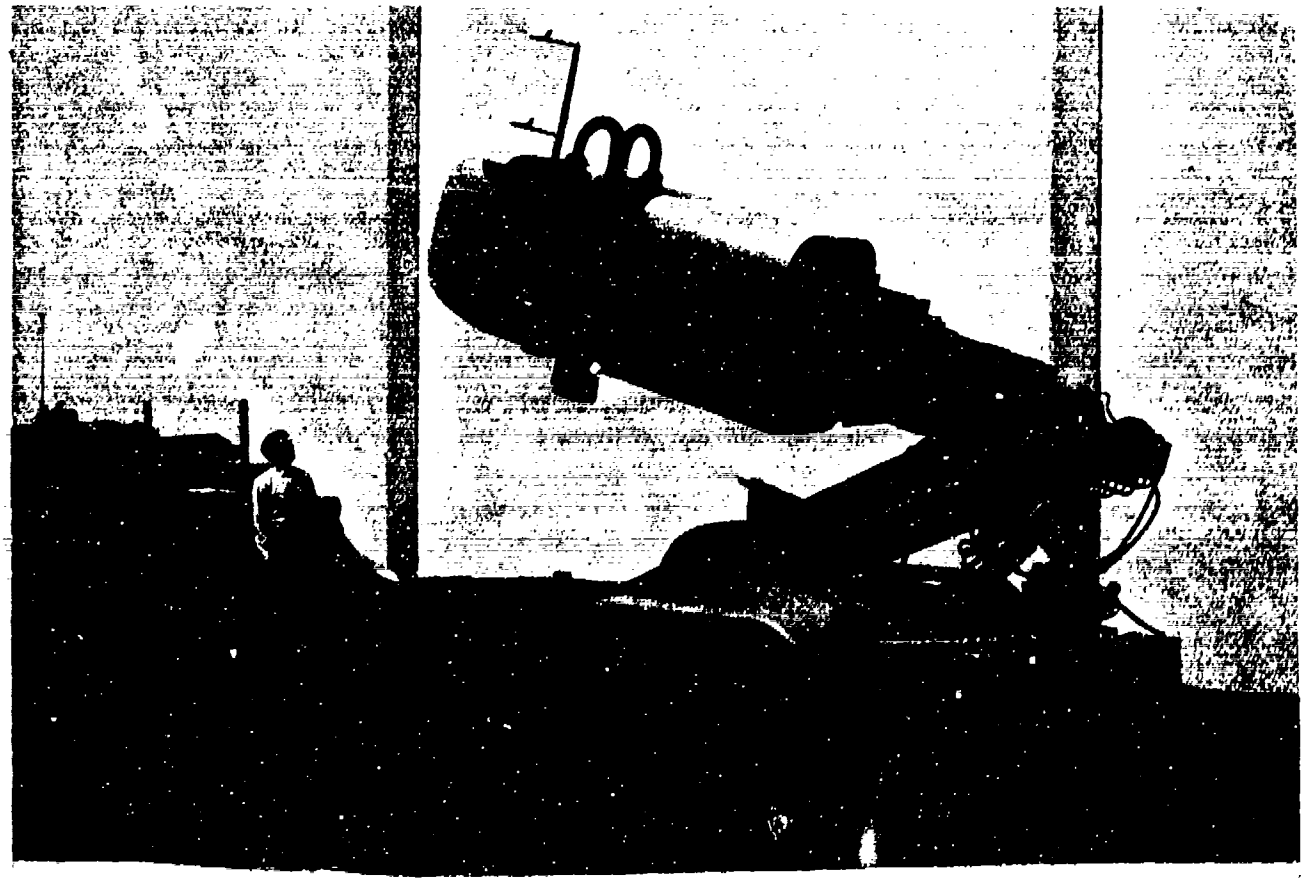


FIGURE 86: PULSE REACTOR TRAILER TEST RIG WITH SHROUDED ENGINES POSITIONED 15° UP



FIGURE 87: VIEW LOOKING DOWN ON TEST SITE AT N.A.S. MOFFETT FIELD, SHOWING TOP VIEW OF SHROUDED PULSE REACTOR ENGINE PACKAGE



FIGURE 88: SHROUDED ENGINES, NOSE DOWN 30° OPERATING OVER DRY HAY FIELD



FIGURE 89: VIEW SHOWING PULSE REACTOR JET DOWNWASH EFFECT AS IT PASSES OVER DRY HAY FIELD AT TWO MILES PER HOUR

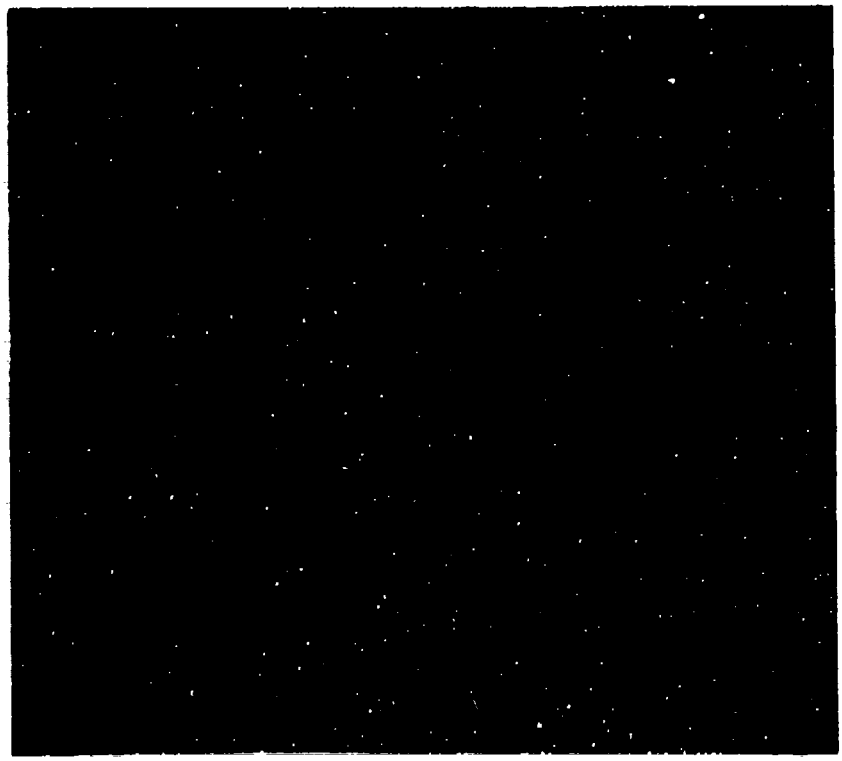


FIGURE 90: TAILPIPE SECTIONS STIFFENED BY ROLLED-IN CORRUGATIONS



FIGURE 91: TESTING OF CORRUGATION STIFFENED
TAILPIPE SECTION ON HH(5.25") COMBUSTOR

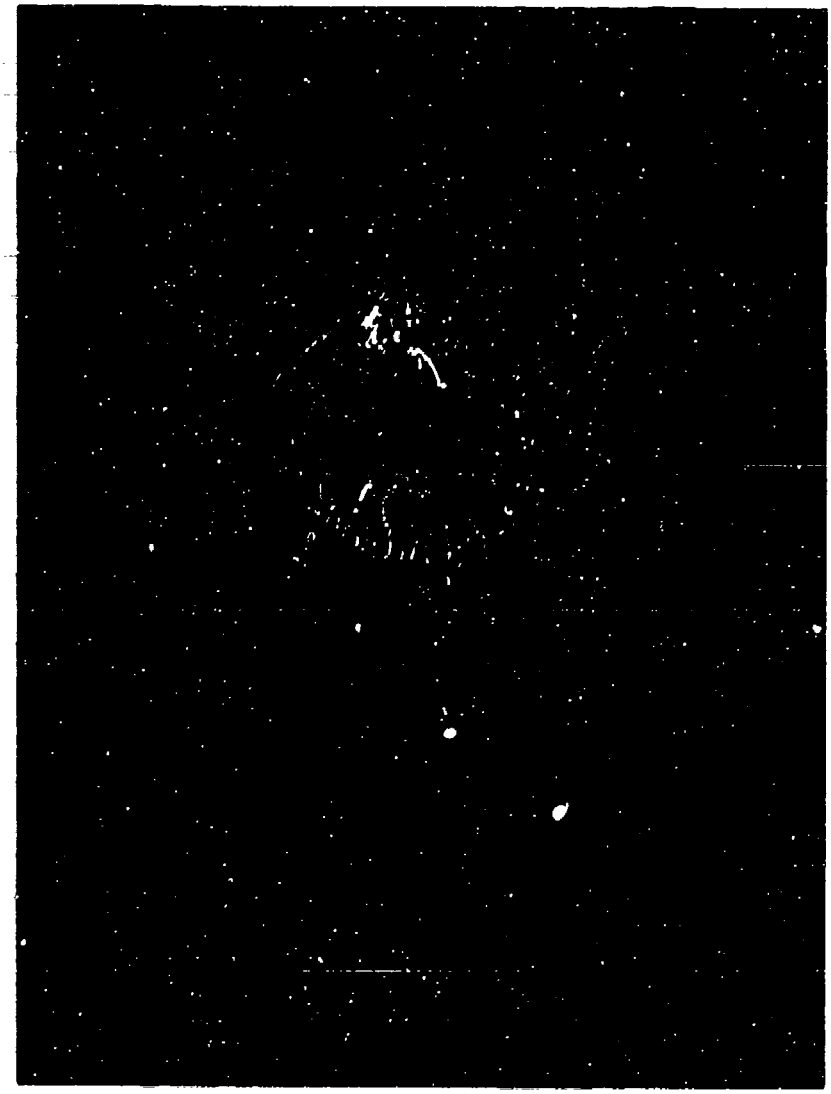


FIGURE 92: HH(5.25") "HORSECOLLAR LIGHTWEIGHT COMBUSTOR WITH RING STIFFENERS AND SHOCK MOUNTS

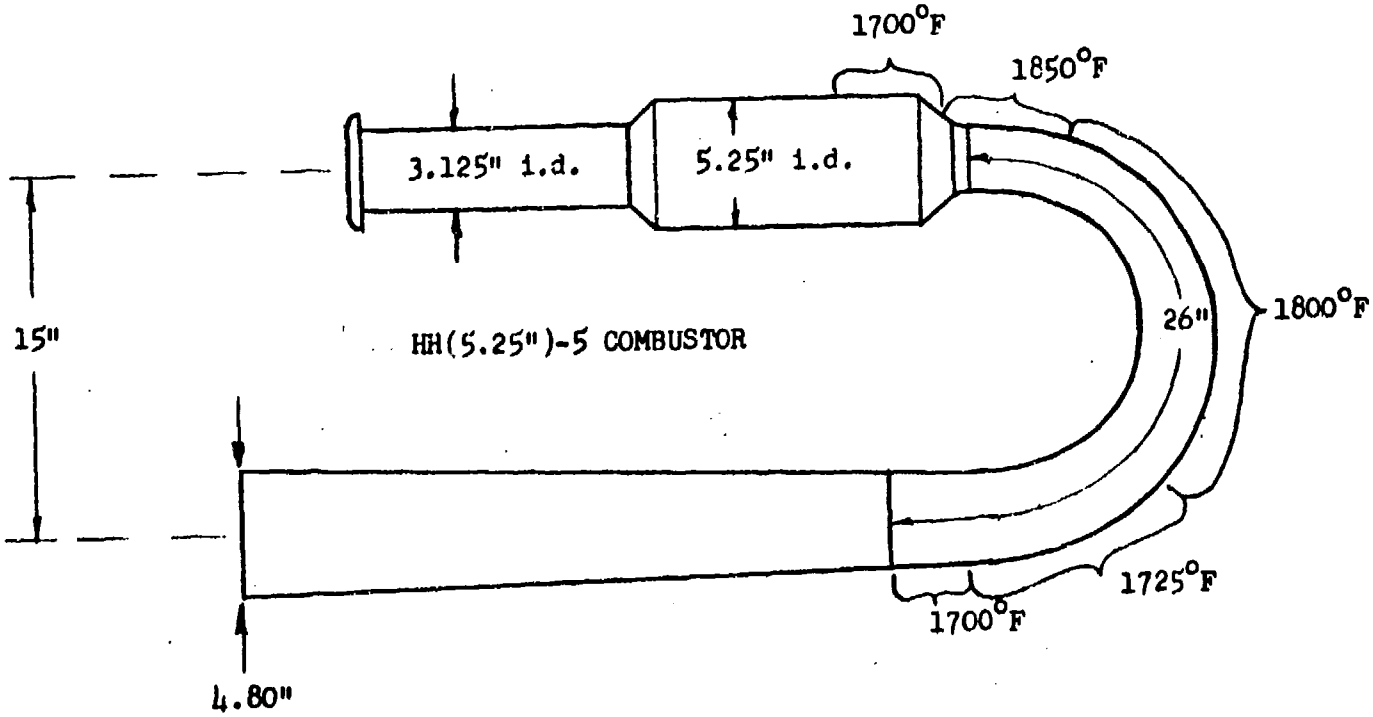
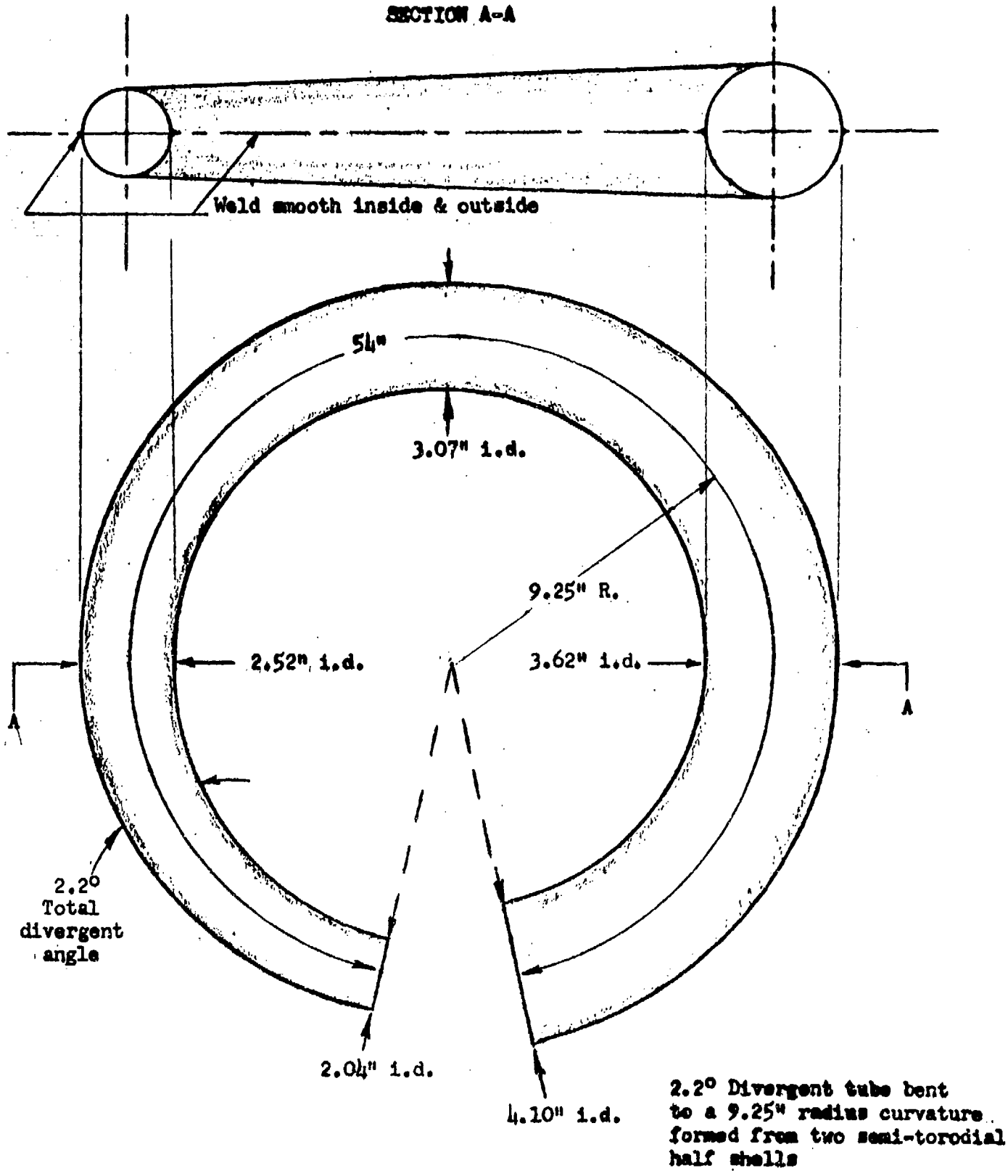


FIGURE 93: SHELL TEMPERATURE DISTRIBUTION HH(5.25")-5 (130 pph FUEL FLOW)

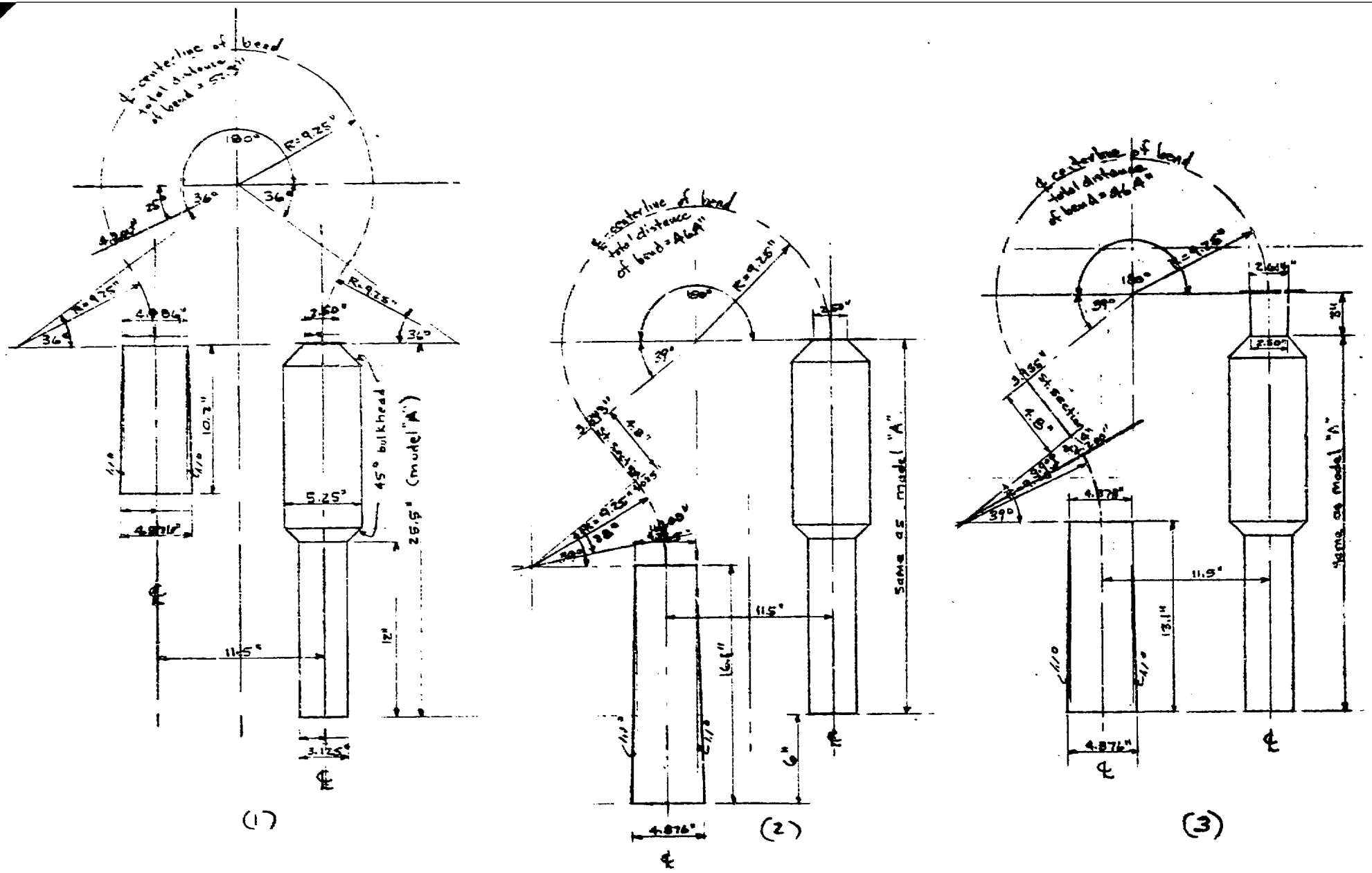


PULSE REACTOR COMBUSTOR TUBULAR TURN SECTION

FIGURE 54



FIGURE 95: PHOTO OF ENGINE CRACK IN HH-5.25-6-7 STAINLESS STEEL (0.050" TYPE 321) NO. 1 COMBUSTOR AFTER 16 HOURS OF OPERATION. FIELD REPAIR WAS MADE AND ENGINE PERFORMANCE RESTORED.



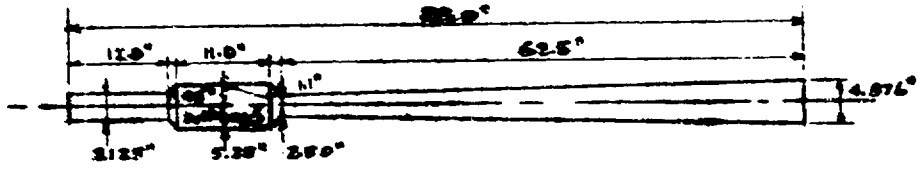


FIGURE 1 SKETCH OF VARIOUS CONFIGURATIONS AVAILABLE FROM TICE TURN

(2)

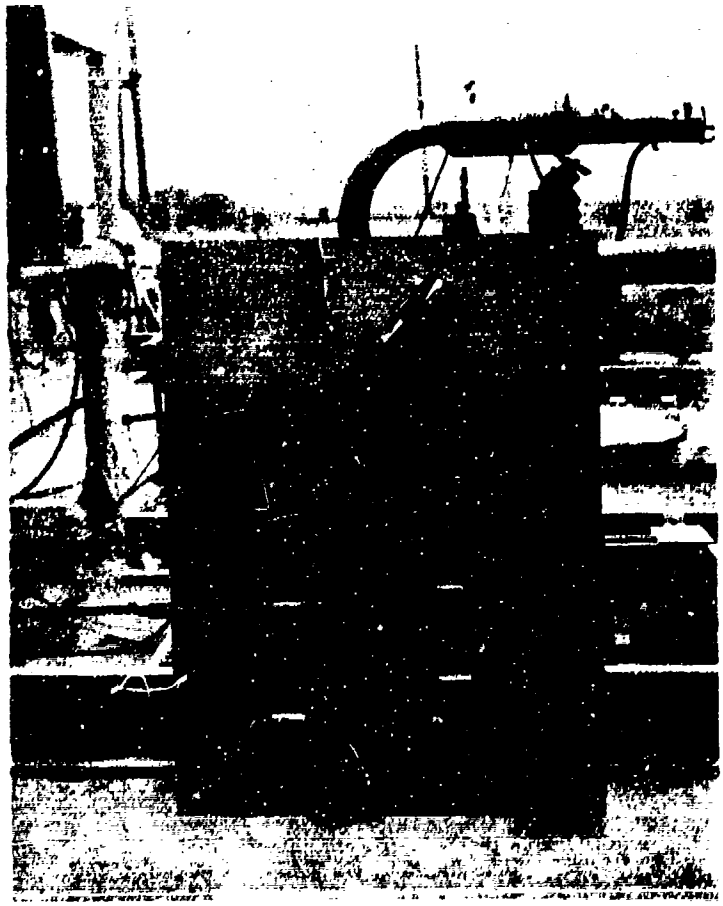


FIGURE 97: ASSEMBLY JIG FOR 180° 5.25-7 COMBUSTOR

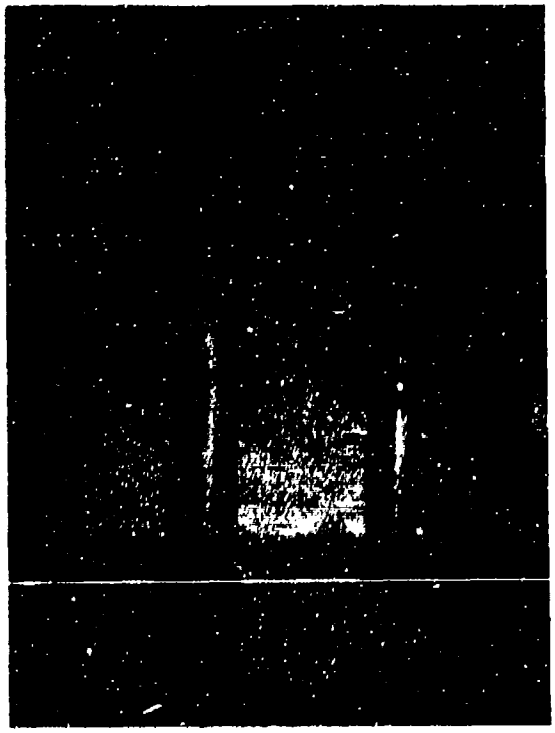


FIGURE 98: 5.25-7 COMBUSTOR MOUNTED IN ASSEMBLY JIG

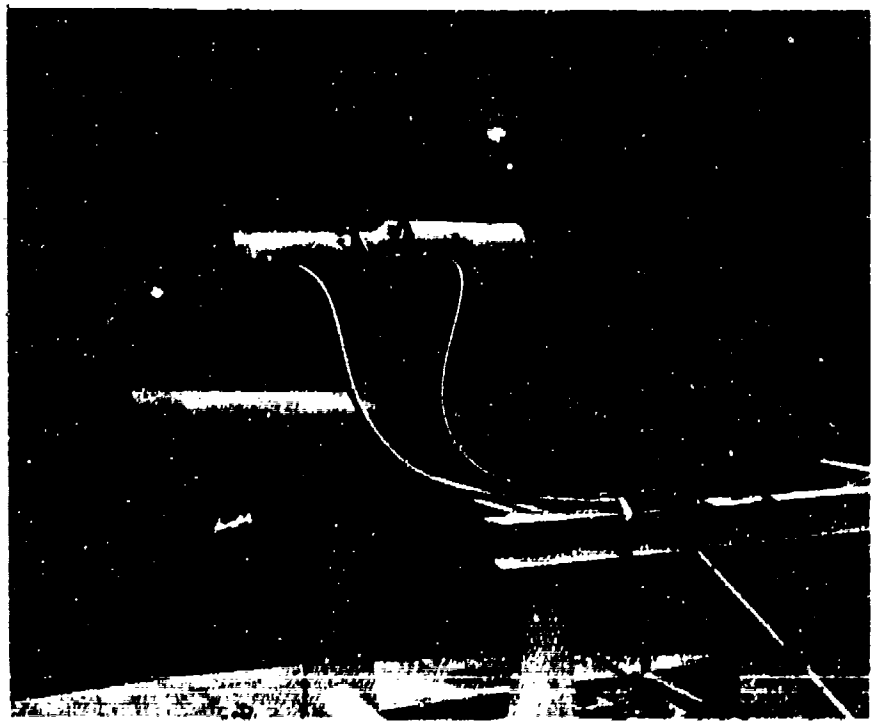


FIGURE 99 180° - 5.25-7 COMBUSTOR MOUNTED ON TEST STAND

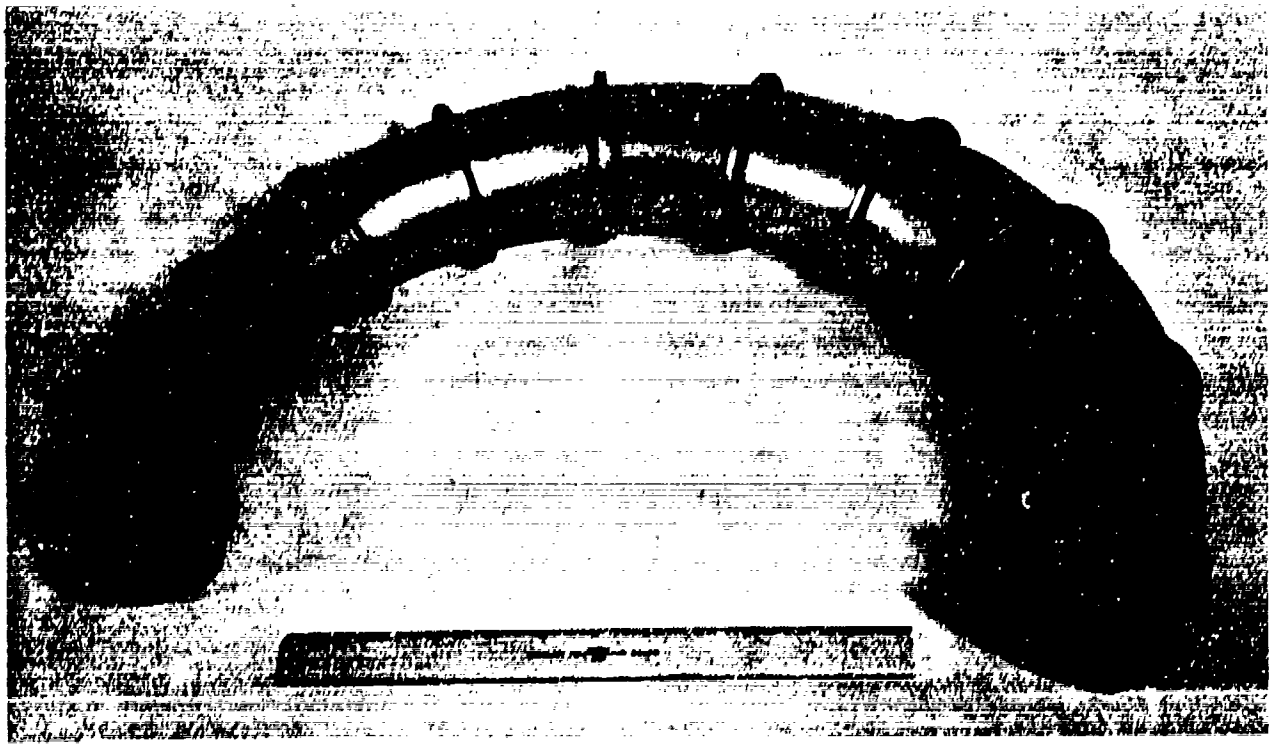


FIGURE 100: LIGHTWEIGHT 220° RING-STIFFENED COMBUSTOR TURN SECTION MANUFACTURED BY TYCE ENGR. CO., 0.017" THICK MATERIAL HAYNES 25 (L-605); WEIGHT 2.55 lb.



FIGURE 101: COMPLETED LIGHTWEIGHT HH(5.25")-7 COMBUSTOR OF 0.017" THICK HAYNES 25 MATERIAL

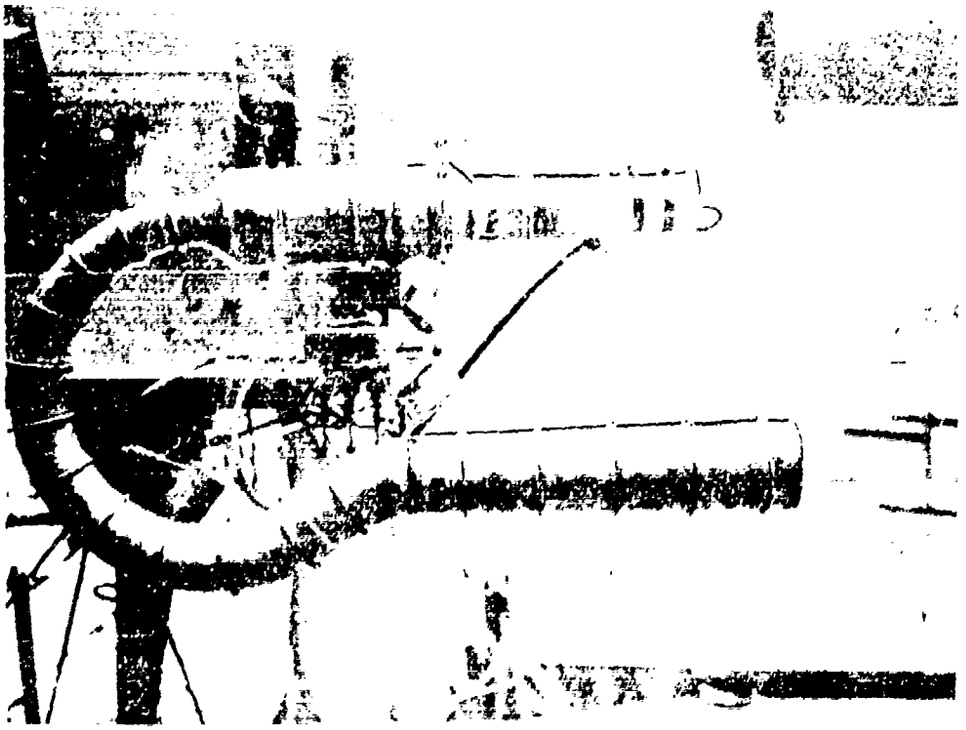


FIGURE 102: UNCOATED LIGHTWEIGHT HH(5.25")-7 COMBUSTOR ON STATIC TEST STAND, USING RUBBER LORD-TYPE SHOCK MOUNTS

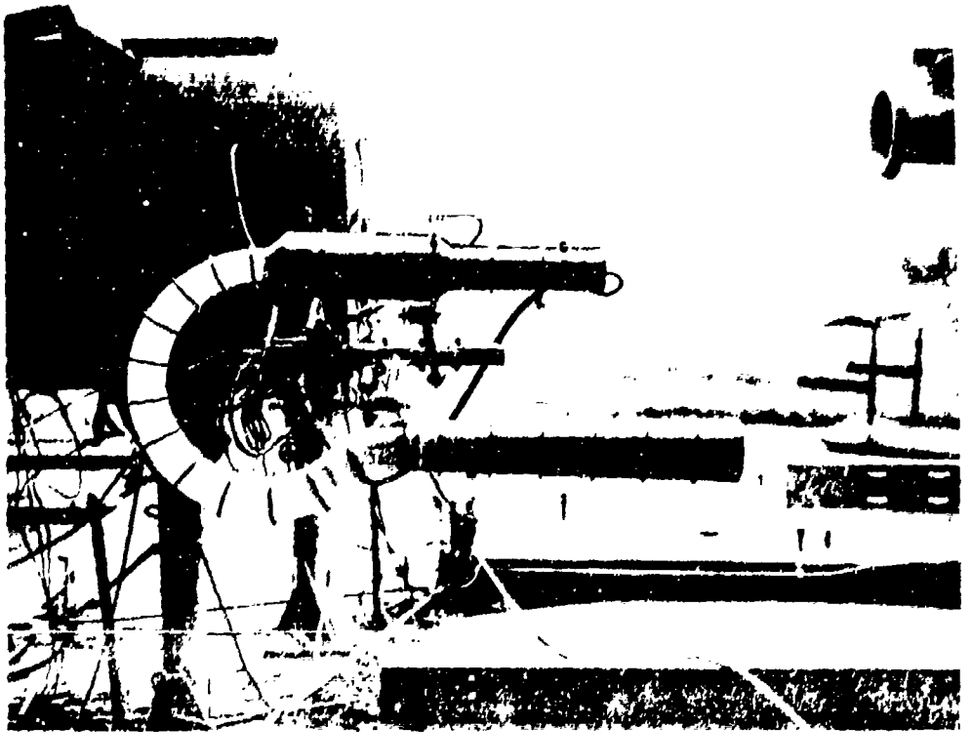


FIGURE 103: SOLARAMIC COATED LIGHTWEIGHT HH(5.25")-7 COMBUSTOR OPERATING ON STATIC TEST STAND, USING ROBINSON-TYPE SHOCK MOUNTS WITH ATTACHMENTS THAT PERMIT DIFFERENTIAL THERMAL EXPANSION OF COMBUSTOR

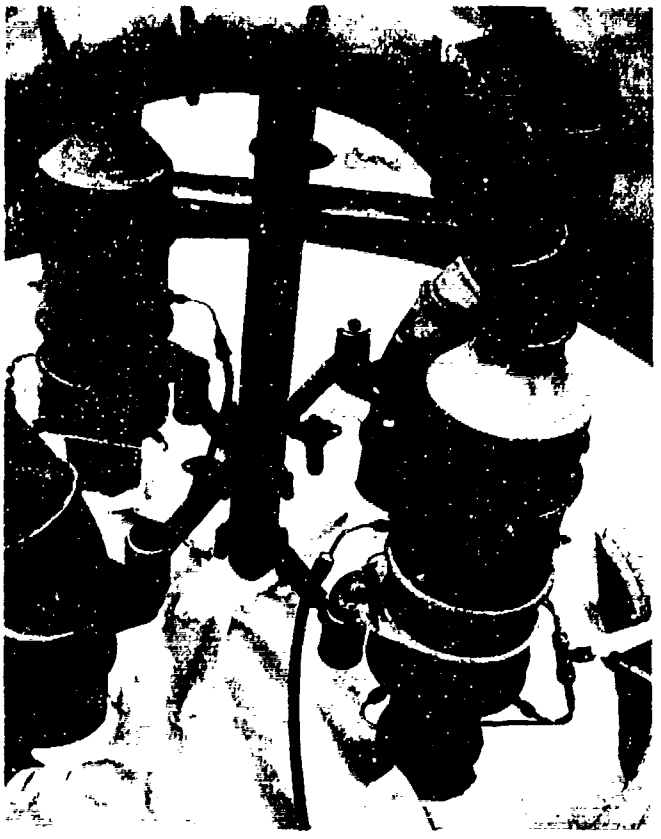


FIGURE 104: OBLIQUE VIEW OF IMPROVED COMBUSTOR SUPPORT MECHANISM

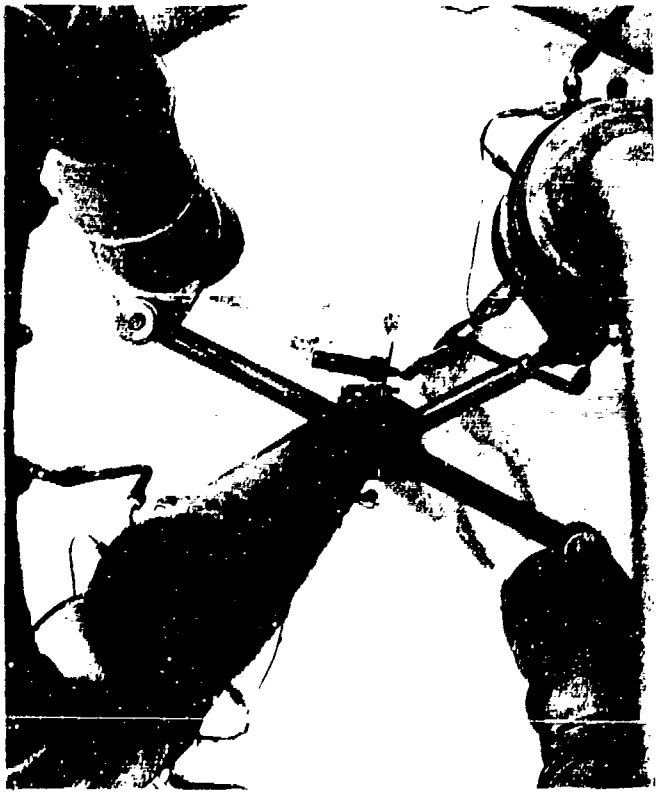


FIGURE 105: AXIAL VIEW OF IMPROVED COMBUSTOR SUPPORT MECHANISM. JOINTED ATTACH ARM ON COMBUSTOR PERMITS DIFFERENTIAL MOTION BETWEEN TAILPIPE AND INLET

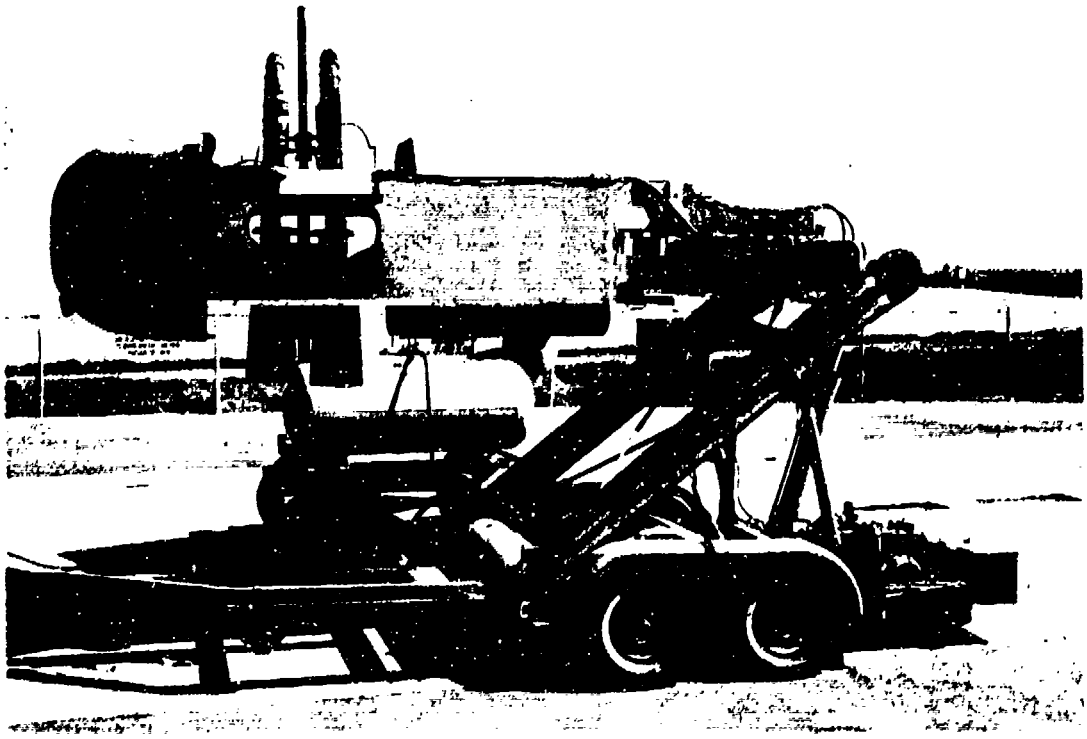


FIGURE 106: LIGHTWEIGHT HH(5.25")-7 PULSE REACTORS INSTALLED IN SHROUD ON TRAILER TEST RIG FOR 50-HR EXPLORATORY DURABILITY TEST PROGRAM

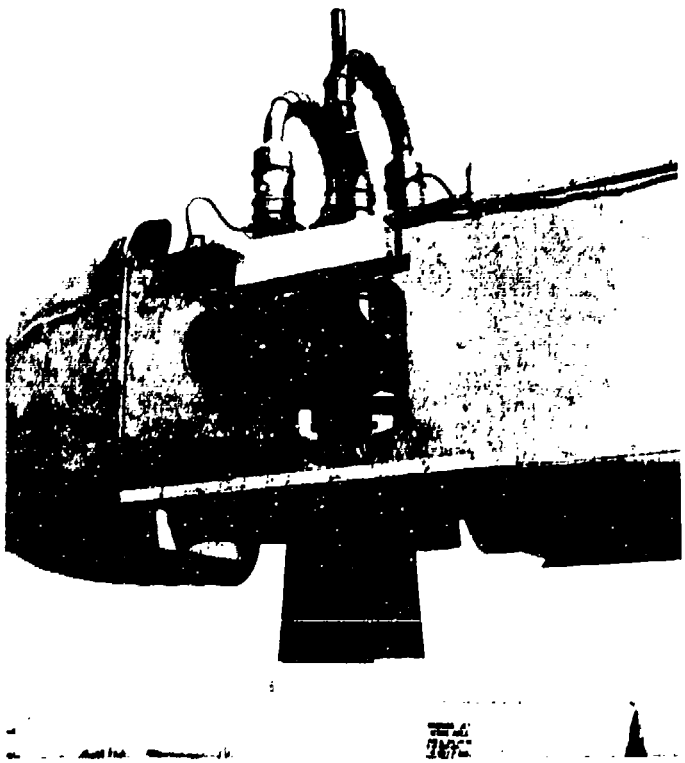


FIGURE 107: CLOSEUP OF INSTALLATION OF LIGHTWEIGHT HH(5.25")-7 ENGINES

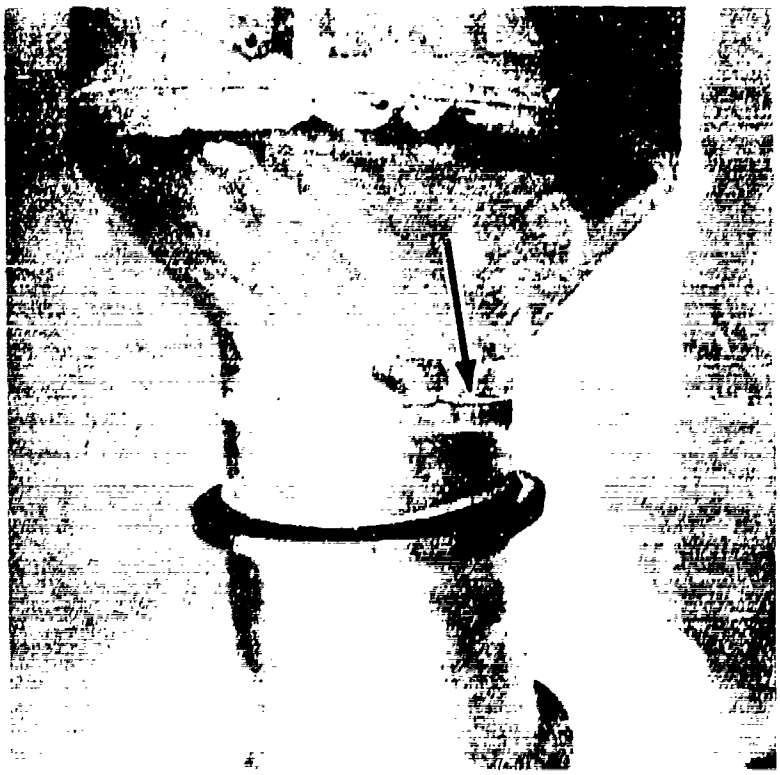


FIGURE 108: FAULTY BRAZED JOINT IN UNCOATED LIGHTWEIGHT HH(5.25")-7 COMBUSTOR



FIGURE 109: TYPICAL FATIGUE CRACK DEVELOPING BENEATH BRAZED-ON STIFFENING RING ON LIGHTWEIGHT HH(5.25")-7 COMBUSTOR



FIGURE 110: SMALL FATIGUE CRACK DEVELOPING AROUND SPARK PLUG BOSS OF UNCOATED COMBUSTOR



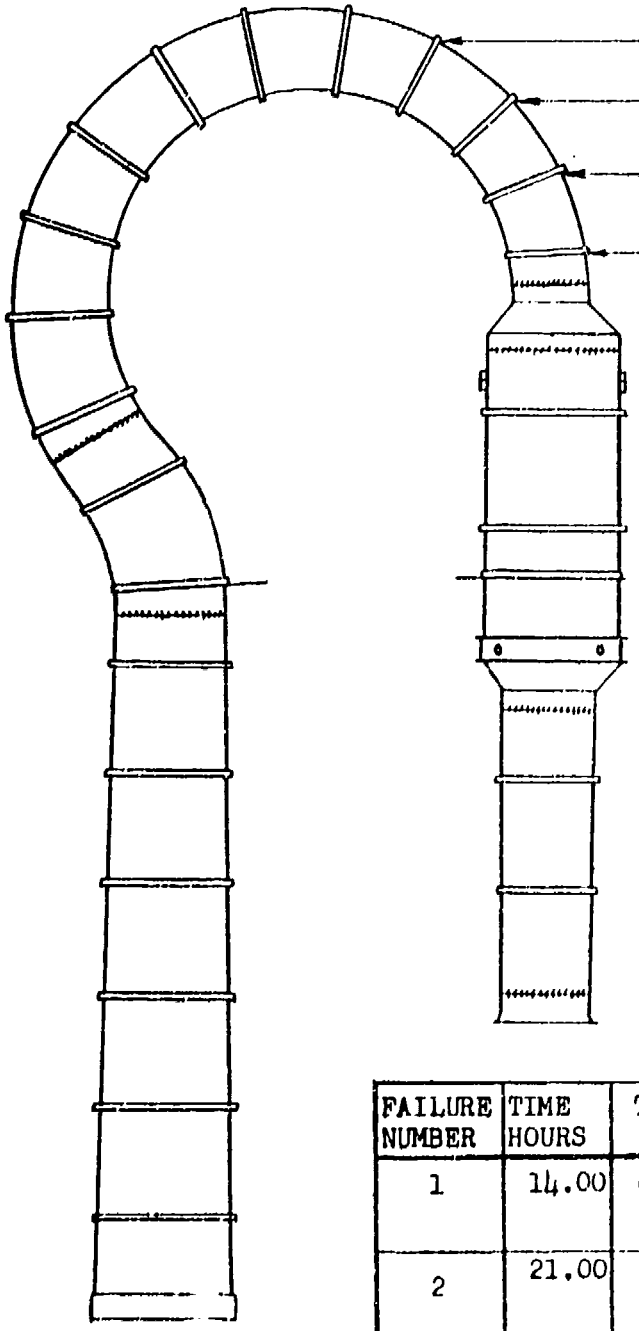
FIGURE 111: CIRCUMFERENTIAL FATIGUE CRACK AT JUNCTURE OF INLET TUBE AND COMBUSTION CHAMBER OF CERAMIC COATED LIGHTWEIGHT III(5.25")-7 COMBUSTOR

CYCLE DESCRIPTION	PERCENT MAX. THRUST	TIME			
		CYCLE, MIN.	NO. OF CYCLE SEQUENCES	UNIT HOURS	SUBTOTAL HOURS
Operator's Checkout -- for procedure, controls, performance, structural shock mounts and support systems		Indef.	Indef. 56	2:12	2:12
Cruising Power Setting	50%	20	36	12:33	14:45
Cruising Power Setting	65%	20	24	8:14	22:59
Cruising Power Setting (for slow forward speed)	75%	20	36	12:45	35:44
Cruising Power Setting (for transition speeds)	85%	20	24	8:20	44:04
Static simulation of hovering out-of-ground effect and low forward speed (5-10 mph). Note: This would normally provide important cooling airflow which was not provided in static runs.	95%	20	15	5:10	49:14
VTOL Throttle Modulation: 7 sec. to max. thrust; 15 sec. at max. thrust; 7 sec. to idle & repeat.	100%	$\frac{1}{2}$	244	1:12	50:26
VTOL Lift-off Cycle: 3 sec. to max. thrust; 1 sec. at max. thrust; 2 sec. to shutdown	100%	$\frac{1}{10}$	261	0:45	51:11

Figure II2: PULSE-REACTOR 50 HOUR DURABILITY TEST, POWER SETTINGS, CYCLES AND TIME

PULSE REACTOR 50 HOUR DURABILITY TEST

HH-5.25-7 ENGINE No. 2 (CERAMIC COATED) (SOLAR 6100)



MATERIAL TYPE: HAYNES 25
MATERIAL THICKNESS: .018
HIGH TEMPERATURE BRAZE "COAST 62"

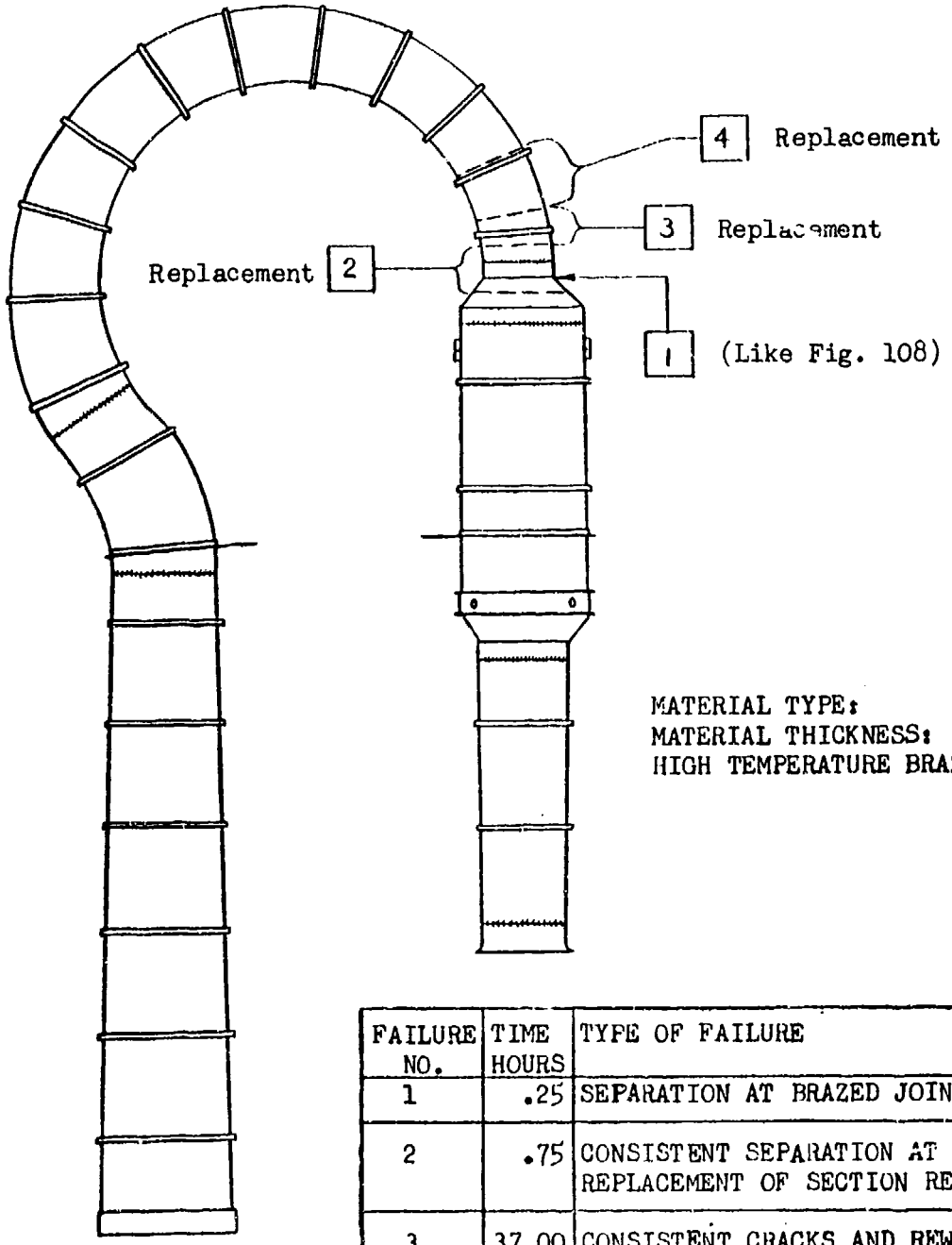
NOTE: THIS ENGINE DID NOT REQUIRE ANY REPLACEMENT SECTIONS, ALL REPAIRS WERE MINOR.

FAILURE NUMBER	TIME HOURS	TYPE OF FAILURE
1	14.00	CONSISTENT CRACKS OF LESS THAN 1" LONG
2	21.00	CONSISTENT CRACKS OF LESS THAN 1/2" LONG
3	24.25	SMALL CRACKS AND SLIGHT ELBOW BULGE AT RING LOCATION
4	28.00	SMALL CRACKS, WITH DEFORMATION OF ELBOW AT RING LOCATION

FIGURE 113: LIGHTWEIGHT HH-5.25-7 PULSE REACTOR SHELL (CERAMIC COATED) SHOWING LOCATION, TIME AND DESCRIPTION OF KEY REPAIRS.

PULSE REACTOR 50 HOUR DURABILITY TEST

HH-5.25-7 ENGINE No.1 (NOT COATED)

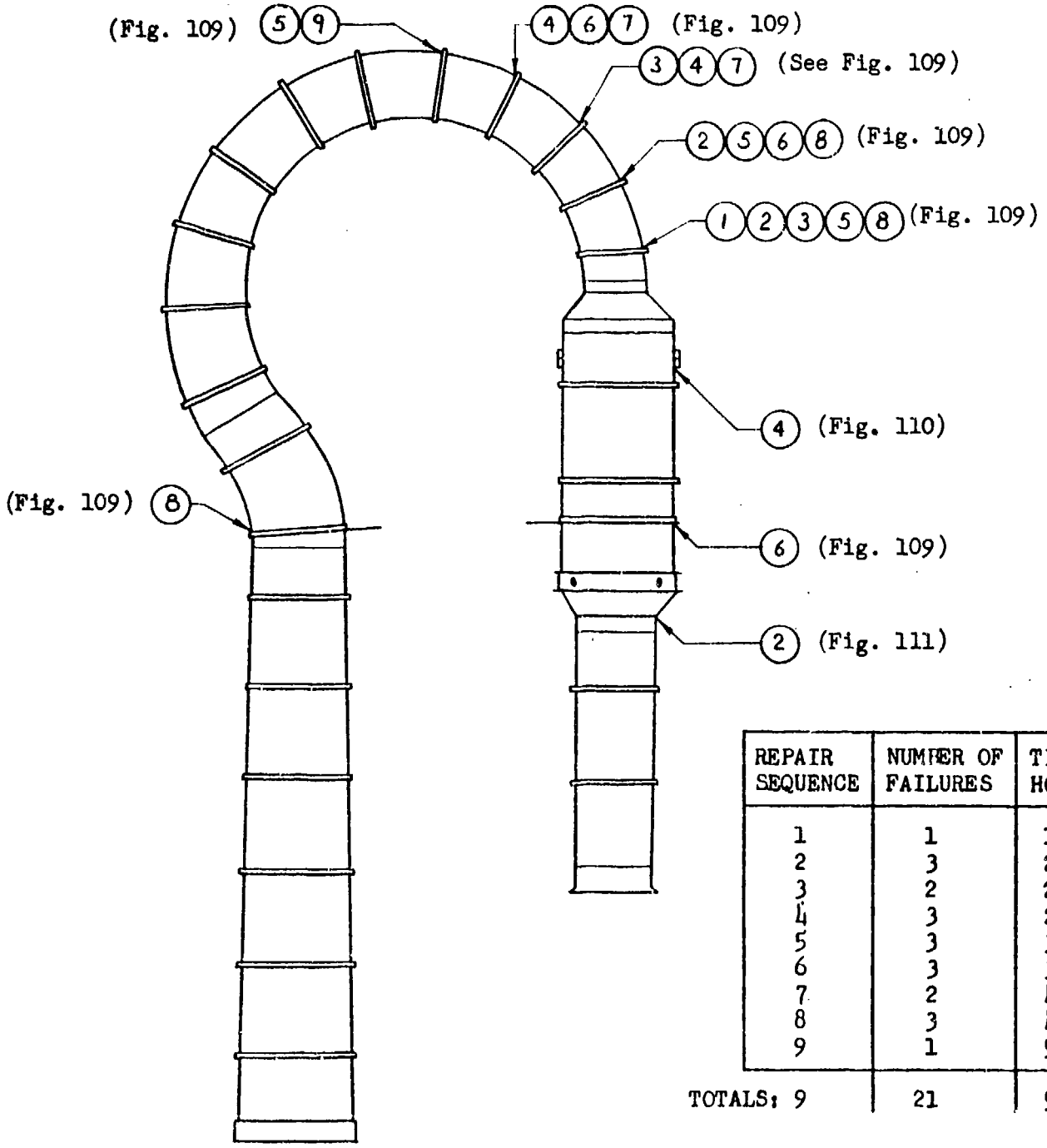


MATERIAL TYPE: HAYNES 25
MATERIAL THICKNESS: .018
HIGH TEMPERATURE BRAZE "COAST 62"

FAILURE NO.	TIME HOURS	TYPE OF FAILURE
1	.25	SEPARATION AT BRAZED JOINT
2	.75	CONSISTENT SEPARATION AT BRAZED JOINT. REPLACEMENT OF SECTION REQUIRED.
3	37.00	CONSISTENT CRACKS AND REWELDS.REQUIRED. REPLACEMENT OF SECTION REQUIRED.
4	47.00	CONSISTENT CRACKS AND REWELDS REQUIRED. REPLACEMENT OF SECTION REQUIRED.

FIGURE 114: LIGHTWEIGHT HH-5.25-7 PULSE REACTOR SHELL (UNCOATED) SHOWING LOCATION, TIME AND DESCRIPTION OF MAJOR REPAIRS.

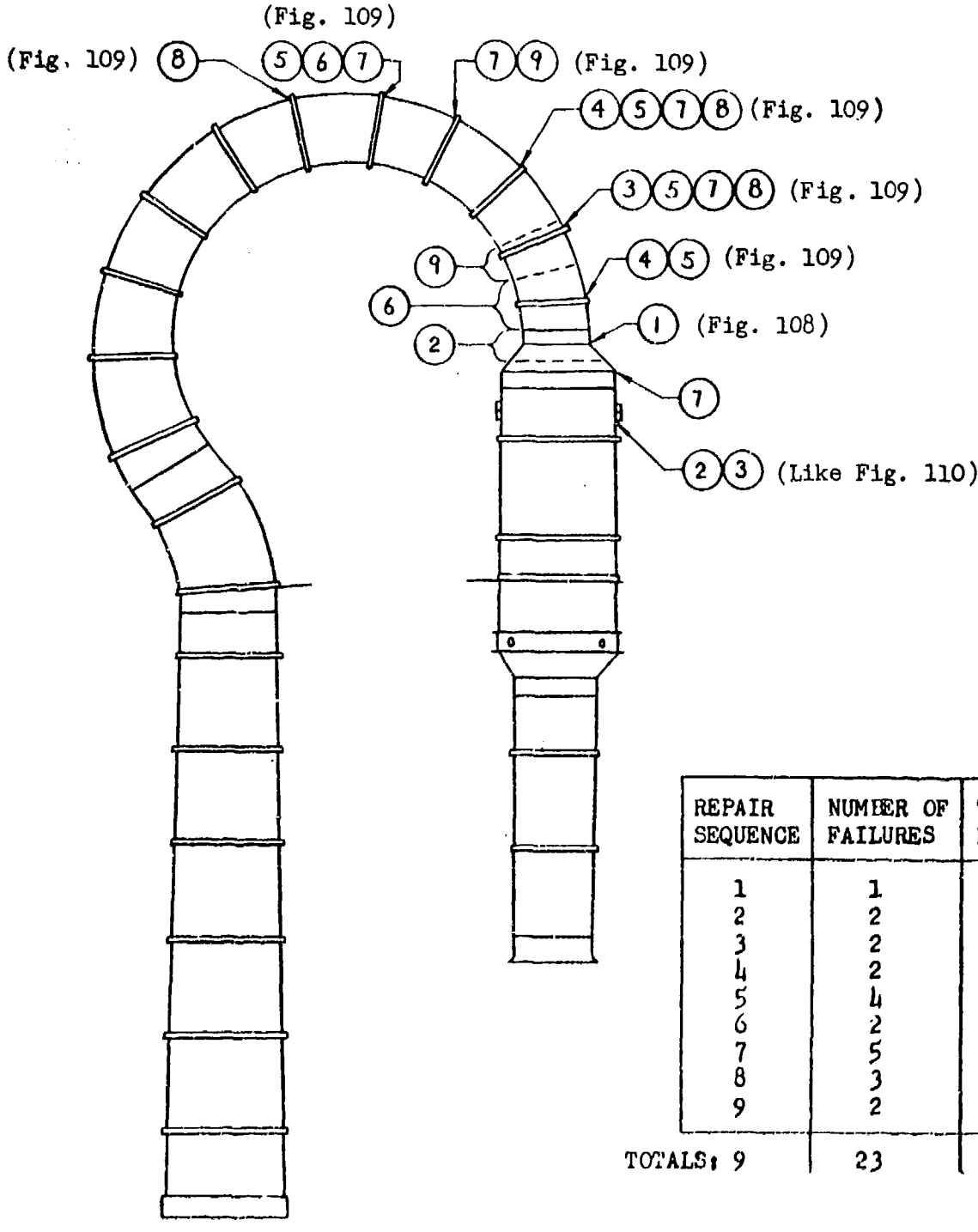
PULSE REACTOR 50 HOUR DURABILITY TEST
HH-5.25-7 ENGINE No. 2 (CERAMIC COATED) (SOLAR 6100)



REPAIR SEQUENCE	NUMBER OF FAILURES	TIME IN HOURS
1	1	14.00
2	3	21.00
3	2	24.25
4	3	28.00
5	3	34.25
6	3	36.00
7	2	42.75
8	3	43.50
9	1	50.50
TOTALS: 9	21	51.10

FIGURE 115: LIGHTWEIGHT HH-5.25-7 PULSE REACTOR (CERAMIC COATED) SHOWING THE COMPLETE HISTORY OF LOCATION AND TIME IN HOURS OF ENGINE SHELL REPAIRS INCLUDING INCIPIENT CRACKS.

PULSE REACTOR 50 HOUR DURABILITY TEST
HH-5.25-7 ENGINE No.1 (NOT COATED)



REPAIR SEQUENCE	NUMBER OF FAILURES	TIME IN HOURS
1	1	.25
2	2	.50
3	2	26.75
4	2	31.00
5	4	32.75
6	2	37.00
7	5	39.00
8	3	43.75
9	2	47.00
TOTALS: 9	23	51.20

FIGURE 116: LIGHTWEIGHT HH-5.25-7 PULSE REACTOR (UNCOATED) SHOWING THE COMPLETE HISTORY OF LOCATION AND TIME IN HOURS OF ENGINE SHELL REPAIRS INCLUDING INCIPIENT CRACKS

TYPES OF FUEL USED	Octane Rating	Initial Boiling Point
WHITE UNLEADED GASOLINE*	72-75	131°F**
AV-GAS	80-87.5	114°F
REGULAR GASOLINE	92	104°F
ETHYL GASOLINE	99.7	104°F
AV-GAS	100-130	120°F

*Considering the fuels shown above, the Pulse-reactor engine's operating characteristics were best when burning unleaded white gasoline (approximately 8 to 10% better) after extended exploratory durability runs.

**No initial boiling point was listed on refiner's test data but telecon from Standard Oil of Calif. Aviation Representative quoted as shown above.

FIGURE 117: VARIOUS TYPES OF FUEL USED DURING PULSE-REACTOR 50 HOUR EXPLORATORY DURABILITY TEST

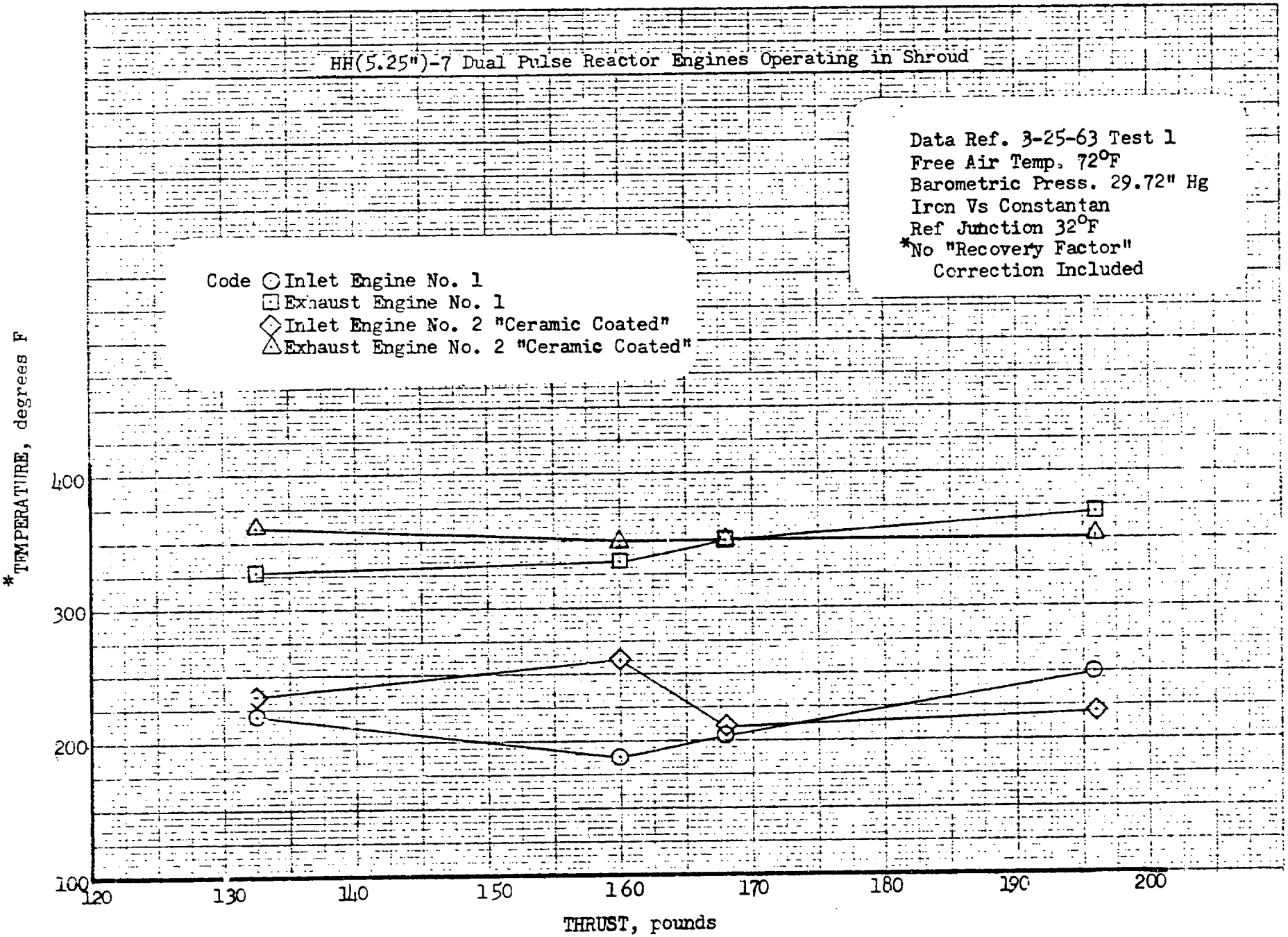


FIGURE 118: AVERAGE TEMPERATURE READING AT AUGMENTER OUTLETS

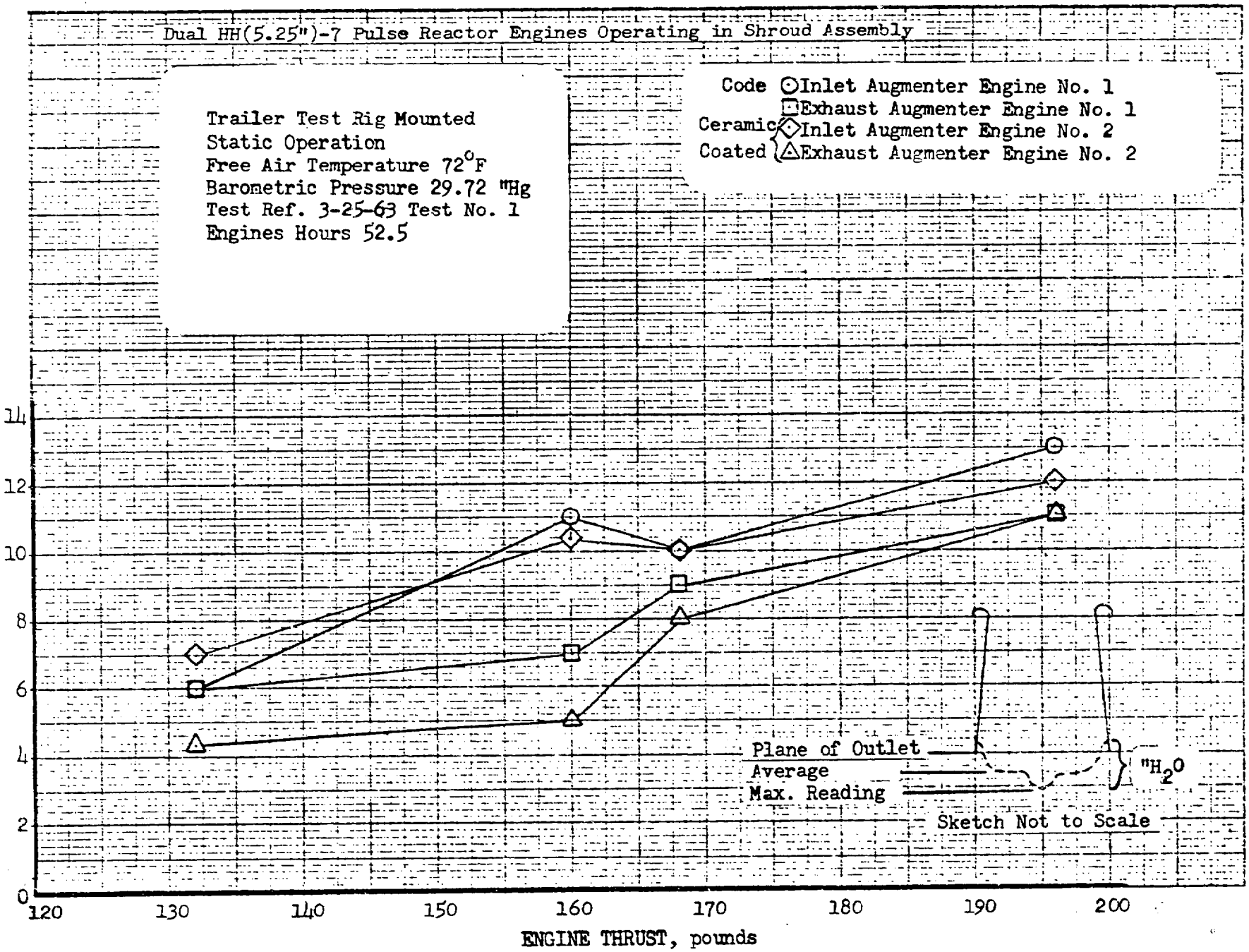


FIGURE 119: MEAN AVERAGE PRESSURE READINGS TAKEN AT AUGMENTER OUTLETS

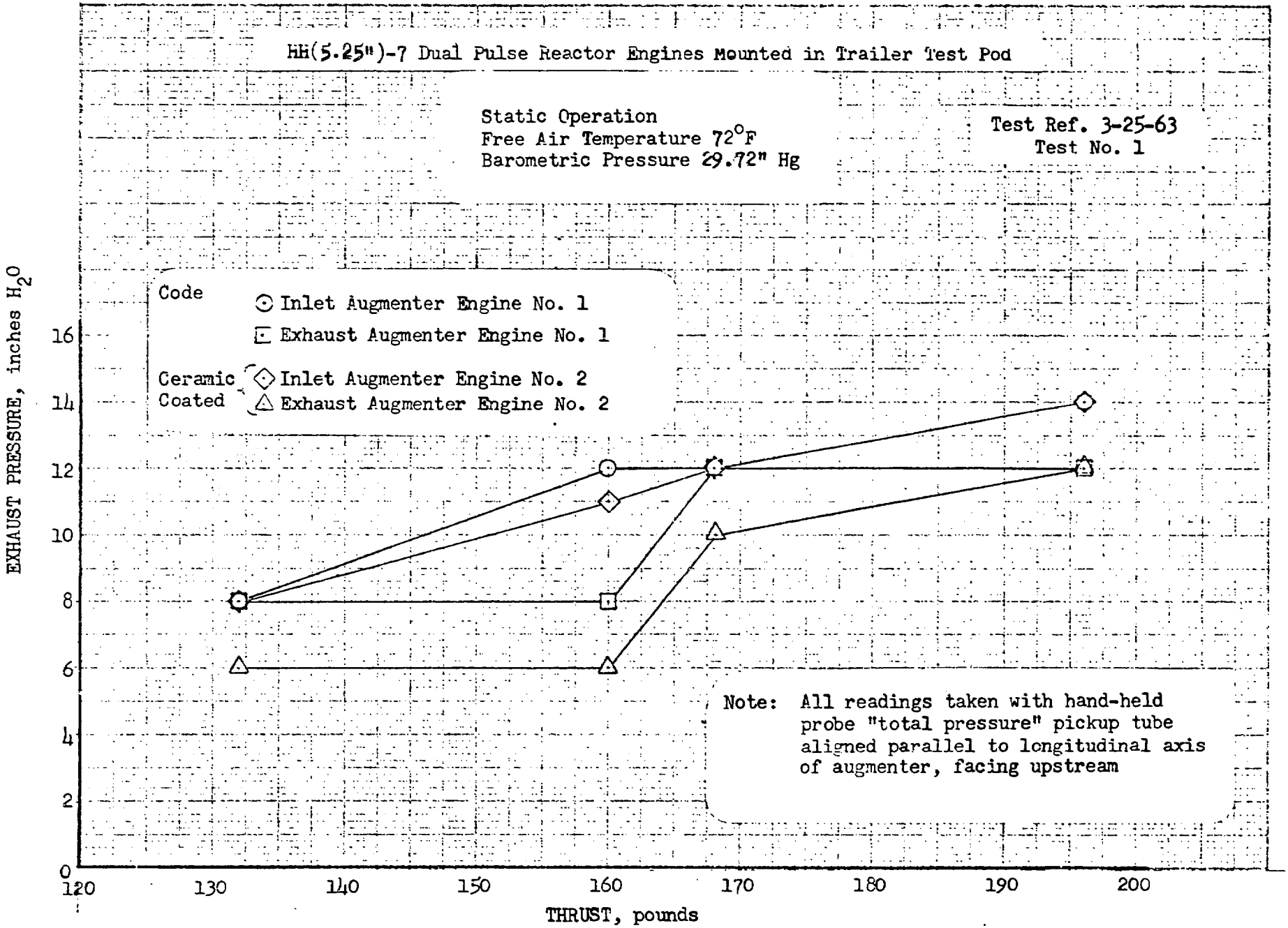


FIGURE 120: MAXIMUM PRESSURE READING TAKEN AT AUGMENTER OUTLETS

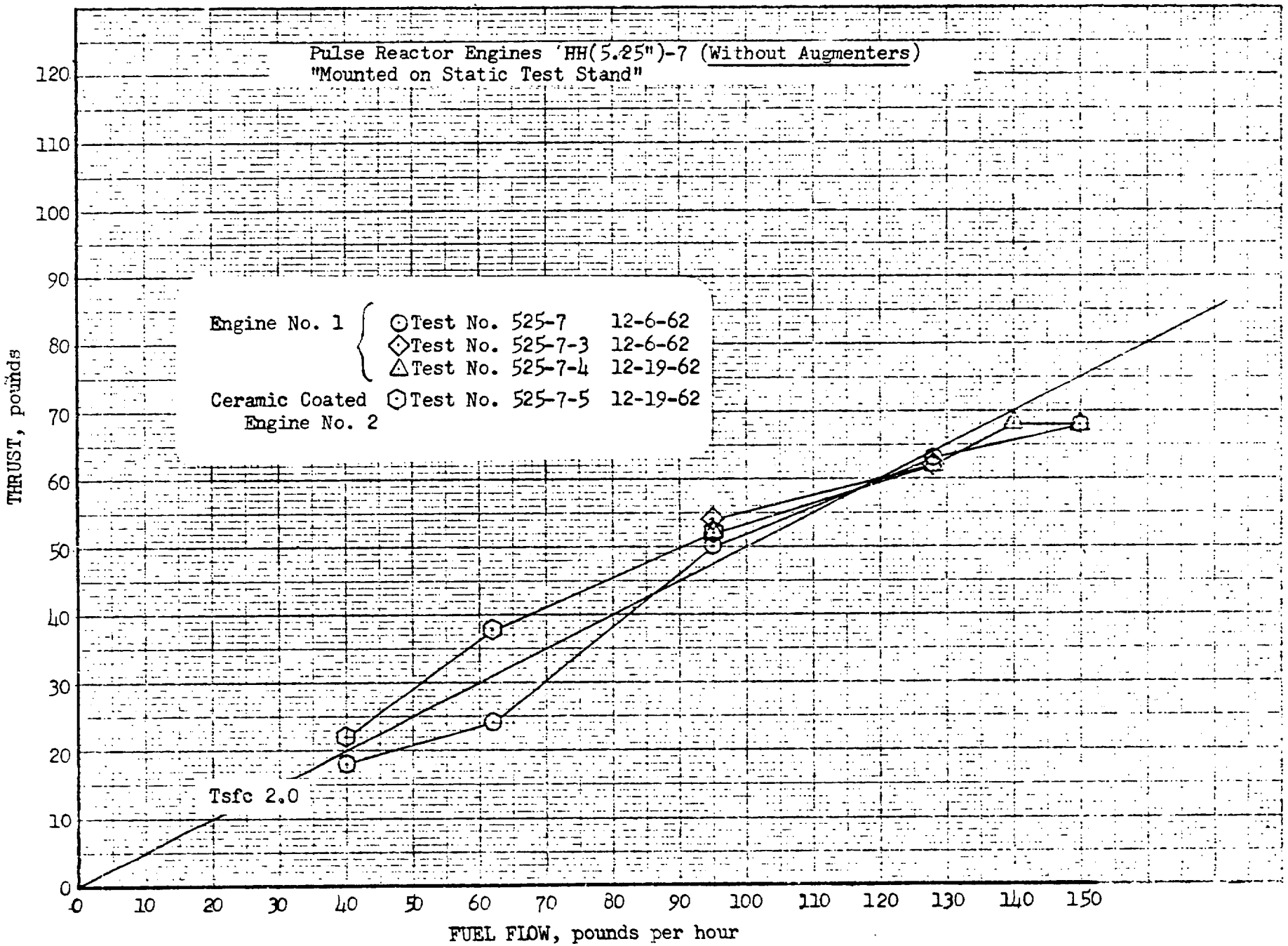


FIGURE 121: INDIVIDUALLY OPERATED HH(5.25")-7 PULSE REACTOR ENGINES WITHOUT AUGMENTERS, PRIOR TO 50-HOUR DURABILITY TEST RUN

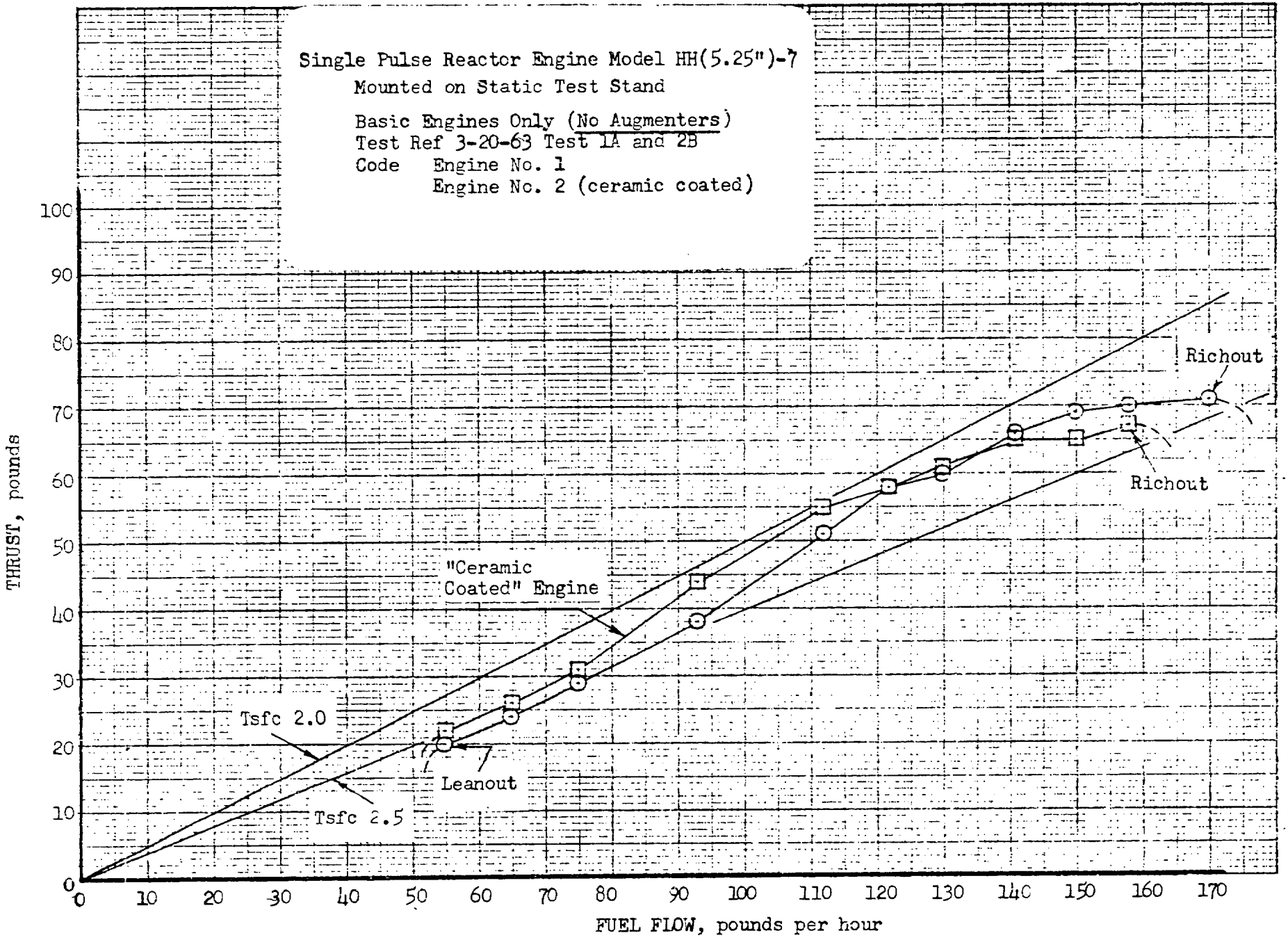


FIGURE 122: HH(5.25")-7 PULSE REACTOR ENGINE PERFORMANCE AT END OF 50-HOUR DURABILITY TEST RUN

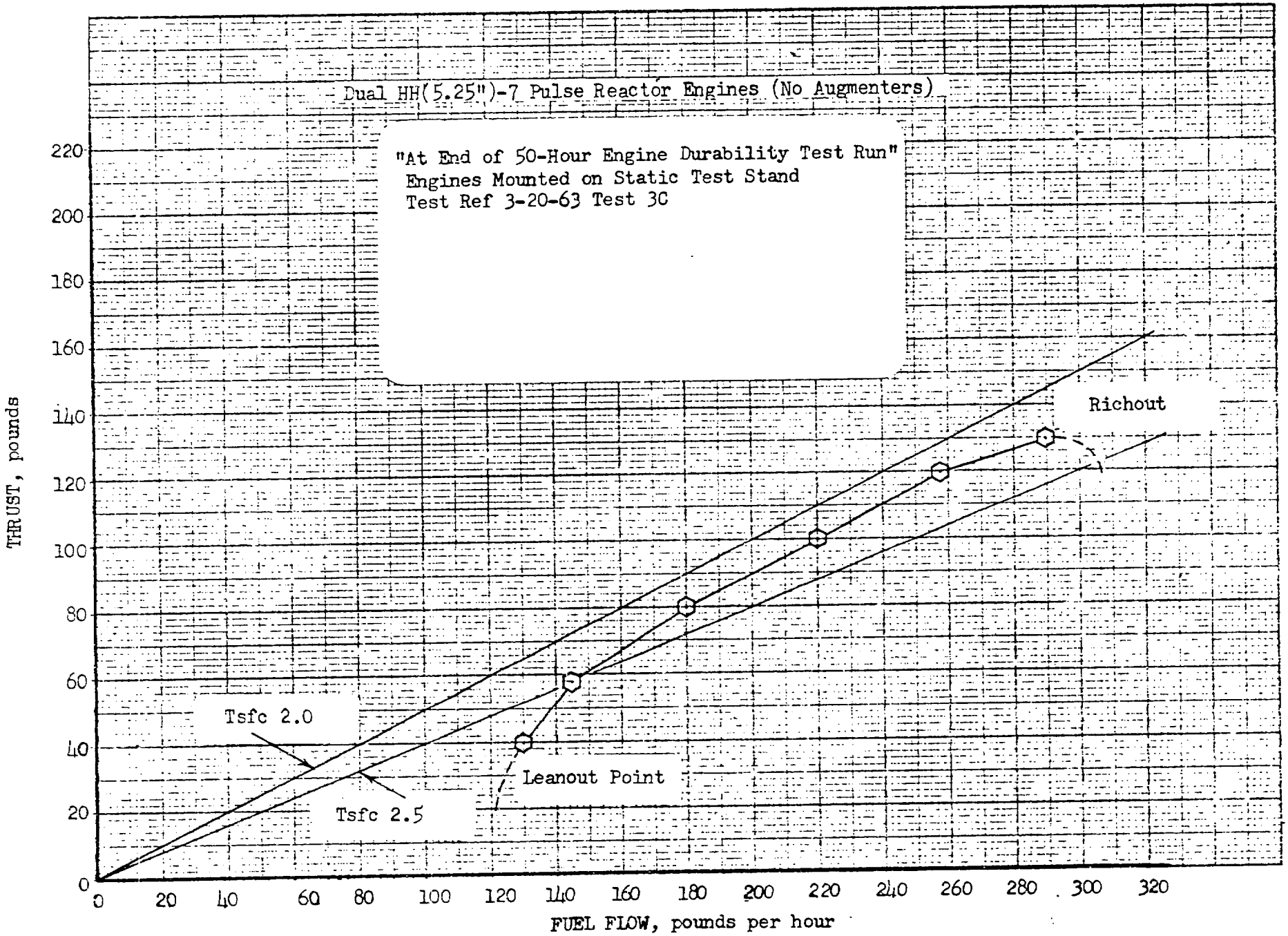


FIGURE 123: DUAL HH(5.25")-7 PULSE REACTOR ENGINES AFTER 50-HOUR DURABILITY TEST, WITHOUT AUGMENTERS

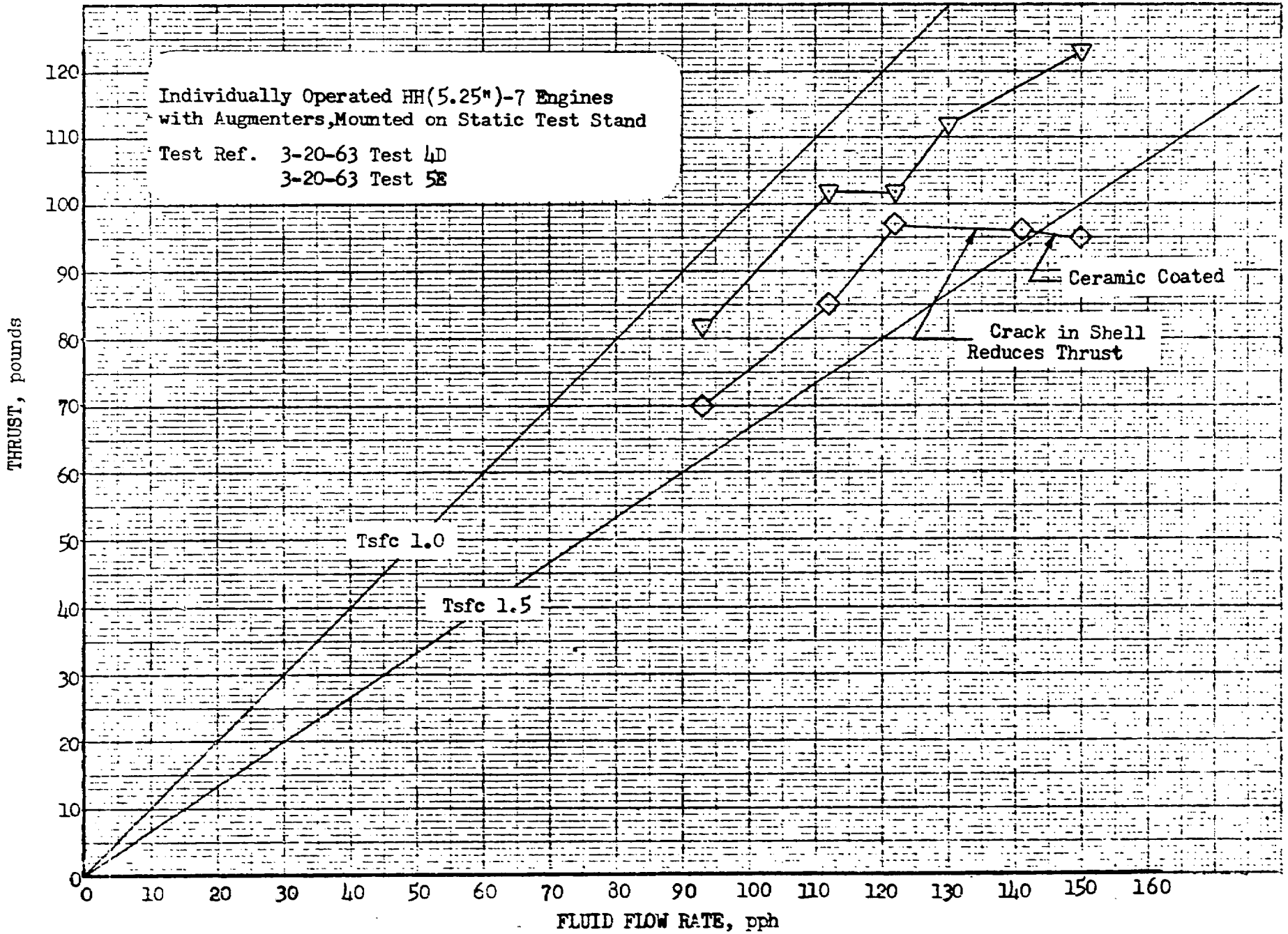


FIGURE 124: INDIVIDUAL HH(5.25")-7 PULSE REACTOR ENGINES WITH AUGMENTERS, AFTER 50-HOUR DURABILITY TEST RUN

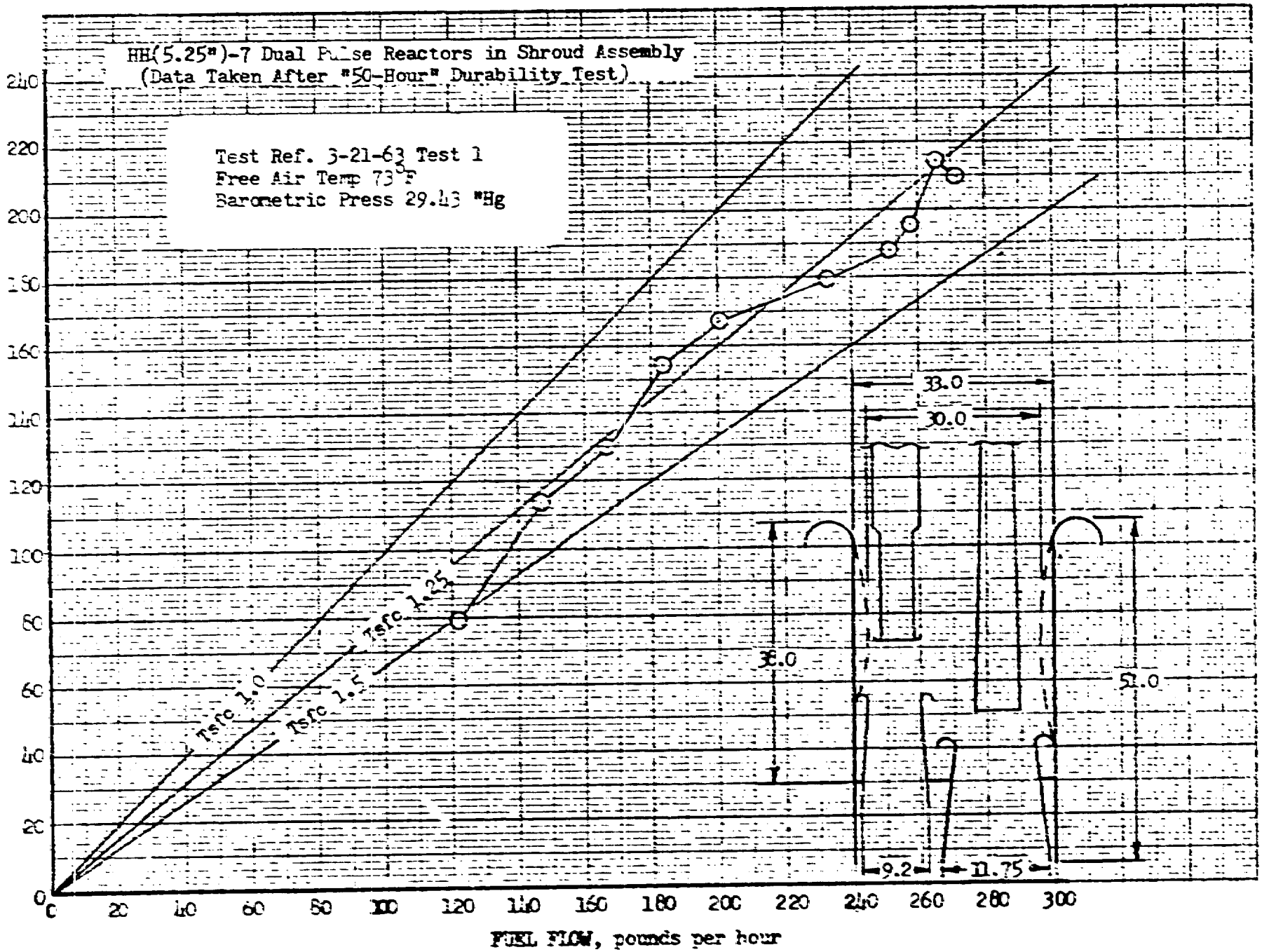


FIGURE 125: HH(5.25")-7 DUAL PULSE REACTORS IN SHROUD ASSEMBLY AFTER 50-HOUR DURABILITY TEST

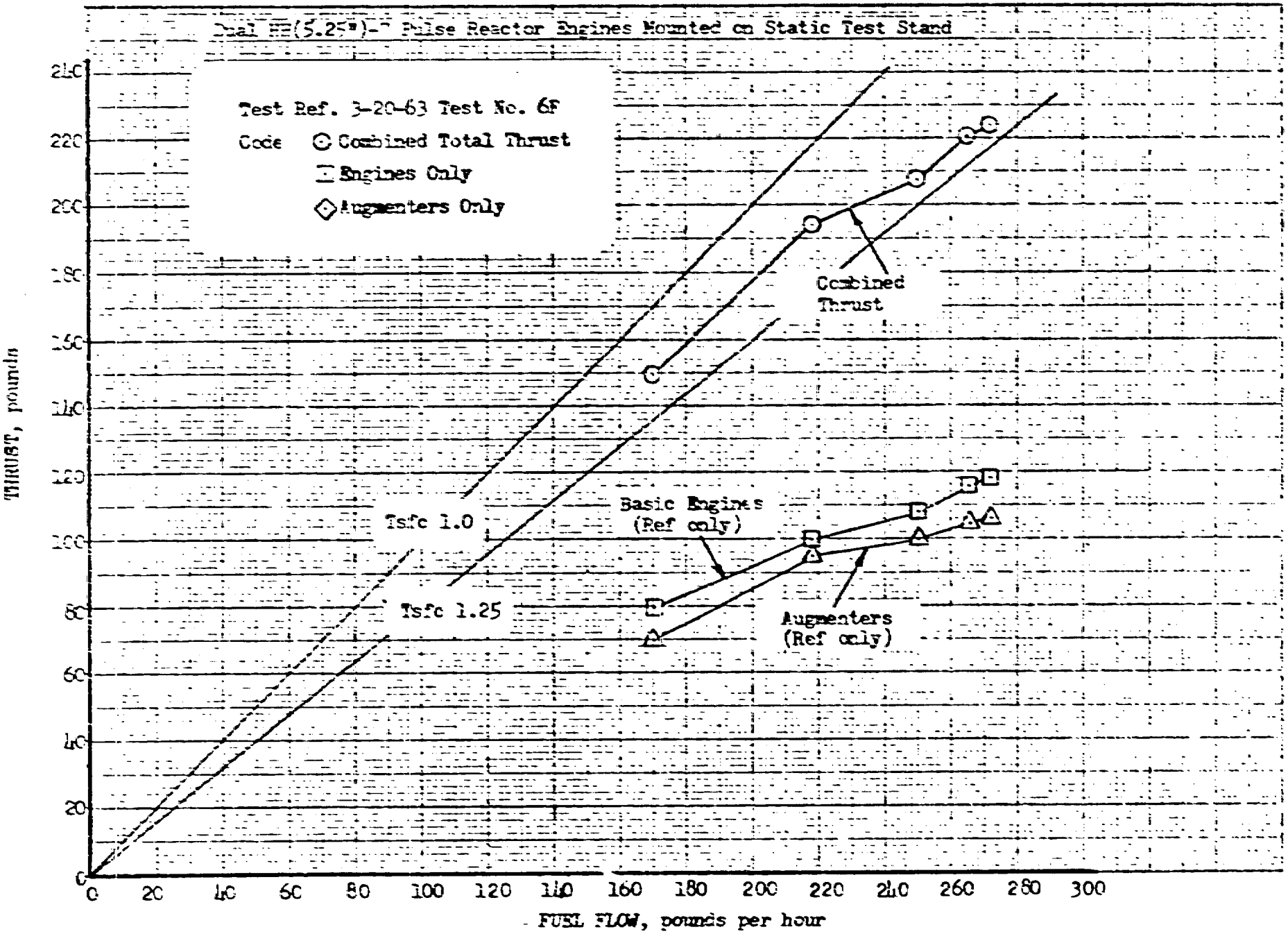


FIGURE 126: DUAL HR(5.25")-7 PULSE REACTOR ENGINES WITH AUGMENTERS AFTER 50-HOUR DURABILITY TEST

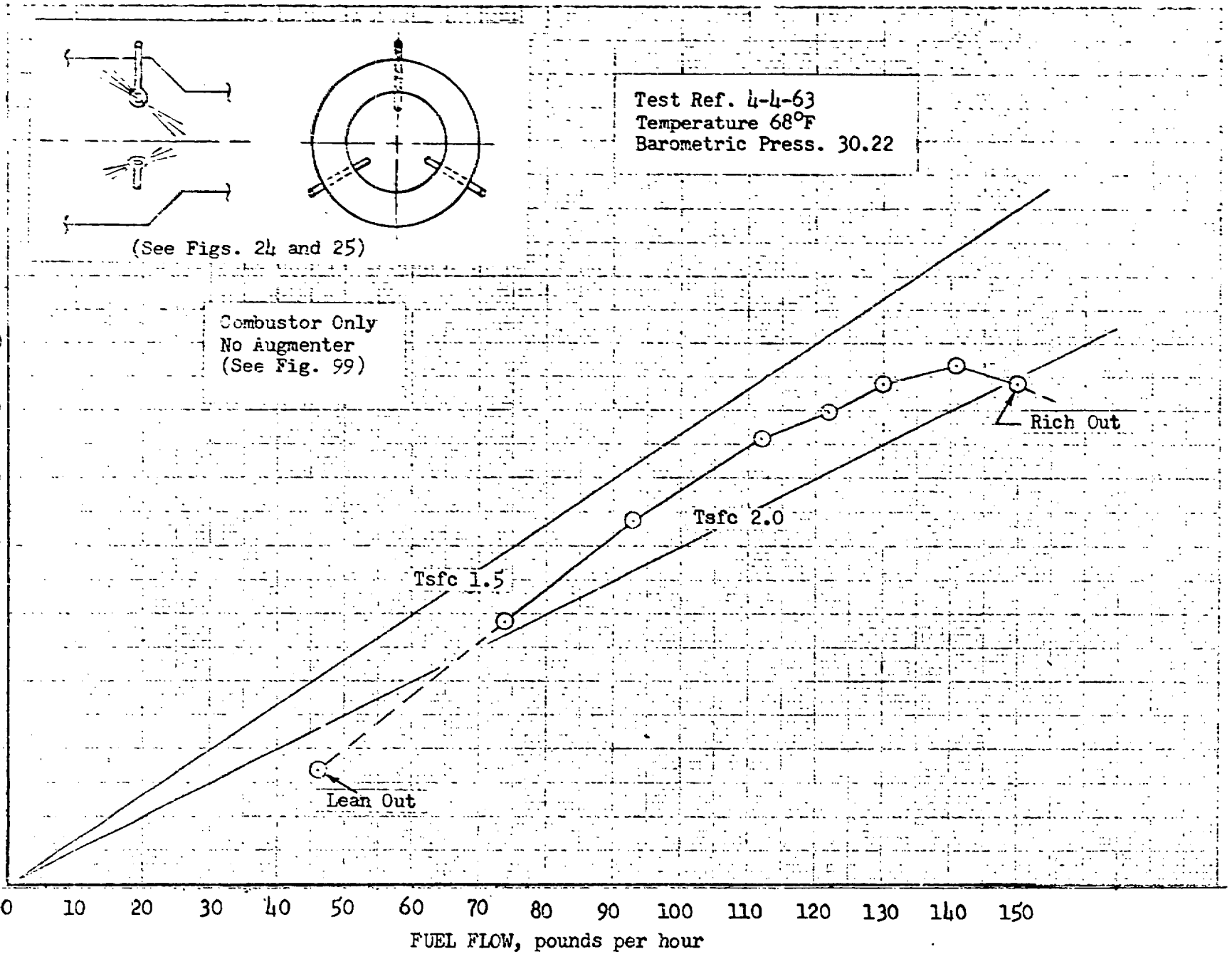


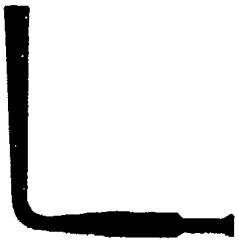
FIGURE 127: HH(5.25")-7 PULSE REACTOR COMBUSTOR WITH (3) FUEL NOZZLES (NO AUGMENTERS)

		Best Operating Engine "U"-Shaped Config. (Single Engine Data)		Best Dual Engine Data "U"-Shaped Config.		Best Engine Data (90° Configuration)	
		Comb.	Comb. + Aug.	2 Combs.	2 Combs + Aug's.	Comb.	Comb + Aug.
	Model Designation	HH5.25-7	HH5.25-5-2	HH5.25-5-2	HH5.25-5-2 +-5 aug.	HH5.25-6-7	HH5.25-5-2 +-5 aug.
Dimensional Data	Combustor: Max. dia/length, inches(Length is total length of combustor centerline)	5.25/88 (Fig.37)	---	5.25/87 (Fig.62)	---	5.25/91 (Figs. 34 and 37)	---
	Inlet Aug: throat dia/outlet dia/length,inches	---	6.25/9.2 /22 (1)	---	6.25/9.2 /22 (3)	---	6.25/9.3 /22 (1) (Fig.37)
	Exit Aug: throat dia/outlet dia/length,inches (1)	---	9.6/11.2 /11.5	---	9.6/11.75 /11.5	---	9.6/11.5 /14.4(Fig.57)
Performance	Test Date	4/63	1/63	1/63	1/63	12/62	12/63
	Max. Thrust, lbs	76 (Fig.127)	128 (3) (Fig.64)	145 (Fig.63)	252 (Fig.64)	86 (Fig.35)	147 (Fig.57)
	Min. Tsfc,lbs/lb/hr	1.7 (Fig.127)	1.0 (2) (Fig.64)	1.85 (Fig.63)	1.0 (Fig.64)	2.0 (Fig.35)	.87 (Fig.57)
	Thrust to Volume ratio, lbs/cu.ft.	122 (3)	72 (4)	122 (3)	72 (4)	124 (2)	83 (4)

(1) Inlet augmenter length can be reduced to 12" with slight loss in performance, see Fig. 55.
(2) Augmenters were optimized for -5 engines. Improved performance can be expected when optimized for -7 engine.
(3) Volume based on duct volume of combustor.
(4) Volume based on combustor plus duct volume of augmenters plus augmenter throat area x throat diameter.

FIGURE 128: SUMMARY TABULATION OF BEST PULSE REACTOR PERFORMANCE DATA

1 90° SINGLE COMBUSTOR



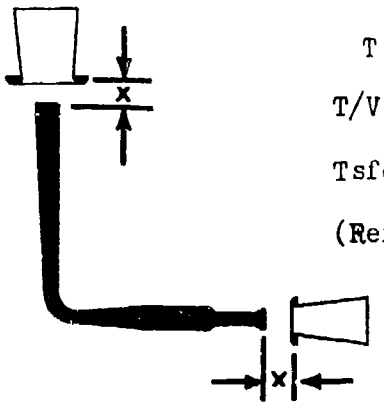
T = 86 lb

T/V = 124

Tsfc = 2.0

(Ref.) Figures -35, 32 & 31
HH 5.25-6-7

2 90° SINGLE PULSE REACTOR



T = 147 lb

T/V = 76

Tsfc. = .87

(Ref.) Figure- 57

HH5.25-5-2

3 180° SINGLE COMBUSTOR



T = 76 lb

T/V = 122

Tsfc = 1.7

(Ref.) Figure 127

HH 5.25-7

4 180° SINGLE PULSE REACTOR



T = 128 lb

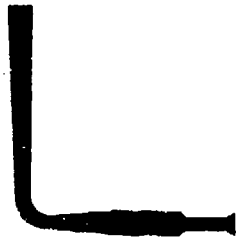
T/V = 72

Tsfc = 1.0

(Ref.) Figure 64
(No. 2 only)

HH5.25-5-2

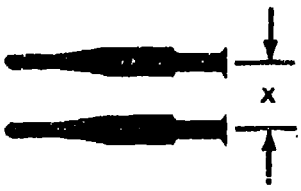
5 90° DUAL COMBUSTORS



(see 1 preceding)

HH5.25-5-2

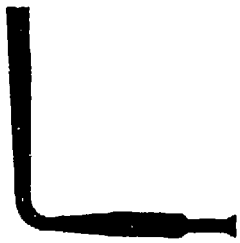
INLET- TO -INLET



11" & 14"

Tested without performance loss

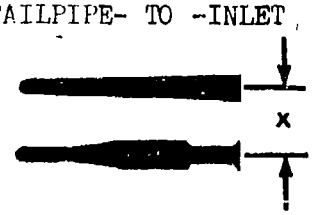
6 90° DUAL COMBUSTORS



(see 1 preceding)

HH5.25-5-2

TAILPIPE- TO -INLET

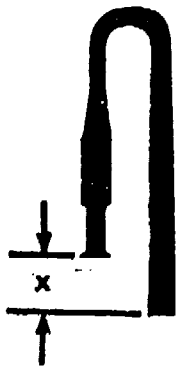


11" & 14"

Tested without performance loss

FIGURE 129a: BEST PULSE REACTOR PERFORMANCE WITH SKETCHES SHOWING VARIOUS CONFIGURATIONS AND COMBINATIONS

7 180° SINGLE COMBUSTOR



T = 76 lb

T/V = 122

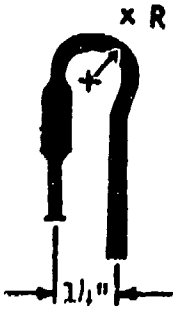
Tsfc = 1.7

(Ref.) Figures 96(2), 102 & 127

HH 5.25-7

Minimum spacing without performance loss; ≈ 11"

8 EFFECT OF TURN RADIUS



Minimum radius without performance loss

T = 76 lb

R = 9.25" T/V = 122

Tsfc = 1.7

(Ref.) Figure 127

HH5.25-7

9 BEST DUAL COMBINATION TO DATE (UNAUGMENTED)



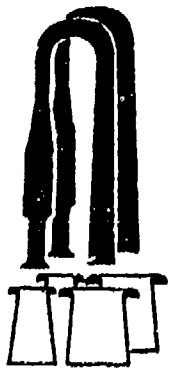
T/V = 122

Tsfc = 1.85

(Ref.) Figure 63

HH5.25-5-2

10 BEST DUAL COMBINATION TO DATE



T = 252 lb.

T/V = 72

Tsfc = 1.0

(Ref.) Figure 64

HH5.25-5-2

FIGURE 129b: BEST PULSE REACTOR PERFORMANCE WITH SKETCHES SHOWING VARIOUS CONFIGURATIONS AND COMBINATIONS

11 BEST DUAL COMBINATION TO DATE FROM SEPARATE COMPONENT TESTS



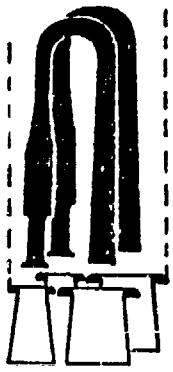
T = 304 lb

T/V = 116.0

Tsfc = .87

(Ref.) Figures 55, 56,63,64 and 127

12 BEST PACKAGE COMBINATIO. TO DATE*



T = 252 lb

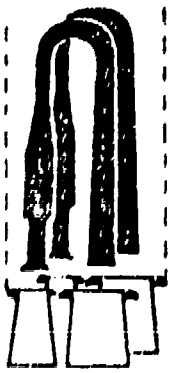
T/V = 17.0

Tsfc = 1.07

(Ref.) Figure 64

*Also see Figure 85

13 BEST COMPOSITE PACKAGE COMBINATION TO DATE



T = 292 lb

T/V = 20.0

Tsfc = .87

(Ref.) Figures 57, 63, 85 and 127

14 PERFORMANCE TARGET PROPOSED



T = 300 lb

T/V = 40.0

Tsfc = .85

(Ref.) See proposal

FIGURE 129c: BEST PULSE REACTOR PERFORMANCE WITH SKETCHES SHOWING VARIOUS CONFIGURATIONS AND COMBINATIONS

APPENDIX I

O R D E R No 30 694 E

C O N T R A C T No 0226 - C

TEST REPORT ON NEW TYPES OF PULSE-REACTORS DEVELOPED FOR HILLER AIRCRAFT CORPORATION

Le Chef de Département EP

P. SERVANTY.

SNECMA

DIVISION ATOMIQUE

CONTENTS

0 - SUMMARY
1 - DESCRIPTION OF THE TEST-BED
2 - DESCRIPTION OF MANUFACTURED UNITS
3 - TEST METHOD
4 - TEST RESULTS
5 - CONCLUSIONS
6 - DRAWINGS
7 - PICTURES

0. SUMMARY

The object of the contract No. 0226-c was to compare the relative qualities of new typesof pulse-reactors for lift purposes.

Within the scope of the agreement, a special test-bed adapted to the particular shapes of the machines to be tested was built at the Saclay Villeras Propulsion test center.

A large number of rigs were studied and built.

These rigs enabled to carry out tests on 97 versions of pulse-reactors up to July 15th, 1962.

The total operating time amounted to 16 hours 20 minutes at that very date.

The most interesting configurations were obtained from combustion chambers of the No 1 and 3 types (see drawing).

Tests enabled to draw important conclusions on the shapes of these new pulse-jets and can also lead to new shapes of thrust augmenters.

A program was set up for later developments.

1. DESCRIPTION OF THE TEST-BED

The test-bed was set up at the Saclay-Villeras Propulsion test center (Seine-et-Oise).

It is hung on 4 steel blades.

The hanging mobile part is constituted by a rectangular parallelepiped made of 3,500 mm long and 1,250 mm wide perforated L -extensions, displacement being perpendicular to the longest side.

According to the shape and dimensions of the tested pulse-reactor, it is mounted either on the top or overhanging at the rear of the rig with rubber dampers. In the last case, the rig-pulse-reactor must be balanced by a counter-weight.

Thrust is measured by two separate dynamometers fitted one behind the other:

- a "BALDWIN" capsule where thrust is read on a "BROWN" recorder
- a hydraulic capsule connected to a manometer

The fixed point of the dynamometers is constituted by a rigid U-shape iron rig, also supporting the calibration scale.

Fuel feeding is ensured by a gear pump fed by a loaded tank, injection pressure being set by a by-pass. Fuel consumption is measured through two gauging vases* fitted one behind the other, having respectively a capacity of 3.7 dm3 and 4.75 dm3.

Starting compressed air, generated by a compressor and kept in a tank, is lead to pulse reactor air inlets by one or several fixed air nozzles.

Ignition is ensured by an electrically driven SNECMA 14 R engine magneto, running at 1400 R P M.

---

*Flowmeter

2. DESCRIPTION OF UNITS

2.1 Combustion Chamber

Ten combustion chambers of 4 distinct types were built.

2.1.1 Five combustion chambers of the No. 1 type respectively designated by symbols 1, 1bis, 1 ter, 1 quater.
Two combustion chambers 1 ter were built, the first one having been damaged during tests.
Chamber 1 quater has not been tested yet due to the interruption of the work.
Respective volumes of these chambers are as follows:

Chamber No. 1	V = 26,9 dm3	(0,95 cub ft)
Chamber 1 bis	V = 24,4 dm3	(0,86 cub ft)
Chamber 1 ter	V = 40,5 dm3	(1,43 cub ft)
Chamber 1 quater	V = 27 dm3	(0,95 cub ft)

2.1.2 Two chambers No. 2

Chamber No. 2	V = 25 dm3	(0,881 cub ft)
Chamber No. 2 bis	V = 31,8 dm3	(1,12 cub ft)

2.1.3 Two chambers No. 3

Chamber No. 3	V = 16,6 dm3	(0,586 cub ft)
Chamber No. 3 bis	V = 30,5 dm3	(1,076 cub ft)

2.1.4 1 chamber No. 4

Chamber No. 4	V = 29,3 dm3	(1,034 cub ft)

2.2 Exhaust Nozzles

Seven pairs of exhaust nozzles were built:

2.2.1 Three pairs of 90°, constant area, elbowed exhaust nozzles having respectively a diameter of 120, 140 and 160 mm (4,62, 5,5 and 6,3 inches)

2.2.2 Two pairs of multi-exhaust nozzles of the No. 1 type
Two exhaust nozzles No. 1 comprising seven 50 mm diameter pipes (1.97 inches)
Volume: 13,5 dm3 (0,476 cub ft)

Two exhaust nozzles No. 1 bis comprising seven 60 mm diameter pipes, the connecting angle of which is different from the previous ones. (2.36 inches)

Volume: 16,5 dm3 (0,582 cub ft)

2.2.3 I pair of exhaust nozzles No. 2
Helmoltz resonator type

Volume: 31,8 dm3 (1,122 cub ft)

2.2.4 I pair of exhaust nozzles No. 3
Constant area elbowed exhaust nozzles which are connected to a cylindroconic capacity.

Volume: 17,4 dm3 (0,614 cub ft)

2.3 Intermediate Nozzles

Seven pairs of intermediate nozzles were built; their characteristics are as follows:

Diameter (inches)	Diameter max. (inches)	length (inches)	Volume (cub ft)
3,15	5,5	47,2	0,411
3,54	6,29	39,3	0,441
3,93	5,5	47,2	0,482
3,93	5,5	66,8	0,752
3,93	6,29	39,3	0,47
3,93	6,29	47,2	0,57
3,93	6,29	62,9	0,8525

2.4 Air Inlet

Machined light alloy bell mouths were fitted on the air inlets of all combustion chambers.

Type No. 1 combustion chambers were successively equipped with straight and 90° elbowed air inlets.

2.5 Fuel Nozzles and Supports

Three types of fuel nozzles were used during tests.

2.5.1 8 mm external diameter type G nozzles, comprising two tangential feeding holes of 9 mm diameter and an exhaust outlet of 1.6 mm diameter. These nozzles are of the vortex type.

2.5.2 10 mm external diameter type G nozzles, comprising two tangential feeding holes of 1 mm diameter and an exhaust outlet of 2.4 mm diameter. These nozzles are of the vortex type.

2.5.3 9 mm external diameter radial nozzles comprising an adjustable slit, fuel being sprayed under the form of a very thin mist.

2.5.4 Various configurations of nozzle supports were built according to the selected location in the combustion chamber.

2.6 Manufacturing Methods

2.6.1 Combustion chambers, intermediate nozzles and outlets were made of stainless steel (1.2 mm and 1.5 mm thick).

All components comprised connecting flanges enabling to achieve a large number of configurations by bolting.

2.6.2 F and G type fuel nozzles were made of brass, radial fuel nozzles of stainless steel Z 10 CNT 18.

2.6.3 Nozzle supports and attachments on the combustion chamber were made of stainless steel Z 10 CNT 18.

3. TEST METHODS

3.1 Each test was preceded with and followed by calibration of the two thrust measuring devices through the scale connected to the test bed. Calibration curves were successively set up with increasing then decreasing loads.

The arithmetic average of indications recorded on the two measuring devices was selected as the thrust measure.

Discrepancy between thrust recorded by the "BALDWIN" and the hydraulic measuring device never exceeds 4%.

Measures were performed under steady conditions, i.e., constant injection pressure and steady thermal state of the pulse-reactor.

Starting maximum thrust generally exceeds by 8 or 10% approximately the steady thrust taken into consideration.

3.2 Fuel mass flows were measured by consumption timing of the gauging vases*, computation of the weight mass flow being based on the density measured by a float densimeter.

Ordinary fuel was used. During tests, fuel density varied between extreme limits of 0,730 kg/dm3 and 0,742 kg/dm3.

3.3 Easy starting and steady operation were first appreciated for each configuration.

For each steady configuration, limitations of poor and rich extinctions were looked for and thrust and fuel consumption were measured.

Worthwhile configurations were submitted to conventional adjustment of air inlet lengths.

---

*Flowmeters

For the best configurations, influence of the type and location of the fuel nozzles was studied.

While changing the type of fuel nozzles remains a rather simple and quick operation, shifting them requires a large amount of work (drilling of new holes in the combustion chamber, blanking of previous ones and welding of nozzle support attachments in their new location). Since No. 1 type chambers comprised 8 fuel nozzles, number of positions tested had to be limited and it is very doubtful that the optimum position is determined yet.

174

As a matter of fact, the direction of the wind during starting seems to affect the direction of such dissymmetry.

4.1.2 In fact, all perfectly steady and easy to start pulse-reactors were fitted with type No. 1, type No. 3 bis and type No. 4 combustion chambers.

4.2 Performance

Performance results of No. 1 type combustion chamber pulse-reactor are limited to the thrust developed by the exhaust nozzles for the following reasons:

4.2.1 During first tests, 90° elbowed air inlets were fitted to these pulse-reactors. In this case, measured thrust represented the sum of the exhaust nozzle thrust and the thrust corresponding to the momentum ejected from the air inlets during backflow following the combustion.

Then the same pulse-reactor was tested with straight air inlets. In this case, the momentum ejected from the air inlets is in a plane perpendicular to the direction of the nozzle exhaust and the thrust of the nozzles is only recorded.

It was noted that the thrust of the nozzles alone in the configuration with straight inlets was higher or at least equal to the total thrust with elbowed air inlets.

Thrusts of nozzles alone have been compared with straight air inlets by rotating the combustion chamber of 90°, the elbowed nozzles being directed to the top at 90° of the nozzles thrust direction.

The result of each test is shown on drawing

It is clearly shown that for the same fuel mass flow, the thrust of the nozzles is much higher with thrust air inlets than with elbowed air inlets.

Further, with the elbowed inlets, rich extinction prematurely occurs as a result of defective filling of the combustion chamber during the rarefaction phase.

It can be concluded that the constant area elbowed air inlet is the cause of important loss and must be given up for the benefit of either specially studied elbows, or more probably, elbowed thrust augmenters.

4.2.2 Performances of pulse-reactors with No. 1 Type combustion chamber are shown on drawings 6-4 to 6-9.

Drawings 6-4 and 6-5 concern pulse-reactors with No. 1bis type chamber; drawings 6.6 and 6.7, pulse-reactors with No. 1 ter type chamber; drawings 6.8 and 6.9 represent thrusts per unit of volume respectively for pulse-reactors with chambers 1 bis and 1 ter.

In every instance, considered thrust is the thrust of nozzles alone, air inlets thrust not included. It seems that chamber 1 bis is largely superior to chamber 1 ter.

The increase of thrust per unit of volume can be explained by similarity laws, but discrepancy of specific fuel consumption seems to be due to an indisputable specific superiority.

For instance, in the best respective configurations a thrust of 49 kg (108 lb) is obtained with a fuel flow of 430 kg/h (947 lb/h) by the pulse reactor with chamber 1 ter and only 278 kg/h (613 lb/h) with chamber 1 bis.

4.2.3 Various considerations resulting from the previous tests have been the cause of drawing chamber I quater which is believed to be superior to chamber 1 bis. Such chamber has not been tested yet.

4.3 Drawing 6 - 10 represents unsatisfactory results obtained with other types of pulse-reactors.

On this drawing, shown thrusts are total thrusts, exhaust nozzle thrust plus air inlet thrust, which could be directly measured for pulse-reactors with chambers 2 bis, 3 bis and 4.

As regards chamber No. 1, it was fitted with elbowed air inlets and it has been explained above that the consequences of this configuration were very unfavorable.

4.4 Drawing 6 - 11 shows the influence of the support type and of the location of the fuel nozzle in the chamber. It is clear that the influence of the support type is almost negligible in comparison with the large influence of the change of location.

As it has already been pointed out, it is doubtful that the optimum location has been found during these tests.

4.5 Succinct tests have finally been performed to measure total thrust of No. 1 type engines.

Because of their shortness, no final conclusion can be presented yet.

It seems that the impulse which could be used on air inlets is about two-thirds of the impulse of the exhaust nozzles, this estimation is in accordance with the results measured on the other types of pulse reactors.

In the straight air inlet configuration, total thrust can be measured only with elbowed thrust augmenters, i.e., measured thrust

would be the thrust with dilution on air inlets.

Elbowed thrust augmenters have been produced; it was not possible, due to the allowed credits, to adjust, even succinctly, such augmenters.

However, it has been clear that the elbowed augmenters with area regularly increasing from upstream to downstream could be favorably replaced by augmenters having a cylindrical upstream part and an elbow with a regularly increasing elbow area.

But this conclusion remains dubious because of the too small number of tests.

5. CONCLUSIONS

From tests performed on 97 different configurations of pulse-reactors, the following conclusions can be made:

5.1 Type No. 1 combustion chambers are superior to all the other ones, as well as for starting easiness, as for operation steadiness and level of performances.

5.1.1 As regards Type 1, chamber 1 bis has been found the most satisfactory as for the level of performance.

5.1.2 For a constant volume, an increase of the diameter to the detriment of the length has always produced, within the tested limits, an improvement of performance.

5.1.3 Among the other types of tested combustion chambers, only chamber No. 3 bis seems capable to reach a satisfactory level of performance.

However, this chamber has the disadvantage to have a complex technology and a dubious life time; it has been damaged several times in spite of rather short operations.

5.1.4 It is advisable to give up all the other types of tested combustion chamber for No. 1 type chambers.

As regards this type, chamber No. 1 bis is the best, but chamber No. 1 quater is deemed to be superior.

5.1.5 No. 1 Type exhaust nozzles (multi-pipe exhaust) are superior to constant area simple elbows and still can be improved. Tested Helmolta resonator Type exhausts operated correctly and gave a thrust rather equal to the thrust of multi-pipe exhausts).

BC

However, their performance is not as good as regards the thrust per unit of volume. The highest thrusts have been obtained with elbows connected with a large volume capacity because of the back-flow.

5.1.6 The fuel nozzle location is very important. Small changes of location are the cause of enormous performance variations.

Unfortunately, tests to determine the best location are very difficult to perform.

5.1.7 It seems necessary to use on No. 1 type pulse-reactors straight air inlets. The best method to use the impulse of these air inlets is not clear yet.

Elbowed thrust augmenters seem to present the most favorable solution.

5.2 Work schedule for the continuation of the development could be as follows:

5.2.1 Test of chamber 1 quater.

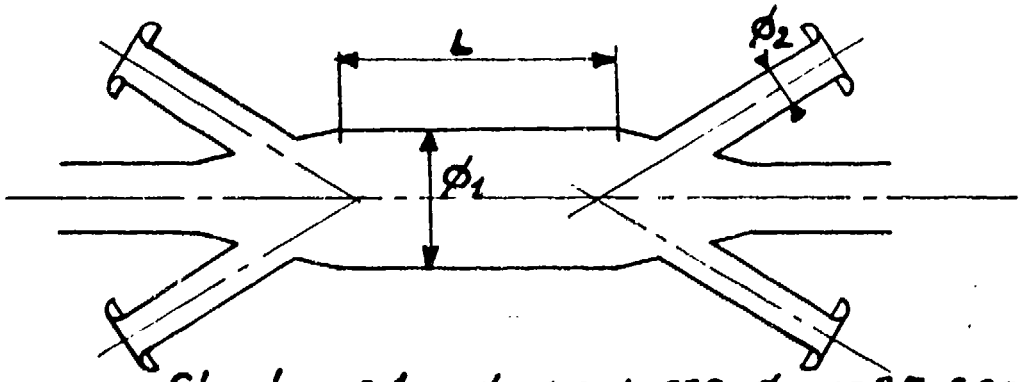
5.2.2 Location of the best position of fuel nozzles.

5.2.3 Study on utilization of impulse of straight air inlets through elbowed thrust augmenters.

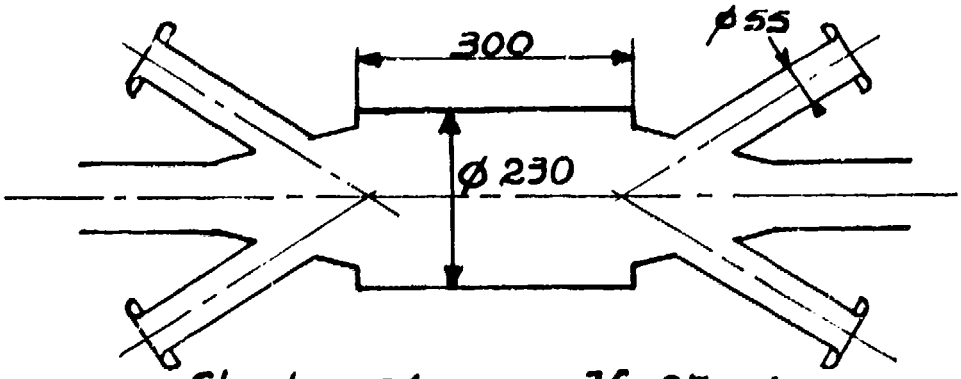
5.2.4 Improvement of multi-pipe exhaust.

5.2.5 Study of augmenters on multi-pipe exhausts.

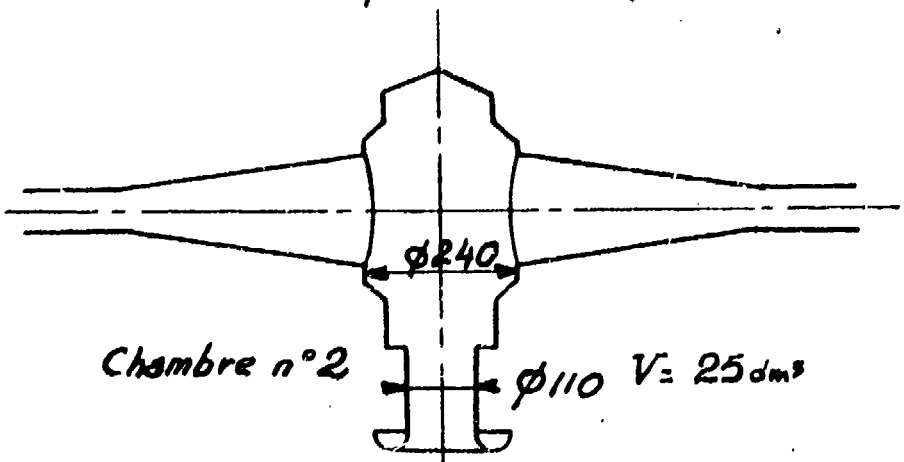
(8)



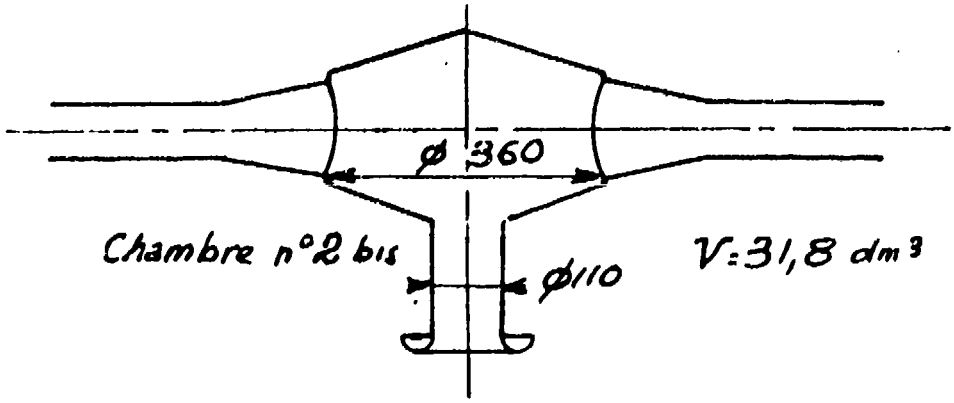
Chambre n°1 ϕ_1 = 160 L = 600 ϕ_2 = 55 V = 269 dm³
1bis " = 200 " = 400 " = 62 " = 24,4
1ter " = 230 " = 500 " = 76 " = 40,5



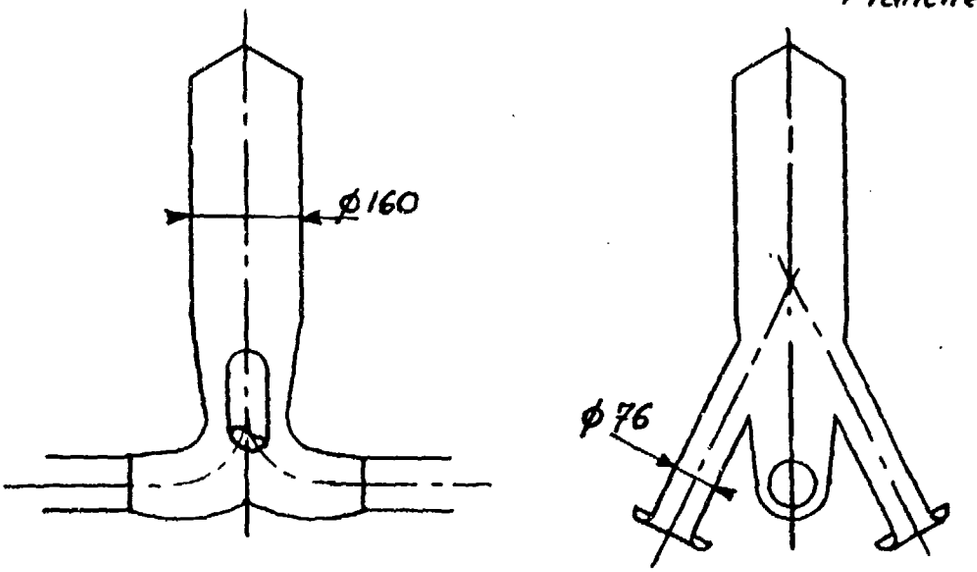
Chambre n°1 quater V = 27 dm³



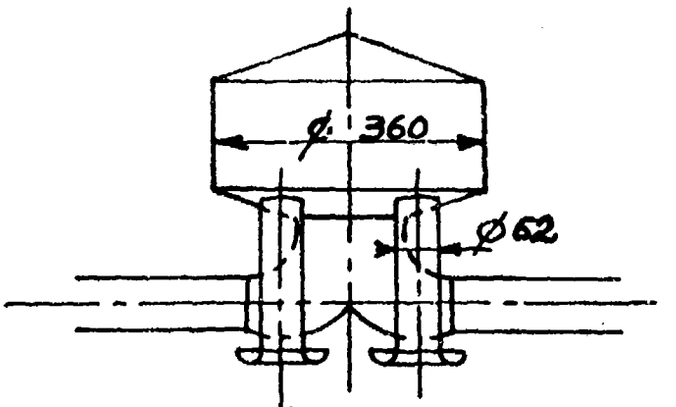
Chambre n°2 V = 25 dm³



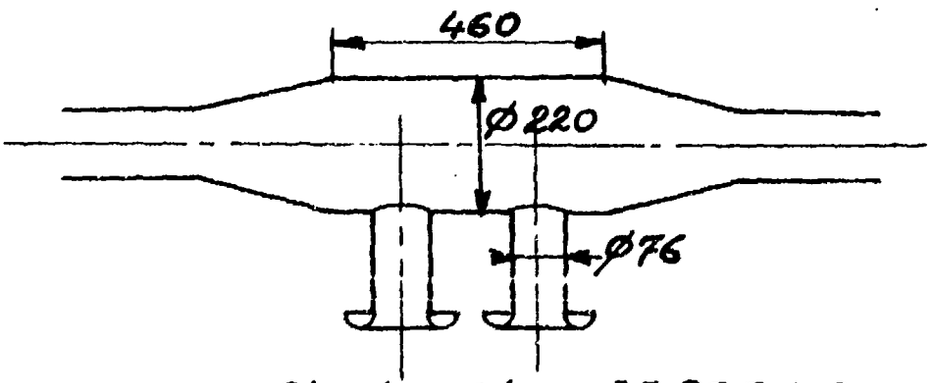
Chambre n°2 bis V = 31,8 dm³



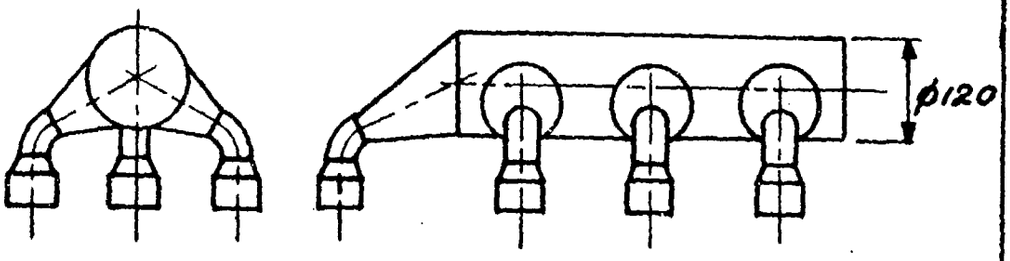
Chambre n°3 V=16,6 Dm³



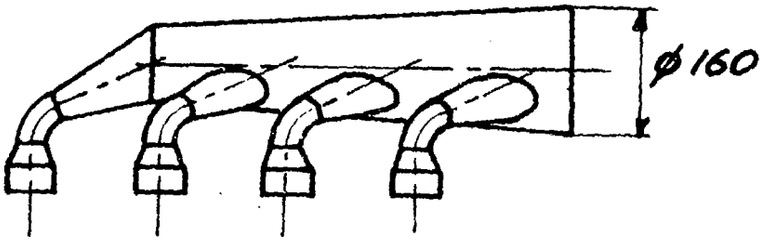
Chambre n°3 bis V= 30,5 dm³



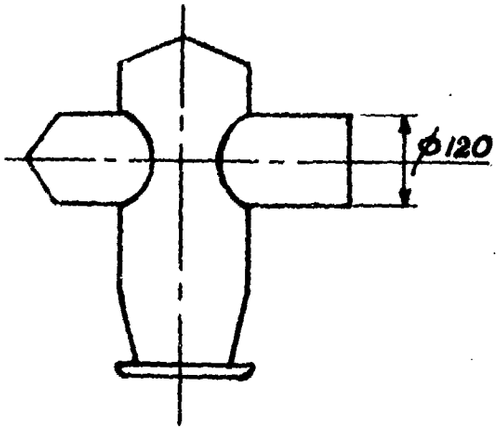
Chambre n°4 V= 29,3 dm³



Sortie n°1 : 7 pipes ϕ50 V = 13,5 dm³
(Outlet)

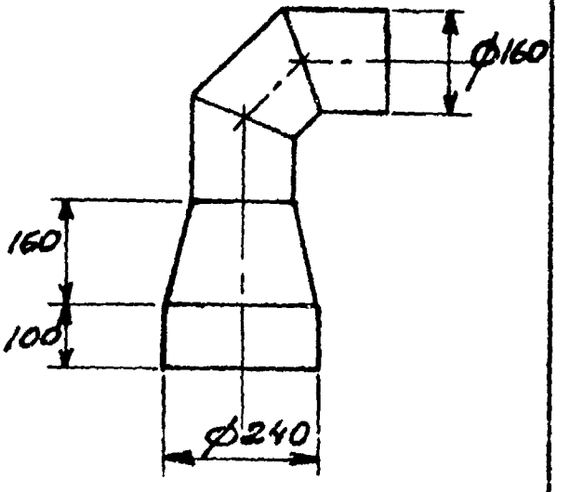


Sortie n°1 bis : 7 pipes ϕ60 V = 16,5 dm³
(Outlet)



Sortie n°2

V = 31,8 dm³



Sortie n° 3
Coude de 160 avec divergent. (Elbow)

V = 17,4 dm³

DATE

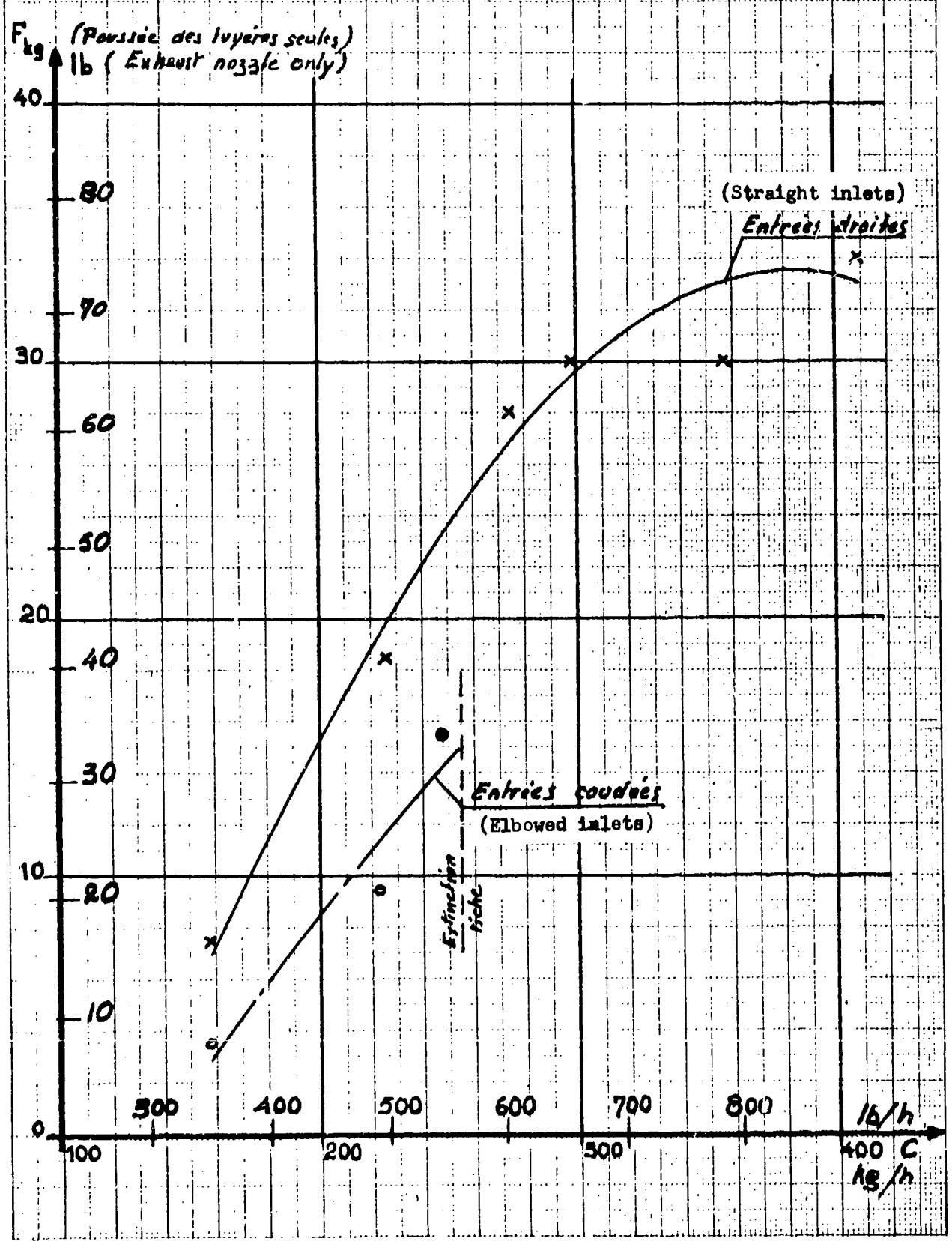
Pulso EP010 type 1ter

Influence des entrées d'air coudées sur la poussée

N°

Planche 6-4

INFLUENCE OF ELBOWED AIR INLETS ON THE THRUST



S.N.E.C.M.A. - 09.03.50 - 445 e.

CE DOCUMENT EST LA PROPRIÉTÉ DE LA S.N.E.C.M.A
IL NE PEUT ÊTRE UTILISÉ, REPRODUIT OU COMMUNIQUÉ
SANS SON AUTORISATION

DATE

SNECMA

Pulso EP010 type 1 bis

Comparaison de différentes tuyères

COMPARISON OF THE DIFFERENT EXHAUST THRUSTS

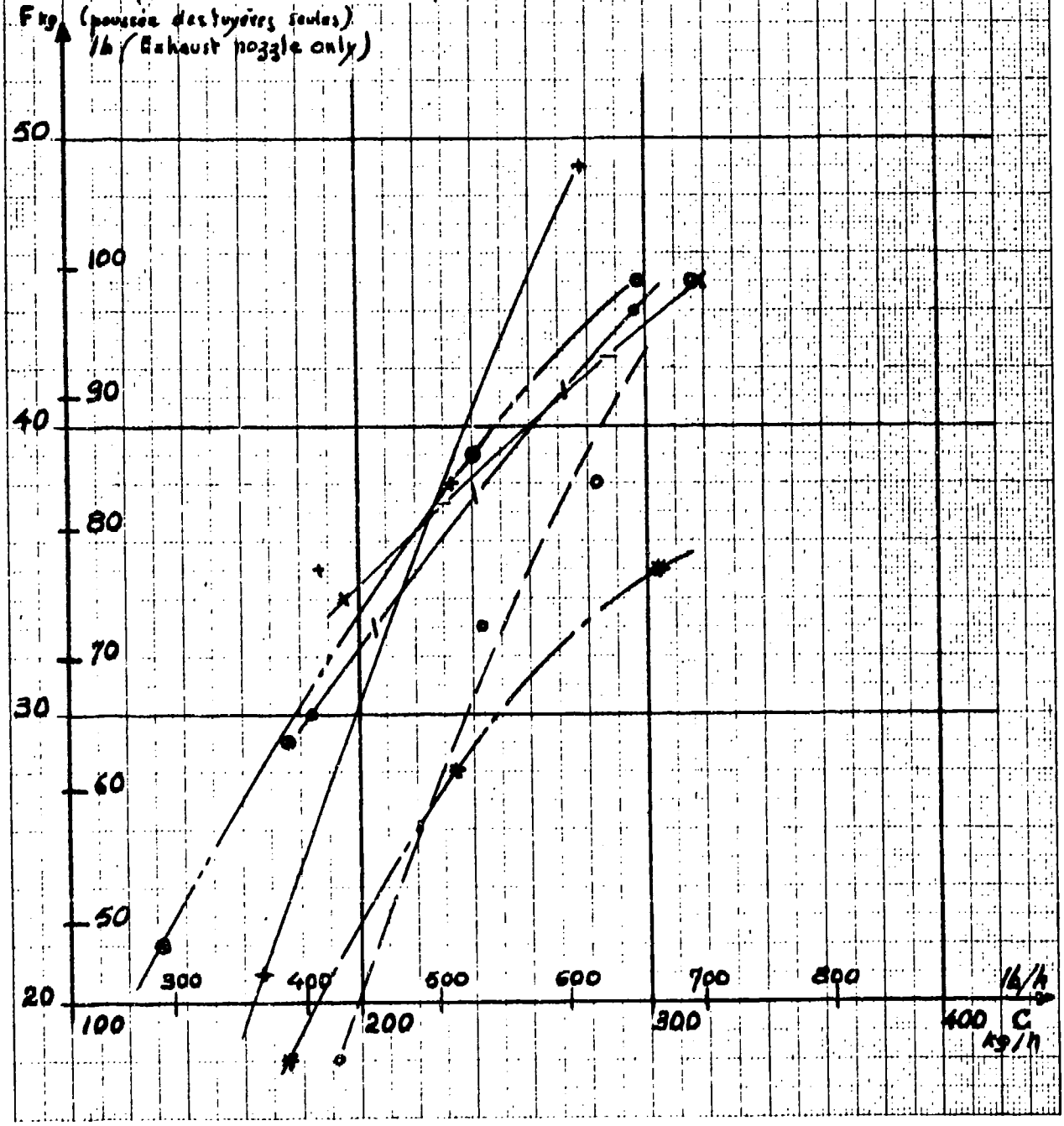
N°

Planche 6-5

(Exhaust) Tuyères ϕ_1/ϕ_2	V_{*_1}	(Comb. chbr.) Rallonge L_{mm}	V	(Elbow) Coude V	V_{radial} Pulso	
80/160	18,7			7,8	77,4	●
90/160	12,5	400	8	9,8	81	×
90/160	12,5	400	8	17,4	100,2	+
70/160	17,4			17,4	94	✱
80/160	18,7			17,4	96,6	○
90/160	12,5			16,5 $*_2$	82,4	●

$*_1$ Pour une seule tuyère. (For one exhaust nozzle)

$*_2$ Sortie n° 1 bis (Outlet)



S.N.E.C.M.A. 080250-445 *

CE DOCUMENT EST LA PROPRIÉTÉ DE LA S.N.E.C.M.A
IL NE PEUT ÊTRE UTILISÉ, REPRODUIT OU COMMUNIQUÉ
SANS SON AUTORISATION

DATE

Pulso EP.010 type 1ter

Comparaison de différentes tuyères

Poussée des tuyères seules.

N°

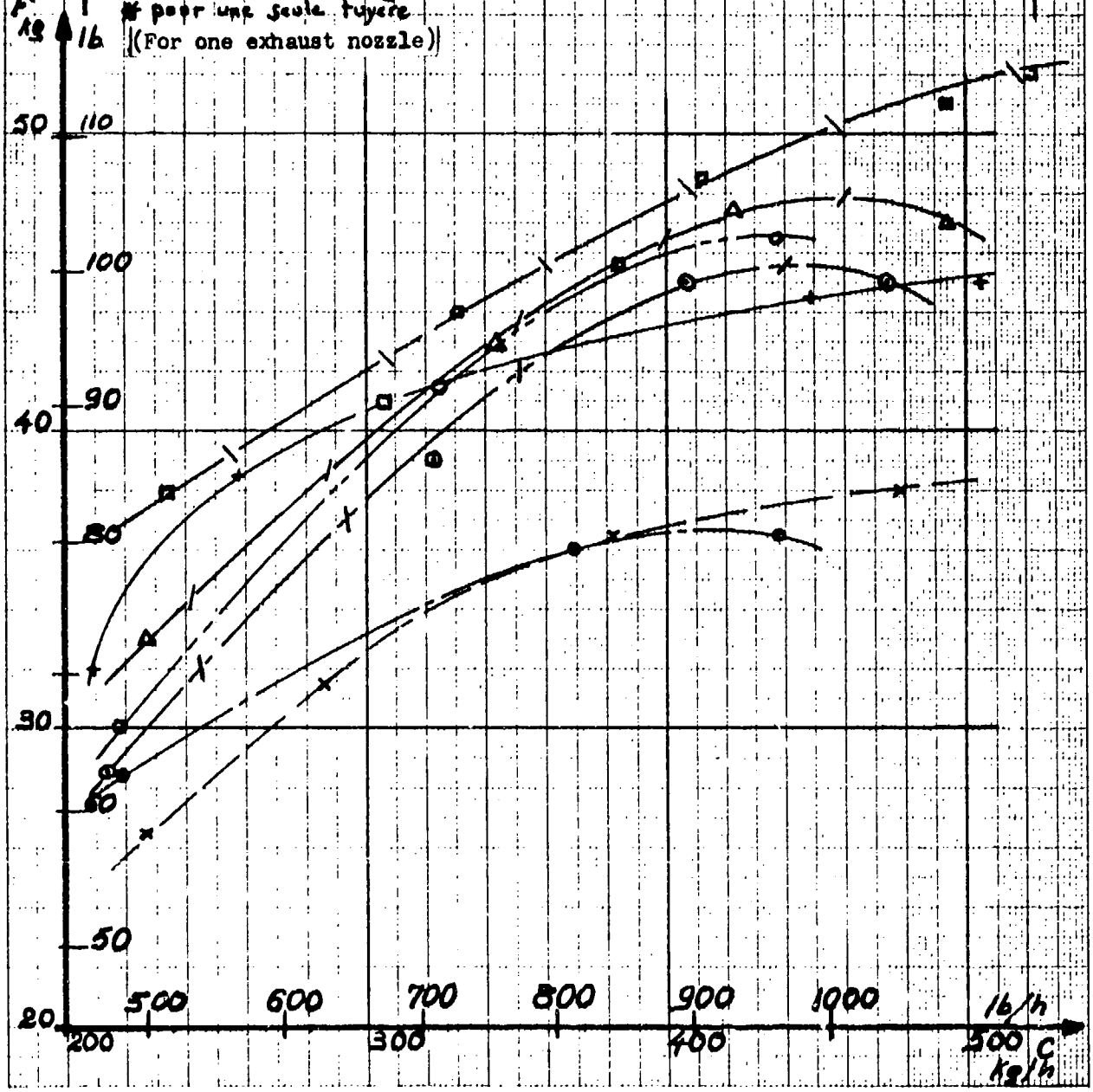
Planche 6-6

COMPARISON OF EFFECT OF DIFFERENT EXHAUST NOZZLE CONFIGURATIONS ON EXHAUST THRUST

Chambre Ø 230 V = 34,98 dm³ (Comb. chbr.)

Dia. Ø col. D.	Tuyère (Exhaust) Ø sortie outlet	Longueur Length	V Dm³	Rallonge Longueur Length, L	V Dm³	(Elbow) V coude Dm³	
80	140	1200	11,68			5,08	+
100	140	1200	13,70			"	×
100	140	1200	13,70	500	7,70	"	●
90	160	1000	12,52			7,85	○
100	160	1000	13,51			"	⊙
100	160	1200	16,20			"	△
100	160	1200	16,20 *	400	8,05	"	□

* pour une seule tuyère (For one exhaust nozzle)



S.N.E.C.M.A. 09.00.30 - 445 ml

CE DOCUMENT EST LA PROPRIÉTÉ DE LA S.N.E.C.M.A
IL NE PEUT ÊTRE UTILISÉ, REPRODUIT OU COMMUNIQUÉ
SANS SON AUTORISATION

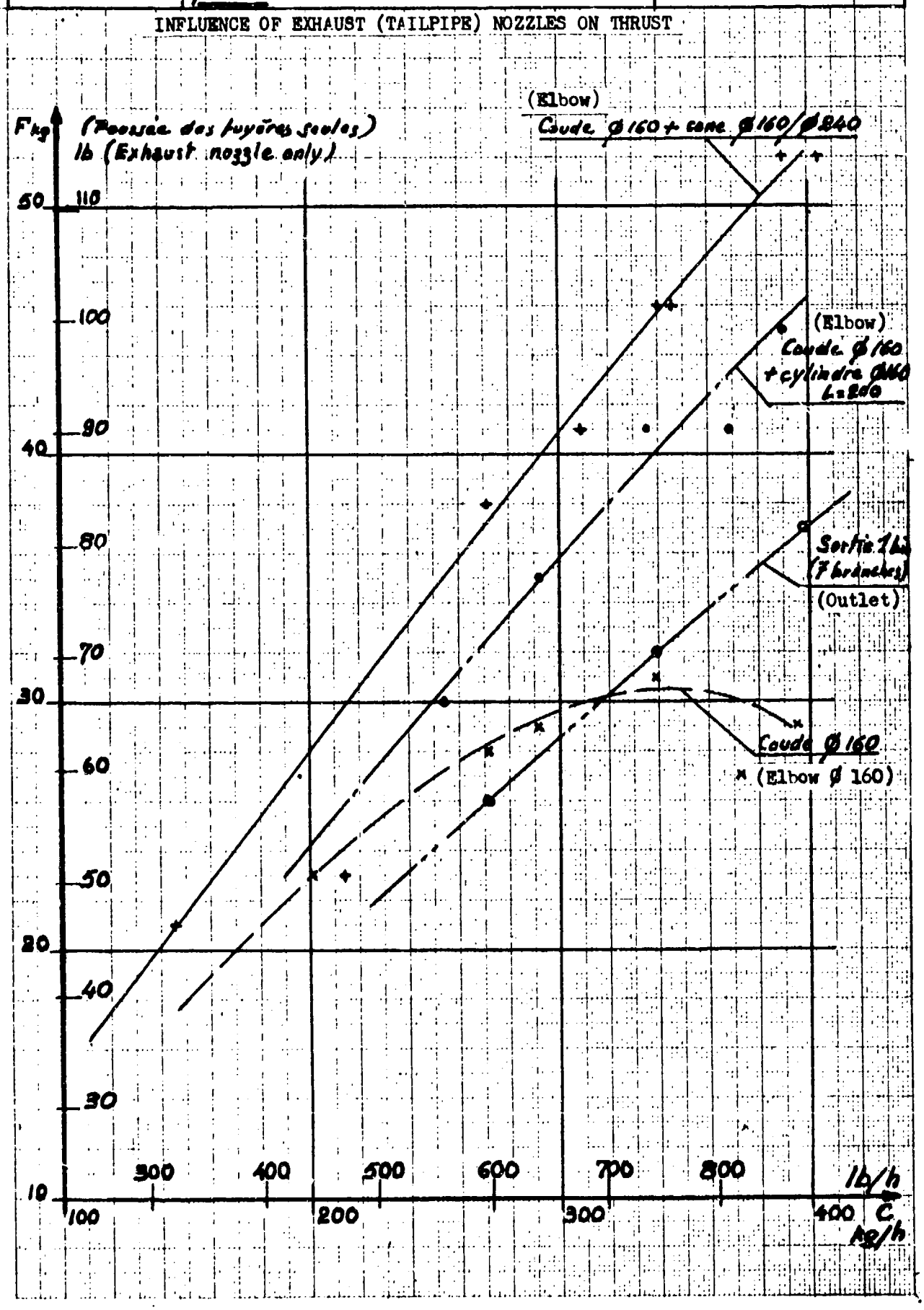
DATE

Pulso EP.010 type 1er

Influence des sorties de tuyères sur la poussée

N°

Planche 6-7



CE DOCUMENT EST LA PROPRIÉTÉ DE LA S.N.E.C.M.A
IL NE PEUT ÊTRE UTILISÉ, REPRODUIT OU COMMUNIQUÉ
SANS SON AUTORISATION

DATE

Pulso EP010 type 1 bis

Comparaison de différentes tuyères

Poussée / Volume du pulso.

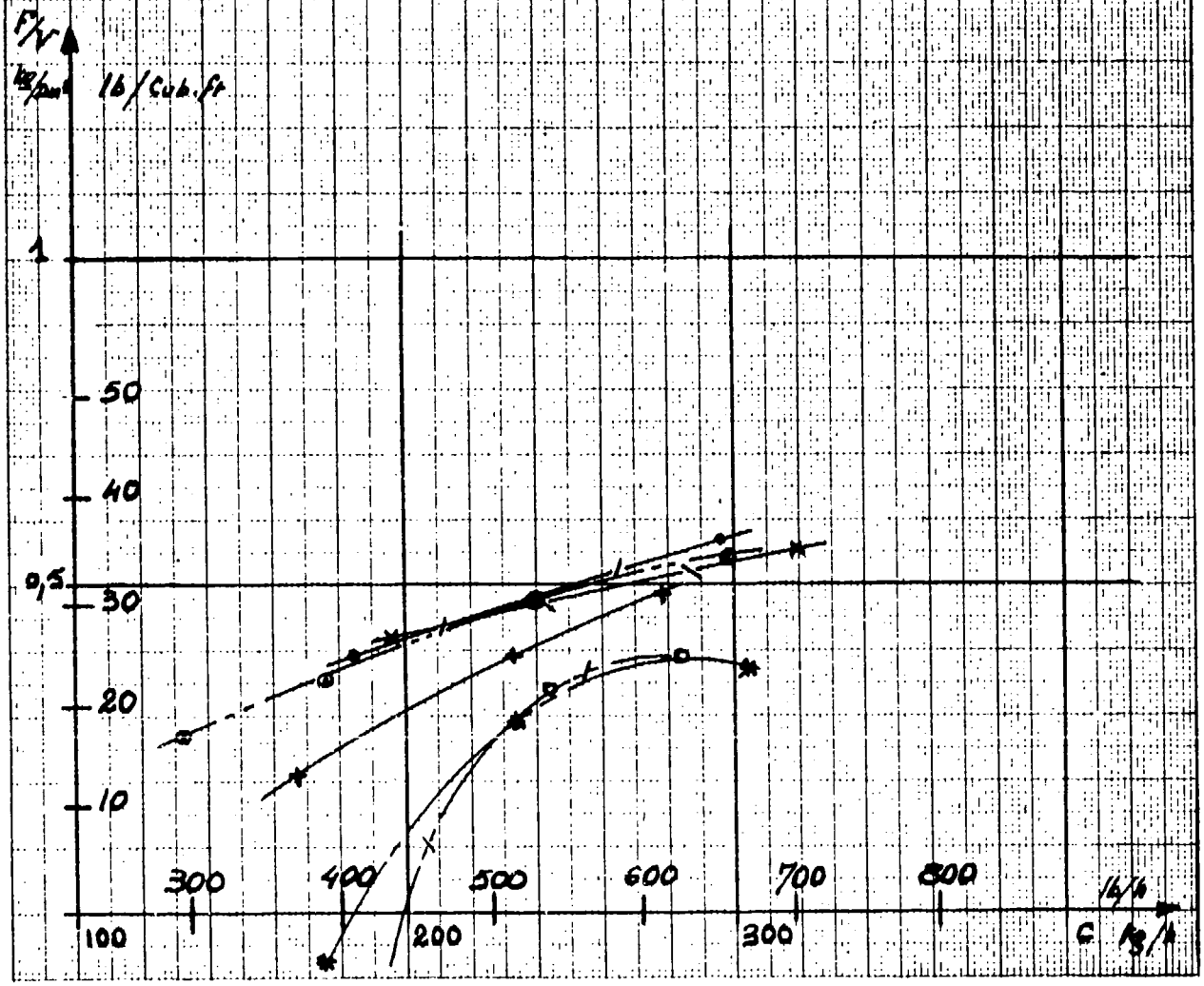
N°

Planche 6-8

COMPARISON OF DIFFERENT EXHAUST THRUST/VOLUME RATIOS

Tuyères Ø col mm	Ø sortie mm	L mm	Volume total du pulso Dm³	Cub.ft	
80	160	1600	77,4	2,74	●
90	160	1400	81	2,85	×
90	160	1400	100,2	3,58	+
70	160	1600	94	3,32	*
80	160	1600	96,6	3,41	○
90	160	1000	82,4	2,91	●

* Dont allonge Ø160 L=400



S.N.E.C.M.A. 09.03.90 445 e

CE DOCUMENT EST LA PROPRIÉTÉ DE LA S.N.E.C.M.A
IL NE PEUT ÊTRE UTILISÉ, REPRODUIT OU COMMUNIQUÉ
SANS SON AUTORISATION

DATE

Pulso EP.010. type 1er

Comparaison de différentes tuyères
Poussée / Volume du pulso.

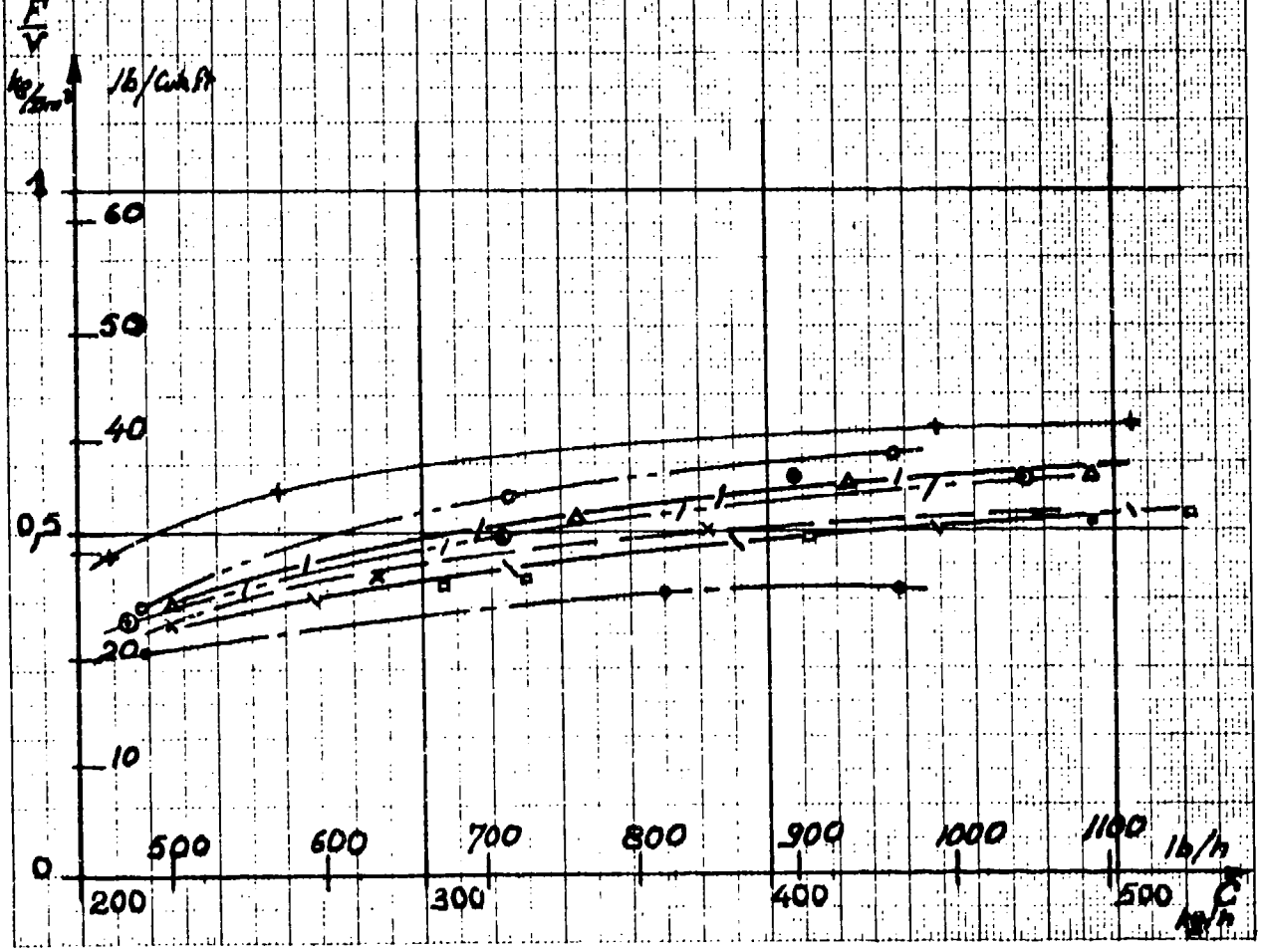
N°

Planche 5-9

COMPARISON OF DIFFERENT EXHAUST THRUST/VOLUME RATIOS

Tuyères (exhaust) Ø col mm	Ø sortie mm	Longueur mm	Volume total du pulso. Dm³	Cub.Ft	
80	140	1200	68,4	2,41	+
100	140	1200	72,4	2,55	x
100	140	1700 (1)	87,8	3,19	•
90	160	1000	75,7	2,67	○
100	160	1000	77,7	2,74	●
100	160	1200	83,1	2,93	△
100	160	1600 (2)	99,1	3,495	□

(1) dont 1 rallonge Ø 140 L = 500
(2) dont 1 rallonge Ø 160 L = 400



S.N.E.C.M.A. - 09.02.26 - 445 m

CE DOCUMENT EST LA PROPRIÉTÉ DE LA S.N.E.C.M.A
IL NE PEUT ÊTRE UTILISÉ, REPRODUIT OU COMMUNIQUÉ
SANS SON AUTORISATION

DATE

Pulso EP. 010.

Comparaison des 4 types de chambre essayés

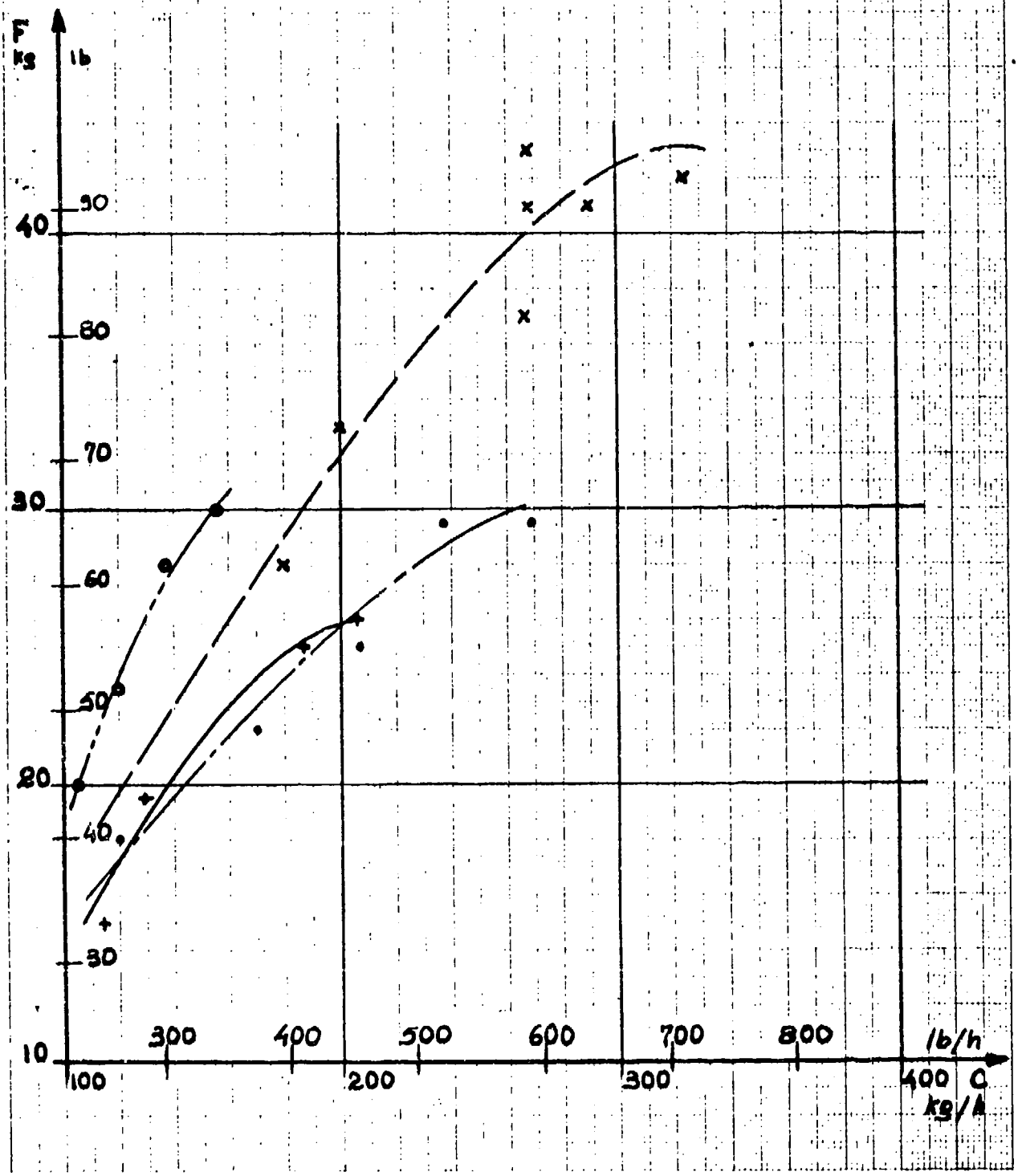
N°

Planche 6.10

COMPARISON OF THE TESTS OF 4 COMBUSTION CHAMBER TYPES

Chambre n°1 : Volume = 73,1 dm^3 ..... o ——·—— PV1 du 5/3/62
Chambre n°2bis " = 56,8 dm^3 ..... • ——·—— PV3 du 24/5/62
Chambre n°3bis " = 56,1 dm^3 ..... x — — — PV2 du 21/5/62
Chambre n°4 : " = 54,3 dm^3 ..... + ——— PV4 du 20/4/62

*1 avec sortie n°1 (With exhaust nozzle)
*2 avec coude Ø 120 (With elbow Ø 120)



S.N.E.C.M.A - 09.03.50 - 445 - 61

CE DOCUMENT EST LA PROPRIÉTÉ DE LA S.N.E.C.M.A
IL NE PEUT ÊTRE UTILISÉ REPRODUIT OU COMMUNIQUÉ
SANS SON AUTORISATION

DATE

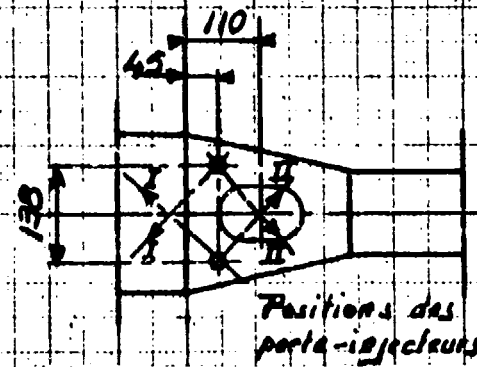
N°

Pulso EP.010 type 1er

Comparaison de differentes positions des injecteurs

Planche 6-11

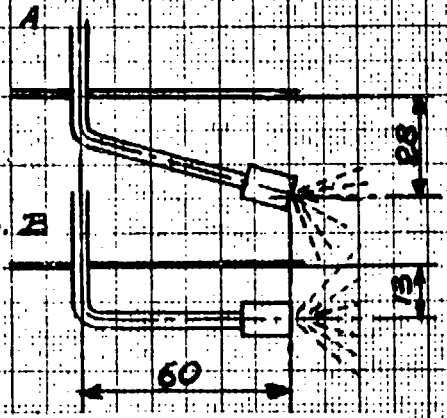
COMPARISON OF DIFFERENT FUEL NOZZLE POSITIONS AND TYPES OF SUPPORT



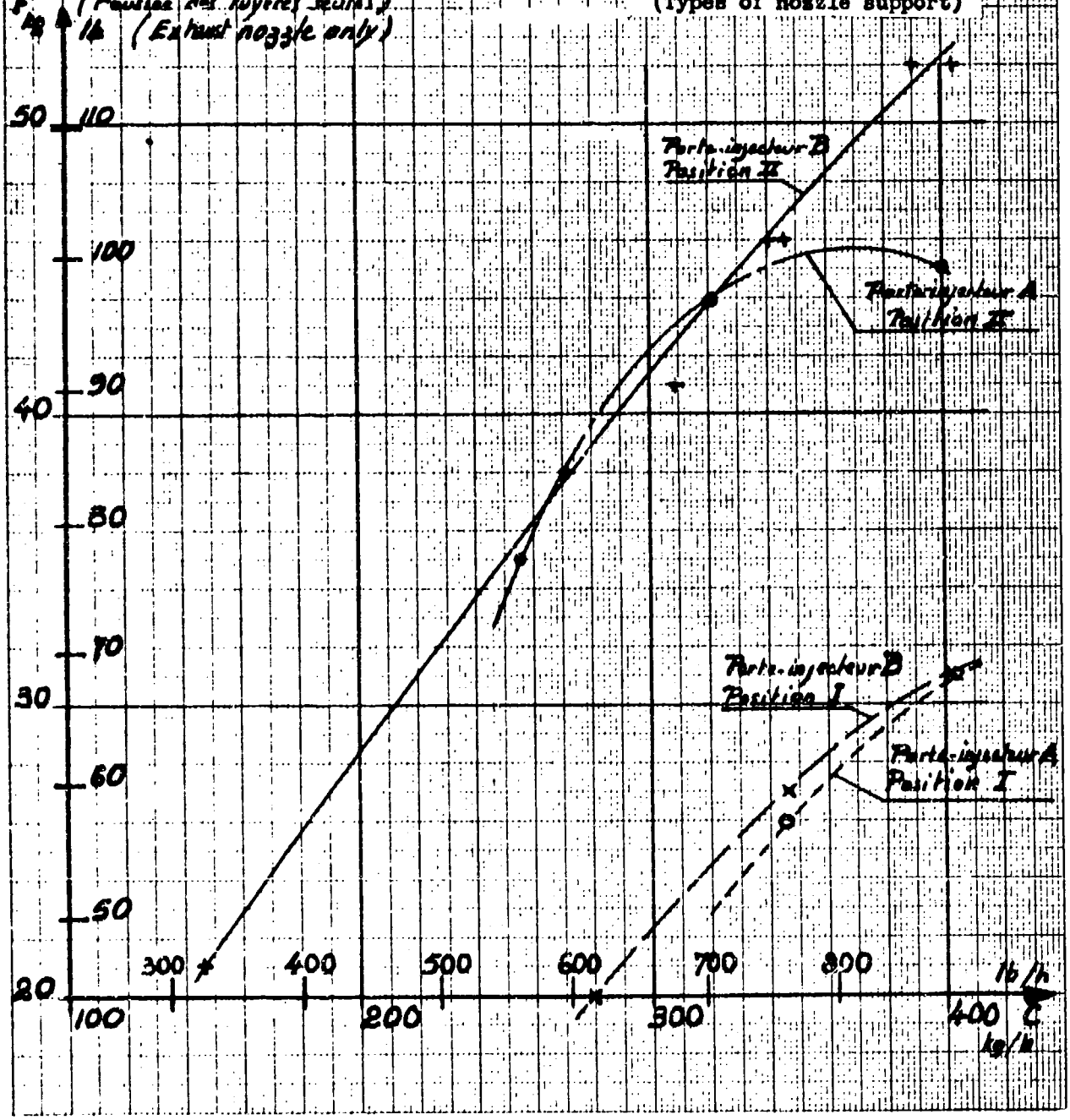
Positions des porte-injecteurs

(Positions of the fuel nozzles)

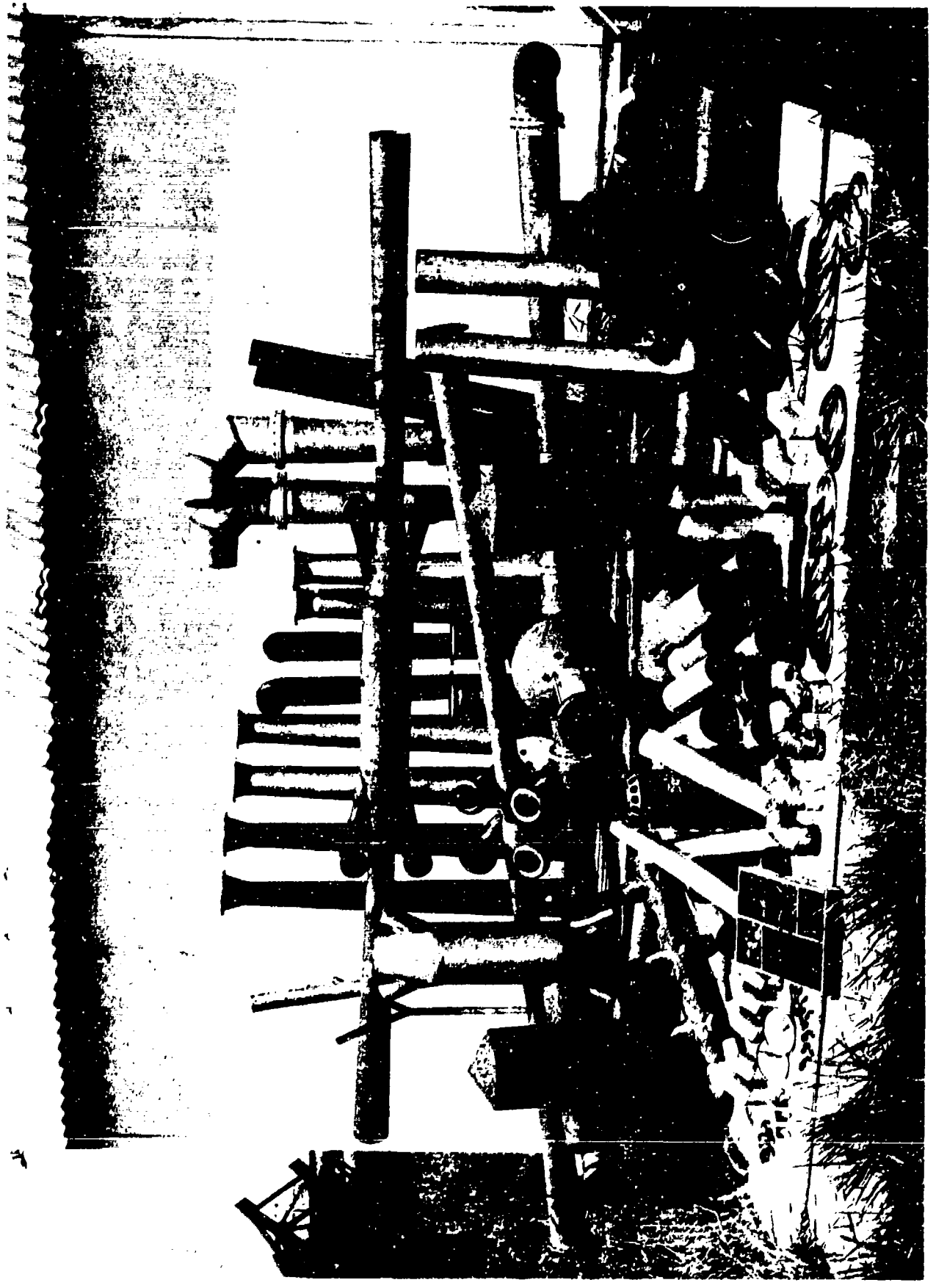
(Position des buses seules)



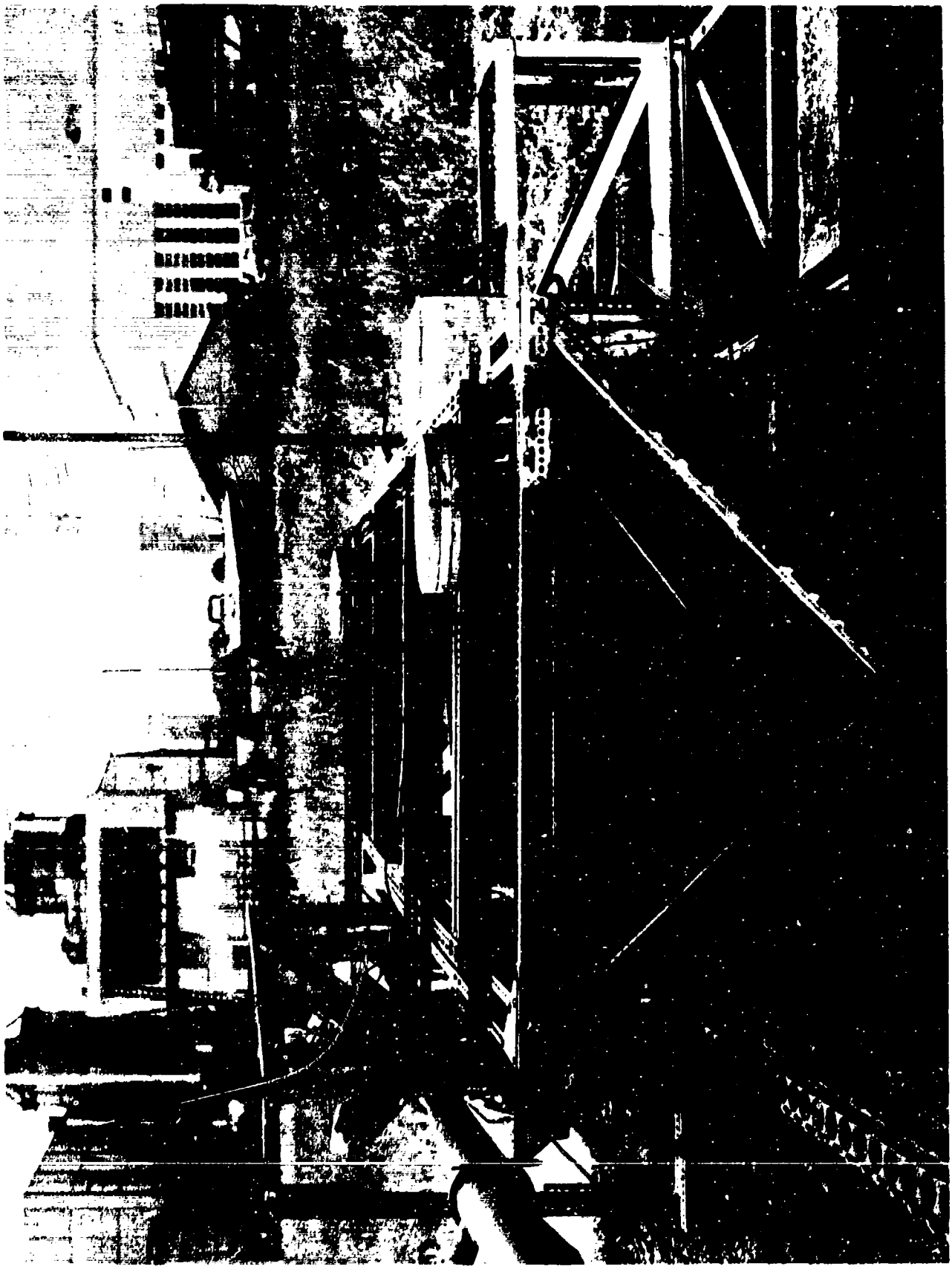
(Types of nozzle support)

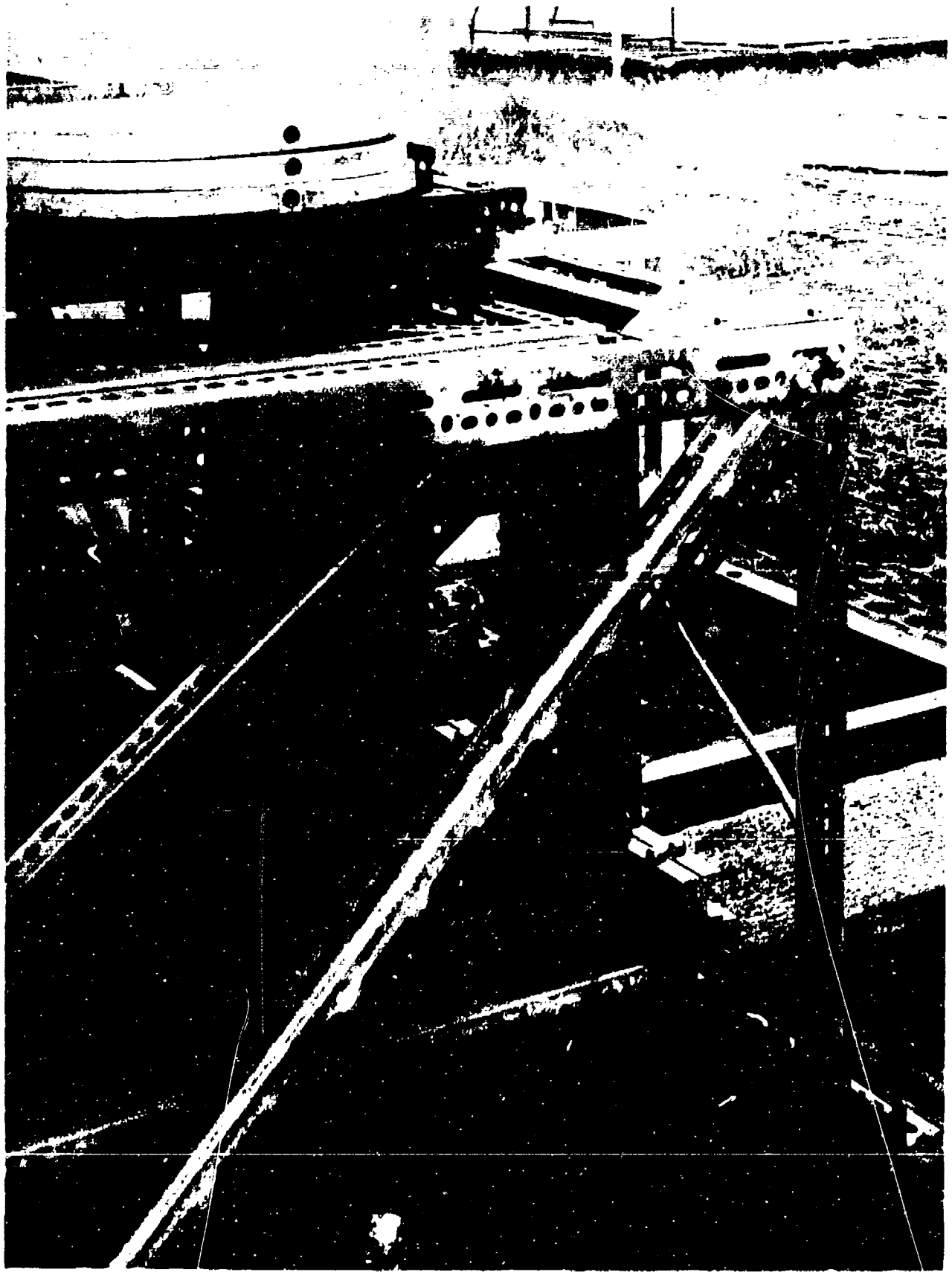


CE DOCUMENT EST LA PROPRIÉTÉ DE LA S.N.E.C.M.A.
IL NE PEUT ÊTRE UTILISÉ, REPRODUIT OU COMMUNIQUÉ SANS SON AUTORISATION

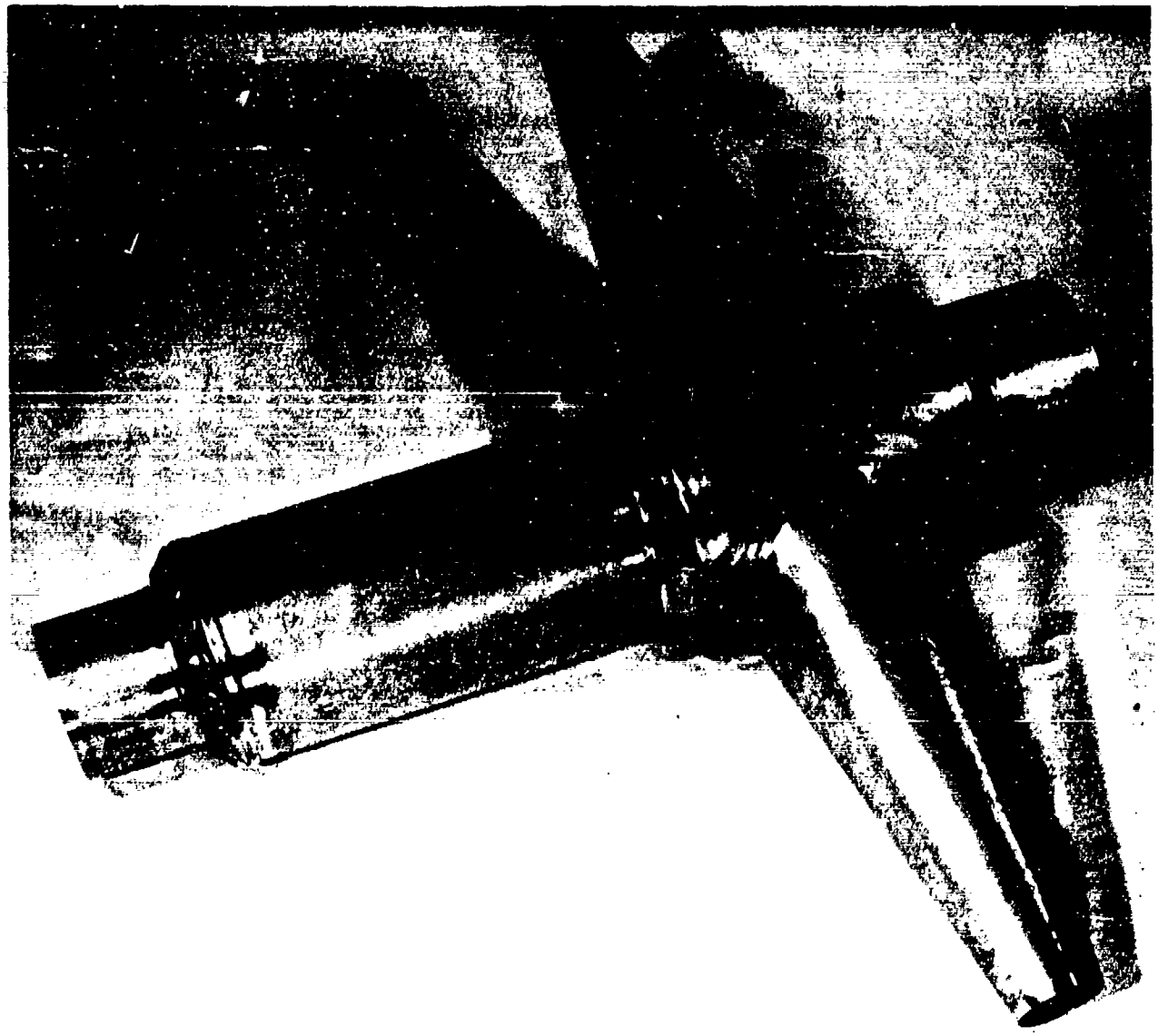


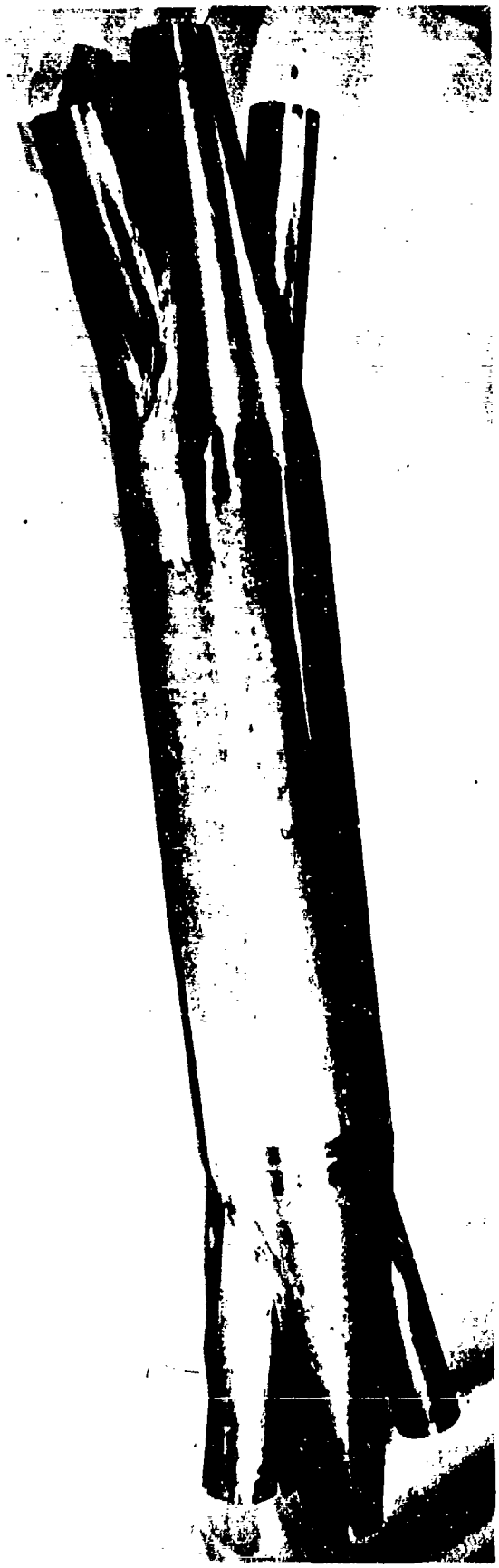




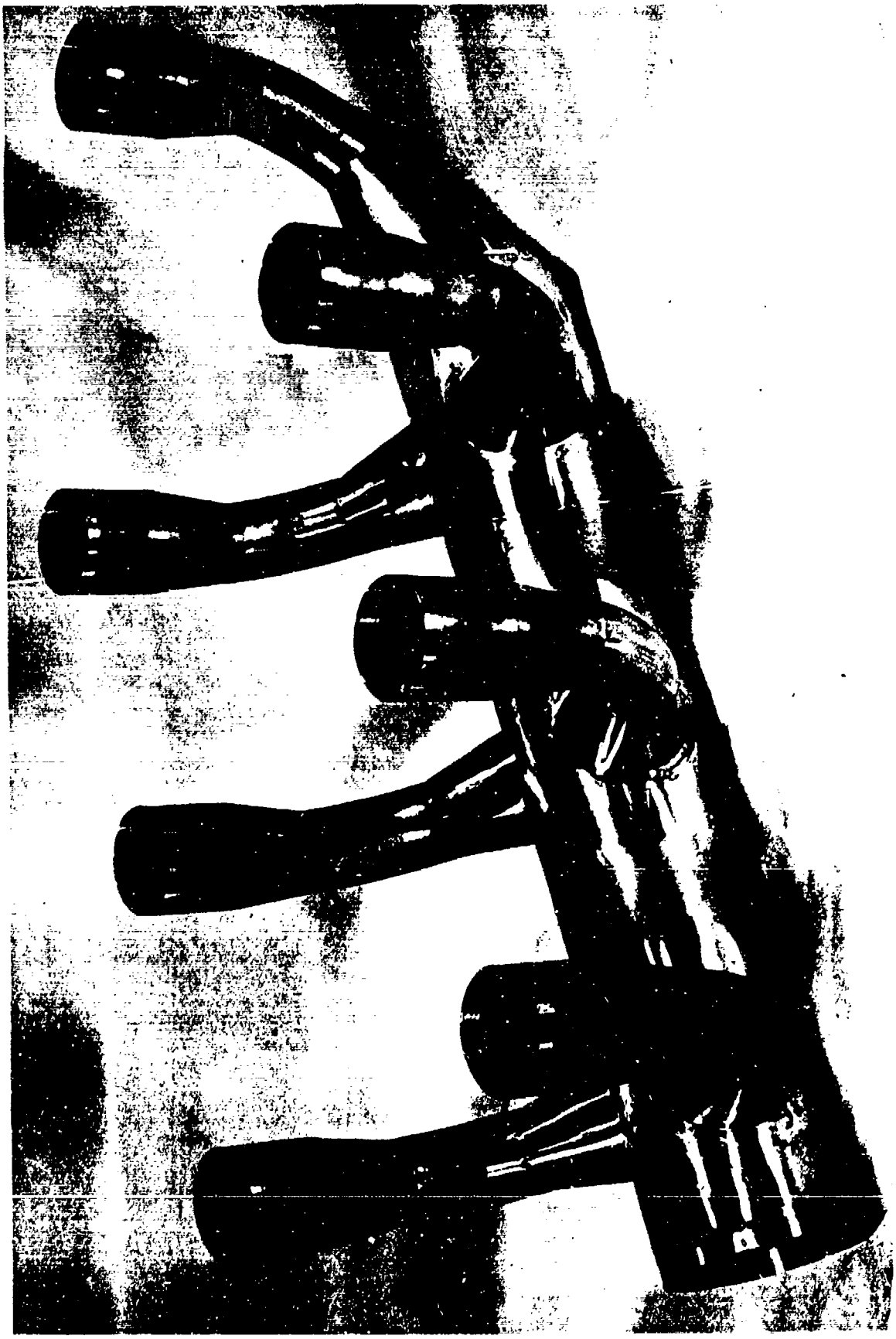




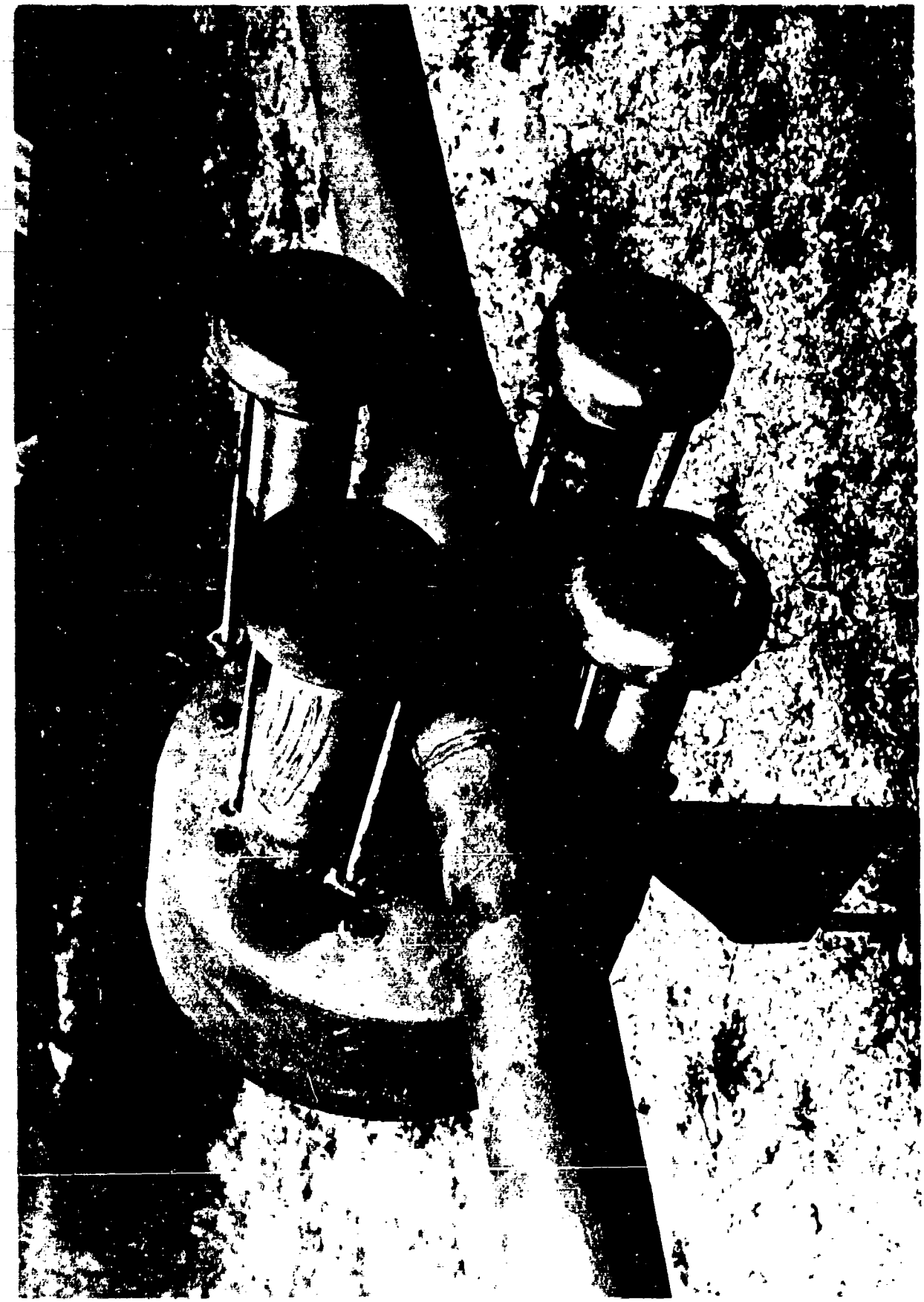


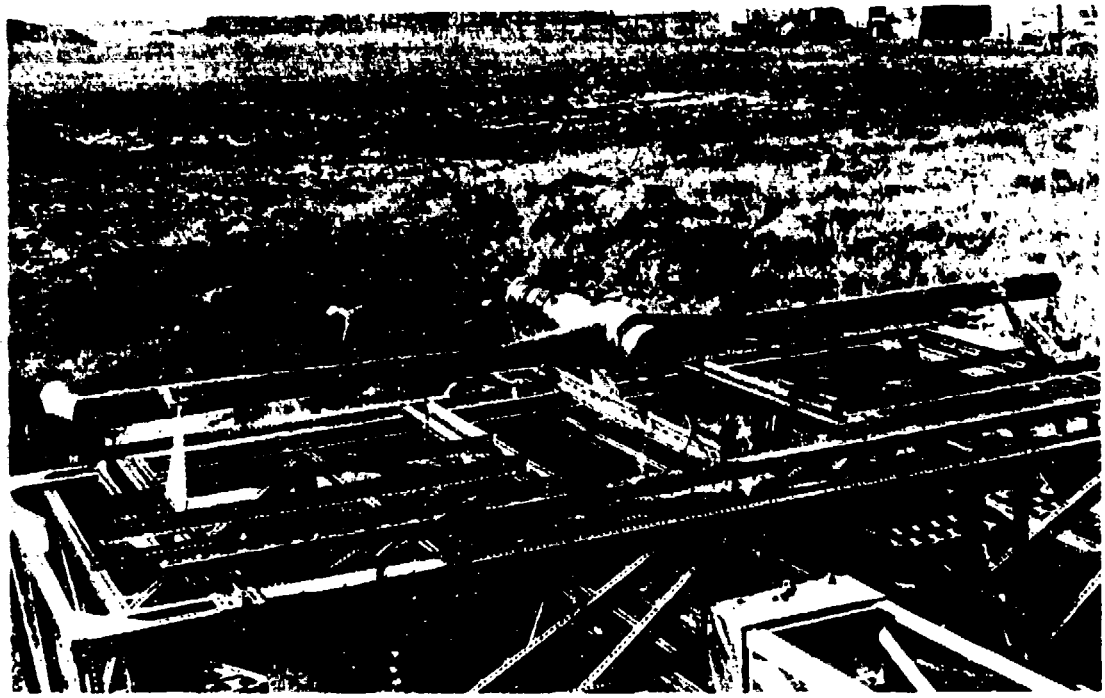


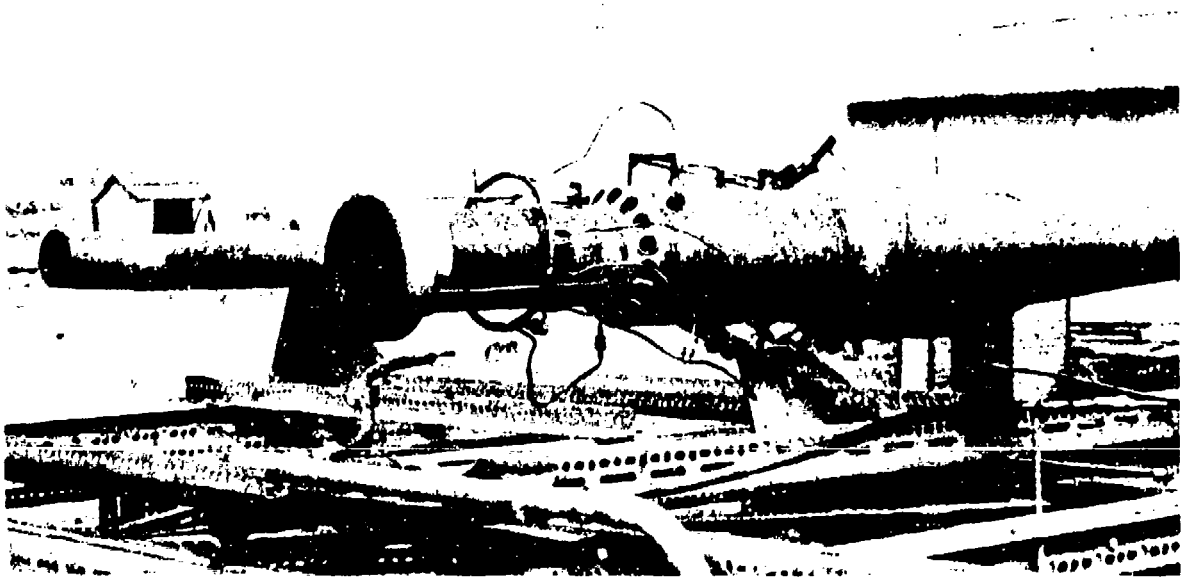




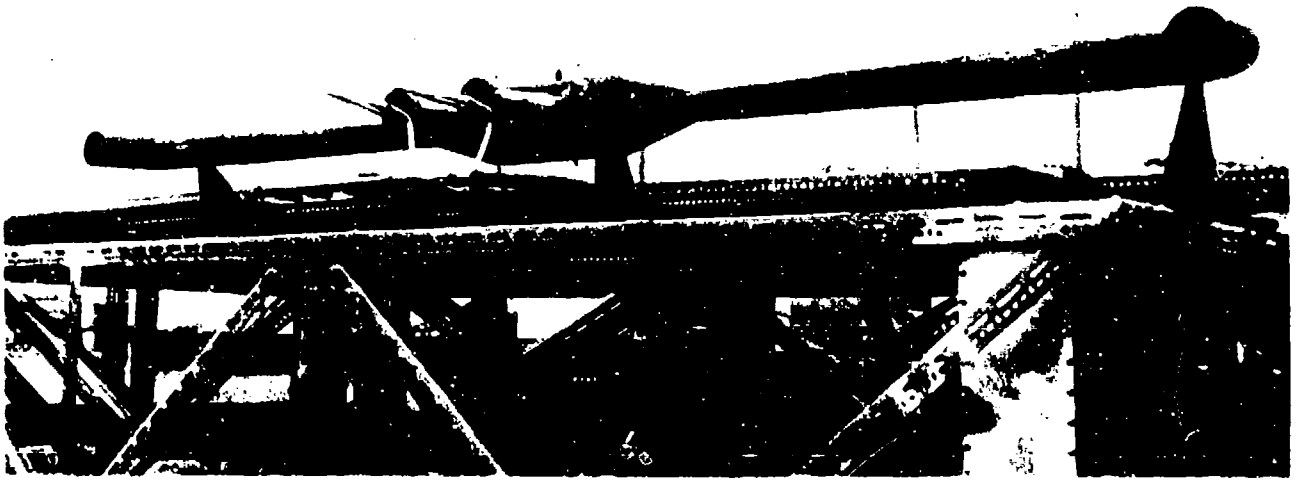




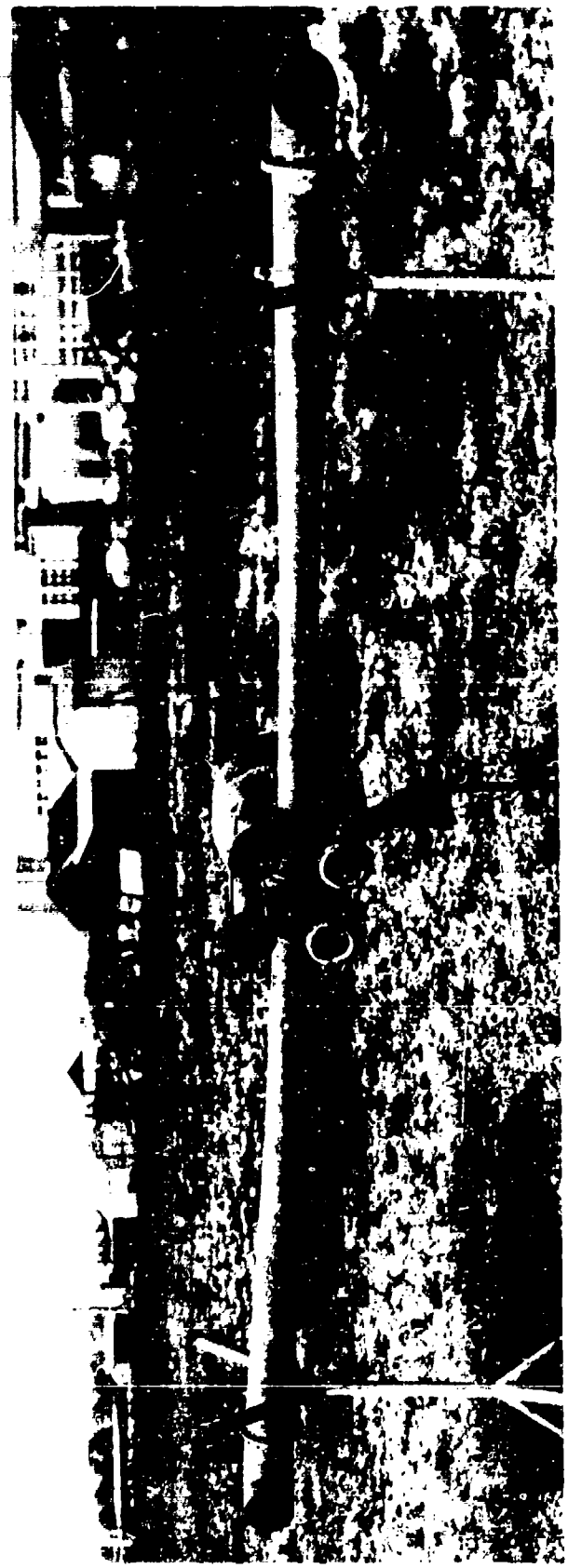








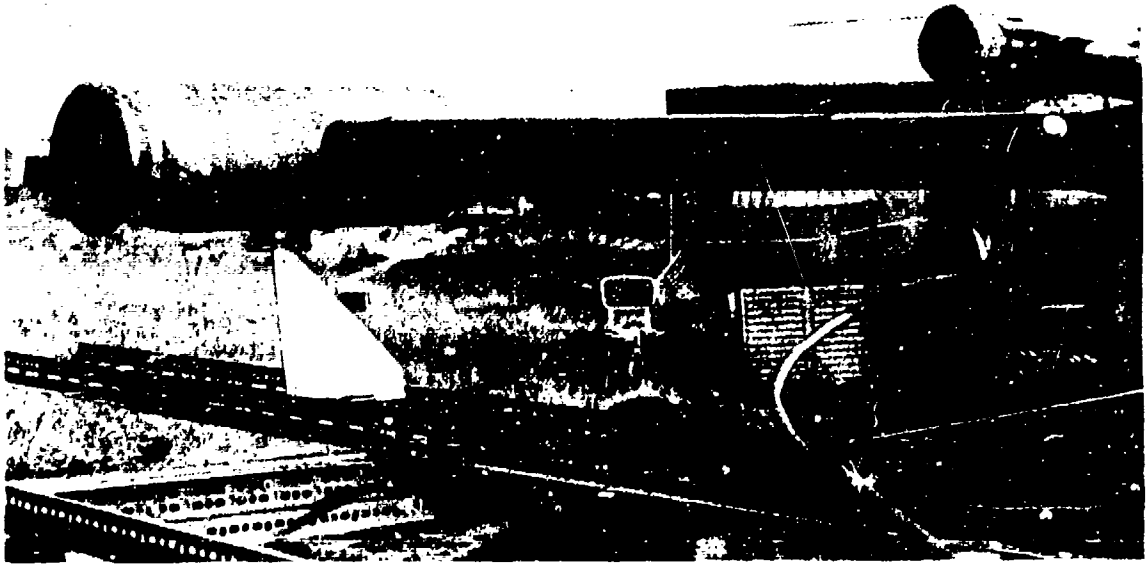


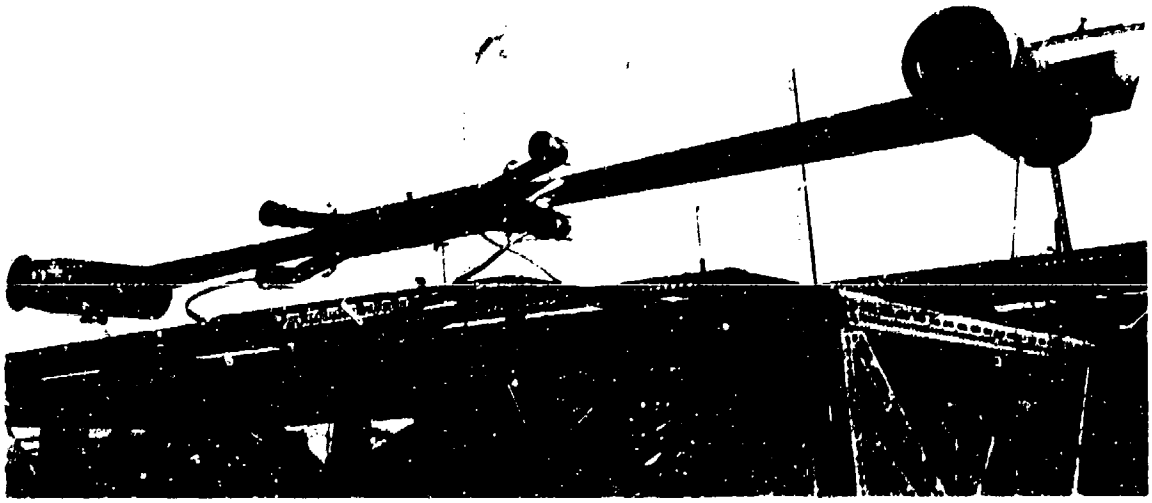




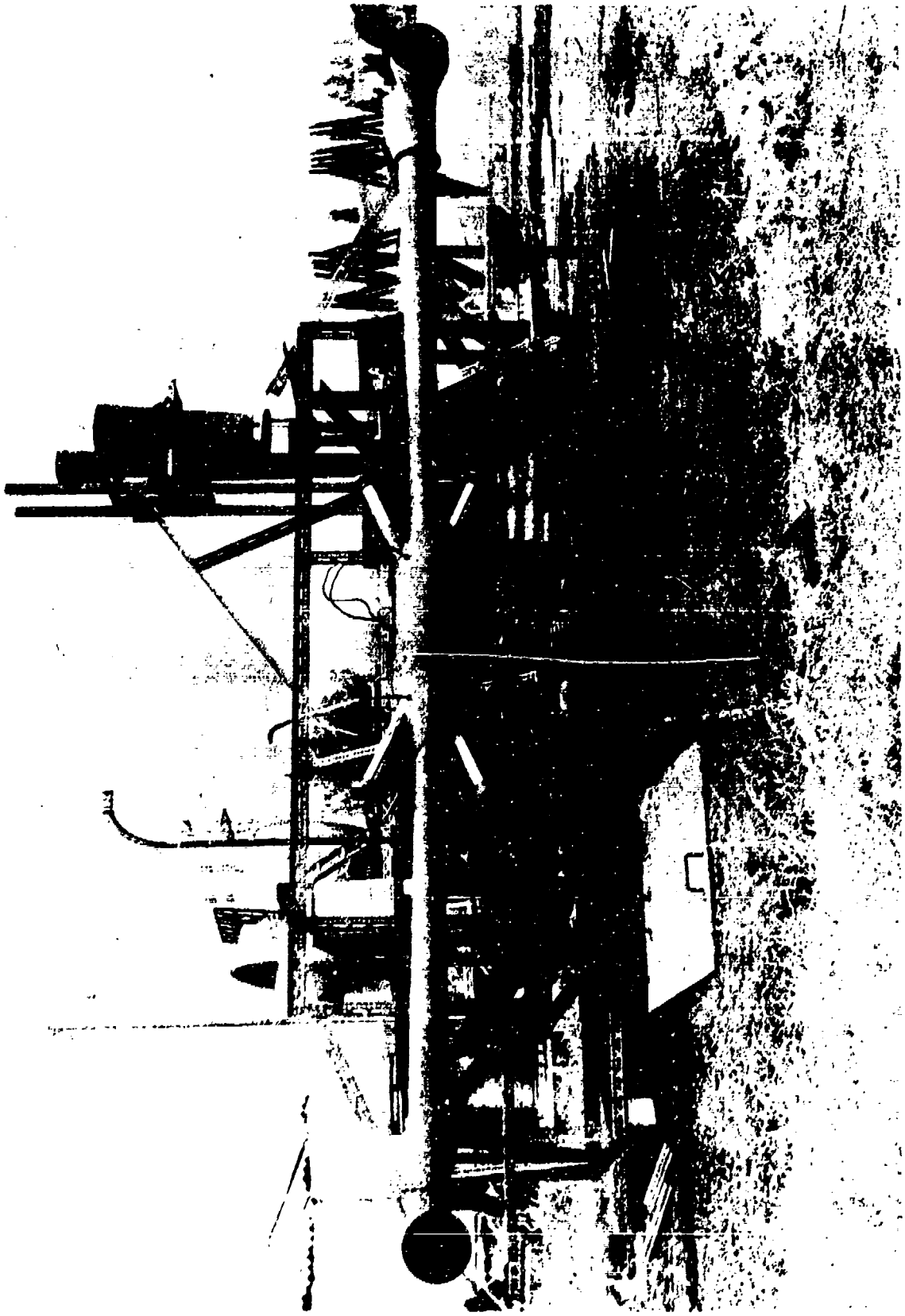


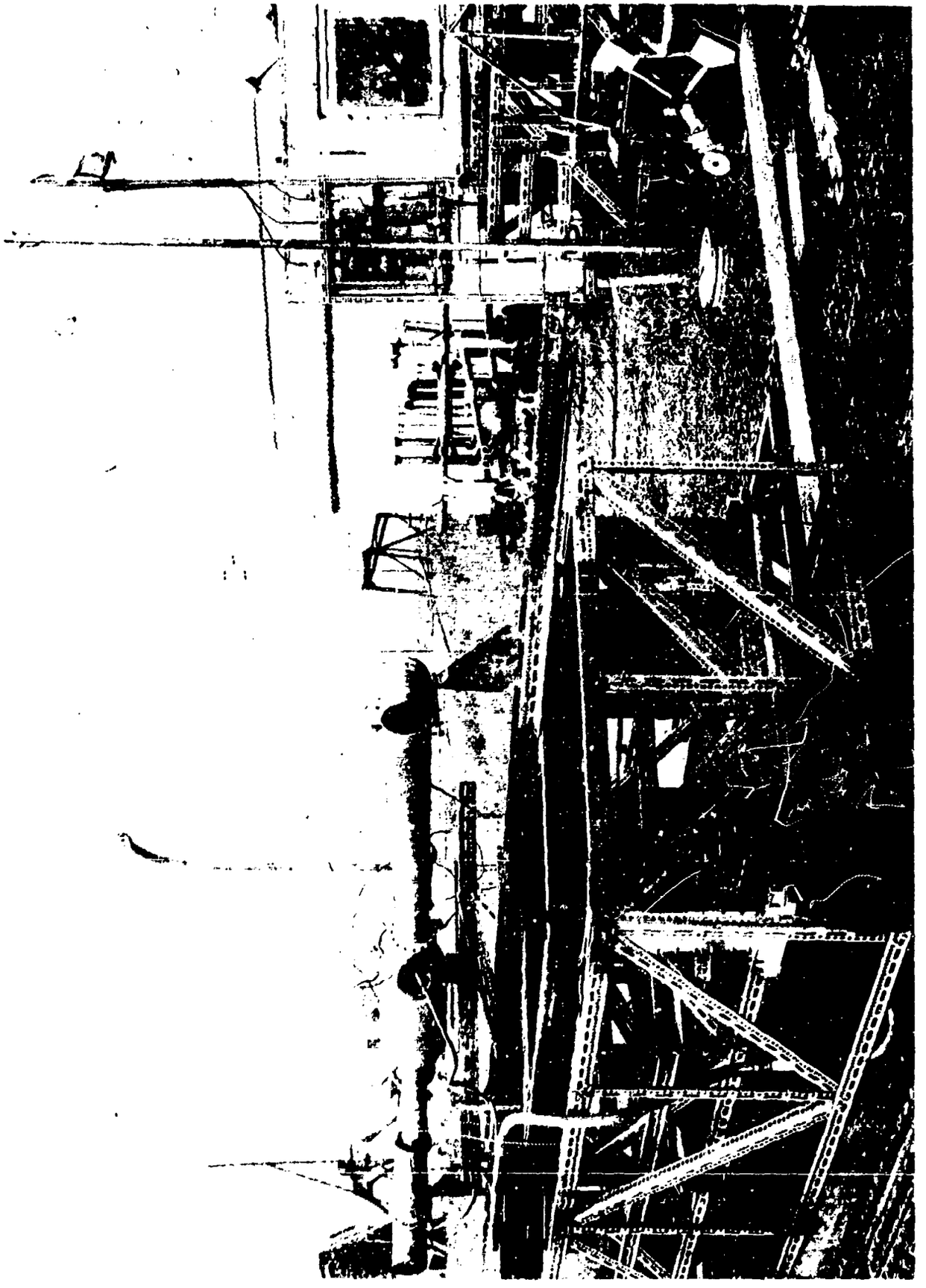


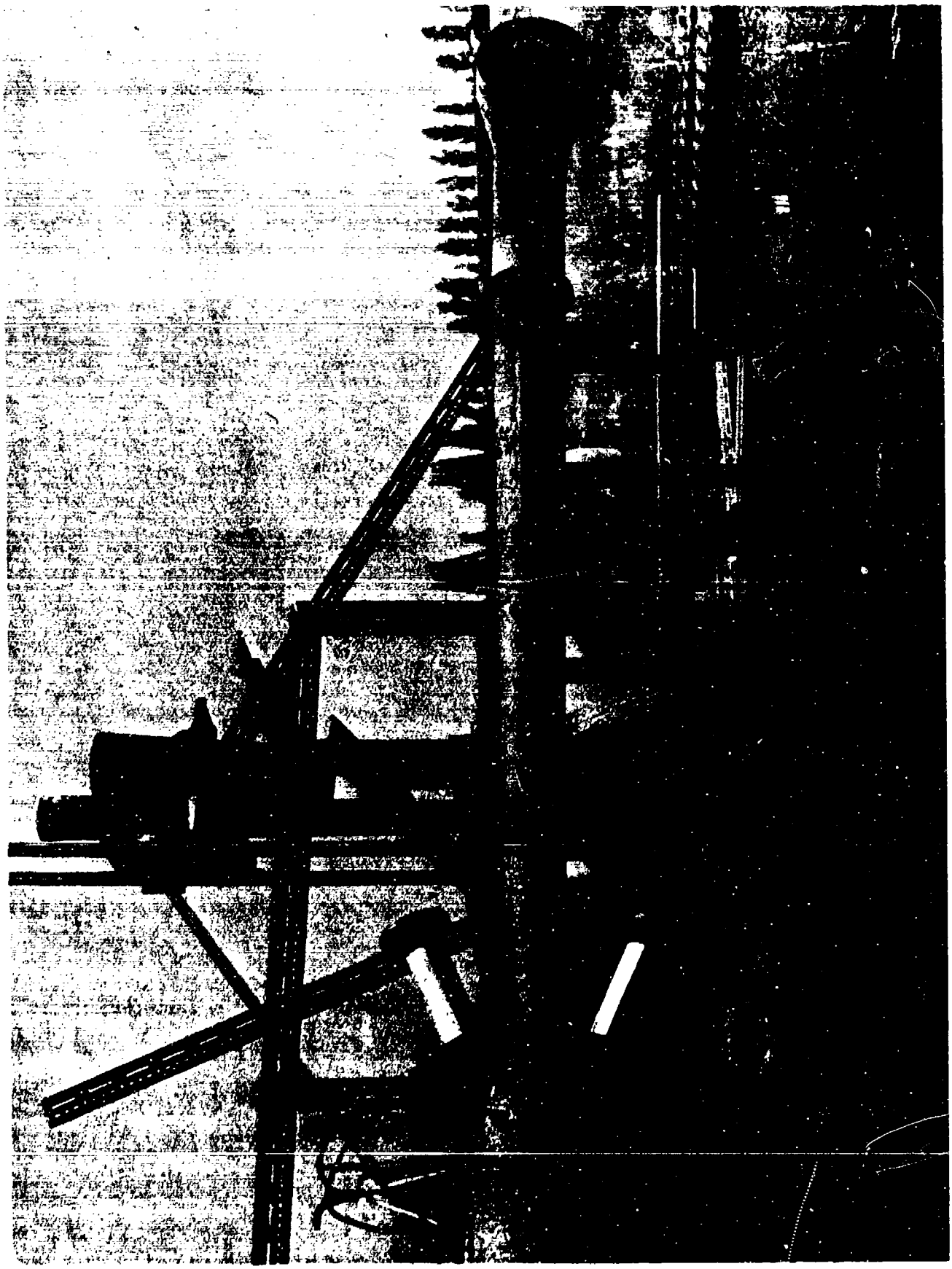


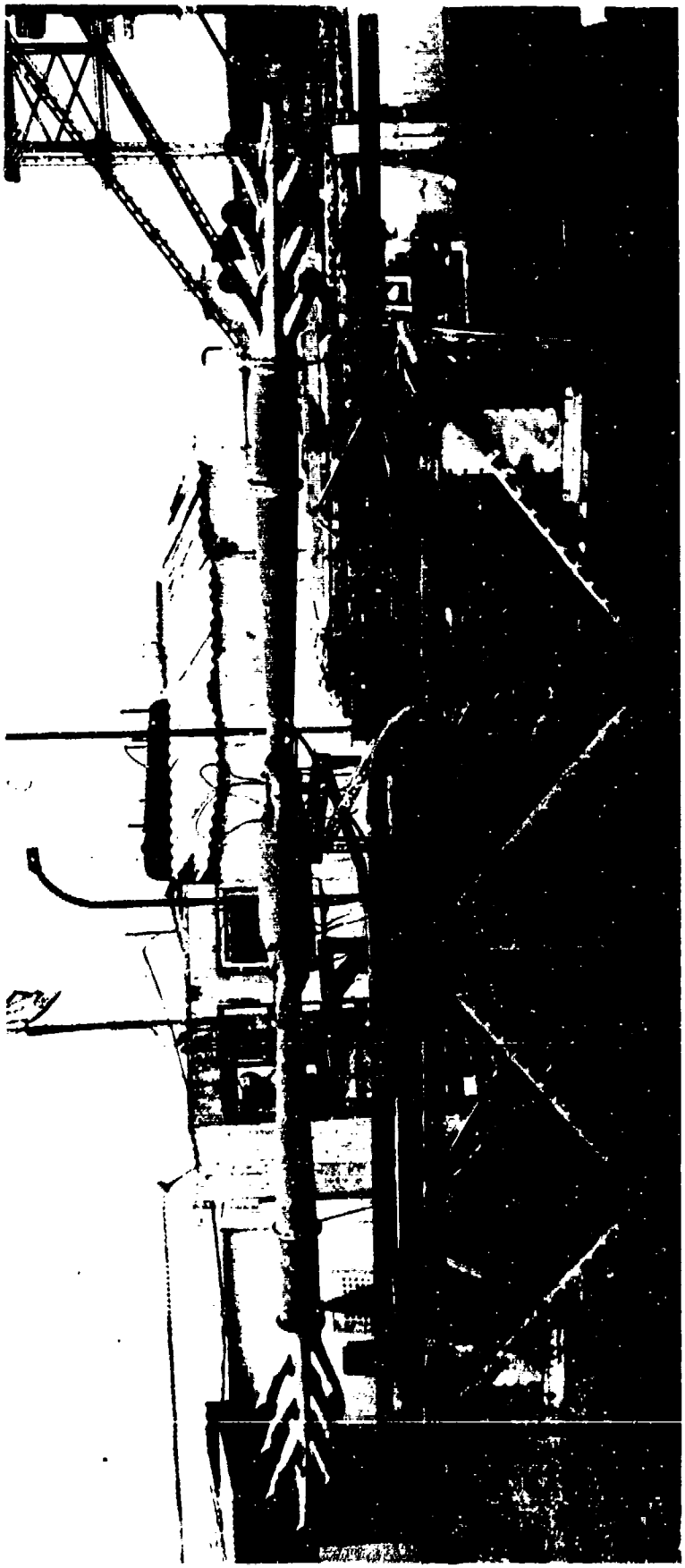


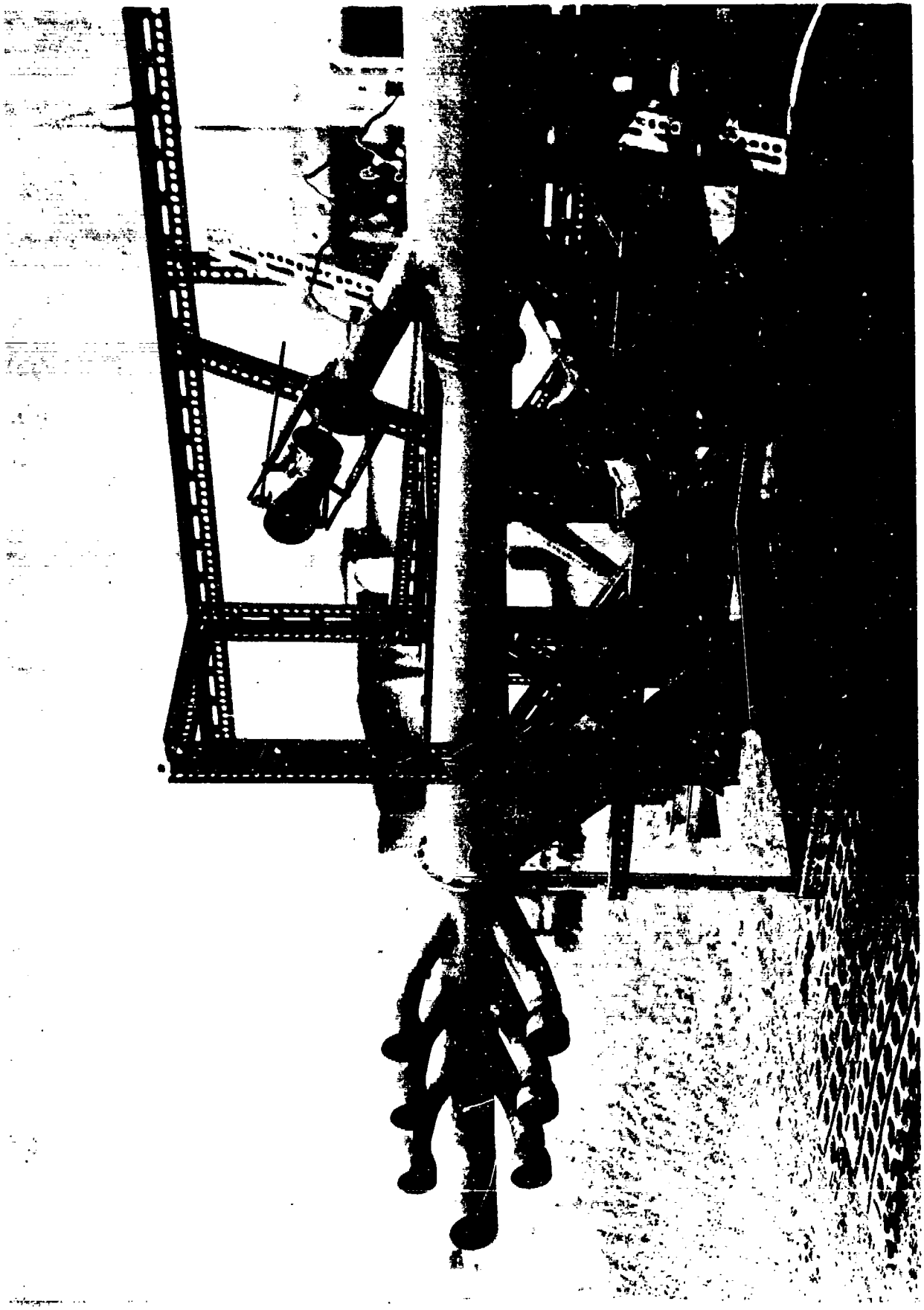














END

FILMED

12-89

DTIC